January 2021

New Conforming Finite Elements Based On The De Rham Complexes For Some Fourth-Order Problems

Qian Zhang
Wayne State University

NEW CONFORMING FINITE ELEMENTS BASED ON THE DE RHAM COMPLEXES FOR SOME FOURTH-ORDER PROBLEMS

by

QIAN ZHANG

DISSERTATION

Submitted to the Graduate School

of Wayne State University,

Detroit, Michigan

in partial fulfillment of the requirements

for the degree of

DOCTOR OF PHILOSOPHY

2021

MAJOR: MATHEMATICS

Approved By:

____

Advisor Date

____

____

____

____

DEDICATION

To My Parents

ACKNOWLEDGEMENTS

Many people helped me along the way on this journey. I would like to take a moment to thank them.

First, I wish to express my greatest gratitude to my advisor, Prof. Zhimin Zhang. When he first gave me the problem of constructing grad curl-conforming elements, I never expected I could come this far on this journey. He is always there, providing support and help to me. Everytime I feel frustrated, it is his constant support that keeps me going forward. He is always very confident at me. Everytime I feel I have solved the problem, he would encourage me to do better. From two dimensions to three dimensions, from 315 degrees of freedom to 18, from grad curl-conforming elements to grad div-conforming elements, we are achieving more and more along this way. For me, he is more than just an advisor; he is also a beacon light in my life.

I would like to thank my collaborator Dr. Kaibo Hu. He brought us the idea of constructing discrete complexes and enriching with bubbles so that we can simplify our elements. Most of this dissertation is based on the collaborations with him. I am impressed by his wide knowledge. Whenever I have a problem, he can always get my point and respond to it promptly. I appreciate every piece of his message, from which I can always learn something new.

I'm truly grateful to Prof. Jiguang Sun from Michigan Technological University. I heard from him the quad-curl problem for the first time. Without him, I could not have found such a great subject that I have enjoyed so much. I appreciate all the helpful discussions we had at Beijing Computational Science Research Center (CSRC) or on Skype, which have helped me understand this problem well.

If it was not for Prof. Ran Zhang recommending me to CSRC, I would never have the chance to meet Prof. Zhimin Zhang. In the last year of my undergraduate program, I went to the fork in the road of my life. She offered me the opportunity to go to Beijing for my master degree study. What I gained from her is not only an opportunity but also some valuable experience. I learned Calculus and the Weak Galerkin method from her; I finished my first paper with her. All of these play a cornerstone role in my future research path.

I would like to thank my collaborator Prof. Jiwei Zhang from Wuhan University. I am so lucky to have him as my co-advisor for my master program. The experience of working with him built up my confidence in research. I would also like to thank my senior, my collaborator, and my friend, Dr. Lixiu Wang. Without her, this journey could have been less colorful.

I wish to express my gratitude to my friends at Wayne State University: Nguyen-Truc-Dao Nguyen, Thi Dai Trang Nguyen, Hongjiang Qian, Handan Shu, Yuxin Wang, Zhexin Wen, and Lewei Zhao. I really enjoyed the time when we went grocery shopping together.

I would like to thank Department of Mathematics at Wayne State University for offering me Graduate Teaching Assistantship, Thomas C. Rumble University Graduate Fellowship, M.F. Janowitz Endowed Mathematics Scholarship, and Outstanding Graduate Award. I could not have come this far without these financial supports. I appreciate all the trainings I received from the department. I learned a lot from the courses instructed by Prof. Peiyong Wang, Prof. George Yin, Prof. Boris Mordukhovich, Prof. Luca Candelori, Prof. Robert Bruner, Mr. Christopher Leirstein, and Ms. Shereen Schultz. I appreciate all the help provided by Carla Sylvester, Maria Vujic, JoAnne Lewan, Barbara Malicke, and Doris E. King. I also appreciate my colleagues, particularly Bakhyt Aitzhanova, Fatemah Alhamede, Priyanka Ahire, Mohammad Kang, Nkechi Nnadi, Oanh Nguyen, Xiang Wan, Charuka Wickramasinghe, Diego Yepez, and Peimeng Yin, for the happy times we have spent together and for the help they have ever provided.

I would like to thank Prof. Peiyong Wang, Prof. Hengguang Li, Prof. Fatih Celiker, and Prof. Weisong Shi for serving as my dissertation committee.

Finally, I would like to thank my parents for their unconditional love and support. I would also like to thank my boyfriend, Hang Du. He is always accompanying me in person or via FaceTime, no matter when I need someone to talk to or I stay up late to figure out a problem. Without them, this journey would not have been filled with such joy, love, and fun.

TABLE OF CONTENTS

LIST OF TABLES

LIST OF FIGURES

CHAPTER 1 INTRODUCTION

1.1 Definition and Some Literature of Finite Elements

In brief, finite elements are piecewise functions with certain global continuity imposed by local degrees of freedom (DOFs). The finite element method (FEM) approximates the solutions of differential equations by these piecewise functions. The FEM has been widely used for numerically solving partial differential equations (PDEs) in a variety of engineering disciplines, e.g., heat transfer, electromagnetism, and fluid dynamics. The history of the FEM can be traced back to early 1940s when Courant [26] proposed the idea of the minimization of a functional by linear approximation over a set of subdomains. A literature survey of some earlier years of FEMs can be found in Babuska's article "Courant element: before and after" in the book [42].

The following definition of a finite element was first introduced by Ciarlet in his lecture notes and became popular after his 1978 book [23].

Definition 1.1.1 (Finite element [23])**.** *A finite element is defined by a triple* (K, P, L)*, where*

- *the domain* K *is a bounded, closed subset of* $\mathbb{R}^d$ *(for* $d = 1, 2, 3, \ldots$*) with nonempty interior and piecewise smooth boundary;*
- *the space* $P = P(K)$ *is a finite dimensional function space on* K *of dimension* n*;*
- *the set of DOFs* $L = \{\ell_1, \ell_2, \ldots, \ell_n\}$ *is a basis for the dual space* P'*, that is, the space of bounded linear functionals on* P*.*

The domain K is called the element domain. It might be a triangle, a rectangle, or a general polygon in two space dimensions (2D), or a tetrahedron, a cube, a prism, etc. in three space dimensions (3D). In FEM, we partition the domain of the problem into a set of element domains, which is known as the finite element mesh. We obtain approximation by refining the mesh. The space P is local function space with approximation property. It is known as the space of shape functions. A popular choice of P is polynomial spaces. The set of DOFs can determine the basis functions of P uniquely. It connects the local function spaces on different element domains to become a global finite element space. By different choices of the DOFs, we can impose different continuity to the global finite element space.

1.2 The Development of Scalar and Vector Finite Elements

According to the dimension of finite element function, the finite elements can be classified into scalar finite elements, vector finite elements, and tensor finite elements.

The scalar finite elements are actually polynomial splines. They may have extra orders of smoothness on lower-dimensional simplices of the mesh, which is known as supersmoothness suggested by Sorokina [60]. This is a trouble of constructing finite elements with high regularity, e.g., the C^1 element (or H^2-conforming element). The study of C^1 element can be dated back to 1960s, when Argyris et al [5] constructed a triangular element, which has 21 DOFs. Bell [15] simplified the Argyris element by removing the three edge DOFs. In 3D, Ženíšek [65] constructed the first C^1 element and later Shangyou Zhang [70] simplified his element and extended it to an arbitrary order. All these elements involve supersmoothness at vertices and/or edges of the meshes, which leads to a large number of DOFs. A way to mitigate this issue is to construct C^1 elements on a split of a given simplex. The Clough-Tocher element [24] and the Hsieh-Clough-Tocher element (the three edge DOFs are removed) [22] are defined on a split of a triangle, which is obtained by connecting each vertex of the triangle to its barycenter. Even if the two elements involve no supersmoothness at vertices of the mesh, they are C^2 at the barycenter, which is first observed by Farin [29]. Alfeld [1] constructed the 3D counterpart of the Clough-Tocher element, which still involves supersmoothness at vertices of the mesh. There are also some conforming elements defined on other splits, see, e.g., [31, 32, 55, 64, 43].

One application of vector finite elements is computational electromagnetics, where the Sobolev spaces $H(\mathrm{div})$ and $H(\mathrm{curl})$ play a vital role in the variational theory. In [51], by using incomplete polynomial spaces, Nédélec proposed two families of finite elements: one is $H(\mathrm{div})$-conforming, the other is $H(\mathrm{curl})$-conforming. These elements are known as Nédélec curl-conforming elements and div-conforming elements of the first kind. The div-conforming elements are also referred to as Raviart-Thomas elements since they are the 3D extension of the elements introduced in [56] by Raviart and Thomas. Later in [52], Nédélec proposed two more families of elements by using complete polynomial spaces, which are known as the Nédélec elements of the second kind. The div-conforming elements therein are the 3D extension of the elements [17] introduced by Brezzi, Douglas, and Marini, and hence are also referred to as Brezzi-Douglas-Marini elements. The tetrahedral elements of the two kinds and the cubical elements of the first kind can be unified as discrete differential forms and fit into discrete complexes [37, 10], which are subcomplexes of the de Rham complex:

$$0 \longrightarrow \mathbb{R} \xrightarrow{\subset} H^1 \xrightarrow{\mathrm{grad}} H(\mathrm{curl}) \xrightarrow{\mathrm{curl}} H(\mathrm{div}) \xrightarrow{\mathrm{div}} L^2 \longrightarrow 0. \tag{1.2.1}$$

Here we dropped the domain Ω in the notation of the function spaces. See Section 2.1.4 for the precise definition of the spaces $H(D;\Omega)$. In [8], Arnold and Awanou developed a new family of discrete differential forms on cubical meshes. The discrete 0-forms are the serendipity finite elements. A periodic table of finite elements [13] has been developed to include the discrete k-forms of arbitrary polynomial degree for simplices and n-dimensional boxes in any dimension. The discrete differential forms together with mixed formulations that respect the underlying cohomological structures of the complex provide a remedy for notorious trouble of spurious solutions [6]. It is also worth mentioning that the lowest-order discrete differential forms on tetrahedra, also known as Whitney forms [63], are highly geometric: the Whitney k-forms have one DOF on each k-dimensional subsimplex, as shown in the following figure.

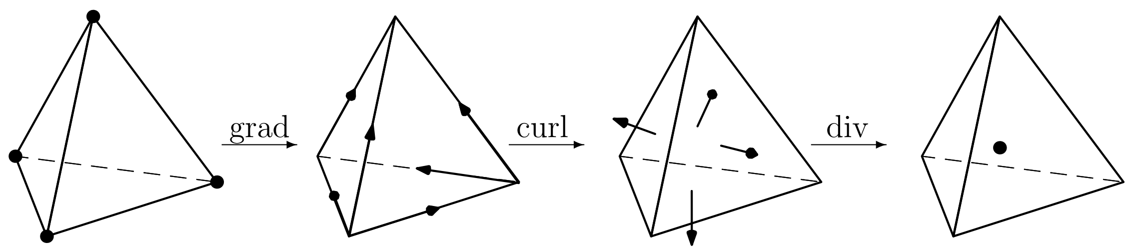

Another application of vector finite elements is incompressible flows. A related complex is the following de Rham complex with enhanced smoothness (also referred to as the Stokes complex):

$$0 \longrightarrow \mathbb{R} \xrightarrow{\subset} H^2 \xrightarrow{\text{grad}} H^1(\text{curl}) \xrightarrow{\text{curl}} H^1 \otimes \mathbb{V} \xrightarrow{\text{div}} L^2 \longrightarrow 0, \tag{1.2.2}$$

where $H^1(\text{curl}) = \{\boldsymbol{u} \in H^1 \otimes \mathbb{V} : \text{curl}\, \boldsymbol{u} \in H^1 \otimes \mathbb{V}\}$. Three desirable properties of a finite element Stokes pair $\boldsymbol{X}_{h,0} \times Y_{h,0}$ are:

- conformity, i.e., $\boldsymbol{X}_{h,0} \subset H_0^1 \otimes \mathbb{V}$ and $Y_{h,0} \subset L_0^2$;
- stability, i.e., the Ladyzenskaja-Babuska-Brezzi (LBB) condition
$$\sup_{\boldsymbol{v} \in \boldsymbol{X}_{h,0} \setminus \{0\}} \frac{\int_\Omega \text{div}\, \boldsymbol{v} q \mathrm{d}x}{\|\boldsymbol{v}\|_{H^1(\Omega)}} \geq C \|q\|_{L^2(\Omega)} \quad \forall q \in Y_{h,0}$$
is satisfied with C independent of h;
- divergence-free velocity approximation [41], i.e., $\text{div}\, \boldsymbol{X}_{h,0} \subset Y_{h,0}$.

However, constructing a finite element velocity-pressure pair that satisfies the three properties is a challenging task drawing decades of attention. In 2D, the Scott-Vogelius finite elements are stable only in the high-order case with certain restrictions on the mesh [58], while the stability in 3D is still an open problem. Motivated by the construction of a stable Stokes pair on general shape-regular triangular meshs [28], Neilan [53] constructed a finite element subcomplex of (1.2.2) on tetrahedral meshes, which includes a stable Stokes pair. Since this construction involves supersmoothness, the number of DOFs is large. In another direction, to fix the stability issue, we may use barycentric refined meshes (see, e.g., [34, 69]) or enrich finite element spaces on general shape-regular meshes by rational bubbles or macro-element bubbles [33, 34].

From the two applications, we can see the construction of vector finite elements is more delicate: they should reproduce some essential structures of the continuous problems.

1.3 Main Work of the Dissertation

The above-mentioned vector finite elements are for low-order differential equations. In this dissertation, we consider the construction of the vector elements for the high-order differential equations which involve the operator $(D^* \circ D)^* \circ (D^* \circ D)$ with $D = \mathrm{curl}$ or div. The fourth-order operators have many science and engineering applications. The operator $(\mathrm{curl}\,\mathrm{curl})^2$ (when $D = \mathrm{curl}$) is applied in inverse electromagnetic scattering theory [18, 50] and magnetohydrodynamics [19]. A variant of $(\mathrm{curl}\,\mathrm{curl})^2$, the operator $-\mathrm{curl}\,\Delta\,\mathrm{curl}$, appears in models of continuum mechanics to incorporate size effects or the coupled stress, see [48, (3.27)], [54, (35)]. The operator $\mathrm{grad}\,\Delta\,\mathrm{div}$ (when $D = \mathrm{div}$) has important applications in linear elasticity [3, 46, 47], where the integration of $\mathrm{grad}\,\Delta\,\mathrm{div}\,\boldsymbol{u}$ represents the shear strain energy with $\boldsymbol{u}$ being the displacement of the elasticity body.

The vector finite elements for the two fourth-order operators are grad curl-conforming elements (curl curl-conforming elements are automatically grad curl-conforming) and grad div-conforming elements, respectively. It bears the both difficulties—high regularity and delicate structures—to construct the grad curl- and grad div-conforming elements. The grad curl-conforming elements are not available until very recently. In [66], the author and her collaborators developed, for the first time, a family of grad rot-conforming

(2D version of curl is rot) finite elements in 2D. To reduce the number of DOFs, they used incomplete polynomials. The polynomial degree k starts from 4 for triangular elements and 3 for rectangular elements, respectively, and the lowest-order elements of both shapes have 24 DOFs. With a rotation, the grad rot-conforming elements can yield grad div-conforming elements. In 3D, there are still no available grad curl- or grad div-conforming elements.

In a broader sense, the existing H^2-conforming elements are both grad curl-conforming and grad div-conforming. In addition, Neilan [53] constructed an $H^1(\text{curl})$-conforming finite element space on tetrahedral meshes, which is the the 3D extension of the $H^1(\text{rot})$-conforming element space in [28]. However, it is still not clear whether we can use these elements to solve the fourth-order problems. In computational electromagnetics, the formulations and elements that violate the delicate structure of the continuous problems might lead to spurious solutions [6]. Will we suffer from the same issue as in computational electromagnetics? If so, when? To answer the questions, we consider the Hodge Laplacian problems of the 2D grad rot complex:

$$0 \longrightarrow H^1 \xrightarrow{\text{grad}} H(\text{grad}\,\text{rot}) \xrightarrow{\text{grad}\,\text{rot}} H(\text{rot}) \xrightarrow{\text{rot}} L^2 \longrightarrow 0. \tag{1.3.1}$$

We apply the grad rot-conforming element [66], the $H^1(\text{rot})$-conforming element [28], and the Argyris element [5] to the primal and/or mixed formulations of the Hodge Laplacian. We observe that the primal formulations with the $H^1(\text{rot})$-conforming element and the H^2-conforming element will produce spurious solutions in certain cases, while the mixed formulations with finite elements that fit into complexes would not. Therefore, in this dissertation, we will design some grad curl-conforming elements and grad div-conforming elements both in 2D and 3D by constructing discrete complexes.

The discrete de Rham complex is now an important tool for the construction of finite elements and analysis of numerical schemes [6, 11, 10, 36, 20]. Motivated by problems in fluid and solid mechanics, there is an increased interest in constructing finite element de Rham complexes with enhanced smoothness [21, 62, 28]. In this dissertation, we will consider several variants of the de Rham complex and construct discrete subcomplexes for them. The discrete complex offers several useful tools, which includes the dimension count and the Poincaré operators. The dimension count motivate us to use bubbles. The Poincaré operators enable us to tailor the shape function spaces to our needs (not necessarily the existing incomplete polynomial spaces which were used before). Therefore, some of our new finite elements will have no restrictions on polynomial degrees like the previous construction. From the complex perspective, we can also fit the $\operatorname{curl}\Delta\operatorname{curl}$, $(\operatorname{curl}\operatorname{curl})^2$, and $\operatorname{grad}\Delta\operatorname{div}$ problems and their finite element approximations in the framework of the finite element exterior calculus (FEEC) [6, 10]. Thus a number of tools from FEEC can be used for the numerical analysis.

The content of this dissertation is based on the results reported in [40, 67, 39, 68] and some new results which have not yet been reported.

1.4 Outline of the Dissertation

The dissertation is organized as follows:

In Chapter 2, we introduce some basic notions of differential complexes and Bernstein-Gelfand-Gelfand (BGG) construction.

In Chapter 3, we introduce the grad curl, grad rot, and grad div complexes derived by the BGG construction. Applying the theoretical framework in [12], we obtain the cohomology of the three complexes. Moreover, we define bounded and surjective trace operators for $H(\operatorname{grad}\operatorname{rot};\Omega)$ and $H(\operatorname{grad}\operatorname{div};\Omega)$, and a bounded trace operator for $H(\operatorname{grad}\operatorname{curl};\Omega)$. We also prove the density of $C^\infty(\overline{\Omega})\otimes\mathbb{V}$ in $H(\operatorname{grad}\operatorname{curl};\Omega)$, $H(\operatorname{grad}\operatorname{rot};\Omega)$, and $H(\operatorname{grad}\operatorname{div};\Omega)$. As a result, we characterize the boundary conditions for all the Hodge Laplacian problems of the grad rot and grad div complexes and one Hodge Laplacian problem of the grad curl complex.

In Chapter 4, we investigate the spurious solutions of the $\operatorname{curl}\Delta\operatorname{rot}$ problems. We consider two Hodge Laplacian problems of the 2D grad rot-complex. We apply different formulations and finite elements to solve the Hodge Laplacian source or eigenvalue problems. We find that the mixed formulations with finite elements that fit into complexes leads to correct solutions, while other combinations may produce spurious solutions. We provide a convergence analysis for both the source and the eigenvalue problems on simply-connected domains. We also provide a theoretical explanation for the numerical phenomena.

In Chapter 5, to construct 2D grad rot-conforming elements, we consider the following variant of the de Rham complex:

$$0 \longrightarrow \mathbb{R} \xrightarrow{\subset} H^1 \xrightarrow{\operatorname{grad}} H(\operatorname{grad}\operatorname{rot}) \xrightarrow{\operatorname{rot}} H^1 \longrightarrow 0. \tag{1.4.1}$$

We consider the space $H(\operatorname{grad}\operatorname{rot})$ instead of $H(\operatorname{curl}\operatorname{rot})$ because $H(\operatorname{grad}\operatorname{curl})$ fits into the complex (1.4.1) naturally. In particular, as we have mentioned earlier, any curl rot-conforming finite element (or curl curl-conforming in 3D) is automatically grad rot-conforming (or grad curl-conforming). Therefore, we will focus on the construction of grad rot-conforming (grad curl-conforming) finite elements in the following. The new finite elements fit into a subcomplex of (1.4.1):

$$0 \longrightarrow \mathbb{R} \xrightarrow{\subset} \Sigma_h \xrightarrow{\operatorname{grad}} V_h \xrightarrow{\operatorname{curl}} \Sigma_h^+ \longrightarrow 0. \tag{1.4.2}$$

In (1.4.2), we choose Lagrange finite element spaces for Σ_h and Lagrange elements enriched with an interior bubble on each element for Σ_h^+. The space $V_h \subset H(\operatorname{grad}\operatorname{rot})$ is thus obtained as the gradient of Σ_h plus a complementary part, the Poincaré operator acting on Σ_h^+. Among the three versions of V_h which we will construct in this dissertation, one of them is consistent with the previous construction [66]. Here we extend it by removing the restriction of the polynomial degree. The simplest elements have only 6 DOFs for a triangle and 8 DOFs for a rectangle. To the best of our knowledge, these elements have the smallest number of DOFs among all the existing grad rot-conforming finite elements.

In Chapter 6 and Chapter 7, to construct 3D grad curl-conforming elements, we consider the following complex:

$$0 \longrightarrow \mathbb{R} \xrightarrow{\subset} H^1 \xrightarrow{\text{grad}} H(\text{grad curl}) \xrightarrow{\text{curl}} H^1 \otimes \mathbb{V} \xrightarrow{\text{div}} L^2 \longrightarrow 0, \qquad (1.4.3)$$

Here, the first two spaces are less smoother than those in (1.2.2), whereas the last two spaces stay the same. This complex is also referred to as the Stokes complex. The complex (1.4.3) relates the construction of the grad curl-conforming elements to the incompressible flows.

Chapter 6 is devoted to constructing the first grad curl-conforming element in 3D. In [53], Neilan constructed a subcomplex for the different Stokes complex (1.2.2), which contains a stable Stokes pair. In this chapter, we apply Poincaré operators and the Stokes pair in [53] to construct a finite element subcomplex of (1.4.3):

$$0 \longrightarrow \mathbb{R} \xrightarrow{\subset} \Sigma_h \xrightarrow{\text{grad}} V_h \xrightarrow{\text{curl}} Z_h \xrightarrow{\text{div}} W_h \longrightarrow 0. \qquad (1.4.4)$$

By changing the polynomial degree of Σ_h, this complex leads to three families of grad curl-conforming elements. Since the construction involves supersmoothness, the number of DOFs is large and the lowest-order element has 279 DOFs.

Chapter 7 is devoted to developing a new finite element subcomplex of (1.4.3) with fewer DOFs:

$$0 \longrightarrow \mathbb{R} \xrightarrow{\subset} \Sigma_h \xrightarrow{\text{grad}} V_h \xrightarrow{\text{curl}} \boldsymbol{\Sigma}_h^+ \xrightarrow{\text{div}} W_h \longrightarrow 0. \qquad (1.4.5)$$

Recently, Guzmán and Neilan [34] enriched the first-order vector-valued Lagrange finite element space with modified Bernardi-Raugel bubbles and constructed a stable Stokes pair. This construction is somewhere between the classic finite elements and the finite elements defined on splits. It does not involve a large number of DOFs or an extensive use of macroelement structures. Therefore, it is a good candidate for $\boldsymbol{\Sigma}_h^+$-W_h. However, the extension to high-order cases is still not available yet. Our construction in this chapter starts by extending Guzmán and Neilan's result in [34] to high-order cases, which is realized by enriching the vector-valued Lagrange finite elements with the modified Bernardi-Raugel bubbles and/or suitable interior bubbles. Then we will apply Poincaré operator and construct a new finite element subcomplex of (1.4.3). The restriction of the new subcomplex to each face coincides with the sequences in 2D construction. In the lowest order case, the spaces in (1.4.5) have 4, 18, 16, and 1 DOFs on each element, respectively. The DOFs are those of the Whitney forms plus vertex evaluation for the 1- and 2-forms (V_h and $\boldsymbol{\Sigma}_h^+$).

In Chapter 8, to construct grad div-conforming elements, we consider the complex

$$0 \longrightarrow \mathbb{R} \xrightarrow{\subset} H^1 \xrightarrow{\text{grad}} H(\text{curl}) \xrightarrow{\text{curl}} H(\text{grad div}) \xrightarrow{\text{div}} H^1 \longrightarrow 0. \tag{1.4.6}$$

The 2D version of the complex (1.4.6) is

$$0 \longrightarrow \mathbb{R} \xrightarrow{\subset} H^1 \xrightarrow{\text{curl}} H(\text{grad div}) \xrightarrow{\text{div}} H^1 \longrightarrow 0. \tag{1.4.7}$$

If we rotate the complex (1.4.7) by $\frac{\pi}{2}$, we will get the complex (1.4.1). Therefore we will focus only on the complex (1.4.6) to construct 3D grad div-conforming elements. Our new finite elements fit into a subcomplex of (1.4.6):

$$0 \longrightarrow \mathbb{R} \xrightarrow{\subset} \Sigma_h \xrightarrow{\text{grad}} V_h \xrightarrow{\text{curl}} W_h \xrightarrow{\text{div}} \Sigma_h^+ \longrightarrow 0, \tag{1.4.8}$$

A starting point is to take Σ_h as the Lagrange finite element spaces. This leads to a natural choice of V_h, which is the Nédélec elements of the first kind. In addition, we choose Lagrange elements enriched with an interior bubble for Σ_h^+. The space $W_h \subset H(\text{grad div})$ is hence obtained as the curl of V_h plus a complementary part, the Poincaré operator acting on Σ_h^+. Different orders of Σ_h can yield different versions of W_h. Among the three versions of W_h which we will construct in this dissertation, the simplest element has only

8 DOFs for a tetrahedron and 14 DOFs for a cube.

In Chapter 9, we summarize our work and provide some promising future directions.

1.5 General Notation

In this section, we recall some basic notation about domains, differential operators, function spaces, and meshes. Throughout the paper, we use C to denote a generic positive h-independent constant.

1.5.1 Domain

Unless otherwise specified, throughout the paper we assume that $\Omega \in \mathbb{R}^d$, $d = 2, 3$ is a bounded Lipschitz domain. A domain $\Omega \in \mathbb{R}^d$ is called a *Lipschitz domain* if its boundary $\partial\Omega$ is locally a graph of a Lipschitz continuous function, i.e., for all $\boldsymbol{x} \in \partial\Omega$, there exists a neighborhood $N(\boldsymbol{x}, r)$ of $\boldsymbol{x}$ and a Lipschitz continuous function $\phi : \mathbb{R}^{d-1} \to \mathbb{R}$ such that

$$\partial\Omega \cap N(\boldsymbol{x}, r) = \{\boldsymbol{y} = (y_1, y_2, \cdots, y_d) : \phi(y_1, y_2, \cdots, y_{d-1}) = y_d\}$$

and

$$\Omega \cap N(\boldsymbol{x}, r) = \{\boldsymbol{y} = (y_1, y_2, \cdots, y_d) : \phi(y_1, y_2, \cdots, y_{d-1}) < y_d\}$$

under a proper local coordinate system.

We say a domain has $C^{1,1}$ boundary if $\partial\Omega$ is locally a graph of a Lipschitz continuous function with Lipschitz continuous derivative.

We define the following *Betti numbers* for the domain Ω:

- the zeroth Betti number b_0 is the number of connected components of the domain;
- the first Betti number b_1 is the number of holes through the domain;
- the second Betti number b_2 is 0 for any bounded in 2D, and it is the number of voids enclosed by the domain in 3D;
- the third Betti number b_3 is 0 for any domain in 2D and 3D.

For simply-connected domain, the first Betti number $b_1 = 0$. The domain Ω is *contractable* if it is homomorphic to a closed unit ball or all the Betti numbers are 0.

For $U \subseteq \Omega$, denote by $\boldsymbol{n}_{\partial U}$ (resp. $\boldsymbol{\tau}_{\partial U}$) the unit outward normal vector (resp. the unit tangential vector) to the boundary ∂U. When $U = \Omega$, we drop the subscript $\partial\Omega$.

1.5.2 Sobolev spaces

We adopt conventional notations for Sobolev spaces. For any sub-domain $U \subset \Omega$ and any integer $1 \leq p < \infty$, the space of functions which are pth-power Lebesgue integrable on U is denoted by

$$L^p(U) = \left\{ v : \int_U |v|^p \mathrm{d}V < \infty \right\},$$

which is equipped with the norm

$$\|v\|_{p,U} = \left(\int_U |v|^p \mathrm{d}V \right)^{1/2}.$$

When $p = 2$, we drop the subscript 2 in $\|v\|_{2,U}$ and equip the space $L^2(U)$ with the following inner product

$$(u, v)_U = \int_U uv \mathrm{d}V.$$

When $U = \Omega$, we drop the subscript U in $\|v\|_{p,U}$ and $(u, v)_U$. We denote by $L_0^2(U)$ the space of L^2 functions with vanishing mean:

$$L_0^2(U) = \left\{ v \in L^2(U) : \int_U v \mathrm{d}V = 0 \right\},$$

Let m be a non-negative integer, then the Sobolev space $H^m(U)$ is defined by

$$H^m(U) = \left\{ v \in L^2(U) : D^\alpha v \in L^2(U) \text{ for all } \alpha \text{ with } |\alpha| \leq m \right\}.$$

This space is equipped with the norm

$$\|v\|_{m,U} = \left(\sum_{|\alpha| \leq k} \|D^\alpha v\|_U \right)^{1/2}$$

and the semi-norm

$$|v|_{m,U} = \left(\sum_{|\alpha|=k} \|D^\alpha v\|_U \right)^{1/2}.$$

We denote by $H_0^m(U)$ the space of $H^m(U)$ functions with trivial trace. In the case of $m = 0$, the space $H^0(U)$ and $H_0^0(U)$ coincide with $L^2(U)$ and $L_0^2(U)$.

When $m = k + \sigma$ with an integer $k \geq 0$ and a real number $\sigma \in (0, 1)$,

$$H^m(U) = \left\{ v \in H^k(U) : D^\alpha v \in H^\sigma(U) \text{ for all } \alpha \text{ with } |\alpha| \leq k \right\},$$

where

$$H^\sigma(U) = \left\{ v \in L^2(U) : \int_U \int_U \frac{|v(x) - v(y)|^2}{|x - y|^{d+2\sigma}} \mathrm{d}x \mathrm{d}y < \infty \right\}.$$

In this case, the space $H^m(U)$ is equipped with the norm

$$\|v\|_{m,U} = \left(\sum_{|\alpha|\leq k} \|D^\alpha v\|_{\sigma,U} \right)^{1/2}$$

and the semi-norm

$$|v|_{m,U} = \left(\sum_{|\alpha|=k} \|D^\alpha v\|_{\sigma,U} \right)^{1/2},$$

where $\|v\|_{\sigma,U}^2 = \|v\|_U^2 + \int_U \int_U \frac{|v(x)-v(y)|^2}{|x-y|^{d+2\sigma}} \mathrm{d}x \mathrm{d}y$.

For $0 \leq k \leq \infty$, we define $C^k(\overline{U})$ and $C^k(U)$ to be the spaces of functions with k-th order continuous derivatives on $\overline{U}$ and U, respectively. We also define $C_0^\infty(U)$ to be the space of infinitely differentiable functions with compact support on U.

Let $\mathbb{V}$ and $\mathbb{M}$ stand for the spaces of vectors and matrices, respectively. For a function space H, we use $H \otimes \mathbb{V}$ (resp. $H \otimes \mathbb{M}$) to denote the vector-valued (resp. matrix-valued) function spaces.

1.5.3 Meshes and Polynomial Spaces

For a Lipschitz polygon or polyhedron, let $\mathcal{T}_h = \{K\}$ be a finite element mesh consisting of triangles or parallelograms in 2D or tetrahedra in 3D. For each element

$K \in \mathcal{T}_h$, we denote by h_K the diameter of K and ρ_K the diameter of the largest circle or ball contained in $\overline{K}$. Let $h = \max_{K\in\mathcal{T}_h} h_K$ be the mesh size of $\mathcal{T}_h$. We assume the mesh is regular, i.e., there is a constant $\sigma_0 > 0$ such that

$$\frac{h_K}{\rho_K} \geq \sigma_0, \text{ for all } K \in \mathcal{T}_h.$$

Let $\mathcal{V}_h$, $\mathcal{E}_h$, and $\mathcal{F}_h$ be the sets of vertices, edges, and faces in $\mathcal{T}_h$. Also let $\mathcal{V}_h(K)$, $\mathcal{E}_h(K)$, and $\mathcal{F}_h(K)$ be the set of vertices, edges, and faces in the element K.

In 2D, we define a reference triangle to be the triangle with vertices $(0,0)$, $(1,0)$, and $(0,1)$, and a reference rectangle to be the rectangle $(-1,1)\times(-1,1)$. In 3D, a reference tetrahedron is the tetrahedron with vertices $(0,0,0)$, $(1,0,0)$, $(0,1,0)$, and $(0,0,1)$, and a reference cube is the cube $(-1,1)\times(-1,1)\times(-1,1)$. Each element $K \in \mathcal{T}_h$ can be obtained by mapping the reference element $\hat{K}$ using the following affine mapping:

$$F_K(\hat{\boldsymbol{x}}) = B_K\hat{\boldsymbol{x}} + \boldsymbol{b}_K. \tag{1.5.1}$$

With the affine mapping,

$$\boldsymbol{n}_i \circ F_K = \frac{B_K^{-\mathrm{T}}\hat{\boldsymbol{n}}_i}{|B_K^{-\mathrm{T}}\hat{\boldsymbol{n}}_i|}, \tag{1.5.2}$$

$$\boldsymbol{\tau}_i \circ F_K = \frac{B_K\hat{\boldsymbol{\tau}}_i}{|B_K\hat{\boldsymbol{\tau}}_i|}, \tag{1.5.3}$$

where $\boldsymbol{n}_i$ and $\hat{\boldsymbol{n}}_i$ are the unit normal vectors to $f_i \in \mathcal{F}_h(K)$ and $\hat{f}_i \in \mathcal{F}_h(\hat{K})$ (or $e_i \in \mathcal{E}_h(K)$ and $\hat{e}_i \in \mathcal{E}_h(\hat{K})$ in 2D), and $\boldsymbol{\tau}_i$ and $\hat{\boldsymbol{\tau}}_i$ are the unit tangential vectors to $e_i \in \mathcal{E}_h(K)$ and $\hat{e}_i \in \mathcal{E}_h(\hat{K})$. We denote a variable on $\hat{K}$ by putting a hat notation above it. For an operator T, we use $T_{\hat{\boldsymbol{x}}}$ to denote the operator is with respect to $\hat{\boldsymbol{x}}$.

We use P_k to denote the space of polynomials with degree at most k, and use $\widetilde{P}_k$ to denote the space of homogeneous polynomials with degree k. We denote by $Q_{i,j,k}$ the space of polynomials with the degrees of the variables $x_1,\ x_2,\ x_3$ no more than $i,\ j,\ k$. Correspondingly, we have $Q_{i,j}$ in 2D. For simplicity, we drop the subscripts i, j when $i = j = k$ in 3D and drop the subscript i when $i = j$ in 2D. Denote $\boldsymbol{P}_k = P_k \otimes \mathbb{V}$ and

$\widetilde{\boldsymbol{P}}_k = \widetilde{P}_k \otimes \mathbb{V}$. We define

$$\mathcal{R}_k = \boldsymbol{P}_{k-1} \oplus \{\boldsymbol{p} \in \widetilde{\boldsymbol{P}}_k : \boldsymbol{x} \cdot \boldsymbol{p} = 0\}. \tag{1.5.4}$$

CHAPTER 2 DIFFERENTIAL COMPLEXES AND THE BERNSTEIN-GELFAND-GELFAND CONSTRUCTION

In this chapter, we introduce some basic notions of differential complexes and BGG construction, which will be used in the subsequent chapters.

2.1 Differential Complexes

2.1.1 Homological Algebra

Given vector spaces V^k, $k = 0, 1, \cdots, n$, and operators $d^k : V^k \to V^{k+1}$, $k = 0, 1, \cdots, n-1$, a *complex* or a *cochain complex* is a sequence

$$0 \longrightarrow V^0 \xrightarrow{d^0} \cdots \xrightarrow{d^{k-1}} V^k \xrightarrow{d^k} V^{k+1} \xrightarrow{d^{k+1}} \cdots \xrightarrow{d^{n-1}} V^n \longrightarrow 0 \qquad (2.1.1)$$

such that $d^{k+1}d^k = 0$, $k = 0, 1, \cdots, n-2$. If d^k, $k = 0, 1, \cdots, n-1$, are differential operators, then the sequence (2.1.1) is called a differential complex.

The complex (2.1.1) gives rise to three spaces at each level k:

- the cocycle space $\mathfrak{Z}^k$: the null space of the operator d^k;
- the coboundary space $\mathfrak{B}^k$: the range space of the operator d^{k-1};
- the cohomology space $\mathcal{H}^k = \mathfrak{Z}^k/\mathfrak{B}^k$;

Due to the complex property $d^k d^{k-1} = 0$, we have $\mathfrak{B}^k \subset \mathfrak{Z}^k$ for each $1 \leq k \leq n-1$. Furthermore, if $\mathfrak{Z}^k = \mathfrak{B}^k$, we say that the complex (2.1.1) is exact at V^k. At the two ends of the sequence, the complex is exact at V^0 if d^0 is injective (with trivial kernel), and is exact at V^n if d^{n-1} is surjective (with trivial cokernel). The complex (2.1.1) is called exact if it is exact at all the spaces V^k, $k = 0, 1, \cdots, n$.

If each space in (2.1.1) has finite dimensions, then a necessary (but not sufficient) condition for the exactness of (2.1.1) is the following dimension condition:

$$\sum_{k=0}^{n} (-1)^k \dim(V^k) = 0.$$

The dimension condition is sufficient if the complex is exact at each level k but i for some $0 \le i \le n$.

2.1.2 Hilbert Complexes

A *Hilbert complex* is a sequence of Hilbert spaces W^k, $k = 0, 1, \cdots, n$, and a sequence of closed densely defined unbounded linear operators $d^k : W^k \to W^{k+1}$, $k = 0, 1, \cdots, n-1$,

$$0 \longrightarrow W^0 \xrightarrow{d^0} \cdots \xrightarrow{d^{k-1}} W^k \xrightarrow{d^k} W^{k+1} \xrightarrow{d^{k+1}} \cdots \xrightarrow{d^{n-1}} W^n \longrightarrow 0 \quad (2.1.2)$$

such that $d^{k+1}d^k = 0$.

Denote $V^k := \mathcal{D}(d^k)$. The operators d^k can be viewed as bounded operators from V^k to V^{k+1}. We equip V^k with the inner product

$$(u, v)_{V^k} := (u, v)_{W^k} + (d^k u, d^k v)_{W^{k+1}}.$$

Suppose $d^k V^k \subset V^{k+1}$. The complex

$$0 \longrightarrow V^0 \xrightarrow{d^0} \cdots \xrightarrow{d^{k-1}} V^k \xrightarrow{d^k} V^{k+1} \xrightarrow{d^{k+1}} \cdots \xrightarrow{d^{n-1}} V^n \longrightarrow 0 \quad (2.1.3)$$

is called the *domain complex*.

We now recall the definition of the adjoint operator. Let X, Y be Hilbert spaces with inner products $(\cdot, \cdot)_X$ and $(\cdot, \cdot)_Y$. Let $T : X \to Y$ be an unbounded operator with domain $\mathcal{D}(T) \subset X$. We assume $\mathcal{D}(T)$ is dense in X. Then we define an unbounded linear operator $T^* : Y \to X$, and define

$$\mathcal{D}(T^*) = \{y \in Y : \text{ there exists } z \in X \ s.t. \ (Tx, y)_Y = (x, z)_X, \ \forall x \in \mathcal{D}(T) \subset X\}.$$

When $y \in \mathcal{D}(T^*)$ and $(Tx, y)_Y = (x, z)_X, \ \forall x \in \mathcal{D}(T)$, we define

$$T^* y := z.$$

Denote by $\delta^{k+1} : W^{k+1} \to W^k$ the adjoint operator of d^k. If $u \in \mathcal{D}(\delta^{k+1})$, we have

$$(\delta^k \delta^{k+1} u, w) = (\delta^{k+1} u, d^{k-1} w) = (u, d^k d^{k-1} w) = 0,$$

and hence $\delta^k\delta^{k+1}u = 0$. Thus, the sequence

$$0 \longleftarrow W^0 \xleftarrow{\delta^1} \cdots \xleftarrow{\delta^k} W^k \xleftarrow{\delta^{k+1}} W^{k+1} \xleftarrow{\delta^{k+2}} \cdots \xleftarrow{\delta^n} W^n \longleftarrow 0 \quad (2.1.4)$$

is also a Hilbert complex with domain complex

$$0 \longleftarrow U^0 \xleftarrow{\delta^1} \cdots \xleftarrow{\delta^k} U^k \xleftarrow{\delta^{k+1}} U^{k+1} \xleftarrow{\delta^{k+2}} \cdots \xleftarrow{\delta^n} U^n \longleftarrow 0. \quad (2.1.5)$$

Here $U^k := \mathcal{D}(\delta^{k+1})$.

2.1.3 Hodge Decomposition

Define the k-coboundary

$$\mathfrak{B}^k := d^{k-1}V^{k-1},$$

and the k-cocycle

$$\mathfrak{Z}^k := \{u \in V^k : d^k u = 0\}.$$

From the definition of the complex, we have $\mathfrak{B}^k \subset \mathfrak{Z}^k$. We also define

$$\mathfrak{B}^*_k := \delta^{k+1}U^{k+1} \text{ and } \mathfrak{Z}^*_k := \{u \in U^k : \delta^k u = 0\}.$$

In the following, we assume $\mathfrak{B}_k$ and $\mathfrak{B}^*_k$, $k = 0, 1, \cdots, n$, are closed.

We have the following decomposition

$$W^k = \mathfrak{Z}^k \oplus \mathfrak{Z}^{k,\perp}.$$

Define the space of harmonic k-forms

$$\mathfrak{H}^k = \mathfrak{Z}^k \cap \mathfrak{Z}^*_k.$$

For a closed Hilbert space, we have

$$\mathfrak{H}^k \cong \mathcal{H}^k.$$

It holds the following Hodge decomposition:

$$W^k = \mathfrak{B}^k \oplus (\mathfrak{B}^{k,\perp} \cap \mathfrak{Z}^k) \oplus \mathfrak{Z}^{k,\perp}$$

$$= \mathfrak{B}^k \oplus (\mathfrak{Z}_k^* \cap \mathfrak{Z}^k) \oplus \mathfrak{Z}^{k,\perp}$$
$$= \mathfrak{B}^k \oplus \mathfrak{H}^k \oplus \mathfrak{Z}^{k,\perp}.$$

Since we assume $\mathfrak{B}_k^*$ is closed, we have, by the definition of the adjoint operator,

$$\mathfrak{Z}^{k,\perp} = \mathfrak{B}_k^*.$$

Therefore,

$$W^k = \mathfrak{B}^k \oplus \mathfrak{H}^k \oplus \mathfrak{Z}^{k,\perp} = \mathfrak{B}^k \oplus \mathfrak{H}^k \oplus \mathfrak{B}_k^*.$$

From the domain complexes (2.1.3), we have

$$V^k = \mathfrak{B}^k \oplus \mathfrak{H}^k \oplus (\mathfrak{B}_k^* \cap V^k).$$

2.1.4 The De Rham Complex

The de Rham complex is the cochain complex of differential forms a domain in $\mathbb{R}^n$ with the exterior derivative as the differential operators. The de Rham complex of smooth differential forms is

$$\mathbb{R} \longrightarrow C^\infty\Lambda^0 \xrightarrow{d^0} C^\infty\Lambda^1 \xrightarrow{d^1} \cdots \xrightarrow{d^{n-1}} C^\infty\Lambda^n \longrightarrow 0. \tag{2.1.6}$$

The sobolev de Rham complex is

$$\mathbb{R} \longrightarrow H^q\Lambda^0 \xrightarrow{d^0} H^{q-1}\Lambda^1 \xrightarrow{d^1} \cdots \xrightarrow{d^{n-1}} H^{q-n}\Lambda^n \longrightarrow 0. \tag{2.1.7}$$

The L^2 de Rham complex is

$$\mathbb{R} \longrightarrow L^2\Lambda^0 \xrightarrow{d^0} L^2\Lambda^1 \xrightarrow{d^1} \cdots \xrightarrow{d^{n-1}} L^2\Lambda^n \longrightarrow 0. \tag{2.1.8}$$

whose domain complex without boundary conditions is

$$\mathbb{R} \longrightarrow H\Lambda^0 \xrightarrow{d^0} H\Lambda^1 \xrightarrow{d^1} \cdots \xrightarrow{d^{n-1}} H\Lambda^n \longrightarrow 0 \tag{2.1.9}$$

with $H\Lambda^k = \{u \in L^2\Lambda^k : d^k u \in L^2\Lambda^{k+1}\}$. The Sobolev de Rham complex (2.1.7) satisfies the following properties.

Theorem 2.1.1 ([25])**.** *For any real number q and on any bounded Lipschitz domain in $\mathbb{R}^n$, the dimension of the cohomology of the Sobolev de Rham complex* (2.1.7) *is finite and independent of q. Moreover, the cohomology can be represented by smooth functions, again independent of q. In other words, there exists a finite-dimensional space $\mathscr{H}_\infty^k \subset C^\infty\Lambda^k$ such that*

$$\mathcal{N}\left(d^k, H^q\Lambda^k\right) = \mathcal{R}\left(d^{k-1}, H^{q+1}\Lambda^{k-1}\right) \oplus \mathscr{H}_\infty^k, \quad k = 0, 1, \cdots, n.$$

According to [12, Theorem 1], $\mathscr{H}_\infty^k$, $k = 0, 1, \cdots, n$ are also the spaces of cohomology representatives of the complex (2.1.9), i.e.,

$$\mathcal{N}\left(d^k, H\Lambda^k\right) = \mathcal{R}\left(d^{k-1}, H\Lambda^{k-1}\right) \oplus \mathscr{H}_\infty^k, \quad k = 0, 1, \cdots, n. \tag{2.1.10}$$

Lemma 2.1.2 ([25])**.** *For the complex* (2.1.7)*, there exist $P^i : H^{q-i}\Lambda^i \to H^{q-i+1}\Lambda^{i-1}$ and $L^i : H^{q-i}\Lambda^i \to C^\infty\Lambda^i$ with finite dimensional range, for $i = 1, 2, \cdots, n$, satisfying*

$$d^{i-1}P^i + P^{i+1}d^i = \mathrm{id} - L^i, \quad i = 1, 2, \cdots, n.$$

In 3D, using vector proxies, for a scalar function u and a vector function $\boldsymbol{u} = (u_1, u_2, u_3)^{\mathrm{T}}$,

$$\begin{aligned}
&d^0 u = \operatorname{grad} u = (\partial_{x_1}u, \partial_{x_2}u, \partial_{x_3}u)^{\mathrm{T}},\\
&d^1 \boldsymbol{u} = \operatorname{curl} \boldsymbol{u} = (\partial_{x_2}u_3 - \partial_{x_3}u_2, \partial_{x_3}u_1 - \partial_{x_1}u_3, \partial_{x_1}u_2 - \partial_{x_2}u_1)^{\mathrm{T}},\\
&d^2 \boldsymbol{u} = \operatorname{div} \boldsymbol{u} = \sum_{i=1}^{3} \partial_{x_i}u_i.
\end{aligned}$$

In 2D, for a scalar function u and a vector function $\boldsymbol{u} = (u_1, u_2)^{\mathrm{T}}$,

$$d^0 u = \operatorname{grad} u = (\partial_{x_1}u, \partial_{x_2}u)^{\mathrm{T}},$$

$$d^1 \boldsymbol{u} = \operatorname{rot} u = \partial_{x_1}u_2 - \partial_{x_2}u_1,$$

or

$$d^0 u = \operatorname{curl} u = (\partial_{x_2}u, -\partial_{x_1}u)^{\mathrm{T}},$$

$$d^1\boldsymbol{u} = \operatorname{div}\boldsymbol{u} = \partial_{x_1}u_1 + \partial_{x_2}u_2.$$

We define

$$H(D;\Omega) := \{\boldsymbol{u} \in L^2(\Omega)\otimes\mathbb{V} :\ D\boldsymbol{u} \in L^2(\Omega),\ L^2(\Omega)\otimes\mathbb{V},\ \text{or}\ L^2(\Omega)\otimes\mathbb{M}.\}$$

with $D = \operatorname{div}$, curl, grad curl, or grad div in 3D and $D = \operatorname{div}$, rot, grad rot, or grad div in 2D. We furnish the the space $H(D;\Omega)$ with the inner product

$$(\boldsymbol{u},\boldsymbol{v})_{H(D;\Omega)} = (\boldsymbol{u},\boldsymbol{v}) + (D\boldsymbol{u}, D\boldsymbol{v})$$

and the norm

$$\|\boldsymbol{u}\|_{H(D;\Omega)} = \|\boldsymbol{u}\| + \|D\boldsymbol{u}\|.$$

We define

$$H_0(\operatorname{div};\Omega) := \{\boldsymbol{u} \in H(\operatorname{div};\Omega) :\ \boldsymbol{u}\cdot\boldsymbol{n} = 0\},$$

$$H_0(\operatorname{curl};\Omega) := \{\boldsymbol{u} \in H(\operatorname{curl};\Omega) :\ \boldsymbol{u}\times\boldsymbol{n} = 0\},$$

$$H_0(\operatorname{rot};\Omega) := \{\boldsymbol{u} \in H(\operatorname{rot};\Omega) :\ \boldsymbol{u}\cdot\boldsymbol{\tau} = 0\}.$$

The 2D domain complex on the domain Ω is

$$\mathbb{R} \xrightarrow{\subset} H^1(\Omega) \xrightarrow{\operatorname{curl}} H(\operatorname{div};\Omega) \xrightarrow{\operatorname{div}} L^2(\Omega) \longrightarrow 0, \tag{2.1.11}$$

or

$$\mathbb{R} \xrightarrow{\subset} H^1(\Omega) \xrightarrow{\operatorname{grad}} H(\operatorname{rot};\Omega) \xrightarrow{\operatorname{rot}} L^2(\Omega) \longrightarrow 0. \tag{2.1.12}$$

The 3D domain complex is

$$\mathbb{R} \xrightarrow{\subset} H^1(\Omega) \xrightarrow{\operatorname{grad}} H(\operatorname{curl};\Omega) \xrightarrow{\operatorname{curl}} H(\operatorname{div};\Omega) \xrightarrow{\operatorname{div}} L^2(\Omega) \longrightarrow 0. \tag{2.1.13}$$

We also have the following complexes with vanishing boundary conditions:

$$\mathbb{R} \xrightarrow{\subset} H_0^1(\Omega) \xrightarrow{\operatorname{curl}} H_0(\operatorname{div};\Omega) \xrightarrow{\operatorname{div}} L_0^2(\Omega) \longrightarrow 0, \tag{2.1.14}$$

$$\mathbb{R} \xrightarrow{\subset} H_0^1(\Omega) \xrightarrow{\text{grad}} H_0(\text{rot};\Omega) \xrightarrow{\text{rot}} L_0^2(\Omega) \longrightarrow 0, \tag{2.1.15}$$

and

$$\mathbb{R} \xrightarrow{\subset} H_0^1(\Omega) \xrightarrow{\text{grad}} H_0(\text{curl};\Omega) \xrightarrow{\text{curl}} H_0(\text{div};\Omega) \xrightarrow{\text{div}} L_0^2(\Omega) \longrightarrow 0. \tag{2.1.16}$$

Motivated by problems in fluid and solid mechanics, there is an increased interest in the de Rham complexes with enhanced smoothness. In this dissertation, to construct grad curl-conforming and grad div-conforming elements, we will consider the complexes (1.4.1), (1.4.3), and (1.4.6).

It is also worth to address the relationship between $H(\operatorname{grad}\operatorname{curl};\Omega)$ and $H(\operatorname{curl}\operatorname{curl};\Omega)$ $= \{\boldsymbol{u} \in L^2(\Omega)\otimes\mathbb{V} : \operatorname{curl}\boldsymbol{u} \in L^2(\Omega)\otimes\mathbb{V} \text{ and } \operatorname{curl}\operatorname{curl}\boldsymbol{u} \in L^2(\Omega)\otimes\mathbb{V}\}$. In 2D, we have $H(\operatorname{grad}\operatorname{rot};\Omega) = H(\operatorname{curl}\operatorname{rot};\Omega) = \{\boldsymbol{u} \in L^2(\Omega)\otimes\mathbb{V} : \operatorname{curl}\operatorname{rot}\boldsymbol{u} \in L^2(\Omega)\otimes\mathbb{V}\}$ since curl is a rotation of grad. In 3D, we have $H(\operatorname{grad}\operatorname{curl};\Omega) \subseteq H(\operatorname{curl}\operatorname{curl};\Omega)$. If Ω is convex or has $C^{1,1}$ boundary, then for any function $\boldsymbol{u} \in H(\operatorname{curl}\operatorname{curl};\Omega)$ with certain boundary conditions, e.g., $\boldsymbol{u}\times\boldsymbol{n} = 0$ on $\partial\Omega$, we have $\operatorname{curl}\boldsymbol{u} \in H^1(\Omega)\otimes\mathbb{V}$ since $\operatorname{curl}\boldsymbol{u} \in H(\operatorname{curl};\Omega)\cap H_0(\operatorname{div};\Omega) \hookrightarrow H^1(\Omega)\otimes\mathbb{V}$ [30, Theorem 3.8]. This implies that for these domains we actually have $H(\operatorname{grad}\operatorname{curl};\Omega)\cap H_0(\operatorname{curl};\Omega) = H(\operatorname{curl}\operatorname{curl};\Omega)\cap H_0(\operatorname{curl};\Omega)$. In particular, for polynomial spaces, $H(\operatorname{grad}\operatorname{curl};\Omega) = H(\operatorname{curl}\operatorname{curl};\Omega)$.

For $D = \operatorname{grad}\operatorname{div}$, $\operatorname{grad}\operatorname{curl}$, or $\operatorname{grad}\operatorname{rot}$, we define another norm for $H(D;\Omega)$:

$$\begin{aligned}
|||\boldsymbol{u}|||_{H(\operatorname{grad}\operatorname{rot};\Omega)} &= \|\boldsymbol{u}\| + \|\operatorname{rot}\boldsymbol{u}\| + \|\operatorname{grad}\operatorname{rot}\boldsymbol{u}\| \text{ when } D = \operatorname{grad}\operatorname{rot},\\
|||\boldsymbol{u}|||_{H(\operatorname{grad}\operatorname{div};\Omega)} &= \|\boldsymbol{u}\| + \|\operatorname{div}\boldsymbol{u}\| + \|\operatorname{grad}\operatorname{div}\boldsymbol{u}\| \text{ when } D = \operatorname{grad}\operatorname{div},\\
|||\boldsymbol{u}|||_{H(\operatorname{grad}\operatorname{curl};\Omega)} &= \|\boldsymbol{u}\| + \|\operatorname{curl}\boldsymbol{u}\| + \|\operatorname{grad}\operatorname{curl}\boldsymbol{u}\| \text{ when } D = \operatorname{grad}\operatorname{curl}.
\end{aligned}$$

It is easy to check that $H(D;\Omega)$ is a Banach space under the two norms $|||\cdot|||_{H(D;\Omega)}$ and $\|\cdot\|_{H(D;\Omega)}$. Applying the bounded inverse theorem, the two norms are equivalent.

2.1.5 Poincaré Operators

For any complex (2.1.1), we call graded operators $\mathfrak{p}^k : V^k \to V^{k-1}$ Poincaré operators if they satisfy

- the null-homotopy property:

$$d^{k-1}\mathfrak{p}^k + \mathfrak{p}^{k+1}d^k = \mathrm{id}_{V^k}; \tag{2.1.17}$$

- the complex property:

$$\mathfrak{p}^{k-1} \circ \mathfrak{p}^k = 0.$$

Lemma 2.1.3. *If there exist Poincaré operators $\mathfrak{p}^\bullet$ for* (2.1.1)*, then* (2.1.1) *is exact.*

Proof. Assume that $d^k u = 0$ for $u \in V^k$. From the null-homotopy identity, $u = d^{k-1}(\mathfrak{p}^k u)$. This implies the exactness of (2.1.1) at V^k. □

For the de Rham complex (2.1.6), there exist Poincaré operators, and their explicit forms in 2D are [36, 44, 21]:

$$\mathfrak{p}^1 \boldsymbol{u} = \int_0^1 \boldsymbol{u}(W + t(\boldsymbol{x} - W)) \cdot (\boldsymbol{x} - W)\mathrm{d}t,\ \forall \boldsymbol{u} \in C^\infty\Lambda^1(\Omega), \tag{2.1.18}$$

$$\mathfrak{p}^2 u = \int_0^1 t u(W + t(\boldsymbol{x} - W))(\boldsymbol{x} - W)^\perp \mathrm{d}t,\ \forall u \in C^\infty\Lambda^2(\Omega), \tag{2.1.19}$$

where $\boldsymbol{x}^\perp = (x_2, -x_1)$. In 3D,

$$\mathfrak{p}^1 \boldsymbol{u} = \int_0^1 \boldsymbol{u}(W + t(\boldsymbol{x} - W)) \cdot (\boldsymbol{x} - W)\mathrm{d}t,\ \forall \boldsymbol{u} \in C^\infty\Lambda^1(\Omega), \tag{2.1.20}$$

$$\mathfrak{p}^2 \boldsymbol{u} = \int_0^1 t\boldsymbol{u}(W + t(\boldsymbol{x} - W)) \times (\boldsymbol{x} - W)\mathrm{d}t,\ \forall \boldsymbol{u} \in C^\infty\Lambda^2(\Omega), \tag{2.1.21}$$

$$\mathfrak{p}^3 u = \int_0^1 t^2 u(W + t(\boldsymbol{x} - W))(\boldsymbol{x} - W)\mathrm{d}t,\ \forall u \in C^\infty\Lambda^3(\Omega), \tag{2.1.22}$$

where W is a base point.

In addition to the complex property and the null-homotopy identity, these operators further satisfy

- the polynomial preserving property: if u is a polynomial of degree r, then $\mathfrak{p}u$ is a polynomial of degree at most $r+1$.

Koszul operators $\kappa^k : V^k \to V^{k-1}$ restricting on homogeneous polynomials have similar properties to the Poincaré operators:

- the homotopy formula:

$$d^{k-1}\kappa^k u + \kappa^{k+1} d^k u = (k+r)u \text{ if } u \in V^k \cap \widetilde{P}_r;$$

- the complex property:

$$\kappa^{k-1} \circ \kappa^k = 0;$$

- the polynomial preserving property: if u is a polynomial of degree r, then κu is a polynomial of degree at most $r+1$.

The explicit forms of Koszul operators in 2D are [6]:

$$\kappa^1 \boldsymbol{u} = \boldsymbol{u} \cdot \boldsymbol{x}, \ \forall \boldsymbol{u} \in C^\infty \Lambda^1(\Omega), \tag{2.1.23}$$

$$\kappa^2 u = u \boldsymbol{x}^\perp, \ \forall u \in C^\infty \Lambda^2(\Omega). \tag{2.1.24}$$

In 3D,

$$\kappa^1 \boldsymbol{u} = \boldsymbol{u} \cdot \boldsymbol{x}, \ \forall \boldsymbol{u} \in C^\infty \Lambda^1(\Omega), \tag{2.1.25}$$

$$\kappa^2 \boldsymbol{u} = \boldsymbol{u} \times \boldsymbol{x}, \ \forall \boldsymbol{u} \in C^\infty \Lambda^2(\Omega), \tag{2.1.26}$$

$$\kappa^3 u = u \boldsymbol{x}, \ \forall u \in C^\infty \Lambda^3(\Omega). \tag{2.1.27}$$

2.2 Bernstein-Gelfand-Gelfand Construction

We can use the BGG construction to derive new differential complexes from the known ones. It is shown in [12] that the cohomology of the output complex of BGG can be related to that of the input complexes. We recall the process of BGG construction and the main conclusion of [12].

Suppose $(Z^\bullet, d^\bullet)$ and $(\widetilde{Z}^\bullet, \widetilde{d}^\bullet)$ are two bounded Hilbert complexes. Suppose also $S^i : \widetilde{Z}^i \to Z^{i+1}$, $i = -1, 0, \cdots, n$ are bounded connecting maps that connects the two Hilbert complexes:

$$\begin{array}{ccccccccccccccc}
0 & \longrightarrow & Z^0 & \xrightarrow{d^0} & Z^1 & \xrightarrow{d^1} & \cdots & \xrightarrow{d^{J-1}} & Z^J & \xrightarrow{d^J} & \cdots & \xrightarrow{d^{n-1}} & Z^n & \longrightarrow & 0 \\
& \overset{S^{-1}}{\nearrow} & & \overset{S^0}{\nearrow} & & \overset{S^1}{\nearrow} & & \overset{S^{J-1}}{\nearrow} & & \overset{S^J}{\nearrow} & & \overset{S^{n-1}}{\nearrow} & & \overset{S^n}{\nearrow} & \\
0 & \longrightarrow & \widetilde{Z}^0 & \xrightarrow{\widetilde{d}^0} & \widetilde{Z}^1 & \xrightarrow{\widetilde{d}^1} & \cdots & \xrightarrow{\widetilde{d}^{J-1}} & \widetilde{Z}^J & \xrightarrow{\widetilde{d}^J} & \cdots & \xrightarrow{\widetilde{d}^{n-1}} & \widetilde{Z}^n & \longrightarrow & 0.
\end{array} \tag{2.2.1}$$

The two complexes $(Z^\bullet, d^\bullet)$ and $(\widetilde{Z}^\bullet, \widetilde{d}^\bullet)$ can not be arbitrary. They are of the form

$$Z^i := V^i \otimes \mathbb{E}^i \quad \text{and} \quad \widetilde{Z}^i := V^{i+1} \otimes \widetilde{\mathbb{E}}^i,$$

where V^i is a Hilbert space and $\mathbb{E}^i, \widetilde{\mathbb{E}}^i$ might be space of scalars $\mathbb{R}$, vectors $\mathbb{V}$, matrices $\mathbb{M}$, etc.

In addition, the connecting operators S^i are of the form

$$S^i = \mathrm{id} \otimes s^i,$$

where $s^i : \widetilde{\mathbb{E}}^i \to \mathbb{E}^{i+1}$ is a linear operator. They satisfy the following two properties:

- Anticommutativity, $S^{i+1}\widetilde{d}^i = -d^{i+1}S^i$, $i = 0, 1, \cdot, n-2$;
- The J-injectivity/surjectivity condition, i.e., for some J with $0 \leq J < n$,

$$s^i \text{ is } \begin{cases} \text{injective}, & 0 \leq i < J, \\ \text{bijective}, & i = J, \\ \text{surjective}, & J < i < n. \end{cases}$$

We are now in a position to define the output complex of the BGG construction:

$$0 \longrightarrow \mathcal{Z}^0 \xrightarrow{D^0} \cdots \xrightarrow{D^{k-1}} \mathcal{Z}^k \xrightarrow{D^{J-1}} \mathcal{Z}^J \xrightarrow{D^J} \cdots \xrightarrow{D^{n-1}} \mathcal{Z}^n \longrightarrow 0 \tag{2.2.2}$$

with

$$\mathcal{Z}^i = \begin{cases} V^i \otimes \mathcal{R}(s^{i-1})^\perp, & 0 \leq i \leq J, \\ V^{i+1} \otimes \mathcal{N}(s^i)^\perp, & J < i \leq n, \end{cases}$$

and

$$D^i = \begin{cases} \mathrm{id} \otimes P_{\mathcal{R}^\perp} d^i, & i < J, \\ \widetilde{d}^i (S^i)^{-1} d^i, & i = J, \\ \widetilde{d}^i, & i > J. \end{cases}$$

Here $\mathcal{R}(s)$ and $\mathcal{N}(s)$ represent the range and the kernel of the operator s, and $P_{\mathcal{R}^\perp}$ represents the L^2 projection to $\mathcal{R}^\perp$.

The output complex (2.2.2) can be read from the input complexes $(Z^\bullet, d^\bullet)$ and $(\widetilde{Z}^\bullet, \widetilde{d}^\bullet)$ in the following way. We start from the left end of the top complex of (2.2.1), and go right along the complex, at each step restricting to the orthogonal complement of the range of the incoming S operator. When we reach the space Z^J, we go to $\widetilde{Z}^{J+1}$ in the bottom complex by following the connecting map S^J in the reverse direction and $\widetilde{d}^J$, and then continue rightwards along the bottom complex, restricting to the kernels of the S operators.

Denote by $\mathcal{H}^i(Z^\bullet, d^\bullet)$ the i-th cohomology space of the complex $(Z^\bullet, d^\bullet)$. Then the cohomology of the output complex can be related to the cohomology of the input complexes by the following theorem.

Theorem 2.2.1 ([12])**.** *Suppose the given bounded Hilbert complexes* $(Z^\bullet, d^\bullet)$ *and* $(\widetilde{Z}^\bullet, \widetilde{d}^\bullet)$ *and bounded connecting maps* $S^i : \widetilde{Z}^i \to Z^{i+1}$ *satisfying the required properties. Then the output complex* (2.2.2) *is a bounded Hilbert complex. Moreover,*

$$\dim \mathcal{H}^i(\mathcal{Z}^\bullet, D^\bullet) \leqslant \dim \mathcal{H}^i(Z^\bullet, d^\bullet) + \dim \mathcal{H}^i(\widetilde{Z}^\bullet, \widetilde{d}^\bullet), \quad \forall i = 0, 1, \cdots, n.$$

The equality holds if and only if S^i *induces the zero maps on cohomology, i.e., if and only if*

$$S^i \mathcal{N}(\widetilde{d}^i) \subset \mathcal{R}(d^i), \quad \forall i = 0, 1, \cdots, n-1. \tag{2.2.3}$$

If there exist bounded operators $K^i : \widetilde{Z}^i \to Z^i, i = 0, 1, \cdots, n$, such that

$$S^i = d^i K^i - K^{i+1}\widetilde{d}^i, \quad i = 0, 1, \cdots, n-1,$$

then the condition (2.2.3) holds. Moreover, the space of cohomology representatives of $(\mathcal{Z}^\bullet, D^\bullet)$ can be represented by the spaces of cohomology representatives of $(Z^\bullet, d^\bullet)$ and $(\widetilde{Z}^\bullet, \widetilde{d}^\bullet)$.

CHAPTER 3 Gradcurl Complex, Gradrot Complex, and Graddiv Complex

The grad curl complex, grad rot complex, and grad div complex can be derived by the BGG construction [12]. In this chapter, we will investigate these complexes and the involved spaces in terms of trace theorems, density, Hodge Laplacian, characterization of boundary conditions of the Hodge Laplacian, etc.

3.1 Gradcurl Complex and Hodge Laplacian

For any real number q, we consider the diagram with two de Rham complexes as the input:

$$
\begin{array}{ccccccccccccc}
0 \longrightarrow & H^q & \xrightarrow{\operatorname{grad}} & H^{q-1}\otimes\mathbb{V} & \xrightarrow{\operatorname{curl}} & H^{q-2}\otimes\mathbb{V} & \xrightarrow{\operatorname{div}} & H^{q-3} & \longrightarrow & 0 & \longrightarrow & 0 & \\
& & {}^{0}\nearrow & & {}^{\operatorname{id}}\nearrow & & {}^{-\operatorname{tr}}\nearrow & & {}^{0}\nearrow & & & & \qquad (3.1.1)\\
0 \longrightarrow & 0 & \longrightarrow & H^{q-2}\otimes\mathbb{V} & \xrightarrow{\operatorname{grad}} & H^{q-3}\otimes\mathbb{M} & \xrightarrow{\operatorname{curl}} & H^{q-4}\otimes\mathbb{M} & \xrightarrow{\operatorname{div}} & H^{q-5}\otimes\mathbb{V} & \longrightarrow & 0. &
\end{array}
$$

Here and after, to ease the presentation, we drop the domain Ω in the function spaces in complexes. The connecting operators satisfy that id is bijective and tr is surjective, and they anti-commute with the differential operators, i.e.,

$$\operatorname{div}\circ\operatorname{id} = \operatorname{tr}\circ\operatorname{grad}.$$

From the general framework presented in the above chapter, we can derive the following grad curl *complex* from (3.1.1):

$$0 \longrightarrow H^q \xrightarrow{\operatorname{grad}} H^{q-1}\otimes\mathbb{V} \xrightarrow{\operatorname{grad}\operatorname{curl}} H^{q-3}\otimes\mathbb{T} \xrightarrow{\operatorname{curl}} H^{q-4}\otimes\mathbb{M} \xrightarrow{\operatorname{div}} H^{q-5}\otimes\mathbb{V} \longrightarrow 0, \quad (3.1.2)$$

where $\mathbb{T}$ is the space of trace-free matrices and the differential operators grad, curl, and div are applied row-rise.

Note that the dimension of cohomology at $H^{q-1}(\Omega)\otimes\mathbb{V}$ in the first row of (3.1.1) is the first Betti number b_1 of the domain, and the dimension of cohomology at $H^{q-2}(\Omega)\otimes\mathbb{V}$ in the second row is 3 (kernel of grad is constants). If we can verify the condition (2.2.3), then, according to Theorem 2.2.1 and Theorem 2.1.1, we have

$$\mathcal{N}(\operatorname{grad}\operatorname{curl}, H^{q-1}(\Omega)\otimes\mathbb{V}) = \mathcal{R}(\operatorname{grad}, H^{q}(\Omega)) \oplus \mathscr{H}^1_\infty, \tag{3.1.3}$$

where $\mathscr{H}^1_\infty$ is a set of smooth cohomology representatives (independent of q) with dimension $\dim \mathscr{H}^1_\infty = 3 + b_1$.

Next we verify the condition (2.2.3). We have a bijection between vectors and skew symmetric matrices defined by

$$\operatorname{mskw}\begin{pmatrix} v_1 \\ v_2 \\ v_3 \end{pmatrix} := \begin{pmatrix} 0 & -v_3 & v_2 \\ v_3 & 0 & -v_1 \\ -v_2 & v_1 & 0 \end{pmatrix}.$$

We define $\widetilde{K}^1 : H^{q-2}(\Omega)\otimes\mathbb{V} \to H^{q-2}(\Omega)\otimes\mathbb{V}$, $\widetilde{K}^2 : H^{q-3}(\Omega)\otimes\mathbb{M} \to H^{q-3}(\Omega)\otimes\mathbb{V}$, and $\widetilde{K}^3 : H^{q-4}(\Omega)\otimes\mathbb{M} \to H^{q-4}(\Omega)$ by

$$\begin{aligned} \widetilde{K}^1\boldsymbol{u} &:= \frac{1}{2}\boldsymbol{u}\times\boldsymbol{x}, \\ \widetilde{K}^2\boldsymbol{U} &:= \frac{1}{2}\big(\boldsymbol{U} - \operatorname{tr}(\boldsymbol{U})\big)\boldsymbol{x}, \\ \widetilde{K}^3\boldsymbol{U} &:= \operatorname{vskw}\boldsymbol{U}\cdot\boldsymbol{x}, \end{aligned}$$

with $\operatorname{vskw} = \operatorname{mskw}^{-1}\circ\operatorname{skw} : \mathbb{M}\to\mathbb{V}$. Then

$$d^i\widetilde{K}^i - \widetilde{K}^{i+1}\widetilde{d}^i = S^i.$$

Recalling the operators P^{i+1} and L^i introduced in Lemma 2.1.2, we define

$$K^i = P^{i+1}S^i + L^i\widetilde{K}^i. \tag{3.1.4}$$

Then

$$\begin{aligned} dK - Kd = d(PS + L\widetilde{K}) - (PS + L\widetilde{K})d &= dPS + PdS + dL\widetilde{K} - L\widetilde{K}d \\ &= (\operatorname{id} - L)S + Ld\widetilde{K} - L\widetilde{K}d = S. \end{aligned}$$

The L^2 version of (3.1.2) with unbounded linear operators, i.e.,

$$0 \longrightarrow L^2 \xrightarrow{\text{grad}} L^2 \otimes \mathbb{V} \xrightarrow{\text{grad curl}} L^2 \otimes \mathbb{T} \xrightarrow{\text{curl}} L^2 \otimes \mathbb{M} \xrightarrow{\text{div}} L^2 \otimes \mathbb{V} \longrightarrow 0 \tag{3.1.5}$$

is closely related to the PDEs.

3.1.1 Gradcurl Complex Without Boundary Conditions

We consider the following domain complex of the L^2 complex (3.1.5):

$$0 \longrightarrow H^1 \xrightarrow{\text{grad}} H(\text{grad curl}) \xrightarrow{\text{grad curl}} H(\text{curl}, \mathbb{T}) \xrightarrow{\text{curl}} H(\text{div}, \mathbb{M}) \xrightarrow{\text{div}} L^2 \otimes \mathbb{V} \longrightarrow 0, \tag{3.1.6}$$

where $H(\text{curl}, \mathbb{T}; \Omega) = \{\boldsymbol{U} \in L^2(\Omega) \otimes \mathbb{T} : \text{curl}\,\boldsymbol{U} \in L^2(\Omega) \otimes \mathbb{M}\}$ and $H(\text{div}, \mathbb{M}; \Omega) = \{\boldsymbol{U} \in L^2(\Omega) \otimes \mathbb{M} : \text{div}\,\boldsymbol{U} \in L^2(\Omega) \otimes \mathbb{V}\}$.

According to Theorem 2.2.1 and (2.1.10), we have

$$\mathcal{N}(\text{grad curl}, H(\text{grad curl}; \Omega)) = \mathcal{R}(\text{grad}, H^1(\Omega)) \oplus \mathscr{H}^1_\infty, \tag{3.1.7}$$

where $\mathscr{H}^1_\infty$ is defined in (3.1.3).

Define

$$H_0(\text{curl}, \mathbb{M}; \Omega) := \{\boldsymbol{U} \in H(\text{curl}, \mathbb{M}; \Omega) : \ \boldsymbol{n} \times \boldsymbol{U} = 0\},$$

where the cross product in $\boldsymbol{n} \times \boldsymbol{U}$ is applied row-wise. The dual complex of (3.1.6) is

$$0 \longleftarrow L^2_0 \xleftarrow{-\text{div}} H_0(\text{div}) \xleftarrow{-\text{curl div}} H_0(\text{curl div}, \mathbb{T}) \xleftarrow{\text{dev curl}} H_0(\text{curl}, \mathbb{M}) \xleftarrow{-\text{grad}} H^1_0 \otimes \mathbb{V} \longleftarrow 0,$$

where $H_0(\text{curl div}, \mathbb{T}; \Omega)$ is a formal notation for the domain of the adjoint of the operator $(\text{grad curl}, H(\text{grad curl}; \Omega))$. We will not characterize $H_0(\text{curl div}, \mathbb{T}; \Omega)$ in this dissertation.

From general results on Hilbert complexes (see Section 2.1.3), we have the Hodge decomposition at $H(\text{grad curl}; \Omega)$:

$$L^2(\Omega) \otimes \mathbb{V} = \text{grad}\, H^1(\Omega) \oplus \text{curl div}\, H_0(\text{curl div}, \mathbb{T}; \Omega) \oplus \mathfrak{H}^1,$$

where $\mathfrak{H}^1$ is the space of harmonic forms with $\dim \mathfrak{H}^1 = \dim \mathscr{H}^1_\infty$.

Define

$$X := H(\operatorname{grad}\operatorname{curl};\Omega) \cap H_0(\operatorname{div};\Omega).$$

The Hodge Laplacian operator follows from the abstract definition:

$$\mathscr{L}^1 := -(\operatorname{curl}\operatorname{div})\operatorname{grad}\operatorname{curl} - \operatorname{grad}\operatorname{div} = -\operatorname{curl}\Delta\operatorname{curl} - \operatorname{grad}\operatorname{div},$$

with the domain $D_{\mathscr{L}^1} = \{\boldsymbol{u} \in X : \operatorname{grad}\operatorname{curl}\boldsymbol{u} \in H_0(\operatorname{curl}\operatorname{div},\mathbb{T};\Omega), \operatorname{div}\boldsymbol{u} \in H^1(\Omega)\}$. For $\boldsymbol{f} \in L^2(\Omega)\otimes\mathbb{V}$, the strong formulation of the Hodge Laplacian boundary value problem seeks $\boldsymbol{u} \in D_{\mathscr{L}^1}$ and $\boldsymbol{u} \perp \mathfrak{H}^1$ such that

$$-\operatorname{curl}\Delta\operatorname{curl}\boldsymbol{u} - \operatorname{grad}\operatorname{div}\boldsymbol{u} = \boldsymbol{f} - P_{\mathfrak{H}^1}\boldsymbol{f} \quad \text{in } \Omega.$$

3.1.2 Gradcurl Complex with Boundary Conditions

Define

$$H_0(\operatorname{div},\mathbb{M};\Omega) := \{\boldsymbol{U} \in H(\operatorname{div},\mathbb{M};\Omega) : \ \boldsymbol{U}\boldsymbol{n} = 0\},$$

$$H_0(\operatorname{grad}\operatorname{curl};\Omega) := \text{ closure of } C_0^\infty(\Omega)\otimes\mathbb{V} \text{ in the sense of } H(\operatorname{grad}\operatorname{curl}) \text{ norm.}$$

We will show in Section 3.1.4 that $H_0(\operatorname{grad}\operatorname{curl};\Omega)$ has the following characterization:

$$H_0(\operatorname{grad}\operatorname{curl};\Omega) := \{\boldsymbol{u} \in H(\operatorname{grad}\operatorname{curl};\Omega) : \ \boldsymbol{u}\times\boldsymbol{n} = 0 \text{ and } \operatorname{curl}\boldsymbol{u} = 0\}.$$

Consider the domain complex of (3.1.5) with vanishing boundary conditions:

$$0 \longrightarrow H_0^1 \xrightarrow{\operatorname{grad}} H_0(\operatorname{grad}\operatorname{curl}) \xrightarrow{\operatorname{grad}\operatorname{curl}} H_0(\operatorname{curl},\mathbb{T}) \xrightarrow{\operatorname{curl}} H_0(\operatorname{div},\mathbb{M}) \xrightarrow{\operatorname{div}} L_0^2\otimes\mathbb{V} \longrightarrow 0, \tag{3.1.8}$$

which is derived from the following diagram:

$$\begin{array}{ccccccccccc}
0 \to H_0^1 \xrightarrow{\operatorname{grad}} & H_0(\operatorname{grad}\operatorname{curl}) & \xrightarrow{\operatorname{curl}} & H_0^1\otimes\mathbb{V} & \xrightarrow{\operatorname{div}} & L_0^2 & \longrightarrow & 0 & \longrightarrow & 0 \\
\nearrow^{0} & & \nearrow^{\mathrm{id}} & & \nearrow^{-\operatorname{tr}} & & \nearrow^{0} & & & \\
0 \longrightarrow 0 \longrightarrow & H_0^1\otimes\mathbb{V} & \xrightarrow{\operatorname{grad}} & H_0(\operatorname{curl},\mathbb{M}) & \xrightarrow{\operatorname{curl}} & H_0(\operatorname{div},\mathbb{M}) & \xrightarrow{\operatorname{div}} & L_0^2\otimes\mathbb{V} & \to & 0.
\end{array} \tag{3.1.9}$$

The dimension of the cohomology at $H_0(\operatorname{grad}\operatorname{curl};\Omega)$ in the first row of (3.1.9) is b_2, and the dimension of the cohomology at $H_0^1(\Omega)\otimes\mathbb{V}$ in the second row of (3.1.9) is 0.

Therefore, we have

$$\mathcal{N}(\operatorname{grad}\operatorname{curl}, H_0(\operatorname{grad}\operatorname{curl};\Omega)) = \mathcal{R}(\operatorname{grad}, H_0^1(\Omega)) \oplus \mathscr{H}_\infty^{1,0},$$

where $\mathscr{H}_\infty^{1,0}$ is a set of smooth cohomology representatives with $\dim \mathscr{H}_\infty^{1,0} = b_2$.

The dual complex of (3.1.8) is

$$0 \longleftarrow L^2 \xleftarrow{-\operatorname{div}} H(\operatorname{div}) \xleftarrow{-\operatorname{curl}\operatorname{div}} H(\operatorname{curl}\operatorname{div}, \mathbb{T}) \xleftarrow{\operatorname{dev}\operatorname{curl}} H(\operatorname{curl}, \mathbb{M}) \xleftarrow{-\operatorname{grad}} H^1 \otimes \mathbb{V} \longleftarrow 0,$$

where $H(\operatorname{curl}\operatorname{div}, \mathbb{T};\Omega) = \{\boldsymbol{U} \in L^2(\Omega) \otimes \mathbb{T} : \operatorname{curl}\operatorname{div}\boldsymbol{U} \in L^2(\Omega) \otimes \mathbb{V}\}$. The Hodge decomposition at $H_0(\operatorname{grad}\operatorname{rot})$ reads:

$$L^2(\Omega) \otimes \mathbb{V} = \operatorname{grad} H_0^1(\Omega) \oplus \operatorname{curl}\operatorname{div} H(\operatorname{curl}\operatorname{div}, \mathbb{T};\Omega) \oplus \mathfrak{H}_0^1$$

with $\dim \mathfrak{H}_0^1 = \dim \mathscr{H}_\infty^{1,0} = b_2$.

Define

$$X_0 := H_0(\operatorname{grad}\operatorname{rot};\Omega) \cap H(\operatorname{div};\Omega).$$

We define the Hodge Laplacian operator $\mathscr{L}^1$ in the previous way but with the domain $D_{\mathscr{L}^1,0} = \{\boldsymbol{u} \in X_0 : \operatorname{grad}\operatorname{curl}\boldsymbol{u} \in H(\operatorname{curl}\operatorname{div}, \mathbb{T};\Omega), \operatorname{div}\boldsymbol{u} \in H_0^1(\Omega)\}$. For $\boldsymbol{f} \in L^2(\Omega) \otimes \mathbb{V}$, the strong formulation of the Hodge Laplacian boundary value problem seeks $\boldsymbol{u} \in D_{\mathscr{L}^1,0}$ and $\boldsymbol{u} \perp \mathfrak{H}_0^1$ such that

$$-\operatorname{curl}\Delta\operatorname{curl}\boldsymbol{u} - \operatorname{grad}\operatorname{div}\boldsymbol{u} = \boldsymbol{f} - P_{\mathfrak{H}_0^1}\boldsymbol{f} \text{ in } \Omega. \tag{3.1.10}$$

In the case of $\boldsymbol{f} \in \operatorname{curl}\operatorname{div} H(\operatorname{curl}\operatorname{div}, \mathbb{T};\Omega)$, the problem (3.1.10) is then to find $\boldsymbol{u}$ such that $\boldsymbol{u} \perp \mathfrak{H}_0^1$ and

$$\begin{aligned} -\operatorname{curl}\Delta\operatorname{curl}\boldsymbol{u} &= \boldsymbol{f} \quad \text{in } \Omega, \\ \operatorname{div}\boldsymbol{u} &= 0 \quad \text{in } \Omega, \\ \boldsymbol{u}\times\boldsymbol{n} &= 0 \quad \text{on } \partial\Omega, \\ \operatorname{curl}\boldsymbol{u} &= 0 \quad \text{on } \partial\Omega. \end{aligned} \tag{3.1.11}$$

3.1.3 Gradcurl Complex with Partial Boundary Conditions

Define

$$H_{\mathrm{curl}}(\operatorname{grad}\operatorname{curl};\Omega) := \{\boldsymbol{u} \in H(\operatorname{grad}\operatorname{curl};\Omega) : \ \operatorname{curl}\boldsymbol{u} = 0\}$$

We consider a domain complex of (3.1.5) with partial vanishing boundary conditions:

$$0 \longrightarrow H^1 \xrightarrow{\operatorname{grad}} H_{\mathrm{curl}}(\operatorname{grad}\operatorname{curl}) \xrightarrow{\operatorname{grad}\operatorname{curl}} H_0(\operatorname{curl},\mathbb{T}) \xrightarrow{\operatorname{curl}} H_0(\operatorname{div},\mathbb{M}) \xrightarrow{\operatorname{div}} L_0^2 \otimes \mathbb{V} \longrightarrow 0, \tag{3.1.12}$$

which is somewhere between the complexes (3.1.6) and (3.1.8). The above complex is derived from the following diagram:

$$\begin{array}{ccccccccccccc}
0 & \longrightarrow & H^1 & \xrightarrow{\operatorname{grad}} & H_{\mathrm{curl}}(\operatorname{grad}\operatorname{curl}) & \xrightarrow{\operatorname{curl}} & H_0^1 \otimes \mathbb{V} & \xrightarrow{\operatorname{div}} & L_0^2 & \longrightarrow & 0 & \longrightarrow & 0 \\
 & & & \overset{0}{\nearrow} & & \overset{\mathrm{id}}{\nearrow} & & \overset{-\operatorname{tr}}{\nearrow} & & \overset{0}{\nearrow} & & & \\
0 & \longrightarrow & 0 & \longrightarrow & H_0^1 \otimes \mathbb{V} & \xrightarrow{\operatorname{grad}} & H_0(\operatorname{curl},\mathbb{M}) & \xrightarrow{\operatorname{curl}} & H_0(\operatorname{div},\mathbb{M}) & \xrightarrow{\operatorname{div}} & L_0^2 \otimes \mathbb{V} & \longrightarrow & 0.
\end{array}$$

The dimension of the de Rham complex cohomology at $H_{\mathrm{curl}}(\operatorname{grad}\operatorname{rot};\Omega)$ in the first row of the above diagram is b_1, and the dimension of the de Rham complex cohomology at $H_0^1(\Omega)$ in the second row is 0. Consequently,

$$\mathcal{N}(\operatorname{grad}\operatorname{curl}, H_{\mathrm{curl}}(\operatorname{grad}\operatorname{curl};\Omega)) = \mathcal{R}(\operatorname{grad}, H^1(\Omega)) \oplus \mathscr{H}_\infty^{1,\mathrm{curl}},$$

where $\mathscr{H}_\infty^{1,\mathrm{curl}}$ is a set of smooth cohomology representatives with $\dim \mathscr{H}_\infty^{1,\mathrm{curl}} = b_1$.

The dual complex of (3.1.12) is:

$$0 \longleftarrow L_0^2 \xleftarrow{-\operatorname{div}} H_0(\operatorname{div}) \xleftarrow{-\operatorname{curl}\operatorname{div}} H_{\operatorname{div}}(\operatorname{curl}\operatorname{div},\mathbb{T}) \xleftarrow{\operatorname{dev}\operatorname{curl}} H(\operatorname{curl},\mathbb{M}) \xleftarrow{-\operatorname{grad}} H^1 \otimes \mathbb{V} \longleftarrow 0,$$

Here $H_{\operatorname{div}}(\operatorname{curl}\operatorname{div},\mathbb{T};\Omega)$ is a formal notation for the domain of the adjoint of the operator $(\operatorname{grad}\operatorname{curl}, H_{\mathrm{curl}}(\operatorname{grad}\operatorname{curl};\Omega))$. Again, we will not characterize $H_{\operatorname{div}}(\operatorname{curl}\operatorname{div},\mathbb{T};\Omega)$ in this dissertation.

The Hodge decomposition at $H_{\mathrm{curl}}(\operatorname{grad}\operatorname{curl})$ reads:

$$L^2(\Omega) \otimes \mathbb{V} = \operatorname{grad} H^1(\Omega) \oplus \operatorname{curl}\operatorname{div} H_{\operatorname{div}}(\operatorname{curl}\operatorname{div},\mathbb{T};\Omega) \oplus \mathfrak{H}_{\mathrm{curl}}^1$$

with $\dim \mathfrak{H}^1_{\mathrm{curl}} = \dim \mathscr{H}^{1,\mathrm{curl}}_{\infty} = b_1$. The space $\mathfrak{H}^1_{\mathrm{curl}}$ is trivial if Ω is simply-connected. Define

$$X_{\mathrm{curl}} := H_{\mathrm{curl}}(\operatorname{grad}\operatorname{curl};\Omega) \cap H_0(\operatorname{div};\Omega).$$

The domain of the Hodge Laplacian operator $\mathscr{L}^1$ is

$$D_{\mathscr{L}^1,\mathrm{curl}} = \{\boldsymbol{u} \in X_{\mathrm{curl}} : \operatorname{grad}\operatorname{curl}\boldsymbol{u} \in H_{\mathrm{div}}(\operatorname{curl}\operatorname{div},\mathbb{T};\Omega), \operatorname{div}\boldsymbol{u} \in H^1(\Omega)\}.$$

For $\boldsymbol{f} \in L^2(\Omega)\otimes\mathbb{V}$, the strong formulation of the Hodge Laplacian boundary value problem seeks $\boldsymbol{u} \in D_{\mathscr{L}^1,\mathrm{curl}}$ and $\boldsymbol{u} \perp \mathfrak{H}^1_{\mathrm{curl}}$ such that

$$-\operatorname{curl}\Delta\operatorname{curl}\boldsymbol{u} - \operatorname{grad}\operatorname{div}\boldsymbol{u} = \boldsymbol{f} - P_{\mathfrak{H}^1_{\mathrm{curl}}}\boldsymbol{f} \quad \text{in } \Omega.$$

3.1.4 Characterization of $H_0(\operatorname{grad}\operatorname{curl})$

In this section, we characterize the space $H_0(\operatorname{grad}\operatorname{curl};\Omega)$.

Theorem 3.1.1. *Define $\gamma_{\tau,\mathrm{curl}}\boldsymbol{u} = \{\boldsymbol{u}\times\boldsymbol{n}, \operatorname{curl}\boldsymbol{u}\}$. Then $\gamma_{\tau,\mathrm{curl}}$ is a linear bounded operator from $H(\operatorname{grad}\operatorname{curl};\Omega)$ to $H^{-1/2}(\partial\Omega)\otimes\mathbb{V}\times H^{1/2}(\partial\Omega)\otimes\mathbb{V}$ with the bound:*

$$\|\gamma_{\tau,\mathrm{curl}}\boldsymbol{u}\|_{H^{-1/2}(\partial\Omega)\times H^{1/2}(\partial\Omega)} \le C\|\boldsymbol{u}\|_{H(\operatorname{grad}\operatorname{curl};\Omega)}.$$

Proof. Since $\gamma_\tau\boldsymbol{u} = \boldsymbol{u}\times\boldsymbol{n}$ is a linear bounded operator from $H(\operatorname{curl};\Omega)$ to $H^{-1/2}(\partial\Omega)\otimes\mathbb{V}$ and $\operatorname{tr}\boldsymbol{v} = \boldsymbol{v}|_{\partial\Omega}$ is a linear bounded operator from $H^1(\Omega)\otimes\mathbb{V}$ to $H^{1/2}(\partial\Omega)\otimes\mathbb{V}$, we have

$$\begin{aligned}
&\|\gamma_{\tau,\mathrm{curl}}\boldsymbol{u}\|^2_{H^{-1/2}(\partial\Omega)\times H^{1/2}(\partial\Omega)}\\
=&\|\boldsymbol{u}\times\boldsymbol{n}\|^2_{H^{-1/2}(\partial\Omega)} + \|\operatorname{curl}\boldsymbol{u}\|^2_{H^{1/2}(\partial\Omega)}\\
\le& C\|\boldsymbol{u}\|^2_{H(\operatorname{curl};\Omega)} + C\|\operatorname{curl}\boldsymbol{u}\|^2_{H^1(\Omega)}\\
\le& C\|\boldsymbol{u}\|^2_{H(\operatorname{grad}\operatorname{curl};\Omega)},
\end{aligned}$$

where we have used the equivalence between the norms $\|\cdot\|_{H(\operatorname{grad}\operatorname{curl};\Omega)}$ and $|||\cdot|||_{H(\operatorname{grad}\operatorname{curl};\Omega)}$, see Section 2.1.4. □

Lemma 3.1.2. *If a function* $\boldsymbol{u} \in H(\operatorname{grad}\operatorname{curl};\Omega)$ *satisfies*

$$(\operatorname{grad}\operatorname{curl}\boldsymbol{u}, \boldsymbol{\Phi}) + (\boldsymbol{u}, \operatorname{curl}\operatorname{div}\boldsymbol{\Phi}) = 0 \textit{ for all } \boldsymbol{\Phi} \in C^\infty(\overline{\Omega}) \otimes \mathbb{T}, \tag{3.1.13}$$

then $\boldsymbol{u} \in H_0(\operatorname{grad}\operatorname{curl};\Omega)$.

Proof. We follow the proof of [49, Lemma 3.27]. Denote $D\boldsymbol{u} = \operatorname{grad}\operatorname{curl}\boldsymbol{u}$. Let $\widetilde{\boldsymbol{u}}$ and $\widetilde{D\boldsymbol{u}}$ be the extension of $\boldsymbol{u}$ and $D\boldsymbol{u}$ by zero outside Ω. Then (3.1.13) can be rewritten as

$$(\widetilde{D\boldsymbol{u}}, \boldsymbol{\Phi}) + (\widetilde{\boldsymbol{u}}, \operatorname{curl}\operatorname{div}\boldsymbol{\Phi}) = 0 \text{ for all } \boldsymbol{\Phi} \in C^\infty(\mathbb{R}^3) \otimes \mathbb{T},$$

which implies $\widetilde{\boldsymbol{u}} \in H(\operatorname{grad}\operatorname{curl};\mathbb{R}^3)$. If we can construct a sequence of functions in $C_0^\infty(\Omega) \otimes \mathbb{V}$ that converges to $\boldsymbol{u}$ in $H(\operatorname{grad}\operatorname{curl})$ norm, then $\boldsymbol{u} \in H_0(\operatorname{grad}\operatorname{curl};\Omega)$.

1). Suppose that Ω is a strictly star-shaped with respect to a point in Ω, say y. Without loss of generality, we suppose y is the origin of the coordinate system. For $\theta \in (0,1)$, define the function

$$\widetilde{\boldsymbol{u}}_\theta(\boldsymbol{x}) = \widetilde{\boldsymbol{u}}(\boldsymbol{x}/\theta), \quad \forall \boldsymbol{x} \in \mathbb{R}^3.$$

Obviously, $\widetilde{\boldsymbol{u}}_\theta \in H(\operatorname{grad}\operatorname{curl};\mathbb{R}^3)$ and $\lim_{\theta\to 1}\widetilde{\boldsymbol{u}}_\theta = \widetilde{\boldsymbol{u}}$ in $H(\operatorname{grad}\operatorname{curl};\mathbb{R}^3)$. Since Ω is strictly star-shaped, the function $\widetilde{\boldsymbol{u}}_\theta$ has a compact support in Ω. Let η_ε be the mollifier

$$\eta_\varepsilon(\boldsymbol{x}) = \varepsilon^{-3}\eta(\boldsymbol{x}/\varepsilon),$$

where

$$\eta(\boldsymbol{x}) = \begin{cases} C_1 \exp\left(\frac{1}{|\boldsymbol{x}|^2-1}\right), & |\boldsymbol{x}| < 1, \\ 0, & |\boldsymbol{x}| \geq 1 \end{cases}$$

with $C_1 = \left(\int_{\mathbb{R}^2} \exp\left(\frac{1}{|\boldsymbol{x}|^2-1}\right)\mathrm{d}\boldsymbol{x}\right)^{-1}$. There exists a $\varepsilon_\theta > 0$ such that, for $0 < \varepsilon < \varepsilon_\theta$, $\eta_\varepsilon * \widetilde{\boldsymbol{u}}_\theta$ belongs to $C_0^\infty(\Omega) \otimes \mathbb{V}$ and

$$\lim_{\varepsilon\to 0} \eta_\varepsilon * \widetilde{\boldsymbol{u}}_\theta = \widetilde{\boldsymbol{u}}_\theta \text{ in } H(\operatorname{grad}\operatorname{curl};\Omega).$$

As a result, there exists $\{\theta_k, \varepsilon_k\}_{k=1}^\infty$ with $0 < \theta_k < 1$ and $0 < \varepsilon_k < \varepsilon_{\theta_k}$ such that $\theta_k \to 1$

and $\varepsilon_k \to 0$. Then

$$\lim_{k\to\infty} \eta_{\varepsilon_k} * \widetilde{\boldsymbol{u}}_{\theta_k} = \widetilde{\boldsymbol{u}} \text{ in } H(\operatorname{grad}\operatorname{curl};\Omega).$$

2). In the general case, there exit finite open sets $\mathcal{O}_i$, $i = 1, 2, \cdots, q$ such that $\Omega \subset \cup_{1\le i\le q}\mathcal{O}_i$ and each $\Omega_i := \Omega \cap \mathcal{O}_i$ is Lipschitz, bounded, and strictly star-shaped. Let $\{\alpha_i\}_{i=1}^q$ be a partition of unity subordinate to $\{\mathcal{O}_i\}_{i=1}^q$, i.e.,

$$\alpha_i \in C_0^\infty(\mathcal{O}_i),\ 0 \le \alpha_i(\boldsymbol{x}) \le 1,\ \text{and} \sum_{i=1}^q \alpha_i(\boldsymbol{x}) \equiv 1 \text{ in } \Omega.$$

Then $\widetilde{\boldsymbol{u}} = \sum_{i=1}^q \alpha_i \widetilde{\boldsymbol{u}}$ in $\mathbb{R}^3$ with $\alpha_i\widetilde{\boldsymbol{u}} \in H(\operatorname{grad}\operatorname{curl};\Omega)$ and $\operatorname{supp}(\alpha_i\widetilde{\boldsymbol{u}}) \subset \overline{\Omega}_i$. We can complete the proof by applying 1) to each $\alpha_i\widetilde{\boldsymbol{u}}$. □

By a modification of the proof of Lemma 3.1.2, we can prove the counterpart for $H(\operatorname{curl}\operatorname{div},\mathbb{T};\Omega)$.

Lemma 3.1.3. *If a function $\boldsymbol{U} \in H(\operatorname{curl}\operatorname{div},\mathbb{T};\Omega)$ satisfies*

$$(\operatorname{curl}\operatorname{div}\boldsymbol{U},\boldsymbol{\phi}) + (\boldsymbol{U},\operatorname{grad}\operatorname{curl}\boldsymbol{\phi}) = 0 \textit{ for all } \boldsymbol{\phi} \in C^\infty(\overline{\Omega}) \otimes \mathbb{V}, \tag{3.1.14}$$

then $\boldsymbol{U} \in H_0(\operatorname{curl}\operatorname{div},\mathbb{T};\Omega) =$ closure of $C_0^\infty(\Omega) \otimes \mathbb{T}$ in $H(\operatorname{curl}\operatorname{div},\mathbb{T};\Omega)$ norm.

Theorem 3.1.4. *$C^\infty(\overline{\Omega}) \otimes \mathbb{V}$ is dense in $H(\operatorname{grad}\operatorname{curl};\Omega)$.*

Proof. We follow the proof of [49, Theorem 3.26]. Rewrite

$$H(\operatorname{grad}\operatorname{curl};\Omega) = C^\infty(\overline{\Omega}) \otimes \mathbb{V} \oplus \left(C^\infty(\overline{\Omega}) \otimes \mathbb{V}\right)^\perp.$$

Suppose $\boldsymbol{u} \in \left(C^\infty(\overline{\Omega}) \otimes \mathbb{V}\right)^\perp$, then

$$(\boldsymbol{u},\boldsymbol{\phi}) + (\operatorname{grad}\operatorname{curl}\boldsymbol{u},\operatorname{grad}\operatorname{curl}\boldsymbol{\phi}) = 0 \text{ for all } \boldsymbol{\phi} \in C^\infty(\overline{\Omega}) \otimes \mathbb{V}. \tag{3.1.15}$$

We shall show $\boldsymbol{u} = 0$. Let $\boldsymbol{V} = \operatorname{grad}\operatorname{curl}\boldsymbol{u} \in L^2(\Omega) \otimes \mathbb{V}$. The equality (3.1.15) implies, in the sense of distributions,

$$\boldsymbol{u} = \operatorname{curl}\operatorname{div}\boldsymbol{V} \in L^2(\Omega) \otimes \mathbb{V}.$$

Then $\boldsymbol{V} \in H(\operatorname{curl}\operatorname{div}, \mathbb{T}; \Omega)$. From the equality (3.1.15), $\boldsymbol{V}$ satisfies

$$(\operatorname{curl}\operatorname{div} \boldsymbol{V}, \boldsymbol{\phi}) + (\boldsymbol{V}, \operatorname{grad}\operatorname{curl} \boldsymbol{\phi}) = 0 \text{ for all } \boldsymbol{\phi} \in C^\infty(\overline{\Omega}) \otimes \mathbb{V}.$$

It follows from Lemma 3.1.3 that $\boldsymbol{V} \in H_0(\operatorname{curl}\operatorname{div}, \mathbb{T}; \Omega)$. Since $C_0^\infty(\Omega) \otimes \mathbb{T}$ is dense in $H_0(\operatorname{curl}\operatorname{div}, \mathbb{T}; \Omega)$, there is a sequence $\{\boldsymbol{V}_n\}_{n=1}^\infty \subset C_0^\infty(\Omega) \otimes \mathbb{T}$ such that $\boldsymbol{V}_n \to \boldsymbol{V}$ in $H_0(\operatorname{curl}\operatorname{div}, \mathbb{T}; \Omega)$ as $n \to \infty$. Then by (3.1.15) and the distributional definition of $\operatorname{grad}\operatorname{curl} \boldsymbol{u}$, we have

$$\begin{aligned} &(\boldsymbol{u}, \boldsymbol{u}) + (\operatorname{grad}\operatorname{curl} \boldsymbol{u}, \operatorname{grad}\operatorname{curl} \boldsymbol{u}) = (\boldsymbol{u}, \operatorname{curl}\operatorname{div} \boldsymbol{V}) + (\boldsymbol{V}, \operatorname{grad}\operatorname{curl} \boldsymbol{u}) \\ &= \lim_{n\to\infty} (\boldsymbol{u}, \operatorname{curl}\operatorname{div} \boldsymbol{V}_n) + (\boldsymbol{V}_n, \operatorname{grad}\operatorname{curl} \boldsymbol{u}) = 0, \end{aligned}$$

which completes the proof. □

Now we are in a position to characterize $H_0(\operatorname{grad}\operatorname{curl}; \Omega)$.

Theorem 3.1.5. *The space* $H_0(\operatorname{grad}\operatorname{curl}; \Omega)$ *can be characterized as*

$$H_0(\operatorname{grad}\operatorname{curl}; \Omega) = \mathcal{N}(\gamma_{\tau,\mathrm{curl}}) := \{\boldsymbol{w} \in H(\operatorname{grad}\operatorname{curl}; \Omega) : \gamma_{\tau,\mathrm{curl}} \boldsymbol{w} = 0 \text{ on } \partial\Omega\}.$$

Proof. It follows from Theorem 3.1.1 that $\mathcal{N}(\gamma_{\tau,\mathrm{curl}})$ is closed. Then it is clear that $H_0(\operatorname{grad}\operatorname{curl}; \Omega) \subset \mathcal{N}(\gamma_{\tau,\mathrm{curl}})$ since $C_0^\infty(\Omega) \otimes \mathbb{V} \subset \mathcal{N}(\gamma_{\tau,\mathrm{curl}})$ and $\mathcal{N}(\gamma_{\tau,\mathrm{curl}})$ is closed. To prove the opposite, we first have

$$\{\boldsymbol{u} \in H(\operatorname{grad}\operatorname{curl}; \Omega) : (\operatorname{grad}\operatorname{curl} \boldsymbol{u}, \boldsymbol{\Phi}) + (\boldsymbol{u}, \operatorname{curl}\operatorname{div} \boldsymbol{\Phi}) = 0 \text{ for all } \boldsymbol{\Phi} \in C^\infty(\overline{\Omega}) \otimes \mathbb{T}\}$$

is a subset of $H_0(\operatorname{grad}\operatorname{curl}; \Omega)$ from Lemma 3.1.2. If $\boldsymbol{u} \in \mathcal{N}(\gamma_{\tau,\mathrm{curl}})$ and $\boldsymbol{u} \in C^\infty(\overline{\Omega}) \otimes \mathbb{V}$, then

$$(\operatorname{grad}\operatorname{curl} \boldsymbol{u}, \boldsymbol{\Phi}) + (\boldsymbol{u}, \operatorname{curl}\operatorname{div} \boldsymbol{\Phi}) = 0.$$

Since $C^\infty(\overline{\Omega}) \otimes \mathbb{V}$ is dense in $H(\operatorname{grad}\operatorname{curl}; \Omega)$ (Theorem 3.1.4), the equality also holds for $\boldsymbol{u} \in H(\operatorname{grad}\operatorname{curl}; \Omega)$. Therefore $\mathcal{N}(\gamma_{\tau,\mathrm{curl}})$ is a subset of

$$\{\boldsymbol{u} \in H(\operatorname{grad}\operatorname{curl}; \Omega) : (\operatorname{grad}\operatorname{curl} \boldsymbol{u}, \boldsymbol{\Phi}) + (\boldsymbol{u}, \operatorname{curl}\operatorname{div} \boldsymbol{\Phi}) = 0 \text{ for all } \boldsymbol{\Phi} \in C^\infty(\overline{\Omega}) \otimes \mathbb{T}\}.$$

□

3.2 Gradrot Complex and Hodge Laplacian

In this section, we present the grad rot complex in 2D. For any real number q, the grad rot *complex* reads:

$$0 \longrightarrow H^q(\Omega) \xrightarrow{\text{grad}} H^{q-1}(\Omega)\otimes\mathbb{V} \xrightarrow{\text{grad rot}} H^{q-3}(\Omega)\otimes\mathbb{V} \xrightarrow{\text{rot}} H^{q-4}(\Omega) \longrightarrow 0, \tag{3.2.1}$$

which is derived from the following diagram:

$$\begin{array}{ccccccccccc} 0 & \longrightarrow & H^q(\Omega) & \xrightarrow{\text{grad}} & H^{q-1}(\Omega)\otimes\mathbb{V} & \xrightarrow{\text{rot}} & H^{q-2}(\Omega) & \longrightarrow & 0 & \longrightarrow & 0 \\ & & & \overset{0}{\nearrow} & & \overset{\text{id}}{\nearrow} & & \overset{0}{\nearrow} & & \overset{0}{\nearrow} & \\ 0 & \longrightarrow & 0 & \longrightarrow & H^{q-2}(\Omega) & \xrightarrow{\text{grad}} & H^{q-3}(\Omega)\otimes\mathbb{V} & \xrightarrow{\text{rot}} & H^{q-4}(\Omega) & \longrightarrow & 0. \end{array} \tag{3.2.2}$$

Note that the dimension of cohomology at $H^{q-1}(\Omega)\otimes\mathbb{V}$ in the first row of (3.2.2) is the first Betti number b_1 of the domain, and the dimension of cohomology at H^{q-2} in the second row is 1 (kernel of grad is constants). According to Theorem 2.2.1 and Theorem 2.1.1

$$\mathcal{N}(\text{grad rot}, H^{q-1}(\Omega)\otimes\mathbb{V}) = \mathcal{R}(\text{grad}, H^q(\Omega)) \oplus \mathscr{H}^1_\infty, \tag{3.2.3}$$

where $\mathscr{H}^1_\infty$ is a set of smooth cohomology representatives (independent of q) with dimension $\dim \mathscr{H}^1_\infty = 1 + b_1$.

Remark 3.2.1. Define $\widetilde{K}_1 u := 1/2u\boldsymbol{x}^\perp$ and $\widetilde{K}_2\boldsymbol{v} := 1/2\boldsymbol{v}\cdot\boldsymbol{x}$. Then we can verify the condition (2.2.3) by defining K_1, K_2 in the way of (3.1.4).

The L^2 version of (3.2.1) with unbounded linear operators is as follows:

$$0 \longrightarrow L^2(\Omega) \xrightarrow{\text{grad}} L^2(\Omega)\otimes\mathbb{V} \xrightarrow{\text{grad rot}} L^2(\Omega)\otimes\mathbb{V} \xrightarrow{\text{rot}} L^2(\Omega) \longrightarrow 0. \tag{3.2.4}$$

3.2.1 Gradrot Complex without Boundary Conditions

Consider the following domain complex of (3.2.4)

$$0 \longrightarrow H^1(\Omega) \xrightarrow{\text{grad}} H(\text{grad rot};\Omega) \xrightarrow{\text{grad rot}} H(\text{rot};\Omega) \xrightarrow{\text{rot}} L^2(\Omega) \longrightarrow 0, \tag{3.2.5}$$

and its dual complex

$$0 \longleftarrow L_0^2(\Omega) \xleftarrow{-\operatorname{div}} H_0(\operatorname{div};\Omega) \xleftarrow{-\operatorname{curl}\operatorname{div}} H_0(\operatorname{curl}\operatorname{div};\Omega) \xleftarrow{\operatorname{curl}} H_0^1(\Omega) \longleftarrow 0. \tag{3.2.6}$$

Here $H_0(\operatorname{curl}\operatorname{div};\Omega)$ is the closure of $C_0^\infty(\Omega) \otimes \mathbb{V}$ in $H(\operatorname{curl}\operatorname{div};\Omega) = \{\boldsymbol{u} \in L^2 \otimes \mathbb{V} : \operatorname{curl}\operatorname{div}\boldsymbol{u} \in L^2 \otimes \mathbb{V}\}$. We will show in Section 3.2.4 that

$$H_0(\operatorname{curl}\operatorname{div};\Omega) = \{\boldsymbol{u} \in H(\operatorname{curl}\operatorname{div};\Omega) : \operatorname{div}\boldsymbol{u} = 0 \text{ and } \boldsymbol{u}\cdot\boldsymbol{n} = 0 \text{ on } \partial\Omega\},$$

and the adjoint of $(\operatorname{grad}\operatorname{rot}, H(\operatorname{grad}\operatorname{rot};\Omega))$ is $(-\operatorname{curl}\operatorname{div}, H_0(\operatorname{curl}\operatorname{div};\Omega))$.

Similar to (3.2.3), we have

$$\mathcal{N}(\operatorname{grad}\operatorname{rot}, H(\operatorname{grad}\operatorname{rot};\Omega)) = \mathcal{R}(\operatorname{grad}, H^1(\Omega)) \oplus \mathscr{H}_\infty^1 \tag{3.2.7}$$

with $\mathscr{H}_\infty^1$ defined in (3.2.3).

The Hodge decomposition at $H(\operatorname{grad}\operatorname{rot};\Omega)$ reads

$$L^2(\Omega)\otimes\mathbb{V} = \operatorname{grad} H^1(\Omega) \oplus \operatorname{curl}\operatorname{div} H_0(\operatorname{curl}\operatorname{div};\Omega) \oplus \mathfrak{H}^1,$$

where $\mathfrak{H}^1$ is the space of harmonic forms with $\dim\mathfrak{H}^1 = \dim\mathscr{H}_\infty^1$. In addition to the harmonic forms of the de Rham complex, i.e., the functions satisfying $\operatorname{rot}\boldsymbol{u} = 0$ and $\operatorname{div}\boldsymbol{u} = 0$, the function $\boldsymbol{u} = \operatorname{grad} p$ with p solving

$$\Delta p = 1 \text{ in } \Omega, \quad p = 0 \text{ on } \partial\Omega$$

is also a harmonic form in $\mathfrak{H}$.

The Hodge Laplacian operator follows from the abstract definition:

$$\mathscr{L}^1 := -(\operatorname{curl}\operatorname{div})\operatorname{grad}\operatorname{rot} - \operatorname{grad}\operatorname{div} = -\operatorname{curl}\Delta\operatorname{rot} - \operatorname{grad}\operatorname{div},$$

with the domain $D_{\mathscr{L}^1} = \{\boldsymbol{u} \in X : \operatorname{grad}\operatorname{rot}\boldsymbol{u} \in H_0(\operatorname{curl}\operatorname{div};\Omega), \operatorname{div}\boldsymbol{u} \in H^1(\Omega)\}$. For $\boldsymbol{f} \in L^2(\Omega)\otimes\mathbb{V}$, the strong formulation of the Hodge Laplacian boundary value problem seeks $\boldsymbol{u} \in D_{\mathscr{L}^1}$ and $\boldsymbol{u} \perp \mathfrak{H}^1$ such that

$$-\operatorname{curl}\Delta\operatorname{rot}\boldsymbol{u} - \operatorname{grad}\operatorname{div}\boldsymbol{u} = \boldsymbol{f} - P_{\mathfrak{H}^1}\boldsymbol{f} \quad \text{in } \Omega. \tag{3.2.8}$$

3.2.2 Gradrot Complex with Boundary Conditions

Define

$$H_0(\operatorname{grad}\operatorname{rot};\Omega) := \text{ closure of } C_0^\infty(\Omega)\otimes\mathbb{V} \text{ in the sense of } H(\operatorname{grad}\operatorname{rot}) \text{ norm.}$$

We will show in Section 3.2.4 that

$$H_0(\operatorname{grad}\operatorname{rot};\Omega) := \{\boldsymbol{u}\in H(\operatorname{grad}\operatorname{rot};\Omega):\ \boldsymbol{u}\cdot\boldsymbol{\tau}=0 \text{ and } \operatorname{rot}\boldsymbol{u}=0\}.$$

Consider the domain complex of (3.2.4) with vanishing boundary conditions:

$$0 \longrightarrow H_0^1(\Omega) \xrightarrow{\operatorname{grad}} H_0(\operatorname{grad}\operatorname{rot};\Omega) \xrightarrow{\operatorname{grad}\operatorname{rot}} H_0(\operatorname{rot};\Omega) \xrightarrow{\operatorname{rot}} L_0^2(\Omega) \longrightarrow 0, \tag{3.2.9}$$

which is derived from the following diagram:

$$\begin{array}{ccccccccccc}
0 & \longrightarrow & H_0^1(\Omega) & \xrightarrow{\operatorname{grad}} & H_0(\operatorname{grad}\operatorname{rot};\Omega) & \xrightarrow{\operatorname{rot}} & H_0^1(\Omega) & \longrightarrow & 0 & \longrightarrow & 0 \\
 & & & \nearrow^{0} & & \nearrow^{\mathrm{id}} & & \nearrow^{0} & & \nearrow^{0} & \\
0 & \longrightarrow & 0 & \longrightarrow & H_0^1(\Omega) & \xrightarrow{\operatorname{grad}} & H_0(\operatorname{rot};\Omega) & \xrightarrow{\operatorname{rot}} & L_0^2(\Omega) & \longrightarrow & 0.
\end{array} \tag{3.2.10}$$

The dimension of the cohomology at $H_0(\operatorname{grad}\operatorname{rot};\Omega)$ in the first row of (3.2.10) is b_2, and the dimension of the cohomology at $H_0^1(\Omega)$ in the second row of (3.2.10) is 0. Therefore, we have

$$\mathcal{N}(\operatorname{grad}\operatorname{rot}, H_0(\operatorname{grad}\operatorname{rot};\Omega)) = \mathcal{R}(\operatorname{grad}, H_0^1(\Omega)) \oplus \mathscr{H}_\infty^{1,0},$$

where $\mathscr{H}_\infty^{1,0}$ is a set of smooth cohomology representatives with $\dim\mathscr{H}_\infty^{1,0} = b_2$.

The dual complex of (3.2.9) is:

$$0 \longleftarrow L^2(\Omega) \xleftarrow{-\operatorname{div}} H(\operatorname{div};\Omega) \xleftarrow{-\operatorname{curl}\operatorname{div}} H(\operatorname{curl}\operatorname{div};\Omega) \xleftarrow{\operatorname{curl}} H^1(\Omega) \longleftarrow 0. \tag{3.2.11}$$

The Hodge decomposition at $H_0(\operatorname{grad}\operatorname{rot})$ reads:

$$L^2(\Omega)\otimes\mathbb{V} = \operatorname{grad} H_0^1(\Omega) \oplus \operatorname{curl}\operatorname{div} H(\operatorname{curl}\operatorname{div};\Omega) \oplus \mathfrak{H}_0^1 \tag{3.2.12}$$

with $\dim\mathfrak{H}_0^1 = \dim\mathscr{H}_\infty^{1,0} = b_2$. The space $\mathfrak{H}_0^1$ is vanishing for any bounded domain in 2D.

Define

$$X_0 := H_0(\operatorname{grad}\operatorname{rot};\Omega) \cap H(\operatorname{div};\Omega).$$

We define the Hodge Laplacian operator $\mathscr{L}^1$ in the previous way but with the domain

$$D_{\mathscr{L}^1,0} = \{\boldsymbol{u} \in X_0 : \operatorname{grad}\operatorname{rot}\boldsymbol{u} \in H(\operatorname{curl}\operatorname{div};\Omega), \operatorname{div}\boldsymbol{u} \in H_0^1(\Omega)\}.$$

For $\boldsymbol{f} \in L^2(\Omega) \otimes \mathbb{V}$, the strong formulation of the Hodge Laplacian boundary value problem seeks $\boldsymbol{u} \in D_{\mathscr{L}^1,0}$ and $\boldsymbol{u} \perp \mathfrak{H}_0^1$ such that

$$-\operatorname{curl}\Delta\operatorname{rot}\boldsymbol{u} - \operatorname{grad}\operatorname{div}\boldsymbol{u} = \boldsymbol{f} - P_{\mathfrak{H}_0^1}\boldsymbol{f} \text{ in } \Omega. \tag{3.2.13}$$

This problem is related to the problem considered in the following chapter, especially when $\boldsymbol{f} \in \operatorname{curl}\operatorname{div} H(\operatorname{curl}\operatorname{div};\Omega)$.

In the case of $\boldsymbol{f} \in \operatorname{curl}\operatorname{div} H(\operatorname{curl}\operatorname{div};\Omega)$, the problem (3.2.13) is then to find $\boldsymbol{u}$ such that $\boldsymbol{u} \perp \mathfrak{H}_0^1$ and

$$\begin{aligned} -\operatorname{curl}\Delta\operatorname{rot}\boldsymbol{u} &= \boldsymbol{f} && \text{in } \Omega,\\ \operatorname{div}\boldsymbol{u} &= 0 && \text{in } \Omega,\\ \boldsymbol{u}\cdot\boldsymbol{\tau} &= 0 && \text{on } \partial\Omega,\\ \operatorname{rot}\boldsymbol{u} &= 0 && \text{on } \partial\Omega. \end{aligned} \tag{3.2.14}$$

3.2.3 Gradrot Complex with Partial Boundary Conditions

Define

$$H_{\mathrm{rot}}(\operatorname{grad}\operatorname{rot};\Omega) := \{\boldsymbol{u} \in H(\operatorname{grad}\operatorname{rot};\Omega) : \ \operatorname{rot}\boldsymbol{u} = 0\}$$

We consider a domain complex of (3.2.4) with partial vanishing boundary conditions:

$$0 \longrightarrow H^1(\Omega) \xrightarrow{\operatorname{grad}} H_{\mathrm{rot}}(\operatorname{grad}\operatorname{rot};\Omega) \xrightarrow{\operatorname{grad}\operatorname{rot}} H_0(\operatorname{rot};\Omega) \xrightarrow{\operatorname{rot}} L_0^2(\Omega) \longrightarrow 0, \tag{3.2.15}$$

which is somewhere between the complexes (3.2.5) and (3.2.9). The above complex is derived from the following diagram:

$$
\begin{array}{ccccccccccc}
0 \longrightarrow & H^1(\Omega) & \xrightarrow{\text{grad}} & H_{\text{rot}}(\operatorname{grad}\operatorname{rot};\Omega) & \xrightarrow{\text{rot}} & H_0^1(\Omega) & \longrightarrow & 0 & \longrightarrow & 0 & \\
 & & \overset{0}{\nearrow} & & \overset{\text{id}}{\nearrow} & & \overset{0}{\nearrow} & & \overset{0}{\nearrow} & & \\
0 \longrightarrow & 0 & \longrightarrow & H_0^1(\Omega) & \xrightarrow{\text{grad}} & H_0(\operatorname{rot};\Omega) & \xrightarrow{\text{rot}} & L_0^2(\Omega) & \longrightarrow & 0. &
\end{array}
\tag{3.2.16}
$$

The dimension of the de Rham complex cohomology at $H_{\text{rot}}(\operatorname{grad}\operatorname{rot};\Omega)$ in the first row of (3.2.16) is b_1, and the dimension of the de Rham complex cohomology at $H_0^1(\Omega)$ in the second row of (3.2.16) is 0. Consequently,

$$\mathcal{N}(\operatorname{grad}\operatorname{rot}, H_{\text{rot}}(\operatorname{grad}\operatorname{rot};\Omega)) = \mathcal{R}(\operatorname{grad}, H^1(\Omega)) \oplus \mathscr{H}_\infty^{1,\text{rot}},$$

where $\mathscr{H}_\infty^{1,\text{rot}}$ is a set of smooth cohomology representatives with $\dim \mathscr{H}_\infty^{1,\text{rot}} = b_1$.

The dual complex of (3.2.15) is:

$$0 \longleftarrow L_0^2(\Omega) \xleftarrow{-\operatorname{div}} H_0(\operatorname{div};\Omega) \xleftarrow{-\operatorname{curl}\operatorname{div}} H_{\text{div}}(\operatorname{curl}\operatorname{div};\Omega) \xleftarrow{\operatorname{curl}} H^1(\Omega) \longleftarrow 0. \tag{3.2.17}$$

Here $H_{\text{div}}(\operatorname{curl}\operatorname{div};\Omega)$ is a formal notation for the domain of the adjoint of the operator $(\operatorname{grad}\operatorname{rot}, H_{\text{rot}}(\operatorname{grad}\operatorname{rot};\Omega))$. We will provide a characterization for this space in Section 3.2.4 to show that it is a subspace of $H(\operatorname{curl}\operatorname{div};\Omega)$ with the boundary condition $\operatorname{div}\boldsymbol{u} = 0$.

The Hodge decomposition at $H_{\text{rot}}(\operatorname{grad}\operatorname{rot})$ reads:

$$L^2(\Omega) \otimes \mathbb{V} = \operatorname{grad} H^1(\Omega) \oplus \operatorname{curl}\operatorname{div} H_{\text{div}}(\operatorname{curl}\operatorname{div};\Omega) \oplus \mathfrak{H}_{\text{rot}}^1 \tag{3.2.18}$$

with $\dim \mathfrak{H}_{\text{rot}}^1 = \dim \mathscr{H}_\infty^{1,\text{rot}} = b_1$. The space $\mathfrak{H}_{\text{rot}}^1$ is trivial if Ω is simply-connected. Define

$$X_{\text{rot}} := H_{\text{rot}}(\operatorname{grad}\operatorname{rot};\Omega) \cap H_0(\operatorname{div};\Omega).$$

The domain of the Hodge Laplacian operator $\mathscr{L}^1$ is

$$D_{\mathscr{L}^1,\text{rot}} = \{\boldsymbol{u} \in X_{\text{rot}} : \operatorname{grad}\operatorname{rot}\boldsymbol{u} \in H_{\text{div}}(\operatorname{curl}\operatorname{div};\Omega), \operatorname{div}\boldsymbol{u} \in H^1(\Omega)\}.$$

For $\boldsymbol{f} \in L^2(\Omega) \otimes \mathbb{V}$, the strong formulation of the Hodge Laplacian boundary value problem seeks $\boldsymbol{u} \in D_{\mathscr{L}^1,\mathrm{rot}}$ and $\boldsymbol{u} \perp \mathfrak{H}^1_{\mathrm{rot}}$ such that

$$-\operatorname{curl} \Delta \operatorname{rot} \boldsymbol{u} - \operatorname{grad} \operatorname{div} \boldsymbol{u} = \boldsymbol{f} - P_{\mathfrak{H}^1_{\mathrm{rot}}} \boldsymbol{f} \quad \text{in } \Omega. \tag{3.2.19}$$

3.2.4 Characterization of $H_0(\operatorname{grad}\operatorname{rot})$, $H_0(\operatorname{curl}\operatorname{div})$ and $H_{\mathrm{div}}(\operatorname{curl}\operatorname{div})$

In this section, we provide a characterization for the spaces $H_0(\operatorname{grad}\operatorname{rot};\Omega)$, $H_0(\operatorname{curl}\operatorname{div};\Omega)$, and $H_{\mathrm{div}}(\operatorname{curl}\operatorname{div};\Omega)$.

Theorem 3.2.1. *Define* $\gamma_{\tau,\mathrm{rot}}\boldsymbol{u} = \{\boldsymbol{u}\cdot\boldsymbol{\tau}, \operatorname{rot}\boldsymbol{u}\}$. *Then* $\gamma_{\tau,\mathrm{rot}}$ *is a linear bounded operator from* $H(\operatorname{grad}\operatorname{rot};\Omega)$ *to* $H^{-1/2}(\partial\Omega) \times H^{1/2}(\partial\Omega)$ *with the bound:*

$$\|\gamma_{\tau,\mathrm{rot}}\boldsymbol{u}\|_{H^{-1/2}(\partial\Omega)\times H^{1/2}(\partial\Omega)} \leq C\|\boldsymbol{u}\|_{H(\operatorname{grad}\operatorname{rot};\Omega)}.$$

Proof. Since $\gamma_\tau \boldsymbol{u} = \boldsymbol{u}\cdot\boldsymbol{\tau}$ is a linear bounded operator from $H(\operatorname{rot};\Omega)$ to $H^{-1/2}(\partial\Omega)$ and $\operatorname{tr} v = v|_{\partial\Omega}$ is a linear bounded operator from $H^1(\Omega)$ to $H^{1/2}(\partial\Omega)$, we obtain

$$\|\gamma_{\tau,\mathrm{rot}}\boldsymbol{u}\|^2_{H^{-1/2}(\partial\Omega)\times H^{1/2}(\partial\Omega)} \leq C\|\boldsymbol{u}\|^2_{H(\mathrm{rot};\Omega)} + C\|\operatorname{rot}\boldsymbol{u}\|^2_{H^1(\Omega)},$$

which completes the proof by the equivalence between the norms $\|\cdot\|_{H(\operatorname{grad}\operatorname{rot};\Omega)}$ and $|||\cdot|||_{H(\operatorname{grad}\operatorname{rot};\Omega)}$, see Section 2.1.4. □

Similarly, we have

Theorem 3.2.2. *Define* $\gamma_{n,\mathrm{div}}\boldsymbol{u} = \{\boldsymbol{u}\cdot\boldsymbol{n}, \operatorname{div}\boldsymbol{u}\}$. *Then* $\gamma_{n,\mathrm{div}}$ *is a linear bounded operator from* $H(\operatorname{curl}\operatorname{div};\Omega)$ *to* $H^{-1/2}(\partial\Omega) \times H^{1/2}(\partial\Omega)$ *with the bound:*

$$\|\gamma_{n,\mathrm{div}}\boldsymbol{u}\|_{H^{-1/2}(\partial\Omega)\times H^{1/2}(\partial\Omega)} \leq C\|\boldsymbol{u}\|_{H(\operatorname{curl}\operatorname{div};\Omega)}.$$

Theorem 3.2.3. *The trace operator* $\gamma_{\tau,\mathrm{rot}}$ *is surjective from* $H(\operatorname{grad}\operatorname{rot};\Omega)$ *to* $H^{-1/2}(\partial\Omega)\times H^{1/2}(\partial\Omega)$. *That is, for any* $g_1 \in H^{-1/2}(\partial\Omega)$ *and* $g_2 \in H^{1/2}(\partial\Omega)$, *there exists* $\boldsymbol{u} \in H(\operatorname{grad}\operatorname{rot};\Omega)$ *such that* $\boldsymbol{u}\cdot\boldsymbol{\tau}|_{\partial\Omega} = g_1$, $\operatorname{rot}\boldsymbol{u}|_{\partial\Omega} = g_2$, *and*

$$\|\boldsymbol{u}\|_{H(\operatorname{grad}\operatorname{rot};\Omega)} \leq C\left(\|g_1\|_{H^{-1/2}(\partial\Omega)} + \|g_2\|_{H^{1/2}(\partial\Omega)}\right).$$

Proof. For $g_2 \in H^{1/2}(\partial\Omega)$, there exists $v \in H^1(\Omega)$ such that $v|_{\partial\Omega} = g_2$ and

$$\|v\|_{H^1(\Omega)} \le C\|g_2\|_{H^{1/2}(\partial\Omega)}.$$

Take $\boldsymbol{x}_0$ and r such that $B(\boldsymbol{x}_0, r) \subset \Omega$ and define

$$\eta_{r,\boldsymbol{x}_0}(\boldsymbol{x}) = \frac{1}{r^2}\eta\Big(\frac{\boldsymbol{x}-\boldsymbol{x}_0}{r}\Big)$$

with η defined in the proof of Theorem 3.1.2. Then we have $\eta_{r,\boldsymbol{x}_0}(x) \in C_0^\infty(\Omega)$ and $\int_\Omega \eta_{r,\boldsymbol{x}_0}(\boldsymbol{x})\mathrm{d}\boldsymbol{x} = 1$. Let $C_0 = \langle g_1, 1\rangle_{\partial\Omega} - (v, 1)$ and $\widetilde{v} = v + C_0\eta_{r,\boldsymbol{x}_0}$. Then we have

$$(\widetilde{v}, 1) = (v, 1) + C_0(\eta_{r,\boldsymbol{x}_0}, 1) = \langle g_1, 1\rangle_{\partial\Omega},$$

and

$$\begin{aligned}\|\widetilde{v}\|_{H^1(\Omega)} &\le \|v\|_{H^1(\Omega)} + C\big(\langle g_1, 1\rangle_{\partial\Omega} - (v, 1)\big)\\ &\le C\left(\|v\|_{H^1(\Omega)} + \|g_1\|_{H^{-1/2}(\partial\Omega)}\right)\\ &\le C\left(\|g_2\|_{H^{1/2}(\partial\Omega)} + \|g_1\|_{H^{-1/2}(\partial\Omega)}\right). \end{aligned} \tag{3.2.20}$$

Now we seek $w \in H^1(\Omega)$ such that

$$\begin{aligned} -\Delta w &= -\widetilde{v} \text{ in } \Omega,\\ \frac{\partial w}{\partial \boldsymbol{n}} &= g_1 \text{ on } \partial\Omega, \end{aligned}$$

where $\widetilde{v}$ and g_1 satisfy

$$-(\widetilde{v}, 1) + \langle g_1, 1\rangle_{\partial\Omega} = 0.$$

By virtual of the regularity result of the elliptic problem [49, Theorem 3.18], we have

$$\|w\|_{H^1(\Omega)} \le C\left(\|\widetilde{v}\| + \|g_1\|_{H^{-1/2}(\partial\Omega)}\right). \tag{3.2.21}$$

Take $\boldsymbol{u} = \operatorname{curl} w$. Then $\boldsymbol{u} \in L^2(\Omega)$ and $\operatorname{rot}\boldsymbol{u} = \Delta w = \widetilde{v} \in H^1(\Omega)$, and hence $\boldsymbol{u} \in H(\operatorname{grad}\operatorname{rot};\Omega)$. Restricted on $\partial\Omega$, $\boldsymbol{u}$ satisfies

$$\boldsymbol{u}\cdot\boldsymbol{\tau} = \operatorname{curl} w\cdot\boldsymbol{\tau} = \operatorname{grad} w\cdot\boldsymbol{n} = g_1,$$

$$\operatorname{rot} \boldsymbol{u} = \Delta w = \widetilde{v} = v = g_2.$$

Combining (3.2.20) and (3.2.21), we obtain

$$\begin{aligned}
\|\boldsymbol{u}\|_{H(\operatorname{grad}\operatorname{rot};\Omega)} &= \|\boldsymbol{u}\| + \|\operatorname{grad}\operatorname{rot} \boldsymbol{u}\| \\
&= \|\operatorname{curl} w\| + \|\operatorname{grad} \widetilde{v}\| \\
&\le \|w\|_{H^1(\Omega)} + \|\widetilde{v}\|_{H^1(\Omega)} \\
&\le C\left(\|\widetilde{v}\| + \|g_1\|_{H^{-1/2}(\partial\Omega)}\right) + \|\widetilde{v}\|_{H^1(\Omega)} \\
&\le C\left(\|g_1\|_{H^{-1/2}(\partial\Omega)} + \|g_2\|_{H^{1/2}(\partial\Omega)}\right).
\end{aligned}$$

□

Proceeding as the proof of Theorem 3.1.4, we can show the following density.

Theorem 3.2.4. *$C^\infty(\overline{\Omega}) \otimes \mathbb{V}$ is dense in $H(\operatorname{grad}\operatorname{rot};\Omega)$.*

Theorem 3.2.5. *$C^\infty(\overline{\Omega}) \otimes \mathbb{V}$ is dense in $H(\operatorname{curl}\operatorname{div};\Omega)$.*

Lemma 3.2.6. *For $\boldsymbol{u} \in H(\operatorname{grad}\operatorname{rot};\Omega)$ and $\boldsymbol{w} \in H(\operatorname{curl}\operatorname{div};\Omega)$, the following identity holds*

$$(\boldsymbol{u}, \operatorname{curl}\operatorname{div} \boldsymbol{w}) + (\operatorname{grad}\operatorname{rot} \boldsymbol{u}, \boldsymbol{w}) = \langle \boldsymbol{u}\cdot\boldsymbol{\tau}, \operatorname{div} \boldsymbol{w}\rangle_{\partial\Omega} + \langle \boldsymbol{w}\cdot\boldsymbol{n}, \operatorname{rot} \boldsymbol{u}\rangle_{\partial\Omega}. \tag{3.2.22}$$

Proof. It is easy to check that (3.2.22) holds for smooth functions $\boldsymbol{u}, \boldsymbol{w}$. By Theorems 3.2.1, 3.2.2, 3.2.4, and 3.2.5, we can prove (3.2.22) for $\boldsymbol{u} \in H(\operatorname{grad}\operatorname{rot};\Omega)$ and $\boldsymbol{w} \in H(\operatorname{curl}\operatorname{div};\Omega)$. □

Now we are in a position to characterize $H_0(\operatorname{grad}\operatorname{rot};\Omega)$ and $H_0(\operatorname{curl}\operatorname{div};\Omega)$.

Theorem 3.2.7. *The space $H_0(\operatorname{grad}\operatorname{rot};\Omega)$ can be characterized as*

$$H_0(\operatorname{grad}\operatorname{rot};\Omega) = \{\boldsymbol{w} \in H(\operatorname{grad}\operatorname{rot};\Omega) : \gamma_{\tau,\mathrm{rot}}\boldsymbol{w} = 0 \text{ on } \partial\Omega\}.$$

Proof. Recalling $H_0(\operatorname{grad}\operatorname{rot};\Omega)$ = closure of $C_0^\infty(\Omega)\otimes\mathbb{V}$ in the sense of $H(\operatorname{grad}\operatorname{rot})$ norm, we write

$$H(\operatorname{grad}\operatorname{rot};\Omega) = H_0(\operatorname{grad}\operatorname{rot};\Omega) \oplus \big(H_0(\operatorname{grad}\operatorname{rot};\Omega)\big)^{\perp}.$$

We then show $\boldsymbol{w}=0$ if $\boldsymbol{w}\in\big(H_0(\operatorname{grad}\operatorname{rot};\Omega)\big)^{\perp}$ and $\gamma_{\tau,\mathrm{rot}}\boldsymbol{w}=\{\boldsymbol{w}\cdot\boldsymbol{\tau},\operatorname{rot}\boldsymbol{w}\}=0$. Since $\boldsymbol{w}\in\big(H_0(\operatorname{grad}\operatorname{rot};\Omega)\big)^{\perp}$,

$$(\boldsymbol{w},\boldsymbol{v}) + (\operatorname{grad}\operatorname{rot}\boldsymbol{w},\operatorname{grad}\operatorname{rot}\boldsymbol{v}) = 0 \text{ for all } \boldsymbol{v}\in C_0^\infty(\Omega)\otimes\mathbb{V},$$

which implies $\boldsymbol{w}=\operatorname{curl}\operatorname{div}\operatorname{grad}\operatorname{rot}\boldsymbol{w}$. Denote $\boldsymbol{u}=\operatorname{grad}\operatorname{rot}\boldsymbol{w}$, then $\boldsymbol{u}\in H(\operatorname{curl}\operatorname{div};\Omega)$. Applying (3.2.22), we obtain

$$\begin{aligned}(\boldsymbol{w},\boldsymbol{w}) + (\operatorname{grad}\operatorname{rot}\boldsymbol{w},\operatorname{grad}\operatorname{rot}\boldsymbol{w}) &= (\boldsymbol{w},\operatorname{curl}\operatorname{div}\boldsymbol{u}) + (\operatorname{grad}\operatorname{rot}\boldsymbol{w},\boldsymbol{u})\\ &=\langle\boldsymbol{w}\cdot\boldsymbol{\tau},\operatorname{div}\boldsymbol{u}\rangle_{\partial\Omega} + \langle\boldsymbol{u}\cdot\boldsymbol{n},\operatorname{rot}\boldsymbol{w}\rangle_{\partial\Omega} = 0,\end{aligned}$$

which yields $\boldsymbol{w}=0$. □

Similarly, we can show

Theorem 3.2.8. *The space* $H_0(\operatorname{curl}\operatorname{div};\Omega)$ *can be characterized as*

$$H_0(\operatorname{curl}\operatorname{div};\Omega) = \{\boldsymbol{w}\in H(\operatorname{curl}\operatorname{div};\Omega) : \gamma_{n,\mathrm{div}}\boldsymbol{w}=0 \textit{ on } \partial\Omega\}.$$

Next we compute the adjoint operators of grad rot with domains $H(\operatorname{grad}\operatorname{rot};\Omega))$ and $H_{\mathrm{rot}}(\operatorname{grad}\operatorname{rot};\Omega))$.

Theorem 3.2.9. *The adjoint of* $(\operatorname{grad}\operatorname{rot}, H(\operatorname{grad}\operatorname{rot};\Omega))$ *is* $(-\operatorname{curl}\operatorname{div}, H_0(\operatorname{curl}\operatorname{div};\Omega))$.

Proof. If $\boldsymbol{w}$ belongs to the domain of the adjoint of $(\operatorname{grad}\operatorname{rot}, H(\operatorname{grad}\operatorname{rot};\Omega))$, then there exists $\boldsymbol{v}\in L^2(\Omega)\otimes\mathbb{V}$ such that

$$(\operatorname{grad}\operatorname{rot}\boldsymbol{u},\boldsymbol{w}) = -(\boldsymbol{u},\boldsymbol{v}), \quad \boldsymbol{u}\in H(\operatorname{grad}\operatorname{rot};\Omega).$$

Such a function $\boldsymbol{w}$ must be in $H(\operatorname{curl}\operatorname{div};\Omega)$ and satisfies $\operatorname{curl}\operatorname{div}\boldsymbol{w}=\boldsymbol{v}$. Therefore, $\boldsymbol{w}$

belongs to the domain of the adjoint of $(\operatorname{grad}\operatorname{rot}, H(\operatorname{grad}\operatorname{rot};\Omega))$ if and only if

$$(\operatorname{grad}\operatorname{rot}\boldsymbol{u},\boldsymbol{w}) = -(\boldsymbol{u},\operatorname{curl}\operatorname{div}\boldsymbol{w}),\quad \boldsymbol{u}\in H(\operatorname{grad}\operatorname{rot};\Omega).$$

From Lemma 3.2.6, the above identity holds if and only if

$$\langle \boldsymbol{u}\cdot\boldsymbol{\tau},\operatorname{div}\boldsymbol{w}\rangle_{\partial\Omega} + \langle \boldsymbol{w}\cdot\boldsymbol{n},\operatorname{rot}\boldsymbol{u}\rangle_{\partial\Omega} = 0.$$

which holds when $\gamma_{n,\operatorname{div}}\boldsymbol{w} = \{\boldsymbol{w}\cdot\boldsymbol{n},\operatorname{div}\boldsymbol{w}\} = 0$ since $\gamma_{\tau,\operatorname{rot}}$ is surjective from $H(\operatorname{grad}\operatorname{rot};\Omega)$ to $H^{-1/2}(\partial\Omega)\times H^{1/2}(\partial\Omega)$ (see Theorem 3.2.3). □

Theorem 3.2.10. *Denote*

$$H_{\operatorname{div}}(\operatorname{curl}\operatorname{div};\Omega) = \{\boldsymbol{w}\in H(\operatorname{curl}\operatorname{div};\Omega) : \operatorname{div}\boldsymbol{w} = 0 \text{ on } \partial\Omega\}.$$

Then the adjoint of $(\operatorname{grad}\operatorname{rot}, H_{\operatorname{rot}}(\operatorname{grad}\operatorname{rot};\Omega))$ *is* $(-\operatorname{curl}\operatorname{div}, H_{\operatorname{div}}(\operatorname{curl}\operatorname{div};\Omega))$.

Proof. The proof is similar to that of Theorem 3.2.9. □

3.3 Graddiv Complex and Hodge Laplacian

In this section, we present the grad div complex. For any real number q, the grad div *complex* reads:

$$0 \longrightarrow H^q \xrightarrow{\operatorname{grad}} H^{q-1}\otimes\mathbb{V} \xrightarrow{\operatorname{curl}} H^{q-2}\otimes\mathbb{V} \xrightarrow{\operatorname{grad}\operatorname{div}} H^{q-4}\otimes\mathbb{V} \xrightarrow{\operatorname{curl}} H^{q-5}\otimes\mathbb{V} \xrightarrow{\operatorname{div}} H^{q-6} \longrightarrow 0,$$

which is derived from the following diagram:

$$\begin{array}{cccccccccccccc}
0 \longrightarrow & H^q & \xrightarrow{\operatorname{grad}} & H^{q-1}\otimes\mathbb{V} & \xrightarrow{\operatorname{curl}} & H^{q-2}\otimes\mathbb{V} & \xrightarrow{\operatorname{div}} & H^{q-3} & \longrightarrow & 0 & \longrightarrow & 0 & \longrightarrow & 0 \\
& & \overset{0}{\nearrow} & & \overset{0}{\nearrow} & & \overset{\operatorname{id}}{\nearrow} & & \overset{0}{\nearrow} & & \overset{0}{\nearrow} & & & \\
0 \longrightarrow & 0 & \longrightarrow & 0 & \longrightarrow & H^{q-3} & \xrightarrow{\operatorname{grad}} & H^{q-4}\otimes\mathbb{V} & \xrightarrow{\operatorname{curl}} & H^{q-5}\otimes\mathbb{V} & \xrightarrow{\operatorname{div}} & H^{q-6} & \longrightarrow & 0.
\end{array}$$

Note that the dimension of cohomology at $H^{q-2}(\Omega)\otimes\mathbb{V}$ in the first row of the above diagram is b_2 of the domain, and the dimension of cohomology at H^{q-3} in the second row is 1. According to Theorem 2.2.1 and Theorem 2.1.1

$$\mathcal{N}(\operatorname{grad}\operatorname{div}, H^{q-2}(\Omega)\otimes\mathbb{V}) = \mathcal{R}(\operatorname{curl}, H^{q-1}(\Omega)) \oplus \mathscr{H}^2_\infty, \tag{3.3.1}$$

where $\mathscr{H}^2_\infty$ is a set of smooth cohomology representatives (independent of q) with dimension $\dim \mathscr{H}^2_\infty = 1 + b_2$.

Remark 3.3.1. Define $\widetilde{K}_1 u := 1/3u\boldsymbol{x}$ and $\widetilde{K}_2 \boldsymbol{v} := 1/3\boldsymbol{v} \cdot \boldsymbol{x}$. Then we can verify the condition (2.2.3) by defining K_1, K_2 in the way of (3.1.4).

The L^2 version of the grad div complex with unbounded linear operators is as follows:

$$0 \longrightarrow L^2 \xrightarrow{\text{grad}} L^2 \otimes \mathbb{V} \xrightarrow{\text{curl}} L^2 \otimes \mathbb{V} \xrightarrow{\text{grad div}} L^2 \otimes \mathbb{V} \xrightarrow{\text{curl}} L^2 \otimes \mathbb{V} \xrightarrow{\text{div}} L^2 \longrightarrow 0. \tag{3.3.2}$$

3.3.1 Graddiv Complex without Boundary Conditions

Consider the following domain complex of (3.3.2)

$$0 \longrightarrow H^1 \xrightarrow{\text{grad}} H(\text{curl}) \xrightarrow{\text{curl}} H(\text{grad div}) \xrightarrow{\text{grad div}} H(\text{curl}) \xrightarrow{\text{curl}} H(\text{div}) \xrightarrow{\text{div}} L^2 \longrightarrow 0.$$

and its dual complex

$$0 \longleftarrow L^2_0 \xleftarrow{-\text{div}} H_0(\text{div}) \xleftarrow{\text{curl}} H_0(\text{curl}) \xleftarrow{\text{grad div}} H_0(\text{grad div}) \xleftarrow{\text{curl}} H_0(\text{curl}) \xleftarrow{-\text{grad}} H^1_0 \longleftarrow 0.$$

Here $H_0(\text{grad div}; \Omega) :=$ closure of $C_0^\infty(\Omega) \otimes \mathbb{V}$ in the sense of $H(\text{grad div})$ norm. We will show in Section 3.3.4 that

$$H_0(\text{grad div}; \Omega) := \{\boldsymbol{u} \in H(\text{grad div}; \Omega) : \ \boldsymbol{u} \cdot \boldsymbol{n} = 0 \text{ and } \operatorname{div} \boldsymbol{u} = 0\},$$

and the adjoint of $(\text{grad div}, H(\text{grad div}; \Omega))$ is $(\text{grad div}, H_0(\text{grad div}; \Omega))$.

Similar to (3.3.1), we have

$$\mathcal{N}(\text{grad div}, H(\text{grad div}; \Omega)) = \mathcal{R}(\text{curl}, H(\text{curl}; \Omega)) \oplus \mathscr{H}^2_\infty \tag{3.3.3}$$

with $\mathscr{H}^2_\infty$ defined in (3.3.1).

The Hodge decomposition at $H(\text{grad div}; \Omega)$ is as follows:

$$L^2(\Omega) \otimes \mathbb{V} = \text{curl}\, H(\text{curl}; \Omega) \oplus \text{grad div}\, H_0(\text{grad div}; \Omega) \oplus \mathfrak{H}^2,$$

where $\mathfrak{H}^2$ is the space of harmonic forms with $\dim \mathfrak{H}^2 = \dim \mathscr{H}^2_\infty$.

Denote

$$Y = H(\operatorname{grad}\operatorname{div};\Omega) \cap H_0(\operatorname{curl}).$$

The Hodge Laplacian operator follows from the abstract definition:

$$\mathscr{L}^2 := (\operatorname{grad}\operatorname{div})\operatorname{grad}\operatorname{div} + \operatorname{curl}\operatorname{curl} = \operatorname{grad}\Delta\operatorname{div} + \operatorname{curl}\operatorname{curl},$$

with the domain $D_{\mathscr{L}^2} = \{\boldsymbol{u} \in Y : \operatorname{grad}\operatorname{div}\boldsymbol{u} \in H_0(\operatorname{grad}\operatorname{div};\Omega), \operatorname{curl}\boldsymbol{u} \in H_0(\operatorname{div};\Omega)\}$. For $\boldsymbol{f} \in L^2(\Omega)\otimes\mathbb{V}$, the strong formulation of the Hodge Laplacian boundary value problem seeks $\boldsymbol{u} \in D_{\mathscr{L}^2}$ and $\boldsymbol{u} \perp \mathfrak{H}^2$ such that

$$\operatorname{grad}\Delta\operatorname{div} - \operatorname{curl}\operatorname{curl} = \boldsymbol{f} - P_{\mathfrak{H}^2}\boldsymbol{f} \quad \text{in } \Omega.$$

3.3.2 Graddiv Complex with Boundary Conditions

Consider the domain complex of (3.3.2) with vanishing boundary conditions:

$$0 \longrightarrow H_0^1 \xrightarrow{\operatorname{grad}} H_0(\operatorname{curl}) \xrightarrow{\operatorname{curl}} H_0(\operatorname{grad}\operatorname{div}) \xrightarrow{\operatorname{grad}\operatorname{div}} H_0(\operatorname{curl}) \xrightarrow{\operatorname{curl}} H_0(\operatorname{div}) \xrightarrow{\operatorname{div}} L_0^2 \longrightarrow 0.$$

and its dual complex

$$0 \longleftarrow L^2 \xleftarrow{-\operatorname{div}} H(\operatorname{div}) \xleftarrow{\operatorname{curl}} H(\operatorname{curl}) \xleftarrow{\operatorname{grad}\operatorname{div}} H(\operatorname{grad}\operatorname{div}) \xleftarrow{\operatorname{curl}} H(\operatorname{curl}) \xleftarrow{-\operatorname{grad}} H^1 \longleftarrow 0.$$

The Hodge decomposition at $H_0(\operatorname{grad}\operatorname{div})$ reads:

$$L^2(\Omega)\otimes\mathbb{V} = \operatorname{curl} H_0(\operatorname{curl};\Omega) \oplus \operatorname{grad}\operatorname{div} H(\operatorname{grad}\operatorname{div};\Omega) \oplus \mathfrak{H}_0^2 \tag{3.3.4}$$

with $\dim \mathfrak{H}_0^2 = b_1$.

Define

$$Y_0 := H_0(\operatorname{grad}\operatorname{div};\Omega) \cap H(\operatorname{curl};\Omega).$$

We define the Hodge Laplacian operator $\mathscr{L}^2$ in the previous way but with the domain

$$D_{\mathscr{L}^2,0} = \{\boldsymbol{u} \in Y_0 : \operatorname{grad}\operatorname{div}\boldsymbol{u} \in H(\operatorname{grad}\operatorname{div};\Omega), \operatorname{curl}\boldsymbol{u} \in H_0(\operatorname{curl};\Omega)\}.$$

For $\boldsymbol{f} \in L^2(\Omega)\otimes\mathbb{V}$, the strong formulation of the Hodge Laplacian boundary value problem seeks $\boldsymbol{u} \in D_{\mathscr{L}^2,0}$ and $\boldsymbol{u} \perp \mathfrak{H}_0^2$ such that

$$\operatorname{grad}\Delta\operatorname{div} - \operatorname{curl}\operatorname{curl} = \boldsymbol{f} - P_{\mathfrak{H}_0^2}\boldsymbol{f} \text{ in } \Omega. \tag{3.3.5}$$

This problem is related to the problem considered in Chapter 8, especially when $\boldsymbol{f} \in \operatorname{grad}\operatorname{div} H(\operatorname{grad}\operatorname{div};\Omega)$.

In the case of $\boldsymbol{f} \in \operatorname{grad}\operatorname{div} H(\operatorname{grad}\operatorname{div};\Omega)$, the problem (3.3.5) is then to find $\boldsymbol{u}$ such that $\boldsymbol{u} \perp \mathfrak{H}_0^2$ and

$$\begin{aligned} \operatorname{grad}\Delta\operatorname{div}\boldsymbol{u} &= \boldsymbol{f} \quad \text{in } \Omega,\\ \operatorname{curl}\boldsymbol{u} &= 0 \quad \text{in } \Omega,\\ \boldsymbol{u}\cdot\boldsymbol{n} &= 0 \quad \text{on } \partial\Omega,\\ \operatorname{div}\boldsymbol{u} &= 0 \quad \text{on } \partial\Omega. \end{aligned} \tag{3.3.6}$$

3.3.3 Graddiv Complex with Partial Boundary Conditions

Define

$$H_{\operatorname{div}}(\operatorname{grad}\operatorname{div};\Omega) := \{\boldsymbol{u} \in H(\operatorname{grad}\operatorname{div};\Omega) : \operatorname{div}\boldsymbol{u} = 0\}.$$

Consider the domain complex of (3.3.2) with partial boundary conditions:

$$0 \longrightarrow H^1 \xrightarrow{\operatorname{grad}} H(\operatorname{curl}) \xrightarrow{\operatorname{curl}} H_{\operatorname{div}}(\operatorname{grad}\operatorname{div}) \xrightarrow{\operatorname{grad}\operatorname{div}} H_0(\operatorname{curl}) \xrightarrow{\operatorname{curl}} H_0(\operatorname{div}) \xrightarrow{\operatorname{div}} L_0^2 \longrightarrow 0.$$

and its dual complex

$$0 \longleftarrow L_0^2 \xleftarrow{-\operatorname{div}} H_0(\operatorname{div}) \xleftarrow{\operatorname{curl}} H_0(\operatorname{curl}) \xleftarrow{\operatorname{grad}\operatorname{div}} H_{\operatorname{div}}(\operatorname{grad}\operatorname{div}) \xleftarrow{\operatorname{curl}} H(\operatorname{curl}) \xleftarrow{-\operatorname{grad}} H^1 \longleftarrow 0.$$

We will show in Section 3.3.4 that the adjoint of $(\operatorname{grad}\operatorname{div}; H_{\operatorname{div}}(\operatorname{grad}\operatorname{div};\Omega))$ is itself.

The Hodge decomposition at $H_{\operatorname{div}}(\operatorname{grad}\operatorname{div})$ reads:

$$L^2(\Omega)\otimes\mathbb{V} = \operatorname{curl} H(\operatorname{curl};\Omega) \oplus \operatorname{grad}\operatorname{div} H_{\operatorname{div}}(\operatorname{grad}\operatorname{div};\Omega) \oplus \mathfrak{H}_{\operatorname{div}}^2 \tag{3.3.7}$$

with $\dim \mathfrak{H}_{\operatorname{div}}^2 = b_2$.

Define

$$Y_{\mathrm{div}} := H_{\mathrm{div}}(\operatorname{grad}\operatorname{div};\Omega) \cap H_0(\operatorname{curl};\Omega).$$

We define the Hodge Laplacian operator $\mathscr{L}^2$ in the previous way but with the domain

$$D_{\mathscr{L}^2,\mathrm{div}} = \{\boldsymbol{u} \in Y_{\mathrm{div}} : \operatorname{grad}\operatorname{div}\boldsymbol{u} \in H_{\mathrm{div}}(\operatorname{grad}\operatorname{div};\Omega), \operatorname{curl}\boldsymbol{u} \in H_0(\operatorname{div};\Omega)\}.$$

For $\boldsymbol{f} \in L^2(\Omega) \otimes \mathbb{V}$, the strong formulation of the Hodge Laplacian boundary value problem seeks $\boldsymbol{u} \in D_{\mathscr{L}^2,\mathrm{div}}$ and $\boldsymbol{u} \perp \mathfrak{H}^2_{\mathrm{div}}$ such that

$$\operatorname{grad}\Delta\operatorname{div} - \operatorname{curl}\operatorname{curl} = \boldsymbol{f} - P_{\mathfrak{H}^2_{\mathrm{div}}}\boldsymbol{f} \text{ in } \Omega. \tag{3.3.8}$$

3.3.4 Characterization of $H_0(\operatorname{grad}\operatorname{div})$

In this section, we characterize the spaces $H_0(\operatorname{grad}\operatorname{div};\Omega)$.

Theorem 3.3.1. *Define* $\gamma_{n,\mathrm{div}}\boldsymbol{u} = \{\boldsymbol{u}\cdot\boldsymbol{n}, \operatorname{div}\boldsymbol{u}\}$. *Then* $\gamma_{n,\mathrm{div}}$ *is a linear bounded operator from* $H(\operatorname{grad}\operatorname{div};\Omega)$ *to* $H^{-1/2}(\partial\Omega) \times H^{1/2}(\partial\Omega)$ *with the bound:*

$$\|\gamma_{n,\mathrm{div}}\boldsymbol{u}\|_{H^{-1/2}(\partial\Omega)\times H^{1/2}(\partial\Omega)} \le C\|\boldsymbol{u}\|_{H(\operatorname{grad}\operatorname{div};\Omega)}.$$

Proof. Since $\gamma_n\boldsymbol{u} = \boldsymbol{u}\cdot\boldsymbol{n}$ is a linear bounded operator from $H(\operatorname{div};\Omega)$ to $H^{-1/2}(\partial\Omega)$ and $\mathrm{tr}v = v|_{\partial\Omega}$ is a linear bounded operator from $H^1(\Omega)$ to $H^{1/2}(\partial\Omega)$, we have

$$\|\gamma_{n,\mathrm{div}}\boldsymbol{u}\|^2_{H^{-1/2}(\partial\Omega)\times H^{1/2}(\partial\Omega)} \le C\|\boldsymbol{u}\|^2_{H(\operatorname{div};\Omega)} + C\|\operatorname{div}\boldsymbol{u}\|^2_{H^1(\Omega)} \le C\|\boldsymbol{u}\|^2_{H(\operatorname{grad}\operatorname{div};\Omega)},$$

where we have used the equivalence between the norms $\|\cdot\|_{H(\operatorname{grad}\operatorname{div};\Omega)}$ and $|||\cdot|||_{H(\operatorname{grad}\operatorname{div};\Omega)}$, see Section 2.1.4. □

Theorem 3.3.2. *For any* $g_1 \in H^{-1/2}(\partial\Omega)$ *and* $g_2 \in H^{1/2}(\partial\Omega)$, *there exists* $\boldsymbol{u} \in H(\operatorname{grad}\operatorname{div};\Omega)$ *such that* $\boldsymbol{u}\cdot\boldsymbol{n}|_{\partial\Omega} = g_1$, $\operatorname{div}\boldsymbol{u}|_{\partial\Omega} = g_2$, *and*

$$\|\boldsymbol{u}\|_{H(\operatorname{grad}\operatorname{div};\Omega)} \le C\left(\|g_1\|_{H^{-1/2}(\partial\Omega)} + \|g_2\|_{H^{1/2}(\partial\Omega)}\right).$$

Proof. The theorem can be proved by taking $\boldsymbol{u} = \operatorname{grad} w$ in the proof of Theorem 3.2.3. □

Theorem 3.3.3. *$C^\infty(\overline{\Omega}) \otimes \mathbb{V}$ is dense in $H(\operatorname{grad}\operatorname{div};\Omega)$.*

Proof. By a suitable modification to the proof of Theorem 3.1.4, we can complete the proof. □

Lemma 3.3.4. *For $\boldsymbol{u} \in H(\operatorname{grad}\operatorname{div};\Omega)$ and $\boldsymbol{w} \in H(\operatorname{grad}\operatorname{div};\Omega)$, the following identity holds*

$$(\boldsymbol{u}, \operatorname{grad}\operatorname{div}\boldsymbol{w}) - (\operatorname{grad}\operatorname{div}\boldsymbol{u}, \boldsymbol{w}) = \langle \boldsymbol{u}\cdot\boldsymbol{n}, \operatorname{div}\boldsymbol{w}\rangle_{\partial\Omega} - \langle \boldsymbol{w}\cdot\boldsymbol{n}, \operatorname{div}\boldsymbol{u}\rangle_{\partial\Omega}. \tag{3.3.9}$$

Proof. It is easy to check that (3.3.9) holds for smooth functions $\boldsymbol{u}, \boldsymbol{w}$. By Theorem 3.3.3 and Theorem 3.3.1, we can prove (3.3.9) for $\boldsymbol{u} \in H(\operatorname{grad}\operatorname{div};\Omega)$ and $\boldsymbol{w} \in H(\operatorname{grad}\operatorname{div};\Omega)$. □

Theorem 3.3.5. *The space $H_0(\operatorname{grad}\operatorname{div};\Omega)$ can be characterized as*

$$H_0(\operatorname{grad}\operatorname{div};\Omega) = \{\boldsymbol{w} \in H(\operatorname{grad}\operatorname{div};\Omega) : \gamma_{n,\operatorname{div}} = 0\}.$$

Proof. Proceeding as the proof of Theorem 3.2.7, we can complete the proof. □

Theorem 3.3.6. *The adjoint of $(\operatorname{grad}\operatorname{div}, H(\operatorname{grad}\operatorname{div};\Omega))$ is $(\operatorname{grad}\operatorname{div}, H_0(\operatorname{grad}\operatorname{div};\Omega))$.*

Proof. According to the proof of Theorem 3.2.9, $\boldsymbol{w}$ belongs to the domain of the adjoint of $(\operatorname{grad}\operatorname{div}, H(\operatorname{grad}\operatorname{div};\Omega))$ if and only if $\boldsymbol{w} \in H(\operatorname{grad}\operatorname{div};\Omega)$ and

$$(\operatorname{grad}\operatorname{div}\boldsymbol{u}, \boldsymbol{w}) = (\boldsymbol{u}, \operatorname{grad}\operatorname{div}\boldsymbol{w}), \qquad \text{for all } \boldsymbol{u} \in H(\operatorname{grad}\operatorname{div};\Omega).$$

From Lemma 3.3.4, the above identity holds if and only if

$$\langle \boldsymbol{u}\cdot\boldsymbol{n}, \operatorname{div}\boldsymbol{w}\rangle_{\partial\Omega} - \langle \boldsymbol{w}\cdot\boldsymbol{n}, \operatorname{div}\boldsymbol{u}\rangle_{\partial\Omega} = 0.$$

which holds when $\gamma_{n,\operatorname{div}}\boldsymbol{w} = \{\boldsymbol{w}\cdot\boldsymbol{n}, \operatorname{div}\boldsymbol{w}\} = 0$ since $\gamma_{n,\operatorname{div}}$ is surjective from $H(\operatorname{grad}\operatorname{div};\Omega)$ to $H^{-1/2}(\partial\Omega) \times H^{1/2}(\partial\Omega)$ (see Theorem 3.3.2). □

Theorem 3.3.7. *The adjoint of the operator $(\operatorname{grad}\operatorname{div}, H_{\operatorname{div}}(\operatorname{grad}\operatorname{div};\Omega))$ is itself.*

Proof. The proof is similar to that of Theorem 3.3.6. □

CHAPTER 4 SPURIOUS SOLUTIONS

It is notorious that spurious solutions would occur when attempting to solve Maxwell's equations by the finite elements smoother than necessary [6]. There is usually no visible sign such as non-convergence or instability to tell them from the correct solutions, which makes the occurrence of spurious solutions dangerous for applications. Because of the similarity shared by the Maxwell equations and the high-order curl problems, we have the reason to doubt spurious solutions would also occur when solving the $\operatorname{curl}\Delta\operatorname{curl}$ problems by inappropriate elements.

In this chapter, we focus on the 2D case and investigate spurious solutions of the $\operatorname{curl}\Delta\operatorname{rot}$ problems. To this end, we consider the source problem (3.2.19) on a simply-connected domain. The explicit boundary conditions are

$$\Delta\operatorname{rot}\boldsymbol{u} = 0,\ \operatorname{rot}\boldsymbol{u} = 0,\ \text{and } \boldsymbol{u}\cdot\boldsymbol{n} = 0 \text{ on } \partial\Omega. \tag{4.0.1}$$

The primal variational formulation of the problem (3.2.19) is to seek $\boldsymbol{u} \in X_{\mathrm{rot}}$ such that

$$(\operatorname{grad}\operatorname{rot}\boldsymbol{u}, \operatorname{grad}\operatorname{rot}\boldsymbol{v}) + (\operatorname{div}\boldsymbol{u}, \operatorname{div}\boldsymbol{v}) = (\boldsymbol{f}, \boldsymbol{v}), \quad \forall \boldsymbol{v} \in X_{\mathrm{rot}}. \tag{4.0.2}$$

Let $\sigma = -\operatorname{div}\boldsymbol{u}$. Then the mixed variational formulation seeks $(\boldsymbol{u}, \sigma) \in H_{\mathrm{rot}}(\operatorname{grad}\operatorname{rot};\Omega) \times H^1(\Omega)$ such that

$$\begin{aligned}(\operatorname{grad}\operatorname{rot}\boldsymbol{u}, \operatorname{grad}\operatorname{rot}\boldsymbol{v}) + (\operatorname{grad}\sigma, \boldsymbol{v}) &= (\boldsymbol{f}, \boldsymbol{v}), \quad \forall \boldsymbol{v} \in H_{\mathrm{rot}}(\operatorname{grad}\operatorname{rot};\Omega),\\ (\boldsymbol{u}, \operatorname{grad}\tau) - (\sigma, \tau) &= 0, \quad \forall \tau \in H^1(\Omega).\end{aligned} \tag{4.0.3}$$

We also consider the corresponding eigenvalue problem on a general domain: find $(\lambda, \boldsymbol{u}) \in \mathbb{R} \times D_{\mathscr{L}^1,\mathrm{rot}}$ such that

$$-\operatorname{curl}\Delta\operatorname{rot}\boldsymbol{u} - \operatorname{grad}\operatorname{div}\boldsymbol{u} = \lambda\boldsymbol{u} \text{ in } \Omega \tag{4.0.4}$$

with the same explicit boundary conditions (4.0.1). The primal variational formulation is to seek $(\lambda, \boldsymbol{u}) \in \mathbb{R} \times X_{\mathrm{rot}}$ such that

$$(\operatorname{grad}\operatorname{rot}\boldsymbol{u}, \operatorname{grad}\operatorname{rot}\boldsymbol{v}) + (\operatorname{div}\boldsymbol{u}, \operatorname{div}\boldsymbol{v}) = \lambda(\boldsymbol{u}, \boldsymbol{v}),\ \forall \boldsymbol{v} \in X_{\mathrm{rot}}. \tag{4.0.5}$$

The mixed variational formulation seeks $(\lambda, \boldsymbol{u}, \sigma) \in \mathbb{R} \times H_{\mathrm{rot}}(\operatorname{grad}\operatorname{rot}; \Omega) \times H^1(\Omega)$ such that

$$\begin{aligned}
(\operatorname{grad}\operatorname{rot}\boldsymbol{u}, \operatorname{grad}\operatorname{rot}\boldsymbol{v}) + (\operatorname{grad}\sigma, \boldsymbol{v}) &= \lambda(\boldsymbol{u}, \boldsymbol{v}),\ \forall \boldsymbol{v} \in H_{\mathrm{rot}}(\operatorname{grad}\operatorname{rot}; \Omega),\\
(\boldsymbol{u}, \operatorname{grad}\tau) - (\sigma, \tau) &= 0,\ \forall \tau \in H^1(\Omega).
\end{aligned} \tag{4.0.6}$$

We also consider the eigenvalue problem corresponding to (3.2.8): find $(\lambda, \boldsymbol{u}) \in \mathbb{R} \times D_{\mathscr{L}^1}$ such that

$$-\operatorname{curl}\Delta\operatorname{rot}\boldsymbol{u} - \operatorname{grad}\operatorname{div}\boldsymbol{u} = \lambda\boldsymbol{u} \text{ in } \Omega \tag{4.0.7}$$

with the explicit boundary conditions:

$$\Delta\operatorname{rot}\boldsymbol{u} = 0,\ \operatorname{grad}\operatorname{rot}\boldsymbol{u}\cdot\boldsymbol{n} = 0,\ \text{and } \boldsymbol{u}\cdot\boldsymbol{n} = 0 \text{ on } \partial\Omega.$$

The primal variational formulation is to find $(\lambda, \boldsymbol{u}) \in \mathbb{R} \times X$ such that

$$(\operatorname{grad}\operatorname{rot}\boldsymbol{u}, \operatorname{grad}\operatorname{rot}\boldsymbol{v}) + (\operatorname{div}\boldsymbol{u}, \operatorname{div}\boldsymbol{v}) = \lambda(\boldsymbol{u}, \boldsymbol{v}),\ \forall \boldsymbol{v} \in X. \tag{4.0.8}$$

The mixed variational formulation is to find $(\lambda, \boldsymbol{u}, \sigma) \in \mathbb{R} \times H(\operatorname{grad}\operatorname{rot}; \Omega) \times H^1(\Omega)$ such that

$$\begin{aligned}
(\operatorname{grad}\operatorname{rot}\boldsymbol{u}, \operatorname{grad}\operatorname{rot}\boldsymbol{v}) + (\operatorname{grad}\sigma, \boldsymbol{v}) &= \lambda(\boldsymbol{u}, \boldsymbol{v}),\ \forall \boldsymbol{v} \in H(\operatorname{grad}\operatorname{rot}; \Omega),\\
(\boldsymbol{u}, \operatorname{grad}\tau) - (\sigma, \tau) &= 0,\ \forall \tau \in H^1(\Omega).
\end{aligned} \tag{4.0.9}$$

4.1 Spurious Numerical Solutions

We apply four FEMs to solve the problems (3.2.19), (4.0.4), and (4.0.7): a primal formulation with the H^2-conforming (Argyris) element, a mixed formulation with the existing grad rot-conforming element [66], and mixed and primal formulations with the $H^1(\mathrm{rot})$-conforming element [28]. Suppose in this chapter $\mathcal{T}_h$ is a partition of the domain

Ω consisting of shape regular triangles. For $K \in \mathcal{T}_h$ and $k \geq 4$, define

$$\mathcal{W}_k(K) := \left\{ \boldsymbol{v} \in \boldsymbol{P}_k(K) : \operatorname{rot} \boldsymbol{v} \in P_{k-3}(K) \cup \left[P_{k-1}(K) \cap H_0^1(K) \right] \right\}.$$

Remark 4.1.1. We can use the Poincaré operator $\mathfrak{p}^2$ to construct $\mathcal{W}_k(K)$. For example, when $k = 4$, $\mathcal{W}_k(K) = \operatorname{grad} P_5(K) \oplus P_1(K)\boldsymbol{x}^\perp \oplus \left\{ \mathfrak{p}^2(\lambda_1\lambda_2\lambda_3) \right\}$.

The grad rot-conforming and $H^1(\mathrm{rot})$-conforming finite element spaces [66, 28] on $\mathcal{T}_h$ are defined for $k \geq 4$ as follows:

$$V_h = \left\{ \boldsymbol{v}_h \in H_{\mathrm{rot}}(\operatorname{grad}\operatorname{rot};\Omega) : \ \boldsymbol{v}_h|_K \in \mathcal{R}_k(K), \ \forall K \in \mathcal{T}_h \right\},$$
$$V_h^1 = \left\{ \boldsymbol{v}_h \in H^1(\mathrm{rot};\Omega) \cap H_{\mathrm{rot}}(\operatorname{grad}\operatorname{rot};\Omega) : \ \boldsymbol{v}_h|_K \in \mathcal{W}_k(K), \ \forall K \in \mathcal{T}_h \right\},$$

where $\mathcal{R}_k$ is defined in (1.5.4).

We also define the following two finite element spaces for the mixed schemes.

$$S_h = \{ w_h \in H^1(\Omega) : \ w_h|_K \in P_k(K), \ \forall K \in \mathcal{T}_h \} \text{ for } k \geq 4,$$
$$S_h^1 = \{ w_h \in H^2(\Omega) : \ w_h|_K \in P_k(K), \ \forall K \in \mathcal{T}_h, \ w_h \in C^2(\mathcal{V}_h) \} \text{ for } k \geq 5.$$

The vector-valued H^2-conforming finite element space is defined as

$$V_h^{Arg} = S_h^1 \otimes \mathbb{V}.$$

We define the following spaces for the primal schemes.

$$\mathring{V}_h^1 = \{ \boldsymbol{v}_h \in V_h^1 : \boldsymbol{v}_h \cdot \boldsymbol{n} = 0 \text{ on } \partial\Omega \},$$
$$\mathring{V}_h^{Arg} = \{ \boldsymbol{v}_h \in V_h^{Arg} : \boldsymbol{v}_h \cdot \boldsymbol{n} = 0 \text{ and } \operatorname{rot} \boldsymbol{v}_h = 0 \text{ on } \partial\Omega \}.$$

4.1.1 Source Problem

We are in a position to present the four finite element schemes for the problem (3.2.19).

Scheme 1. Mixed formulation with the $\operatorname{grad}\operatorname{rot}$**-conforming element:**

Find $(\boldsymbol{u}_h, \sigma_h) \in V_h \times S_h$ *such that*

$$(\operatorname{grad}\operatorname{rot}\boldsymbol{u}_h, \operatorname{grad}\operatorname{rot}\boldsymbol{v}_h) + (\operatorname{grad}\sigma_h, \boldsymbol{v}_h) = (\boldsymbol{f}, \boldsymbol{v}_h),\ \forall \boldsymbol{v}_h \in V_h,$$

$$(\boldsymbol{u}_h, \operatorname{grad}\tau_h) - (\sigma_h, \tau_h) = 0,\ \forall \tau_h \in S_h.$$

Scheme 2. Mixed formulation with the $H^1(\operatorname{rot})$**-conforming element:**

Find $(\boldsymbol{u}_h, \sigma_h) \in V_h^1 \times S_h^1$ *such that*

$$(\operatorname{grad}\operatorname{rot}\boldsymbol{u}_h, \operatorname{grad}\operatorname{rot}\boldsymbol{v}_h) + (\operatorname{grad}\sigma_h, \boldsymbol{v}_h) = (\boldsymbol{f}, \boldsymbol{v}_h),\ \forall \boldsymbol{v}_h \in V_h^1,$$

$$(\boldsymbol{u}_h, \operatorname{grad}\tau_h) - (\sigma_h, \tau_h) = 0,\ \forall \tau_h \in S_h^1.$$

Scheme 3. Primal formulation with the $H^1(\operatorname{rot})$**-conforming element:**

Find $\boldsymbol{u}_h \in \mathring{V}_h^1$ *such that*

$$(\operatorname{grad}\operatorname{rot}\boldsymbol{u}_h, \operatorname{grad}\operatorname{rot}\boldsymbol{v}_h) + (\operatorname{div}\boldsymbol{u}_h, \operatorname{div}\boldsymbol{v}_h) = (\boldsymbol{f}, \boldsymbol{v}_h), \quad \forall \boldsymbol{v}_h \in \mathring{V}_h^1.$$

Scheme 4. Primal formulation with the Argyris element:

Find $\boldsymbol{u}_h \in \mathring{V}_h^{Arg}$ *such that*

$$(\operatorname{grad}\operatorname{rot}\boldsymbol{u}_h, \operatorname{grad}\operatorname{rot}\boldsymbol{v}_h) + (\operatorname{div}\boldsymbol{u}_h, \operatorname{div}\boldsymbol{v}_h) = (\boldsymbol{f}, \boldsymbol{v}_h), \quad \forall \boldsymbol{v}_h \in \mathring{V}_h^{Arg}.$$

The numerical results for the Hodge Laplacian boundary value problem with $\boldsymbol{f} = (1, 0)^{\mathrm{T}}$ on an L-shape domain are shown in Figure 4.1.1. As we can see in Figure 4.1.1, the primal formulations with the $H^1(\operatorname{rot})$-conforming element and the Argyris element (Schemes 3 and 4) show different solutions compared with the mixed formulations with the $\operatorname{grad}\operatorname{rot}$- and $H^1(\operatorname{rot})$-conforming elements (Schemes 1 and 2). In fact, the primal formulations produce spurious solutions. We will provide a theoretical explanation on this numerical phenomenon in Section 4.2.

4.1.2 Eigenvalue Problem

Similar to the source problem, we consider the following four numerical schemes for the eigenvalue problem (4.0.4).

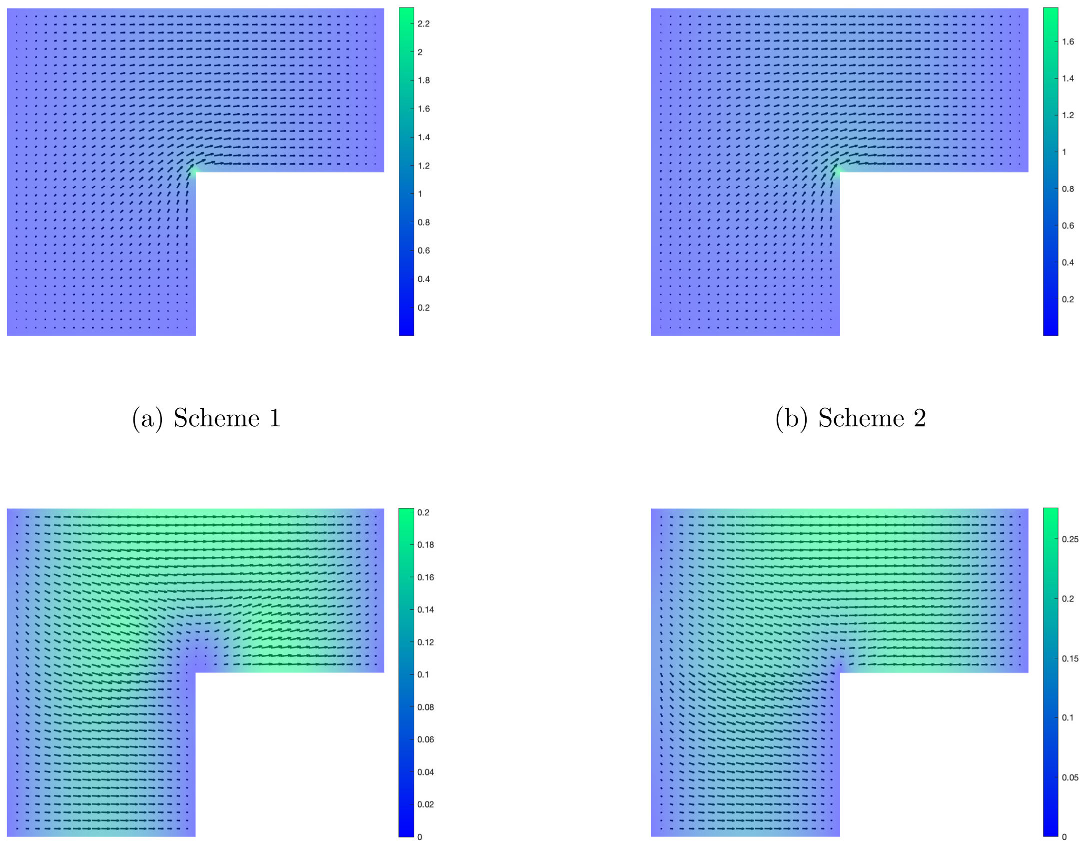

(a) Scheme 1

(b) Scheme 2

(c) Scheme 3

(d) Scheme 4

Figure 4.1.1: Finite element solutions to the problem (3.2.19) on an L-shape domain with $\boldsymbol{f} = (1, 0)^{\mathrm{T}}$.

Scheme 5. Mixed formulation with the $\operatorname{grad}\operatorname{rot}$**-conforming element:**

Find $(\lambda_h, \boldsymbol{u}_h, \sigma_h) \in \mathbb{R} \times V_h \times S_h$ *such that*

$$(\operatorname{grad}\operatorname{rot}\boldsymbol{u}_h, \operatorname{grad}\operatorname{rot}\boldsymbol{v}_h) + (\operatorname{grad}\sigma_h, \boldsymbol{v}_h) = \lambda_h(\boldsymbol{u}_h, \boldsymbol{v}_h),\ \forall \boldsymbol{v}_h \in V_h,$$

$$(\boldsymbol{u}_h, \operatorname{grad}\tau_h) - (\sigma_h, \tau_h) = 0,\ \forall \tau_h \in S_h.$$

Scheme 6. Mixed formulation with the $H^1(\mathrm{rot})$-conforming element:

Find $(\lambda_h, \boldsymbol{u}_h, \sigma_h) \in \mathbb{R} \times V_h^1 \times S_h^1$ *such that*

$$(\operatorname{grad}\operatorname{rot}\boldsymbol{u}_h, \operatorname{grad}\operatorname{rot}\boldsymbol{v}_h) + (\operatorname{grad}\sigma_h, \boldsymbol{v}_h) = \lambda_h(\boldsymbol{u}_h, \boldsymbol{v}_h),\ \ \forall \boldsymbol{v}_h \in V_h^1,$$

$$(\boldsymbol{u}_h, \operatorname{grad}\tau_h) - (\sigma_h, \tau_h) = 0,\ \ \forall \tau_h \in S_h^1.$$

Scheme 7. Primal formulation with the $H^1(\mathrm{rot})$-conforming element:

Find $(\lambda_h, \boldsymbol{u}_h) \in \mathbb{R} \times \mathring{V}_h^1$ *such that*

$$(\operatorname{grad}\operatorname{rot}\boldsymbol{u}_h, \operatorname{grad}\operatorname{rot}\boldsymbol{v}_h) + (\operatorname{div}\boldsymbol{u}_h, \operatorname{div}\boldsymbol{v}_h) = \lambda_h(\boldsymbol{u}_h, \boldsymbol{v}_h), \quad \forall \boldsymbol{v}_h \in \mathring{V}_h^1.$$

Scheme 8. Primal formulation with the Argyris element:

Find $(\lambda_h, \boldsymbol{u}_h) \in \mathbb{R} \times \mathring{V}_h^{Arg}$ *such that*

$$(\operatorname{grad}\operatorname{rot}\boldsymbol{u}_h, \operatorname{grad}\operatorname{rot}\boldsymbol{v}_h) + (\operatorname{div}\boldsymbol{u}_h, \operatorname{div}\boldsymbol{v}_h) = \lambda_h(\boldsymbol{u}_h, \boldsymbol{v}_h), \quad \forall \boldsymbol{v}_h \in \mathring{V}_h^{Arg}.$$

We apply Schemes 5 – 8 to solve the eigenvalue problem (4.0.4) on three different domains (see Figure 4.1.2):

- $\Omega_1 = (0,1) \times (0,1)$.
- $\Omega_2 = (0,1) \times (0,1)/[1/3, 3/4] \times [1/4, 2/3]$.
- $\Omega_3 = (-1,1) \times (-1,1)/[0,1) \times (-1,0]$.

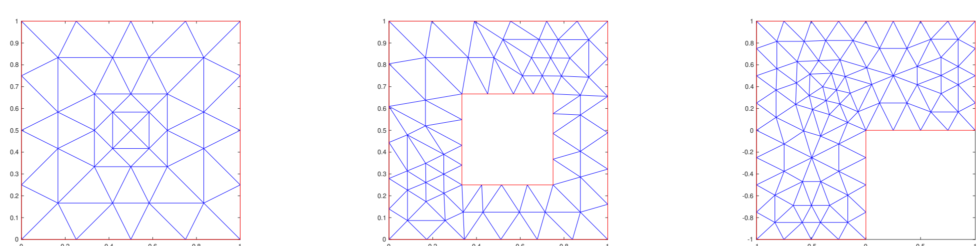

Figure 4.1.2: Initial meshes ($n = 0$) for Ω_1, Ω_2, and Ω_3

We observe from Tables 4.1.1 – 4.1.12 that the four schemes lead to the same numerical eigenvalues on Ω_1 and different numerical eigenvalues on Ω_2 and Ω_3. We will prove in

Section 4.2 that Scheme 5 yields correctly convergent numerical eigenvalues on simply-connected domains. Therefore, Scheme 7 and Scheme 8 lead to spurious eigenvalues on Ω_3.

Table 4.1.1: Numerical eigenvalues with units π^2 on Ω_1 obtained by **Scheme 5** with $k = 4$ for (4.0.4)

n	λ_1	λ_2	λ_3	λ_4	λ_5	λ_6	λ_7	λ_8
0	1.000000	1.000000	2.000000	4.000001	4.000001	5.000002	5.000002	8.000011
1	1.000000	1.000000	2.000000	4.000000	4.000000	5.000000	5.000000	8.000000
2	1.000000	1.000000	2.000000	4.000000	4.000000	5.000000	5.000000	8.000000

Table 4.1.2: Numerical eigenvalues with units π^2 on Ω_1 obtained by **Scheme 6** with $k = 4$ for (4.0.4)

n	λ_1	λ_2	λ_3	λ_4	λ_5	λ_6	λ_7	λ_8
0	1.000000	1.000000	2.000000	4.000000	4.000000	5.000000	5.000000	8.000001
1	1.000000	1.000000	2.000000	4.000000	4.000000	5.000000	5.000000	8.000000
2	1.000000	1.000000	2.000000	4.000000	4.000000	5.000000	5.000000	8.000000

Table 4.1.3: Numerical eigenvalues with units π^2 on Ω_1 obtained by **Scheme 7** with $k = 4$ for (4.0.4)

n	λ_1	λ_2	λ_3	λ_4	λ_5	λ_6	λ_7	λ_8
0	1.000000	1.000000	2.000000	4.000001	4.000001	5.000004	5.000004	8.000077
1	1.000000	1.000000	2.000000	4.000000	4.000000	5.000000	5.000000	8.000000
2	1.000000	1.000000	2.000000	4.000000	4.000000	5.000000	5.000000	8.000000

4.1.3 Eigenvalue Problem with Different Boundary Conditions

We consider four numerical schemes similar to Schemes 5 – 8 but without the boundary condition $\operatorname{rot} \boldsymbol{u}_h = 0$ on the three domains. Again, we observe that the four schemes lead to different numerical eigenvalues. In particular, the mixed formulations produce

Table 4.1.4: Numerical eigenvalues with units π^2 on Ω_1 obtained by **Scheme 8** with $k = 5$ for (4.0.4)

n	λ_1	λ_2	λ_3	λ_4	λ_5	λ_6	λ_7	λ_8
0	1.000000	1.000000	2.000000	4.000000	4.000000	5.000000	5.000000	8.000003
1	1.000000	1.000000	2.000000	4.000000	4.000000	5.000000	5.000000	8.000000
2	1.000000	1.000000	2.000000	4.000000	4.000000	5.000000	5.000000	8.000000

Table 4.1.5: Numerical eigenvalues with units π^2 on Ω_2 obtained by **Scheme 5** with $k = 4$ for (4.0.4)

n	λ_1	λ_2	λ_3	λ_4	λ_5	λ_6	λ_7	λ_8
0	0.000000	0.594212	0.595733	1.802009	2.843750	4.460286	4.495899	5.463774
1	0.000000	0.593616	0.595336	1.801970	2.839489	4.458673	4.493247	5.463500
2	0.000000	0.593379	0.595179	1.801959	2.837796	4.458048	4.492200	5.463407

Table 4.1.6: Numerical eigenvalues with units π^2 on Ω_2 obtained by **Scheme 6** with $k = 4$ for (4.0.4)

n	λ_1	λ_2	λ_3	λ_4	λ_5	λ_6	λ_7	λ_8
0	0.000000	0.596944	0.597564	1.802182	2.863546	4.467690	4.508052	5.465057
1	0.000000	0.594698	0.596060	1.802016	2.847332	4.461544	4.498047	5.463929
2	0.000000	0.593808	0.595466	1.801975	2.840909	4.459177	4.494100	5.463565

Table 4.1.7: Numerical eigenvalues with units π^2 on Ω_2 obtained by **Scheme 7** with $k = 4$ for (4.0.4)

n	λ_1	λ_2	λ_3	λ_4	λ_5	λ_6	λ_7	λ_8
0	2.645076	3.202686	3.607223	4.369787	6.145767	7.964110	8.167482	8.213072
1	2.269742	2.874862	3.141026	4.063906	5.846892	7.677691	7.894476	7.971607
2	2.065438	2.689171	2.882076	3.886972	5.659409	7.489803	7.694887	7.864160
3	1.947637	2.579732	2.731537	3.781333	5.542562	7.373284	7.571471	7.797919

Table 4.1.8: Numerical eigenvalues with units π^2 on Ω_2 obtained by **Scheme 8** with $k = 5$ for (4.0.4)

n	λ_1	λ_2	λ_3	λ_4	λ_5	λ_6	λ_7	λ_8
0	2.996956	3.517662	3.946885	4.626899	6.440491	8.154377	8.449486	8.484641
1	2.462447	3.063195	3.349072	4.229950	6.010834	7.860474	8.069506	8.098664
2	2.178163	2.802148	3.008808	3.990078	5.760831	7.614372	7.802093	7.935650
3	2.015498	2.648156	2.808560	3.844587	5.606347	7.451910	7.636857	7.841693

Table 4.1.9: Numerical eigenvalues with units π^2 on Ω_3 obtained by **Scheme 5** with $k = 4$ for (4.0.4)

n	λ_1	λ_2	λ_3	λ_4	λ_5	λ_6	λ_7	λ_8
0	0.149678	0.358073	1.000000	1.000000	1.153997	1.274383	2.000000	2.172031
1	0.149578	0.358072	1.000000	1.000000	1.153996	1.274062	2.000000	2.171278
2	0.149538	0.358072	1.000000	1.000000	1.153996	1.273934	2.000000	2.170978

Table 4.1.10: Numerical eigenvalues with units π^2 on Ω_3 obtained by **Scheme 6** with $k = 4$ for (4.0.4)

n	λ_1	λ_2	λ_3	λ_4	λ_5	λ_6	λ_7	λ_8
0	0.150209	0.358082	1.000000	1.000000	1.154010	1.276086	2.000000	2.176030
1	0.149788	0.358074	1.000000	1.000000	1.153998	1.274741	2.000000	2.172873
2	0.149621	0.358072	1.000000	1.000000	1.153996	1.274203	2.000000	2.171612

Table 4.1.11: Numerical eigenvalues with units π^2 on Ω_3 obtained by **Scheme 7** with $k = 4$ for (4.0.4)

n	λ_1	λ_2	λ_3	λ_4	λ_5	λ_6	λ_7	λ_8
0	0.416285	0.665296	1.000000	1.000000	1.181067	1.558700	2.000000	2.447851
1	0.393230	0.635841	1.000000	1.000000	1.170019	1.536785	2.000000	2.416211
2	0.379644	0.618841	1.000000	1.000000	1.163726	1.524513	2.000000	2.396893

Table 4.1.12: Numerical eigenvalues with units π^2 on Ω_3 obtained by **Scheme 8** with $k = 5$ for (4.0.4)

n	λ_1	λ_2	λ_3	λ_4	λ_5	λ_6	λ_7	λ_8
0	0.431506	0.667232	1.000000	1.000000	1.185750	1.559335	2.000000	2.471656
1	0.401863	0.638780	1.000000	1.000000	1.173429	1.538747	2.000000	2.429102
2	0.384768	0.621402	1.000000	1.000000	1.165924	1.526300	2.000000	2.404445

one zero eigenvalue on Ω_1, Ω_3 and two zero eigenvalues on Ω_2, whereas the primal formulations do not produce zero numerical eigenvalues. We will explain this difference in Section 4.2.

Table 4.1.13: Numerical eigenvalues with units π^2 on Ω_1 obtained by **Scheme 5** with $k = 4$ for (4.0.7)

n	λ_1	λ_2	λ_3	λ_4	λ_5	λ_6	λ_7	λ_8
0	0.000000	1.000000	1.000000	2.000000	4.000000	4.000001	5.000002	5.000002
1	0.000000	1.000000	1.000000	2.000000	4.000000	4.000000	5.000000	5.000000
2	-0.000000	1.000000	1.000000	2.000000	4.000000	4.000000	5.000000	5.000000

Table 4.1.14: Numerical eigenvalues with units π^2 on Ω_1 obtained by **Scheme 6** with $k = 4$ for (4.0.7)

n	λ_1	λ_2	λ_3	λ_4	λ_5	λ_6	λ_7	λ_8
0	0.000000	1.000000	1.000000	2.000000	4.000000	4.000000	5.0000001	5.0000001
1	0.000000	1.000000	1.000000	2.000000	4.000000	4.000000	5.0000000	5.0000000
2	-0.000000	1.000000	1.000000	2.000000	4.000000	4.000000	5.0000000	5.0000000

4.2 Convergence Analysis and Explanations of Spurious Solutions

We prove that the mixed formulations provide correct solutions for both the source (3.2.19) and the eigenvalue problem (4.0.4) on simply-connected domains. Therefore the different solutions by the primal formulations in Section 4.1 are spurious. Since Ω is

Table 4.1.15: Numerical eigenvalues with units π^2 on Ω_1 obtained by **Scheme 7** with $k = 4$ for (4.0.7)

n	λ_1	λ_2	λ_3	λ_4	λ_5	λ_6	λ_7	λ_8
0	1.000000	1.000000	2.000000	4.000002	4.000002	5.000004	5.000004	7.762197
1	1.000000	1.000000	2.000000	4.000000	4.000000	5.000000	5.000000	5.940076
2	1.000000	1.000000	2.000000	4.000000	4.000000	4.833375	5.000000	5.000000
3	1.000000	1.000000	2.000000	4.000000	4.000000	4.078384	5.000000	5.000000

Table 4.1.16: Numerical eigenvalues with units π^2 on Ω_1 obtained by **Scheme 8** with $k = 5$ for (4.0.7)

n	λ_1	λ_2	λ_3	λ_4	λ_5	λ_6	λ_7	λ_8
0	1.000000	1.000000	2.000000	4.000000	4.000000	4.353529	5.000000	5.000000
1	1.000000	1.000000	2.000000	3.732480	4.000000	4.000000	5.000000	5.000000
2	1.000000	1.000000	2.000000	3.266372	4.000000	4.000000	5.000000	5.000000
3	1.000000	1.000000	2.000000	2.903702	4.000000	4.000000	5.000000	5.000000

Table 4.1.17: Numerical eigenvalues with units π^2 on Ω_2 obtained by **Scheme 5** with $k = 4$ for (4.0.7)

n	λ_1	λ_2	λ_3	λ_4	λ_5	λ_6	λ_7	λ_8
0	0.000000	-0.000000	0.594212	0.595733	1.802009	2.843750	4.460286	4.495899
1	0.000000	-0.000000	0.593616	0.595336	1.801970	2.839489	4.458673	4.493248
2	0.000000	-0.000000	0.593379	0.595179	1.801960	2.837797	4.458049	4.492195

Table 4.1.18: Numerical eigenvalues with units π^2 on Ω_2 obtained by **Scheme 6** with $k = 4$ for (4.0.7)

n	λ_1	λ_2	λ_3	λ_4	λ_5	λ_6	λ_7	λ_8
0	0.000000	-0.000000	0.596944	0.597564	1.802182	2.863546	4.467690	4.508052
1	0.000000	-0.000000	0.594698	0.596060	1.802016	2.847329	4.461542	4.498048
2	0.000000	-0.000000	0.593808	0.595465	1.801975	2.840909	4.459231	4.494105

Table 4.1.19: Numerical eigenvalues with units π^2 on Ω_2 obtained by **Scheme 7** with $k = 4$ for (4.0.7)

n	λ_1	λ_2	λ_3	λ_4	λ_5	λ_6	λ_7	λ_8
0	2.640174	3.189826	3.594658	4.335878	6.144269	7.950591	8.156921	8.201252
1	2.267177	2.860417	3.128707	4.010749	5.845370	7.650719	7.875648	7.961485
2	2.063909	2.673185	2.869503	3.813822	5.657945	7.452232	7.668946	7.852054
3	1.946566	2.562122	2.718412	3.687886	5.541129	7.326460	7.539070	7.783510

Table 4.1.20: Numerical eigenvalues with units π^2 on Ω_2 obtained by **Scheme 8** with $k = 5$ for (4.0.7)

n	λ_1	λ_2	λ_3	λ_4	λ_5	λ_6	λ_7	λ_8
0	2.987390	3.489137	3.927939	4.570472	6.438141	8.140561	8.420141	8.469386
1	2.457624	3.037089	3.331364	4.148755	6.008541	7.823479	8.045921	8.078550
2	2.175539	2.777434	2.992092	3.886997	5.758800	7.562974	7.770874	7.918637
3	2.013865	2.623800	2.792272	3.720863	5.604514	7.391764	7.599227	7.823772

Table 4.1.21: Numerical eigenvalues with units π^2 on Ω_3 obtained by **Scheme 5** with $k = 4$ for (4.0.7)

n	λ_1	λ_2	λ_3	λ_4	λ_5	λ_6	λ_7	λ_8
0	0.000000	0.149678	0.358073	1.000000	1.000000	1.153996	1.274383	2.000000
1	0.000000	0.149578	0.358072	1.000000	1.000000	1.153996	1.274062	2.000000
2	0.000000	0.149538	0.358072	1.000000	1.000000	1.153996	1.273934	2.000000

Table 4.1.22: Numerical eigenvalues with units π^2 on Ω_3 obtained by **Scheme 6** with $k = 4$ for (4.0.7)

n	λ_1	λ_2	λ_3	λ_4	λ_5	λ_6	λ_7	λ_8
0	0.000000	0.150209	0.358082	1.000000	1.000000	1.154010	1.276086	2.000000
1	0.000000	0.149788	0.358074	1.000000	1.000000	1.153998	1.274741	2.000000
2	-0.000000	0.149621	0.358072	1.000000	1.000000	1.153996	1.274203	2.000000

Table 4.1.23: Numerical eigenvalues with units π^2 on Ω_3 obtained by **Scheme 7** with $k = 4$ for (4.0.7)

n	λ_1	λ_2	λ_3	λ_4	λ_5	λ_6	λ_7	λ_8
0	0.415525	0.607103	1.000000	1.000000	1.180641	1.471030	2.000000	2.203868
1	0.392873	0.556247	1.000000	1.000000	1.169824	1.399646	1.989572	2.000000
2	0.379489	0.518223	1.000000	1.000000	1.163642	1.330472	1.856537	2.000000
3	0.371374	0.487486	1.000000	1.000000	1.159955	1.265016	1.776840	2.000000

Table 4.1.24: Numerical eigenvalues with units π^2 on Ω_3 obtained by **Scheme 8** with $k = 4$ for (4.0.7)

n	λ_1	λ_2	λ_3	λ_4	λ_5	λ_6	λ_7	λ_8
0	0.429946	0.569639	1.000000	1.000000	1.184886	1.369446	1.913935	2.000000
1	0.401203	0.520021	1.000000	1.000000	1.173065	1.292529	1.813290	2.000000
2	0.384498	0.482939	1.000000	1.000000	1.165775	1.227369	1.751382	2.000000
3	0.374438	0.453274	1.000000	1.000000	1.161302	1.172738	1.711802	2.000000

assumed simply-connected, $\mathfrak{H}^1_{\mathrm{rot}}$ vanishes. Define

$$\mathfrak{Z}_h = \{\boldsymbol{v}_h \in V_h : \operatorname{grad}\operatorname{rot}\boldsymbol{v}_h = 0\}.$$

Because of the vanishing $\mathfrak{H}^1_{\mathrm{rot}}$ and the boundary condition of V_h, $\mathfrak{Z}_h = \operatorname{grad} S_h$.

4.2.1 Source Problem

We show the convergence for the source problem.

We first apply the theoretical framework of FEEC to show the problem (3.2.19) is well-posed. According to Theorem 4.7 in [6], the strong formulation (3.2.19), the primal formulation (4.0.2), and the mixed formulation (4.0.3) are equivalent. The well-posedness of (3.2.19) follows from standard results on the Hodge Laplacian problems of Hilbert complexes (see [6, Theorem 4.8]). It holds the following estimate

$$\|\boldsymbol{u}\| + \|\operatorname{grad}\operatorname{rot}\boldsymbol{u}\| + \|\operatorname{div}\boldsymbol{u}\|_1 + \|\operatorname{curl}\Delta\operatorname{rot}\boldsymbol{u}\| \leq C\|\boldsymbol{f}\|. \tag{4.2.1}$$

Since $\boldsymbol{u} \in D_{\mathscr{L}^1,\mathrm{rot}}$, by the Poincaré inequality, we have

$$\|\Delta \operatorname{rot} \boldsymbol{u}\| \leq C\|\boldsymbol{f}\|. \tag{4.2.2}$$

Since the two norms $|||\cdot|||_{H(\operatorname{grad}\operatorname{rot};\Omega)}$ and $\|\cdot\|_{H(\operatorname{grad}\operatorname{rot};\Omega)}$ are equivalent, we have

$$\|\operatorname{rot} \boldsymbol{u}\| \leq |||\boldsymbol{u}|||_{H(\operatorname{grad}\operatorname{rot};\Omega)} \leq C\|\boldsymbol{u}\|_{H(\operatorname{grad}\operatorname{rot};\Omega)} \leq C\|\boldsymbol{f}\|. \tag{4.2.3}$$

Next we investigate the regularity of the solutions.

Theorem 4.2.1. *In addition to the assumptions on Ω, we further assume that Ω is a polygon. There exists a constant $\alpha > 1/2$ such that the solution $\boldsymbol{u}$ of* (3.2.19) *satisfies*

$$\boldsymbol{u} \in H^{\alpha}(\Omega) \otimes \mathbb{V} \text{ and } \operatorname{rot} \boldsymbol{u} \in H^{1+\alpha}(\Omega),$$

and it holds

$$\|\boldsymbol{u}\|_{\alpha} + \|\operatorname{rot} \boldsymbol{u}\|_{1+\alpha} \leq C\|\boldsymbol{f}\|.$$

Moreover, if $\boldsymbol{f} \in H(\mathrm{div};\Omega)$ and $\boldsymbol{f}\cdot\boldsymbol{n} \in H^{\alpha-1/2}(\partial\Omega)$, then $\operatorname{div}\boldsymbol{u} \in H^{1+\alpha}(\Omega)$ and it holds

$$\|\operatorname{div} \boldsymbol{u}\|_{1+\alpha} \leq C\left(\|\operatorname{div}\boldsymbol{f}\| + \|\boldsymbol{f}\cdot\boldsymbol{n}\|_{\alpha-1/2,\partial\Omega}\right).$$

Proof. It follows from the embedding $H(\mathrm{rot};\Omega)\cap H_0(\mathrm{div};\Omega) \hookrightarrow H^{\alpha}(\Omega)\otimes\mathbb{V}$ with $\alpha > 1/2$ [4] that $\boldsymbol{u} \in H^{\alpha}(\Omega) \otimes \mathbb{V}$, and

$$\|\boldsymbol{u}\|_{\alpha} \leq C\left(\|\boldsymbol{u}\| + \|\operatorname{div}\boldsymbol{u}\| + \|\operatorname{rot}\boldsymbol{u}\|\right) \leq C\|\boldsymbol{f}\|,$$

where we have used (4.2.1) and (4.2.3). Therefore it suffices to show that $\operatorname{rot}\boldsymbol{u} \in H^{1+\alpha}(\Omega)$. Since $\operatorname{curl}\Delta\operatorname{rot}\boldsymbol{u} \in L^2(\Omega)\otimes\mathbb{V}$, we have

$$-\Delta\operatorname{rot}\boldsymbol{u} \in H^1(\Omega).$$

Moreover, $\operatorname{rot}\boldsymbol{u}$ satisfies the boundary condition $\operatorname{rot}\boldsymbol{u} = 0$. By the regularity of the Laplace problem [49, Theorem 3.18], there exists an $\alpha > 1/2$ such that $\operatorname{rot}\boldsymbol{u} \in H^{1+\alpha}(\Omega)$, and

$$\|\operatorname{rot}\boldsymbol{u}\|_{1+\alpha} \leq C\|\Delta\operatorname{rot}\boldsymbol{u}\| \leq C\|\boldsymbol{f}\|,$$

where we have used (4.2.2).

Multiplying both sides of (3.2.19) by $-\operatorname{grad} q \in \operatorname{grad} H^1(\Omega)$ and integrating over Ω, we obtain

$$(\operatorname{grad}\operatorname{div}\boldsymbol{u}, \operatorname{grad} q) = (\operatorname{div}\boldsymbol{f}, q) - \langle \boldsymbol{f}\cdot\boldsymbol{n}, q\rangle,$$

Applying the regularity of the Laplace problem [49, Theorem 3.18] again, there exists a constant $\alpha > 1/2$ such that

$$\|\operatorname{div}\boldsymbol{u}\|_{1+\alpha} \leq C\left(\|\operatorname{div}\boldsymbol{f}\| + \|\boldsymbol{f}\cdot\boldsymbol{n}\|_{\alpha-1/2,\partial\Omega}\right).$$

□

Remark 4.2.1. If Ω is a convex polygon, then α in Theorem 4.2.1 can be 1.

According to [6, Theorem 5.4], Scheme 1 is stable if the following discrete Poincaré inequality holds. The discrete Poincaré inequality for V_h is due to special structures of the grad rot-conforming elements.

Lemma 4.2.2 (discrete Poincaré inequality for V_h)**.** *For $\boldsymbol{v}_h \in V_h \cap \mathfrak{Z}_h^{\perp}$, we have*

$$\|\boldsymbol{v}_h\|_{H(\operatorname{grad}\operatorname{rot};\Omega)} \leq C\|\operatorname{grad}\operatorname{rot}\boldsymbol{v}_h\|, \tag{4.2.4}$$

where C is a constant independent of h.

Proof. Let $P_k^-\Lambda^l$ be the standard finite element differential l-forms on triangles [6], i.e., $l = 0$ corresponds to the Lagrange element and $l = 1$ corresponds to the Nédélec elements of the first kind. Due to the interelement continuity, $V_h \subset P_k^-\Lambda^1$. Moreover, $\mathfrak{Z}_h = \operatorname{grad} S_h = \operatorname{grad} P_k^-\Lambda^0$. Then (4.2.4) follows from the discrete Poincaré inequalities of $P_k^-\Lambda^1$ and $P_k^-\Lambda^0$. □

Theorem 4.2.3. *Under the domain assumptions of Theorem 4.2.1. Suppose also $\boldsymbol{f}$ is sufficiently smooth. Let $(\boldsymbol{u}_h, \sigma_h)$ be the numerical solution of Scheme 1 and $(\boldsymbol{u}, \sigma)$ be the* *exact solution of the problem* (3.2.19)*. Then*

$$\|\boldsymbol{u}-\boldsymbol{u}_h\|_{H(\operatorname{grad}\operatorname{rot};\Omega)}+\|\sigma-\sigma_h\|_1\leq Ch^{\alpha}(\|\boldsymbol{u}\|_{\alpha}+\|\operatorname{rot}\boldsymbol{u}\|_{1+\alpha}+\|\sigma\|_{1+\alpha}).$$

Proof. From [6, Theorem 5.5] for the case where the harmonic function space vanishes, we have

$$\|\boldsymbol{u}-\boldsymbol{u}_h\|_{H(\operatorname{grad}\operatorname{rot};\Omega)}+\|\sigma-\sigma_h\|_1\leq C\big(\inf_{\tau_h\in S_h}\|\sigma-\tau_h\|+C\inf_{\boldsymbol{v}_h\in V_h}\|\boldsymbol{u}-\boldsymbol{v}_h\|\big).$$

Let π_h and Π_h be the canonical interpolations to S_h and V_h. From their approximation properties [66] and Theorem 4.2.1, we have

$$\|\boldsymbol{u}-\boldsymbol{u}_h\|_{H(\operatorname{grad}\operatorname{rot};\Omega)}+\|\sigma-\sigma_h\|_1\leq Ch^{\alpha}(\|\boldsymbol{u}\|_{\alpha}+\|\operatorname{rot}\boldsymbol{u}\|_{1+\alpha}+\|\sigma\|_{1+\alpha}).$$

□

4.2.2 Eigenvalue Problem

To obtain the convergence estimate for Scheme 5, we rewrite (4.0.6) and Scheme 5 as follows.

Seek $(\widetilde{\lambda},\boldsymbol{u},\sigma)\in\mathbb{R}\times H_{\mathrm{rot}}(\operatorname{grad}\operatorname{rot};\Omega)\times H^1(\Omega)$ such that

$$\begin{aligned}(\operatorname{grad}\operatorname{rot}\boldsymbol{u},\operatorname{grad}\operatorname{rot}\boldsymbol{v})+(\boldsymbol{u},\boldsymbol{v})+(\operatorname{grad}\sigma,\boldsymbol{v})&=\widetilde{\lambda}(\boldsymbol{u},\boldsymbol{v}),\ \forall\boldsymbol{v}\in H_{\mathrm{rot}}(\operatorname{grad}\operatorname{rot};\Omega),\\(\boldsymbol{u},\operatorname{grad}\tau)-(\sigma,\tau)&=0,\ \forall\tau\in H^1(\Omega).\end{aligned}\tag{4.2.5}$$

Find $(\widetilde{\lambda}_h,\boldsymbol{u}_h,\sigma_h)\in\mathbb{R}\times V_h\times S_h$, such that

$$\begin{aligned}(\operatorname{grad}\operatorname{rot}\boldsymbol{u}_h,\operatorname{grad}\operatorname{rot}\boldsymbol{v}_h)+(\boldsymbol{u}_h,\boldsymbol{v}_h)+(\operatorname{grad}\sigma_h,\boldsymbol{v}_h)&=\widetilde{\lambda}_h(\boldsymbol{u}_h,\boldsymbol{v}_h),\ \forall\boldsymbol{v}_h\in V_h,\\(\boldsymbol{u}_h,\operatorname{grad}\tau_h)-(\sigma_h,\tau_h)&=0,\ \forall\tau_h\in S_h.\end{aligned}\tag{4.2.6}$$

Note that $\widetilde{\lambda}=\lambda+1$ and $\widetilde{\lambda}_h=\lambda_h+1$. We also consider the corresponding source problem and its finite element discretization.

Seek $(\boldsymbol{u},\sigma)\in H_{\mathrm{rot}}(\operatorname{grad}\operatorname{rot};\Omega)\times H^1(\Omega)$ such that

$$\begin{aligned}(\operatorname{grad}\operatorname{rot}\boldsymbol{u},\operatorname{grad}\operatorname{rot}\boldsymbol{v})+(\boldsymbol{u},\boldsymbol{v})+(\operatorname{grad}\sigma,\boldsymbol{v})&=(\boldsymbol{f},\boldsymbol{v}),\ \forall\boldsymbol{v}\in H_{\mathrm{rot}}(\operatorname{grad}\operatorname{rot};\Omega),\\(\boldsymbol{u},\operatorname{grad}\tau)-(\sigma,\tau)&=0,\ \forall\tau\in H^1(\Omega).\end{aligned}\tag{4.2.7}$$

Find $(\boldsymbol{u}_h, \sigma_h) \in V_h \times S_h$, such that

$$\begin{aligned}(\operatorname{grad}\operatorname{rot}\boldsymbol{u}_h, \operatorname{grad}\operatorname{rot}\boldsymbol{v}_h) + (\boldsymbol{u}_h, \boldsymbol{v}_h) + (\operatorname{grad}\sigma_h, \boldsymbol{v}_h) &= (\boldsymbol{f}, \boldsymbol{v}_h),\ \forall \boldsymbol{v}_h \in V_h,\\ (\boldsymbol{u}_h, \operatorname{grad}\tau_h) - (\sigma_h, \tau_h) &= 0,\ \forall \tau_h \in S_h.\end{aligned} \tag{4.2.8}$$

By suitable modification to the proof of [6, Theorem 4.8]) and [6, Theorem 4.9]), we can show the problem (4.2.7) is well-posed, and (4.2.1) holds. Similar to the problem (3.2.19), we can get the same regularity estimate as in Theorem 4.2.1.

Define the solution operators $T : L^2(\Omega)\otimes\mathbb{V} \to L^2(\Omega)\otimes\mathbb{V}$ and $S : L^2(\Omega)\otimes\mathbb{V} \to H^1(\Omega)$ by

$$T\boldsymbol{f} := \boldsymbol{u} \text{ and } S\boldsymbol{f} := \sigma.$$

We also define the discrete solution operators $T_h : L^2(\Omega) \otimes \mathbb{V} \to L^2(\Omega) \otimes \mathbb{V}$ and $S_h : L^2(\Omega) \otimes \mathbb{V} \to H^1(\Omega)$ by

$$T_h\boldsymbol{f} := \boldsymbol{u}_h \text{ and } S_h\boldsymbol{f} := \sigma_h.$$

From (4.2.7) and (4.2.8), these operators are bounded and satisfy

$$\begin{aligned}&\|T\boldsymbol{f}\|_{H(\operatorname{grad}\operatorname{rot};\Omega)} \le \|\boldsymbol{f}\|,\ \|T_h\boldsymbol{f}\|_{H(\operatorname{grad}\operatorname{rot};\Omega)} \le \|\boldsymbol{f}\|,\\ &\|S\boldsymbol{f}\|_1 \le \|\boldsymbol{f}\|,\ \text{and } \|S_h\boldsymbol{f}\|_1 \le \|\boldsymbol{f}\|.\end{aligned} \tag{4.2.9}$$

We have the following orthogonality:

$$\begin{aligned}(T\boldsymbol{f} - T_h\boldsymbol{f}, \boldsymbol{v}_h)_{H(\operatorname{grad}\operatorname{rot};\Omega)} + (\operatorname{grad}(S\boldsymbol{f} - S_h\boldsymbol{f}), \boldsymbol{v}_h) &= 0,\ \forall\ \boldsymbol{v}_h \in V_h,\\ (T\boldsymbol{f} - T_h\boldsymbol{f}, \operatorname{grad}\tau_h) - (S\boldsymbol{f} - S_h\boldsymbol{f}, \tau_h) &= 0,\ \forall\ \tau_h \in S_h.\end{aligned} \tag{4.2.10}$$

Taking $\boldsymbol{v}_h = \operatorname{grad}\tau_h$ in the first equation of (4.2.10) and subtracting the second equation from the first one, we obtain

$$(\operatorname{grad}(S\boldsymbol{f} - S_h\boldsymbol{f}), \operatorname{grad}\tau_h) + (S\boldsymbol{f} - S_h\boldsymbol{f}, \tau_h) = 0. \tag{4.2.11}$$

If we can prove $\|T - T_h\|_{\mathcal{L}(L^2\otimes\mathbb{V}, L^2\otimes\mathbb{V})} \to 0$, then from the spectral approximation theory in [14], the eigenvalues of (4.2.6) converge to the eigenvalues of (4.2.5), and hence, the eigenvalues of Scheme 5 converge to the eigenvalues of (4.0.6).

Theorem 4.2.4. *Under the domain assumptions of Theorem 4.2.1, the eigenvalues of Scheme 5 converge to the eigenvalues of* (4.0.6)*.*

To obtain the uniform convergence, we present some preliminary results. First, we will need the Hodge mapping $\boldsymbol{H}\boldsymbol{q}_h$ of $\boldsymbol{q}_h$ [35, 38]. In fact, for any $\boldsymbol{q}_h \in \mathfrak{Z}_h^{\perp} \cap V_h$, there exists $\boldsymbol{H}\boldsymbol{q}_h \in H(\mathrm{rot};\Omega) \cap H_0(\mathrm{div};\Omega)$ satisfying $\mathrm{rot}\,\boldsymbol{q}_h = \mathrm{rot}\,\boldsymbol{H}\boldsymbol{q}_h$ and $\mathrm{div}\,\boldsymbol{H}\boldsymbol{q}_h = 0$.

Lemma 4.2.5. *There exists a constant C independent of $\boldsymbol{q}_h$ and h such that*

$$\|\boldsymbol{H}\boldsymbol{q}_h - \boldsymbol{q}_h\| \leq Ch^{\alpha}\|\mathrm{rot}\,\boldsymbol{q}_h\|, \quad \forall \boldsymbol{q}_h \in \mathfrak{Z}_h^{\perp} \cap V_h.$$

Proof. Proceeding as the proof of [49, Lemma 7.6] or [38, Lemma 4.5], we can complete the proof. □

Lemma 4.2.6. *Under the domain assumptions of Theorem 4.2.1, the solutions of* (4.2.7) *and* (4.2.8) *satisfy*

$$\|\sigma - \sigma_h\| \leq Ch^{\alpha}\|\boldsymbol{f}\|.$$

Proof. We introduce the following auxiliary problem: find $\check{\sigma} \in H^1(\Omega)$ such that

$$(\mathrm{grad}\,\check{\sigma}, \mathrm{grad}\,\tau) + (\check{\sigma}, \tau) = (\sigma - \sigma_h, \tau)\,, \quad \forall \tau \in H^1(\Omega). \tag{4.2.12}$$

The discrete problem is to find $\check{\sigma}_h \in S_h$ such that

$$(\mathrm{grad}\,\check{\sigma}_h, \mathrm{grad}\,\tau_h) + (\check{\sigma}_h, \tau_h) = (\sigma - \sigma_h, \tau_h)\,, \quad \forall \tau_h \in S_h.$$

According to Theorem 3.18 in [49] again, there exists the same constant $\alpha > 1/2$ such that

$$\|\check{\sigma}\|_{1+\alpha} \leq C\,\|\sigma - \sigma_h\|\,.$$

From the Ceá lemma, we have

$$\|\check{\sigma} - \check{\sigma}_h\|_1 \leq Ch^{\alpha}\|\check{\sigma}\|_{1+\alpha} \leq Ch^{\alpha}\,\|\sigma - \sigma_h\|\,.$$

Taking $\tau = \sigma - \sigma_h$ in (4.2.12) and applying (4.2.11), we obtain

$$
\begin{aligned}
(\sigma - \sigma_h, \sigma - \sigma_h) &= (\check{\sigma}, \sigma - \sigma_h) + (\operatorname{grad} \check{\sigma}, \operatorname{grad}(\sigma - \sigma_h)) \\
&= (\check{\sigma} - \check{\sigma}_h, \sigma - \sigma_h) + (\operatorname{grad}(\check{\sigma} - \check{\sigma}_h), \operatorname{grad}(\sigma - \sigma_h)) \\
&\leq \|\check{\sigma} - \check{\sigma}_h\|_1 \|\sigma - \sigma_h\|_1 \leq Ch^\alpha \|\sigma - \sigma_h\| \|\sigma - \sigma_h\|_1,
\end{aligned}
$$

which together with (4.2.9) leads to

$$\|\sigma - \sigma_h\| \leq Ch^\alpha \|\sigma - \sigma_h\|_1 \leq Ch^\alpha \|\boldsymbol{f}\|.$$

□

We are now in a position to estimate $\|T - T_h\|_{\mathcal{L}(L^2 \otimes \mathbb{V}, L^2 \otimes \mathbb{V})}$.

Theorem 4.2.7. *Under the domain assumptions of Theorem 4.2.1, we have*

$$\|T - T_h\|_{\mathcal{L}(L^2 \otimes \mathbb{V}, L^2 \otimes \mathbb{V})} \leq Ch^\alpha.$$

Proof. We shall prove $\|\boldsymbol{u} - \boldsymbol{u}_h\| \leq Ch^\alpha \|\boldsymbol{f}\|$. Denote $\widetilde{\boldsymbol{u}} = T(\boldsymbol{u} - \boldsymbol{u}_h)$, $\widetilde{\boldsymbol{u}}_h = T_h(\boldsymbol{u} - \boldsymbol{u}_h)$, $\widetilde{\sigma} = S(\boldsymbol{u} - \boldsymbol{u}_h)$, and $\widetilde{\sigma}_h = S_h(\boldsymbol{u} - \boldsymbol{u}_h)$. Proceeding as the dual argument, we have

$$
\begin{aligned}
&(\boldsymbol{u} - \boldsymbol{u}_h, \boldsymbol{u} - \boldsymbol{u}_h) = (\widetilde{\boldsymbol{u}}, \boldsymbol{u} - \boldsymbol{u}_h)_{H(\operatorname{grad}\operatorname{rot};\Omega)} + (\operatorname{grad} \widetilde{\sigma}, \boldsymbol{u} - \boldsymbol{u}_h) \\
&= (\widetilde{\boldsymbol{u}} - \widetilde{\boldsymbol{u}}_h, \boldsymbol{u} - \boldsymbol{u}_h)_{H(\operatorname{grad}\operatorname{rot};\Omega)} + (\operatorname{grad} \widetilde{\sigma}, \boldsymbol{u} - \boldsymbol{u}_h) - (\operatorname{grad}(\sigma - \sigma_h), \widetilde{\boldsymbol{u}}_h) \qquad \text{by (4.2.10)} \\
&= (\widetilde{\boldsymbol{u}} - \widetilde{\boldsymbol{u}}_h, \boldsymbol{u} - \Pi_h \boldsymbol{u})_{H(\operatorname{grad}\operatorname{rot};\Omega)} + (\operatorname{grad}(\widetilde{\sigma} - \widetilde{\sigma}_h), \boldsymbol{u} - \Pi_h \boldsymbol{u}) \qquad \text{by (4.2.10), (4.2.11)} \\
&\quad + (\sigma - \sigma_h, \widetilde{\sigma}_h) - (\operatorname{grad}(\sigma - \sigma_h), \widetilde{\boldsymbol{u}}_h) =: \mathrm{I} + \mathrm{II} + \mathrm{III} + \mathrm{IV}.
\end{aligned}
$$

Applying (4.2.9) and the approximation property of Π_h [66], we have

$$
\begin{aligned}
\mathrm{I} + \mathrm{II} &\leq \|\boldsymbol{u} - \Pi_h \boldsymbol{u}\|_{H(\operatorname{grad}\operatorname{rot};\Omega)} \left(\|\widetilde{\boldsymbol{u}} - \widetilde{\boldsymbol{u}}_h\|_{H(\operatorname{grad}\operatorname{rot};\Omega)} + \|\operatorname{grad}(\widetilde{\sigma} - \widetilde{\sigma}_h)\| \right) \\
&\leq C \|\boldsymbol{u} - \Pi_h \boldsymbol{u}\|_{H(\operatorname{grad}\operatorname{rot};\Omega)} \|\boldsymbol{u} - \boldsymbol{u}_h\| \\
&\leq Ch^\alpha \|\boldsymbol{u} - \boldsymbol{u}_h\| \left(\|\boldsymbol{u}\|_\alpha + \|\operatorname{rot} \boldsymbol{u}\|_{1+\alpha} \right) \\
&\leq Ch^\alpha \|\boldsymbol{f}\| \|\boldsymbol{u} - \boldsymbol{u}_h\|.
\end{aligned}
$$

Using Lemma 4.2.6, we get

$$\mathrm{III} \le Ch^{\alpha}\|\boldsymbol{f}\|\|\widetilde{\sigma}_h\| \le Ch^{\alpha}\|\boldsymbol{f}\|\|\boldsymbol{u}-\boldsymbol{u}_h\|.$$

Now it remains to estimate IV. We decompose $\widetilde{\boldsymbol{u}}_h = \boldsymbol{p}_h + \boldsymbol{q}_h$ with $\boldsymbol{p}_h \in \mathfrak{Z}_h$ and $\boldsymbol{q}_h \in \mathfrak{Z}_h^{\perp} \cap V_h$. Then

$$\mathrm{IV} = (\operatorname{grad}(\sigma-\sigma_h), \widetilde{\boldsymbol{u}}_h) = (\operatorname{grad}(\sigma-\sigma_h), \boldsymbol{q}_h) + (\operatorname{grad}(\sigma-\sigma_h), \boldsymbol{p}_h) =: \mathrm{IV}_{\mathrm{I}} + \mathrm{IV}_{\mathrm{II}}.$$

Applying Lemma 4.2.5, we obtain

$$\begin{aligned}\mathrm{IV}_{\mathrm{I}} &= (\operatorname{grad}(\sigma-\sigma_h), \boldsymbol{q}_h - \boldsymbol{H}\boldsymbol{q}_h) \le Ch^{\alpha}\|\operatorname{rot}\boldsymbol{q}_h\|\|\boldsymbol{f}\| \\ &\le Ch^{\alpha}\|\operatorname{rot}\widetilde{\boldsymbol{u}}_h\|\|\boldsymbol{f}\| \le Ch^{\alpha}\|\boldsymbol{u}-\boldsymbol{u}_h\|\|\boldsymbol{f}\|.\end{aligned}$$

Since $\mathfrak{Z}_h = \operatorname{grad} S_h$, there exists a function $\phi_h \in S_h$ satisfying $(\phi_h, 1) = 0$ and $\boldsymbol{p}_h = \operatorname{grad}\phi_h$. By (4.2.11), we get

$$\begin{aligned}\mathrm{IV}_{\mathrm{II}} =& \big(\operatorname{grad}(\sigma-\sigma_h), \operatorname{grad}\phi_h\big) = -\big(\sigma-\sigma_h, \phi_h\big) \le C\|\sigma-\sigma_h\|\|\operatorname{grad}\phi_h\| \\ =& C\|\sigma-\sigma_h\|\|\boldsymbol{p}_h\| \le C\|\sigma-\sigma_h\|\|\widetilde{\boldsymbol{u}}_h\| \le Ch^{\alpha}\|\boldsymbol{f}\|\|\boldsymbol{u}-\boldsymbol{u}_h\|.\end{aligned}$$

Collecting all the estimates, we complete the proof. □

4.2.3 Theoretical Explanation of the Numerical Phenomena

Let $H^1_{n,\mathrm{rot}}(\mathrm{rot};\Omega) = H^1(\mathrm{rot};\Omega) \cap X_{\mathrm{rot}}$ denote the space of $H^1(\mathrm{rot};\Omega)$ vector fields with vanishing normal components and rot on the boundary, which is a closed subspaces of $H^1(\mathrm{rot};\Omega)$. Clearly, $H^1_{n,\mathrm{rot}}(\mathrm{rot};\Omega) \subset X_{\mathrm{rot}}$. For $\boldsymbol{u} \in H^1_{n,\mathrm{rot}}(\mathrm{rot};\Omega)$, by the Poincaré inequality and the identity $\|\operatorname{grad}\boldsymbol{u}\|^2 = \|\operatorname{rot}\boldsymbol{u}\|^2 + \|\operatorname{div}\boldsymbol{u}\|^2$ [6], we have

$$C(\|\operatorname{grad}\operatorname{rot}\boldsymbol{u}\|^2 + \|\operatorname{grad}\boldsymbol{u}\|^2) \le \|\operatorname{grad}\operatorname{rot}\boldsymbol{u}\|^2 + \|\operatorname{div}\boldsymbol{u}\|^2 \le \|\operatorname{grad}\operatorname{rot}\boldsymbol{u}\|^2 + \|\operatorname{grad}\boldsymbol{u}\|^2.$$

Therefore, the restriction of the X-norm to $H^1_{n,\mathrm{rot}}(\mathrm{rot};\Omega)$ is equivalent to the full norm of $H^1(\mathrm{rot};\Omega)$. It follows from the fact $H^1_{n,\mathrm{rot}}(\mathrm{rot};\Omega)$ is closed in $H^1(\mathrm{rot};\Omega)$ that $H^1_{n,\mathrm{rot}}(\mathrm{rot};\Omega)$ is a closed subspace of X_{rot}. To prove $X_{\mathrm{rot}} \ne H^1_{n,\mathrm{rot}}(\mathrm{rot};\Omega)$, it suffices to find a function in X_{rot} which is not in $H^1_{n,\mathrm{rot}}(\mathrm{rot};\Omega)$. Consider the function $\phi \in H^1(\Omega)$ such that $\Delta\phi \in$

$L^2(\Omega)$ and $\frac{\partial \phi}{\partial \boldsymbol{n}} = 0$ on $\partial\Omega$. When Ω is a nonconvex polygonal domain, we have $\phi \notin H^2(\Omega)$. Setting $\boldsymbol{u} = \operatorname{grad} \phi$, we see that $\boldsymbol{u} \in X_{\text{rot}}$ but $\boldsymbol{u} \notin H^1_{n,\text{rot}}(\text{rot};\Omega)$. For any such function $\boldsymbol{u}$, we have $\inf_{\boldsymbol{v} \in H^1_{n,\text{rot}}(\text{rot};\Omega)} \|\boldsymbol{u} - \boldsymbol{v}\|_X = \delta_{\boldsymbol{u}} > 0$, where $\delta_{\boldsymbol{u}}$ is the distance of $\boldsymbol{u}$ from $H^1_{n,\text{rot}}(\text{rot};\Omega)$. Therefore, if the finite element space V_h is contained in $H^1_{n,\text{rot}}(\text{rot};\Omega)$, then the numerical solution $\boldsymbol{u}_h \in V_h$ can not converge to $\boldsymbol{u}$ in general. The mixed variational formulation, however, does not suffer from this restriction, and hence does not lead to spurious solutions. On the other hand, the choice of finite elements are crucial for the success of the mixed formulations. The grad rot- and $H^1(\text{rot})$-conforming finite elements are stable as they fit into complexes.

Since $\dim \mathfrak{H}^1_{\text{rot}} = b_1 = 1$ on Ω_2, there is a zero eigenvalue on Ω_2 corresponding to the harmonic forms in $\mathfrak{H}^1_{\text{rot}}$. However, Scheme 7 and Scheme 8 fail to capture this zero eigenmode. The same issue occurs for the numerical solutions of the problem (4.0.7). The harmonic forms are generally smooth functions but not polynomials. Therefore, the finite element spaces V_h^1 and V_h^{Arg} do not contain any harmonic forms. That is why Scheme 7 and Scheme 8 can not capture the vanishing eigenvalue.

CHAPTER 5 2D GRADROT-CONFORMING ELEMENTS

Chapter 4 tells us the importance of constructing finite elements that fit into complexes. From this chapter on, we will construct grad rot-conforming elements, grad curl-conforming elements, and grad div-conforming elements by designing discrete complexes.

In this chapter, we focus on the construction of grad rot-conforming elements. To this end, we consider the de Rham complex with enhanced smoothness (1.4.1). To make this chapter more readable, we put the complex (1.4.1) here

$$0 \longrightarrow \mathbb{R} \xrightarrow{\subset} H^1 \xrightarrow{\text{grad}} H(\operatorname{grad}\operatorname{rot}) \xrightarrow{\text{rot}} H^1 \longrightarrow 0. \tag{5.0.1}$$

From the complex, we can see the grad rot-conforming elements satisfy that

- the tangential component of $\boldsymbol{u}_h$ is continuous across two adjacent elements;
- $\operatorname{rot}\boldsymbol{u}_h$ is continuous across two adjacent elements.

In [66], the author and her collaborators combine the first kind of Nédélec elements and the Lagrange elements to define grad rot-conforming elements that satisfy the above continuity conditions. The construction is based on the existing polynomial spaces, $Q_{k-1,k} \times Q_{k,k-1}$ or $\mathcal{R}_k$ (see (1.5.4) for its definition). The restriction of $k \geq 4$ for the triangular elements or $k \geq 3$ for the rectangular elements has to be imposed since an interior bubble should be included in the finite element space of $\operatorname{rot}\boldsymbol{u}$. Therefore the lowest-order element has 24 DOFs on both a triangular and rectangular element.

We will construct the following finite element subcomplexes of (5.0.1):

$$0 \longrightarrow \mathbb{R} \xrightarrow{\subset} \Sigma_h^r \xrightarrow{\text{grad}} V_h^{r-1,k+1} \xrightarrow{\text{rot}} \Sigma_h^{k,+} \longrightarrow 0. \tag{5.0.2}$$

Here we introduce two parameters r and k with $r = k$, $r = k+1$, or $r = k+2$ to specify degrees of spaces, which lead to several versions of complexes. The complexes (5.0.2) include two new grad rot-conforming element spaces $V_h^{k-1,k+1}$ and $V_h^{k+1,k+1}$. We also fit the existing finite element space into the complex and extend it to lower-order cases. Among the three versions of V_h, the new finite element space $V_h^{k-1,k+1}$ has fewest DOFs.

5.1 Local Shape Function Spaces and Polynomial Complexes

To define a finite element space, we must supply, for each element $K \in \mathcal{T}_h$, the space of shape functions and the DOFs. In this section, we will define the local complex of the local shape function spaces on each $K \in \mathcal{T}_h$ for (5.0.2):

$$0 \longrightarrow \mathbb{R} \xrightarrow{\subset} \Sigma_h^r(K) \xrightarrow{\text{grad}} V_h^{r-1,k+1}(K) \xrightarrow{\text{rot}} \Sigma_h^{k,+}(K) \longrightarrow 0. \tag{5.1.1}$$

To this end, we first consider the following local complex on the reference element $\hat{K}$:

$$0 \longrightarrow \mathbb{R} \xrightarrow{\subset} \hat{\Sigma}_h^r(\hat{K}) \xrightarrow{\text{grad}_{\hat{\boldsymbol{x}}}} \hat{V}_h^{r-1,k+1}(\hat{K}) \xrightarrow{\text{rot}_{\hat{\boldsymbol{x}}}} \hat{\Sigma}_h^{k,+}(\hat{K}) \longrightarrow 0. \tag{5.1.2}$$

Let $\hat{\Sigma}_h^r(\hat{K})$ be $P_r(\hat{K})$ for the triangular element $\hat{K}$ or $Q_r(\hat{K})$ for the rectangular element $\hat{K}$. For the triangular element $\hat{K}$, we set

$$\hat{\Sigma}_h^{k,+}(\hat{K}) = \begin{cases} P_k(\hat{K}), & k \geq 3, \\ P_k(\hat{K}) \oplus \text{span}\{\hat{B}_t\}, & k = 1, 2, \end{cases}$$

where $\hat{B}_t = \hat{x}_1\hat{x}_2(1 - \hat{x}_1 - \hat{x}_2)$. For the rectangular element $\hat{K}$, we set

$$\hat{\Sigma}_h^{k,+}(\hat{K}) = \begin{cases} Q_k(\hat{K}), & k \geq 2, \\ Q_k(\hat{K}) \oplus \text{span}\{\hat{B}_r\}, & k = 1, \end{cases}$$

where $\hat{B}_r = (\hat{x}_1 + 1)(\hat{x}_1 - 1)(\hat{x}_2 + 1)(\hat{x}_2 - 1)$. We define

$$\hat{V}_h^{r-1,k+1}(\hat{K}) = \text{grad}_{\hat{\boldsymbol{x}}} \hat{\Sigma}_h^r(\hat{K}) \oplus \mathfrak{p}_{\hat{\boldsymbol{x}}}^2 \hat{\Sigma}_h^{k,+}(\hat{K}), \tag{5.1.3}$$

where the Poincaré operator $\mathfrak{p}_{\hat{\boldsymbol{x}}}^2$ is defined by (2.1.19) with the base point $W = 0$. As a special case of Poincaré operators, $\mathfrak{p}_{\hat{\boldsymbol{x}}}^2$ satisfies the following null-homotopy identities:

$$\text{rot}_{\hat{\boldsymbol{x}}} \mathfrak{p}_{\hat{\boldsymbol{x}}}^2 \hat{u} = \hat{u}, \ \forall \hat{u} \in C^\infty\Lambda^2(\hat{K}), \tag{5.1.4}$$

$$\text{grad}_{\hat{\boldsymbol{x}}} \mathfrak{p}_{\hat{\boldsymbol{x}}}^1 \hat{\boldsymbol{u}} + \mathfrak{p}_{\hat{\boldsymbol{x}}}^2 \text{rot}_{\hat{\boldsymbol{x}}} \hat{\boldsymbol{u}} = \hat{\boldsymbol{u}}, \ \forall \hat{\boldsymbol{u}} \in C^\infty\Lambda^1(\hat{K}). \tag{5.1.5}$$

By the null-homotopy identity (5.1.4), the right hand side of (5.1.3) is a direct sum.

Remark 5.1.1. For the reference rectangle $\hat{K}$, we can also use the serendipity elements $\mathcal{S}_r(\hat{K}) := P_r(\hat{K}) \oplus \mathrm{span}\{\hat{x}_1^r\hat{x}_2, \hat{x}_1\hat{x}_2^r\}$ [7] for $\hat{\Sigma}_h^r(\hat{K})$ and use $\mathcal{S}_k(\hat{K})$ when $k \geq 4$ or $\mathcal{S}_k(\hat{K}) \oplus \mathrm{span}\{\hat{B}_r\}$ when $k < 4$ for $\hat{\Sigma}_h^{k,+}(\hat{K})$. This leads to another three families of rectangular elements with fewer DOFs and the same accuracy.

Remark 5.1.2. For polynomial bases in $\hat{\Sigma}_h^{k,+}(\hat{K})$ other than the bubbles $\hat{B}_t$ or $\hat{B}_r$, we can replace the Poincaré operator $\mathfrak{p}_{\hat{\boldsymbol{x}}}^2$ by the Koszul operator $\kappa_{\hat{\boldsymbol{x}}}^2$. It seems necessary to use the Poincaré operator for the bubbles to get the complex property. For the bubble function $\hat{B}_t$ or $\hat{B}_r$, we have

$$\begin{aligned}\mathfrak{p}_{\hat{\boldsymbol{x}}}^2\hat{B}_t =& \frac{\hat{x}_1\hat{x}_2(4\hat{x}_1+4\hat{x}_2-5)}{20}\hat{\boldsymbol{x}}^{\perp},\\ \mathfrak{p}_{\hat{\boldsymbol{x}}}^2\hat{B}_r =& -\frac{2\hat{x}_1^2\hat{x}_2^2-3\hat{x}_1^2-3\hat{x}_2^2+6}{12}\hat{\boldsymbol{x}}^{\perp}.\end{aligned}$$

By the definition of the shape function spaces, it is easy to show that the sequence (5.1.2) is a complex. By the properties of the Poincaré operators, we can verify that the sequence

$$0 \longleftarrow \mathbb{R} \longleftarrow \hat{\Sigma}_h^r(\hat{K}) \xleftarrow{\mathfrak{p}_{\hat{\boldsymbol{x}}}^1} \hat{V}_h^{r-1,k+1}(\hat{K}) \xleftarrow{\mathfrak{p}_{\hat{\boldsymbol{x}}}^2} \hat{\Sigma}_h^{k,+}(\hat{K}) \longleftarrow 0 \qquad (5.1.6)$$

is also a complex with the Poincaré operators in (2.1.18) – (2.1.19). From Lemma 2.1.3, we obtain the exactness.

Lemma 5.1.1. *The complex* (5.1.2) *is exact.*

Lemma 5.1.2. *The inclusion* $\boldsymbol{P}_{r-1}(\hat{K}) \subseteq \hat{V}_h^{r-1,k+1}(\hat{K})$ *holds. More precisely, we have*

$$\hat{V}_h^{k,k+1}(\hat{K}) = \begin{cases}\mathcal{R}_{k+1}(\hat{K}) & \text{when } k \geq 3 \text{ and } \hat{K} \text{ is a triangle,}\\ Q_{k,k+1}(\hat{K}) \times Q_{k+1,k}(\hat{K}) & \text{when } k \geq 2 \text{ and } \hat{K} \text{ is a rectangle.}\end{cases}$$

Proof. From the null-homotopy property (5.1.5),

$$\boldsymbol{P}_{r-1}(\hat{K}) = \mathrm{grad}_{\hat{\boldsymbol{x}}}\, \mathfrak{p}_{\hat{\boldsymbol{x}}}^1 \boldsymbol{P}_{r-1}(\hat{K}) + \mathfrak{p}_{\hat{\boldsymbol{x}}}^2\, \mathrm{rot}_{\hat{\boldsymbol{x}}}\, \boldsymbol{P}_{r-1}(\hat{K}).$$

By definition, $\hat{V}_h^{r-1,k+1}(\hat{K}) = \operatorname{grad}_{\hat{\boldsymbol{x}}} \hat{\Sigma}_h^r(\hat{K}) + \mathfrak{p}_{\hat{\boldsymbol{x}}}^2 \hat{\Sigma}_h^{k,+}(\hat{K})$. We have $\mathfrak{p}_{\hat{\boldsymbol{x}}}^1 \boldsymbol{P}_{r-1}(\hat{K}) \subseteq P_r(\hat{K}) \subseteq \hat{\Sigma}_h^r(\hat{K})$ and $\operatorname{rot}_{\hat{\boldsymbol{x}}} \boldsymbol{P}_{r-1}(\hat{K}) \subseteq P_k(\hat{K}) \subseteq \hat{\Sigma}_h^{k,+}(\hat{K})$. Therefore the desired inclusion holds.

Now we show $\mathcal{R}_{k+1}(\hat{K}) = \operatorname{grad}_{\hat{\boldsymbol{x}}} P_{k+1}(\hat{K}) + \mathfrak{p}_{\hat{\boldsymbol{x}}}^2 P_k(\hat{K})$ which is exactly $\hat{V}_h^{k,k+1}(\hat{K})$ when $k \geq 3$ and $\hat{K}$ is a triangle. Since $\operatorname{grad}_{\hat{\boldsymbol{x}}} P_{k+1}(\hat{K}) + \mathfrak{p}_{\hat{\boldsymbol{x}}}^2 P_{k-1}(\hat{K}) \subseteq P_k(\hat{K})$ and $\mathfrak{p}_{\hat{\boldsymbol{x}}}^2 \widetilde{P}_k(\hat{K}) \subseteq \{\hat{\boldsymbol{u}} \in \widetilde{P}_{k+1}(\hat{K}) : \hat{\boldsymbol{x}} \cdot \hat{\boldsymbol{u}} = 0\}$, we have $\operatorname{grad}_{\hat{\boldsymbol{x}}} P_{k+1}(\hat{K}) + \mathfrak{p}_{\hat{\boldsymbol{x}}}^2 P_k(\hat{K}) \subseteq \mathcal{R}_{k+1}(\hat{K})$. It suffices to show that they have the some dimension. From the exactness of (5.1.2), $\dim \hat{V}_h^{k,k+1}(\hat{K}) = \dim P_{k+1}(\hat{K}) + \dim P_k(\hat{K}) - 1 = (k+1)(k+3) = \dim \mathcal{R}_{k+1}(\hat{K})$ when $k \geq 3$.

Similarly, we can prove $\hat{V}_h^{k,k+1}(\hat{K}) = Q_{k,k+1}(\hat{K}) \times Q_{k+1,k}(\hat{K})$ when $k \geq 2$ and $\hat{K}$ is a rectangle.

□

We adopt the following transformation to relate the function $\hat{\boldsymbol{u}} \in \hat{V}_h^{r-1,k+1}(\hat{K})$ to a function $\boldsymbol{u} \in V_h^{r-1,k+1}(K)$:

$$\boldsymbol{u} \circ F_K = B_K^{-\mathrm{T}} \hat{\boldsymbol{u}}, \tag{5.1.7}$$

where the affine mapping F_K is defined in (1.5.1). By a simple computation, we have

$$\operatorname{rot} \boldsymbol{u} \circ F_K = \frac{1}{\det(B_K)} \operatorname{rot}_{\hat{\boldsymbol{x}}} \hat{\boldsymbol{u}}. \tag{5.1.8}$$

We are now in a position to define the spaces in (5.1.1):

$$\begin{aligned} \Sigma_h^r(K) &= \left\{ u : u \circ F_K \in \hat{\Sigma}_h^r(\hat{K}) \right\}, \\ V_h^{r-1,k+1}(K) &= \left\{ \boldsymbol{u} : B_K^{\mathrm{T}} \boldsymbol{u} \circ F_K \in \hat{V}_h^{r-1,k+1}(\hat{K}) \right\}, \\ \Sigma_h^{k,+}(K) &= \left\{ u : u \circ F_K \in \hat{\Sigma}_h^{k,+}(\hat{K}) \right\}. \end{aligned}$$

Remark 5.1.3. We do not use $\operatorname{grad} \Sigma_h^r(K) \oplus \mathfrak{p}^2 \Sigma_h^{k,+}(K)$ to define $V_h^{r-1,k+1}(K)$ because $\operatorname{grad} \Sigma_h^r(K) \oplus \mathfrak{p}^2 \Sigma_h^{k,+}(K)$ can not be related to $\hat{V}_h^{r-1,k+1}(\hat{K})$ via (5.1.7) when $r = k$.

By the definition of the spaces and Lemma 5.1.1, we can show (5.1.1) is also an exact complex.

5.2 Degrees of Freedom

In this section, we define DOFs for each space in (5.1.1). Taking $r = k$, $k+1$, and $k+2$ in (5.1.1) yields three versions of grad rot-conforming element spaces $V_h^{k-1,k+1}(K)$, $V_h^{k,k+1}(K)$, and $V_h^{k+1,k+1}(K)$. Fig. 5.2.1 demonstrates the complex (5.1.1) for the case $k = 1$.

Among the three versions of $V_h(K)$, the simplest elements have only 6 DOFs for a triangle and 8 DOFs for a rectangle. To the best of our knowledge, these elements have the smallest number of DOFs among all the existing grad rot-conforming finite elements.

The DOFs for the Lagrange element $\Sigma_h^r(K)$ can be given as follows.

- Vertex DOFs $M_v(u)$ at all the vertices $v_i \in \mathcal{V}_h(K)$:

$$M_v(u) = \{u(v_i)\}.$$

- Edge DOFs $M_e(u)$ on all the edges $e_i \in \mathcal{E}_h(K)$:

$$M_e(u) = \left\{\int_{e_i} uv\mathrm{d}s \text{ for all } v \in P_{r-2}(e_i)\right\}.$$

- Interior DOFs $M_K(u)$ in the element K:

$$M_K(u) = \left\{\int_K uv\mathrm{d}A \text{ for all } v \in P_{r-3}(K)\right\}, \text{ when } K \text{ is a triangular element;}$$

$$M_K(u) = \left\{\int_K uv\mathrm{d}A \text{ for all } v \in Q_{r-2}(K)\right\}, \text{ when } K \text{ is a rectangular element.}$$

For $u \in H^{1+\delta}(K)$ with $\delta > 0$, we can define an H^1 interpolation operator $\pi_K : H^{1+\delta}(K) \to \Sigma_h^r(K)$ by the above DOFs such that

$$M_v(u - \pi_K u) = \{0\},\ M_e(u - \pi_K u) = \{0\},\ \text{and } M_K(u - \pi_K u) = \{0\}. \tag{5.2.1}$$

The DOFs for $\Sigma_h^{k,+}(K)$ can be given similarly, with only one additional interior integration DOF to take care of the interior bubble. We denote $\widetilde{\pi}_K$ as the H^1 interpolation operator to $\Sigma_h^{k,+}(K)$ by these DOFs.

We define the following DOFs for $V_h^{r-1,k+1}(K)$:

- Vertex DOFs $\boldsymbol{M}_v(\boldsymbol{u})$ at all the vertices $v_i \in \mathcal{V}_h(K)$:

$$\boldsymbol{M}_v(\boldsymbol{u}) = \{\mathrm{rot}\, \boldsymbol{u}(v_i)\}\,. \tag{5.2.2}$$

- Edge DOFs $\boldsymbol{M}_e(\boldsymbol{u})$ on all the edges $e_i \in \mathcal{E}_h(K)$ with the unit tangential vector $\boldsymbol{\tau}_i$:

$$\begin{aligned}\boldsymbol{M}_e(\boldsymbol{u}) = &\left\{\int_{e_i} \boldsymbol{u}\cdot\boldsymbol{\tau}_i q \mathrm{d}s \text{ for all } q \in P_{r-1}(e_i)\right\}\\ &\cup \left\{\int_{e_i} \mathrm{rot}\,\boldsymbol{u} q \mathrm{d}s \text{ for all } q \in P_{k-2}(e_i)\right\}.\end{aligned} \tag{5.2.3}$$

- Interior DOFs $\boldsymbol{M}_K(\boldsymbol{u})$ in the element K:

$$\begin{aligned}\boldsymbol{M}_K(\boldsymbol{u}) = &\left\{\int_K \boldsymbol{u}\cdot\boldsymbol{q} \mathrm{d}A \text{ for all } \boldsymbol{q}\circ F_K = B_K\hat{\boldsymbol{q}},\ \hat{\boldsymbol{q}} \in P_{r-3}(\hat{K})\hat{\boldsymbol{x}}\right\}\\ &\cup \left\{\int_K \mathrm{rot}\,\boldsymbol{u} q \mathrm{d}A \text{ for all } q \in P_{k-3}(K)/\mathbb{R}\right\},\end{aligned} \tag{5.2.4}$$

  when K is a triangular element;

$$\begin{aligned}\boldsymbol{M}_K(\boldsymbol{u}) = &\left\{\int_K \boldsymbol{u}\cdot\boldsymbol{q} \mathrm{d}A \text{ for all } \boldsymbol{q}\circ F_K = B_K\hat{\boldsymbol{q}},\ \hat{\boldsymbol{q}} \in Q_{r-2}(\hat{K})\hat{\boldsymbol{x}}\right\}\\ &\cup \left\{\int_K \mathrm{rot}\,\boldsymbol{u} q \mathrm{d}A \text{ for all } q \in Q_{k-2}(K)/\mathbb{R}\right\},\end{aligned} \tag{5.2.5}$$

  when K is a rectangular element.

  Here B_K is defined in (1.5.1), $P_k(\hat{K})\hat{\boldsymbol{x}} = \left\{\hat{\boldsymbol{q}} :\ \hat{\boldsymbol{q}} = \hat{\varphi}\hat{\boldsymbol{x}},\ \forall\hat{\varphi} \in P_k(\hat{K})\right\}$, and $Q_k(\hat{K})\hat{\boldsymbol{x}} = \left\{\hat{\boldsymbol{q}} :\ \hat{\boldsymbol{q}} = \hat{\varphi}\hat{\boldsymbol{x}},\ \forall\hat{\varphi} \in Q_k(\hat{K})\right\}$.

Remark 5.2.1. The DOFs in $\boldsymbol{M}_K(\boldsymbol{u})$ can also be given by

$$\left\{\int_K \boldsymbol{u}\cdot\boldsymbol{q} \mathrm{d}A \text{ for all } \boldsymbol{q}\circ F_K = B_K\hat{\boldsymbol{q}},\ \hat{\boldsymbol{q}} \in \mathscr{P}(\hat{K})\right\},\ \text{when } K \text{ is a triangular element;}$$

$$\left\{\int_K \boldsymbol{u}\cdot\boldsymbol{q} \mathrm{d}A \text{ for all } \boldsymbol{q}\circ F_K = B_K\hat{\boldsymbol{q}},\ \hat{\boldsymbol{q}} \in \mathscr{Q}(\hat{K})\right\},\ \text{when } K \text{ is a rectangular element,}$$

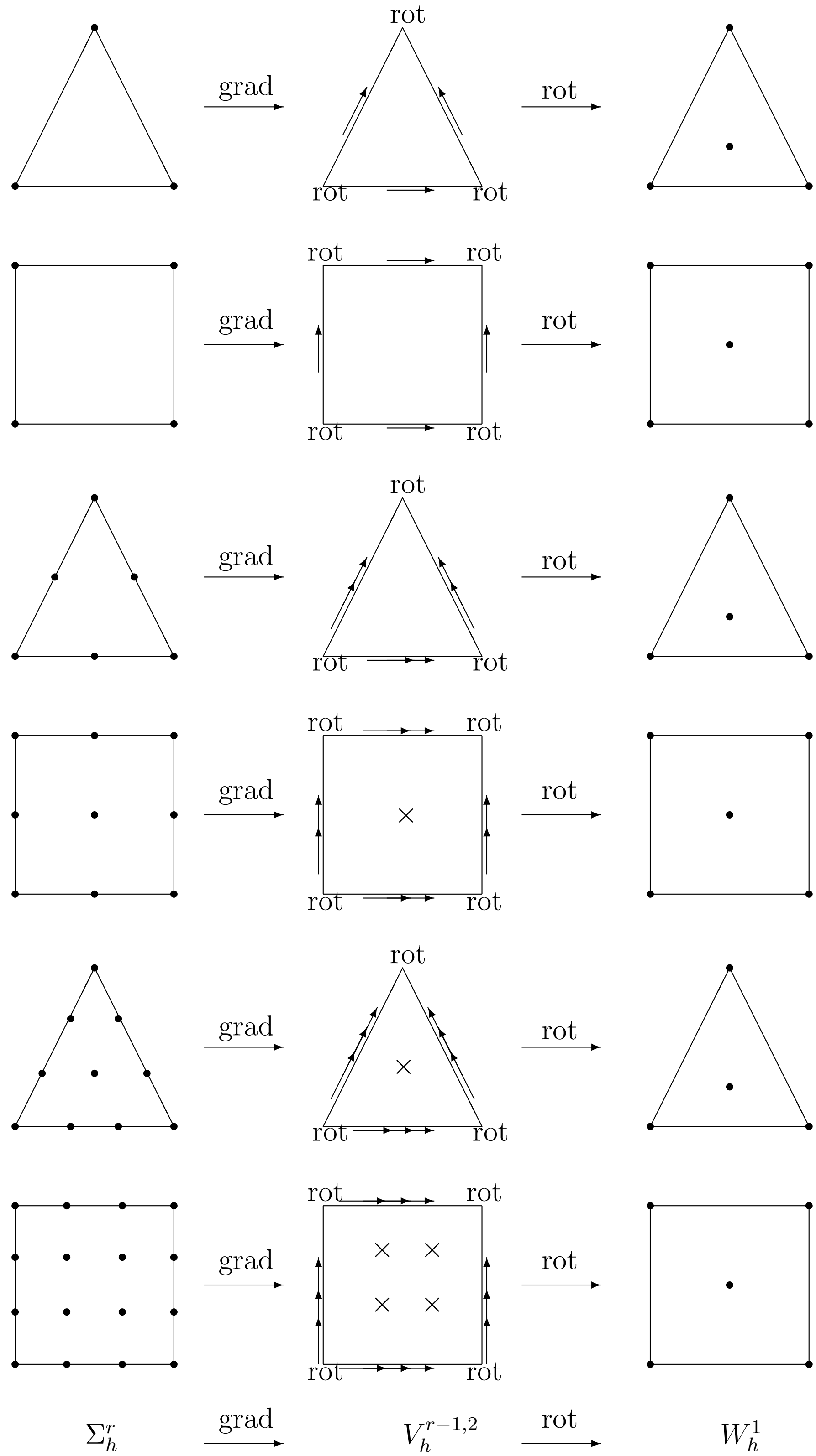

Figure 5.2.1: The lowest-order finite element complexes (5.1.1) in 2D with $r = k$ in the first two rows, $r = k + 1$ in the middle two rows, and $r = k + 2$ in the last two rows.

where $\mathscr{P}(\hat{K}) = \boldsymbol{P}_{k-4}(\hat{K}) \oplus \widetilde{P}_{k-4}(\hat{K})\hat{\boldsymbol{x}} \oplus \cdots \oplus \widetilde{P}_{r-3}(\hat{K})\hat{\boldsymbol{x}}$ and $\mathscr{Q}(\hat{K}) = Q_{r-2}(\hat{K})\hat{\boldsymbol{x}} \oplus \{\hat{\boldsymbol{q}} : \hat{\boldsymbol{q}} = \operatorname{curl}_{\hat{\boldsymbol{x}}} \hat{\varphi},\ \forall \hat{\varphi} \in Q_{k-2}(\hat{K})/\mathbb{R}\}$.

Remark 5.2.2. By Lemma 5.1.2 and the definition of $V_h^{k,k+1}$, we have

$$V_h^{k,k+1}(K) = \begin{cases} \mathcal{R}_{k+1}(K) & \text{when } k \geq 3 \text{ and } K \text{ is a triangle,} \\ Q_{k,k+1}(K) \times Q_{k+1,k}(K) & \text{when } k \geq 2 \text{ and } K \text{ is a rectangle.} \end{cases}$$

Therefore $V_h^{k,k+1}(K)$ coincides with the finite elements constructed in [66]. Here we extend these finite elements to lower-order cases by allowing $k = 1$ and/or 2.

Lemma 5.2.1. *The DOFs* (5.2.2) – (5.2.5) *are well-defined for any* $\boldsymbol{u} \in H^{1/2+\delta}(K) \otimes \mathbb{V}$ *and* $\operatorname{rot} \boldsymbol{u} \in H^{1+\delta}(K)$ *with* $\delta > 0$.

Proof. By the embedding theorem in [27], we have $\operatorname{rot} \boldsymbol{u} \in H^{1+\delta}(K) \subset C^{0,\delta}(K)$, then the DOFs about $\operatorname{rot} \boldsymbol{u}$ are well-defined. It follows Cauchy-Schwarz inequality that other DOFs defined in $\boldsymbol{M}_e(\boldsymbol{u})$ and $\boldsymbol{M}_K(\boldsymbol{u})$ are well-defined since $\boldsymbol{u} \in H^{1/2+\delta}(K) \otimes \mathbb{V}$ and $\boldsymbol{u}|_{\partial K} \in H^{\delta}(\partial K) \otimes \mathbb{V}$. □

Lemma 5.2.2. *The DOFs for* $V_h^{r-1,k+1}(K)$ *are unisolvent.*

Proof. Since the decomposition (5.1.3) is a direct sum, $\dim V_h^{r-1,k+1}(K) = \dim \Sigma_h^{k,+}(K) + \dim \operatorname{grad} \Sigma_h^r(K)$. By counting the number of DOFs, the DOF set has the same dimension. Then it suffices to show that if all the DOFs vanish on a function $\boldsymbol{u} \in V_h^{r-1,k+1}(K)$, then $\boldsymbol{u} = 0$. To see this, we first show that $\operatorname{rot} \boldsymbol{u} = 0$. By integration by parts, the following DOF for $\Sigma_h^{k,+}(K)$ vanishes on $\operatorname{rot} \boldsymbol{u}$:

$$\int_K \operatorname{rot} \boldsymbol{u} \mathrm{d}A = \int_{\partial K} \boldsymbol{u} \cdot \boldsymbol{\tau}_{\partial K} \mathrm{d}s = 0.$$

It follows from $\operatorname{rot} V_h^{r-1,k+1}(K) \subset \Sigma_h^{k,+}(K)$ and the unisolvence of the DOFs for $\Sigma_h^{k,+}(K)$ that $\operatorname{rot} \boldsymbol{u} = 0$. Then $\boldsymbol{u} = \operatorname{grad} \phi$ for some $\phi \in \Sigma_h^r(K)$. By the edge DOFs of $V_h^{r-1,k+1}(K)$, $\boldsymbol{u} \cdot \boldsymbol{\tau}_i = 0$ on the edge e_i. Then there exists a $\psi \in P_{r-3}(K)$ or $Q_{r-2}(K)$ such that $\phi = B_\star \psi$

with $B_\star = B_r$ or B_t. By the property of 2D Koszul operator (see Chapter 2), there exists $\boldsymbol{q}$ such that $B_K^{-1}\boldsymbol{q} \circ F_K \in \hat{\boldsymbol{q}} \in P_{r-3}(\hat{K})\hat{\boldsymbol{x}}$ or $Q_{r-2}(\hat{K})\hat{\boldsymbol{x}}$ and $\operatorname{div}\boldsymbol{q} = \psi$. By the interior DOFs, we have

$$0 = (\boldsymbol{u}, \boldsymbol{q}) = (\operatorname{grad}\phi, \boldsymbol{q}) = -(\phi, \operatorname{div}\boldsymbol{q}) = (B_\star\psi, \psi)\,.$$

This implies that $\psi = 0$ and hence $\boldsymbol{u} = 0$. □

For $\delta > 0$, provided $\boldsymbol{u} \in H^{1/2+\delta}(K) \otimes \mathbb{V}$ with $\operatorname{rot}\boldsymbol{u} \in H^{1+\delta}(K)$ (see Lemma 5.2.1), we can define an $H(\operatorname{grad}\operatorname{rot})$ interpolation operator $\Pi_K\boldsymbol{u} \in V_h^{r-1,k+1}(K)$ such that

$$\boldsymbol{M}_v(\boldsymbol{u} - \Pi_K\boldsymbol{u}) = \{0\},\ \boldsymbol{M}_e(\boldsymbol{u} - \Pi_K\boldsymbol{u}) = \{0\},\ \text{and } \boldsymbol{M}_K(\boldsymbol{u} - \Pi_K\boldsymbol{u}) = \{0\},$$

where $\boldsymbol{M}_v$, $\boldsymbol{M}_e$ and $\boldsymbol{M}_K$ are the sets of DOFs in (5.2.2) – (5.2.5).

5.3 Global Finite Element Complexes

For all $K \in \mathcal{T}_h$, we glue $V_h^{r-1,k+1}(K)$ together by the DOFs (5.2.2) – (5.2.5) to get the global finite element space $V_h^{r-1,k+1}$. Similarly, we can get Σ_h^r and $\Sigma_h^{k,+}$. The global finite element spaces lead to the complex (5.0.2).

Lemma 5.3.1. *The following conformity holds:*

$$V_h^{r-1,k+1} \subset H(\operatorname{grad}\operatorname{rot};\Omega).$$

Proof. To verify $V_h^{r-1,k+1} \subset H(\operatorname{grad}\operatorname{rot};\Omega)$, we must show $\boldsymbol{u}\cdot\boldsymbol{\tau}_i = 0$ and $\operatorname{rot}\boldsymbol{u} = 0$ on each $e_i \in \mathcal{E}_h(K)$ if the DOFs (5.2.2) – (5.2.3) vanish on $\boldsymbol{u} \in V_h^{r-1,k+1}(K)$. It is easy to see that $(\operatorname{rot}\boldsymbol{u})|_{e_i} \in P_k(e_i)$. Since $\hat{\boldsymbol{x}}^\perp\hat{\boldsymbol{\tau}}_i = 0$ on $\hat{e}_i$, $\boldsymbol{u}\cdot\boldsymbol{\tau}_i = \frac{(\hat{\boldsymbol{u}}\cdot\hat{\boldsymbol{\tau}}_i)\circ F_K^{-1}}{|B_K\hat{\boldsymbol{\tau}}_i|} = \frac{(\operatorname{grad}_{\hat{\boldsymbol{x}}}\mathfrak{p}^1_{\hat{\boldsymbol{x}}}\hat{\boldsymbol{u}}\cdot\hat{\boldsymbol{\tau}}_i + \mathfrak{p}^2_{\hat{\boldsymbol{x}}}\operatorname{rot}_{\hat{\boldsymbol{x}}}\hat{\boldsymbol{u}}\cdot\hat{\boldsymbol{\tau}}_i)\circ F_K^{-1}}{|B_K\hat{\boldsymbol{\tau}}_i|} = \frac{(\operatorname{grad}_{\hat{\boldsymbol{x}}}\mathfrak{p}^1_{\hat{\boldsymbol{x}}}\hat{\boldsymbol{u}}\cdot\hat{\boldsymbol{\tau}}_i)\circ F_K^{-1}}{|B_K\hat{\boldsymbol{\tau}}_i|} \in P_{r-1}(e_i)$. From the vanishing DOFs in (5.2.2) –(5.2.3), we have $\boldsymbol{u}\cdot\boldsymbol{\tau}_i = 0$ and $\operatorname{rot}\boldsymbol{u} = 0$ on e_i. □

Theorem 5.3.2. *The complex* (5.0.2) *is exact on contractible domains.*

Proof. We first show the exactness at $V_h^{r-1,k+1}$. To this end, we show that, for any $\boldsymbol{v}_h \in V_h^{r-1,k+1} \subset H(\operatorname{grad}\operatorname{rot};\Omega)$ satisfying $\operatorname{rot}\boldsymbol{v}_h = 0$, there exists $p \in \Sigma_h^r$ such that

$\boldsymbol{v}_h = \operatorname{grad} p$. On one hand, from the exactness of the complex (5.0.1), we have $\boldsymbol{v}_h = \operatorname{grad} p$ for some $p \in H^1(\Omega)$. On the other hand, from Lemma 5.1.1, there exists $p_K \in \Sigma_h^r(K)$ such that $\boldsymbol{v}_h|_K = \operatorname{grad} p|_K = \operatorname{grad} p_K$ for all $K \in \mathcal{T}_h$. Comparing the two aspects, we have $\boldsymbol{v}_h = \operatorname{grad} p$ with $p \in H^1$ and $p|_K \in \Sigma_h^r(K)$ which implies $p \in \Sigma_h^r$. To prove the exactness at $\Sigma_h^{k,+}$, that is to prove the operator rot from $V_h^{r-1,k+1}$ to $\Sigma_h^{k,+}$ is surjective, we count the dimensions. Take the triangular element as an example, the dimension count of the Lagrange elements reads:

$$\dim \Sigma_h^r = \mathcal{V} + (r-1)\mathcal{E} + \frac{1}{2}(r-2)(r-1)\mathcal{K},$$

where $\mathcal{V}$, $\mathcal{E}$, and $\mathcal{K}$ denote the number of vertices, edges, and 2D cells, respectively. Moreover, $\dim \Sigma_h^{k,+} = \dim \Sigma_h^k$ for $k \geq 3$ and $\dim \Sigma_h^{k,+} = \dim \Sigma_h^k + \mathcal{K}$ for $k = 1, 2$. From the DOFs (5.2.2) – (5.2.4),

$$\dim V_h^{r-1,k+1} = \mathcal{V} + (r+k-1)\mathcal{E} + \frac{(r-2)(r-1) + (k-2)(k-1) - 2}{2}\mathcal{K} \text{ for } k \geq 3,$$
$$\dim V_h^{r-1,k+1} = \mathcal{V} + (r+k-1)\mathcal{E} + \frac{(r-2)(r-1) + (k-2)(k-1)}{2}\mathcal{K} \text{ for } k = 1, 2.$$

From the above dimension count, we have

$$\dim V_h^{r-1,k+1} = \dim \Sigma_h^{k,+} + \dim \Sigma_h^r - 1,$$

where we have used Euler's formula $\mathcal{V} - \mathcal{E} + \mathcal{K} = 1$. This completes the proof. $\square$

For $\delta > 0$, denote $\Sigma = H^{1+\delta}(\Omega)$ and $V = \{\boldsymbol{u} \in H^{1/2+\delta}(\Omega) \otimes \mathbb{V} : \operatorname{rot} \boldsymbol{u} \in H^{1+\delta}(\Omega)\}$. We define three global interpolations $\pi_h : \Sigma \to \Sigma_h^r$, $\widetilde{\pi}_h : \Sigma \to \Sigma_h^{k,+}$, and $\Pi_h : V \to V_h^{r-1,k+1}$ in the following way:

$$(\pi_h u)|_K = \pi_K u, \ (\widetilde{\pi}_h u)|_K = \widetilde{\pi}_K u, \text{ and } (\Pi_h \boldsymbol{u})|_K = \Pi_K \boldsymbol{u}, \ \forall K \in \mathcal{T}_h,$$

where the interpolations π_K, $\widetilde{\pi}_K$, and Π_K are defined in Section 5.2.

We summarize the interpolations in the following diagram.

$$
\begin{array}{ccccccccccc}
0 & \longrightarrow & \mathbb{R} & \xrightarrow{\subset} & H^1(\Omega) & \xrightarrow{\operatorname{grad}} & H(\operatorname{grad}\operatorname{rot};\Omega) & \xrightarrow{\operatorname{rot}} & H^1(\Omega) & \longrightarrow & 0 \\
 & & & & \downarrow & & \downarrow & & \downarrow & & \\
0 & \longrightarrow & \mathbb{R} & \xrightarrow{\subset} & \Sigma & \xrightarrow{\operatorname{grad}} & V & \xrightarrow{\operatorname{rot}} & \Sigma & \longrightarrow & 0 \\
 & & & & \downarrow{\scriptstyle \pi_h} & & \downarrow{\scriptstyle \Pi_h} & & \downarrow{\scriptstyle \widetilde{\pi}_h} & & \\
0 & \longrightarrow & \mathbb{R} & \xrightarrow{\subset} & \Sigma_h^r & \xrightarrow{\operatorname{grad}} & V_h^{r-1,k+1} & \xrightarrow{\operatorname{rot}} & \Sigma_h^{k,+} & \longrightarrow & 0,
\end{array}
\tag{5.3.1}
$$

Now we show that the interpolations in (5.3.1) commute with the differential operators. This result will play a key role in the error analysis of the interpolation Π_h.

Lemma 5.3.3. *The last two rows of the complex* (5.3.1) *form a commuting diagram, i.e.,*

$$\operatorname{grad}\pi_h u = \Pi_h \operatorname{grad} u \textit{ for all } u \in \Sigma, \tag{5.3.2}$$

$$\operatorname{rot}\Pi_h \boldsymbol{u} = \widetilde{\pi}_h \operatorname{rot}\boldsymbol{u} \textit{ for all } \boldsymbol{u} \in V. \tag{5.3.3}$$

Proof. We only prove (5.3.2). A similar trick can be used to prove (5.3.3). From the diagram (5.3.1), we know both $\Pi_h \operatorname{grad} u$ and $\operatorname{grad}\pi_h u$ are in the space $V_h^{r-1,k+1}$. It suffices to prove that the DOFs (5.2.2) – (5.2.5) for $\Pi_h \operatorname{grad} u$ and $\operatorname{grad}\pi_h u$ agree for each element $K \in \mathcal{T}_h$. For each $v_i \in \mathcal{V}(K)$, we have

$$\operatorname{rot}\big(\Pi_h \operatorname{grad} u - \operatorname{grad}\pi_h u\big)(v_i) = \operatorname{rot}\big(\operatorname{grad} u - \operatorname{grad}\pi_h u\big)(v_i) = 0.$$

On each edge $e_i \in \mathcal{E}(K)$ with a tangent vector $\boldsymbol{\tau}_i$ and two endpoints v_1 and v_2, we have

$$\int_{e_i}\big(\Pi_h \operatorname{grad} u - \operatorname{grad}\pi_h u\big)\cdot\boldsymbol{\tau}_i q \mathrm{d}s = \int_{e_i}\big(\operatorname{grad} u - \operatorname{grad}\pi_h u\big)\cdot\boldsymbol{\tau}_i q \mathrm{d}s$$

$$= q(v_2)(u-\pi_h u)(v_2) - q(v_1)(u-\pi_h u)(v_1) - \int_{e_i}\big(u-\pi_h u\big)\frac{\partial q}{\partial \boldsymbol{\tau}_i}\mathrm{d}s = 0,\ \forall q \in P_{r-1}(e_i).$$

Here we used integration by parts and the definition of the interpolations. By the definition of Π_h, we have

$$\int_{e_i}\operatorname{rot}\big(\Pi_h \operatorname{grad} u - \operatorname{grad}\pi_h u\big) q \mathrm{d}s = 0,\ \forall q \in P_{k-2}(K).$$

For the interior DOFs, we see that for any $\boldsymbol{q}$ satisfying $B_K^{-1}\boldsymbol{q}\circ F_K \in \mathscr{P}(\hat{K})$ or $\mathscr{Q}(\hat{K})$,

$$\int_K \big(\Pi_h \operatorname{grad} u - \operatorname{grad} \pi_h u\big)\cdot \boldsymbol{q}\mathrm{d}S = \int_K \big(\operatorname{grad} u - \operatorname{grad} \pi_h u\big)\cdot \boldsymbol{q}\mathrm{d}S$$
$$= -\int_K \big(u - \pi_h u\big) \operatorname{div} \boldsymbol{q}\mathrm{d}S + \int_{\partial K} \big(u-\pi_h u\big)\boldsymbol{q}\cdot\boldsymbol{n}\mathrm{d}s = 0.$$

This completes the proof. □

Lemma 5.3.4. *Suppose $\boldsymbol{u}\in V$. Under the transformation* (5.1.7)*, we have*

$$\Pi_K \boldsymbol{u}\circ F_K = B_K^{-\mathrm{T}}\Pi_{\hat{K}}\hat{\boldsymbol{u}}.$$

Proof. We will show that $\widehat{\Pi_K \boldsymbol{u}} = B_K^{\mathrm{T}}\Pi_K\boldsymbol{u}\circ F_K$ as an interpolation on $\hat{K}$ is equal to $\Pi_{\hat{K}}\hat{\boldsymbol{u}}$. Suppose $\Pi_K\boldsymbol{u} = \sum_i d_i(\boldsymbol{u})\boldsymbol{N}_i$ where the DOFs $\{d_i(\boldsymbol{u})\}$ are defined in (5.2.2) – (5.2.5) and $\{\boldsymbol{N}_i\}$ is the corresponding dual basis, then $\widehat{\Pi_K\boldsymbol{u}} = \sum_i d_i(\boldsymbol{u})B_K^{\mathrm{T}}\boldsymbol{N}_i\circ F_K$. According to Proposition 3.4.7 in [16], it suffices to show that each DOF $d_i(\boldsymbol{u})$ is a linear combination of the DOFs $d_i(\hat{\boldsymbol{u}})$ to define $\Pi_{\hat{K}}\hat{\boldsymbol{u}}$.

We now check all the DOFs in (5.2.2) – (5.2.5) one by one:

$$\operatorname{rot}\boldsymbol{u}(v_i) = \frac{\operatorname{rot}_{\hat{\boldsymbol{x}}}\hat{\boldsymbol{u}}(\hat{v}_i)}{\det(B_K)},\ \int_{e_i}\operatorname{rot}\boldsymbol{u}q\mathrm{d}s = \frac{|e_i|}{|\hat{e}_i|}\frac{\int_{\hat{e}_i}\operatorname{rot}_{\hat{\boldsymbol{x}}}\hat{\boldsymbol{u}}\hat{q}\mathrm{d}\hat{s}}{\det(B_K)},$$
$$\int_{e_i}\boldsymbol{u}\cdot\boldsymbol{\tau}_i q\mathrm{d}s = \int_{\hat{e}_i} B_K^{-\mathrm{T}}\hat{\boldsymbol{u}}\cdot\frac{B_K\hat{\boldsymbol{\tau}}_i}{|B_K\hat{\boldsymbol{\tau}}_i|}\frac{|e_i|}{|\hat{e}_i|}\hat{q}\mathrm{d}\hat{s} = \int_{\hat{e}_i}\hat{\boldsymbol{u}}\cdot\hat{\boldsymbol{\tau}}_i\hat{q}\mathrm{d}\hat{s},$$
$$\int_K \boldsymbol{u}\cdot\boldsymbol{q}\mathrm{d}A = \int_{\hat{K}} B_K^{-\mathrm{T}}\hat{\boldsymbol{u}}\cdot B_K\hat{\boldsymbol{x}}\hat{q}\det(B_K)\mathrm{d}\hat{A} = \det(B_K)\int_{\hat{K}}\hat{\boldsymbol{u}}\cdot\hat{\boldsymbol{x}}\hat{q}\mathrm{d}\hat{A},$$
$$\int_K \operatorname{rot}\boldsymbol{u}q\mathrm{d}A = \int_{\hat{K}}\frac{\operatorname{rot}_{\hat{\boldsymbol{x}}}\hat{\boldsymbol{u}}}{\det(B_K)}\hat{q}\det(B_K)\mathrm{d}\hat{A} = \int_{\hat{K}}\operatorname{rot}_{\hat{\boldsymbol{x}}}\hat{\boldsymbol{u}}\hat{q}\mathrm{d}\hat{A}.$$

Here $|e_i|$ is the length of e_i.

□

Lemma 5.3.5 ([49, 2])**.** *Suppose that $\boldsymbol{v}$ and $\hat{\boldsymbol{v}}$ are related by the transformation* (5.1.7)*. Then for any $s\geq 0$, we have*

$$|\hat{\boldsymbol{v}}|_{s,\hat{K}} \leq Ch_K^s\,\|\boldsymbol{v}\|_{s,K}\,,$$
$$\big|\operatorname{rot}_{\hat{\boldsymbol{x}}}\hat{\boldsymbol{v}}\big|_{s,\hat{K}} \leq Ch_K^{s+1}\,\|\operatorname{rot}\boldsymbol{v}\|_{s,K}\,.$$

Theorem 5.3.6. *Suppose* $\boldsymbol{u} \in H^{\max\{s+(r-k-1),1/2+\delta\}}(\Omega) \otimes \mathbb{V}$ *and* $\operatorname{rot} \boldsymbol{u} \in H^s(\Omega)$ *with* $s \geq 1+\delta$*, then we have the following error estimates for the interpolation* Π_h*,*

$$\|\boldsymbol{u} - \Pi_h \boldsymbol{u}\| \leq C h^{r_1} (\|\boldsymbol{u}\|_{\max\{s+(r-k-1),1/2+\delta\}} + \|\operatorname{rot} \boldsymbol{u}\|_s), \tag{5.3.4}$$

$$\|\operatorname{rot}(\boldsymbol{u} - \Pi_h \boldsymbol{u})\| \leq C h^{r_2} \|\operatorname{rot} \boldsymbol{u}\|_s, \tag{5.3.5}$$

$$\|\operatorname{grad} \operatorname{rot}(\boldsymbol{u} - \Pi_h \boldsymbol{u})\| \leq C h^{r_2 - 1} \|\operatorname{rot} \boldsymbol{u}\|_s. \tag{5.3.6}$$

Here $r_1 = \min\{\max\{s + (r-k-1), 1/2+\delta\}, r\}$ *and* $r_2 = \min\{s, k+1\}$*.*

Proof. (i). We divide our proof in three steps. We apply the transformation (5.1.7) and Lemma 5.3.4 to derive

$$\begin{aligned}
&\|\boldsymbol{u} - \Pi_K \boldsymbol{u}\|_K \\
=& \left(\int_{\hat{K}} \left| B_K^{-\mathrm{T}} (\hat{\boldsymbol{u}} - \widehat{\Pi_K \boldsymbol{u}}) \right|^2 |\det(B_K)| \, \mathrm{d}\hat{V} \right)^{\frac{1}{2}} \\
\leq& |\det(B_K)|^{\frac{1}{2}} \left\| B_K^{-1} \right\| \|\hat{\boldsymbol{u}} - \Pi_{\hat{K}} \hat{\boldsymbol{u}}\|_{\hat{K}}.
\end{aligned} \tag{5.3.7}$$

Denote by $\widetilde{r}_1$ the largest integer strictly less than r_1. Noting the fact that $\Pi_{\hat{K}} \hat{\boldsymbol{p}} = \hat{\boldsymbol{p}}$ when $\hat{\boldsymbol{p}} \in \boldsymbol{P}_{\widetilde{r}_1}(\hat{K}) \subseteq \boldsymbol{P}_{r-1}(\hat{K}) \subseteq V_h^{r-1,k+1}(\hat{K})$ (see Lemma 5.1.2), we obtain, with the help of Lemma 5.2.1

$$\begin{aligned}
&\|\hat{\boldsymbol{u}} - \Pi_{\hat{K}} \hat{\boldsymbol{u}}\|_{\hat{K}} = \|(I - \Pi_{\hat{K}})(\hat{\boldsymbol{u}} + \hat{\boldsymbol{p}})\|_{\hat{K}} \\
\leq& C \left(\|\hat{\boldsymbol{u}} + \hat{\boldsymbol{p}}\|_{1/2+\delta,\hat{K}} + \|\operatorname{rot}_{\hat{\boldsymbol{x}}}(\hat{\boldsymbol{u}} + \hat{\boldsymbol{p}})\|_{1+\delta,\hat{K}} \right) \\
\leq& C \left(\|\hat{\boldsymbol{u}} + \hat{\boldsymbol{p}}\|_{r_1,\hat{K}} + \|\operatorname{rot}_{\hat{\boldsymbol{x}}}(\hat{\boldsymbol{u}} + \hat{\boldsymbol{p}})\|_{r_2,\hat{K}} \right).
\end{aligned}$$

Denote by $[s]$ the integer part of s. Applying Theorem 5.5 in [49], we have when $r = k$ (in this case $r_1 + 1 = r_2$),

$$\begin{aligned}
&\|\hat{\boldsymbol{u}} - \Pi_{\hat{K}} \hat{\boldsymbol{u}}\|_{\hat{K}} = \inf_{\hat{\boldsymbol{p}} \in \boldsymbol{P}_{\widetilde{r}_1}(\hat{K})} \|(I - \Pi_{\hat{K}})(\hat{\boldsymbol{u}} + \hat{\boldsymbol{p}})\|_{\hat{K}} \\
\leq& \inf_{\hat{\boldsymbol{p}} \in \boldsymbol{P}_{\widetilde{r}_1}(\hat{K})} C \left(\|\hat{\boldsymbol{u}} + \hat{\boldsymbol{p}}\|_{r_1,\hat{K}} + \|\operatorname{rot}_{\hat{\boldsymbol{x}}}(\hat{\boldsymbol{u}} + \hat{\boldsymbol{p}})\|_{r_1,\hat{K}} + |\operatorname{rot}_{\hat{\boldsymbol{x}}} \hat{\boldsymbol{u}}|_{r_2,\hat{K}} + |\operatorname{rot}_{\hat{\boldsymbol{x}}} \hat{\boldsymbol{u}}|_{[r_2],\hat{K}} \right) \\
\leq& C \left(|\hat{\boldsymbol{u}}|_{r_1,\hat{K}} + |\operatorname{rot}_{\hat{\boldsymbol{x}}} \hat{\boldsymbol{u}}|_{[r_1],\hat{K}} + |\operatorname{rot}_{\hat{\boldsymbol{x}}} \hat{\boldsymbol{u}}|_{r_1,\hat{K}} + |\operatorname{rot}_{\hat{\boldsymbol{x}}} \hat{\boldsymbol{u}}|_{[r_2],\hat{K}} + |\operatorname{rot}_{\hat{\boldsymbol{x}}} \hat{\boldsymbol{u}}|_{r_2,\hat{K}} \right),
\end{aligned}$$

when $r = k+1$ (in this case $r_1 = r_2$),

$$\begin{aligned}
\|\hat{\boldsymbol{u}} - \Pi_{\hat{K}}\hat{\boldsymbol{u}}\|_{\hat{K}} &= \inf_{\hat{\boldsymbol{p}}\in \boldsymbol{P}_{\widetilde{r}_1}(\hat{K})} \|(I-\Pi_{\hat{K}})\,(\hat{\boldsymbol{u}}+\hat{\boldsymbol{p}})\|_{\hat{K}} \\
&\le \inf_{\hat{\boldsymbol{p}}\in \boldsymbol{P}_{\widetilde{r}_1}(\hat{K})} C\left(\|\hat{\boldsymbol{u}}+\hat{\boldsymbol{p}}\|_{r_1,\hat{K}} + \|\mathrm{rot}_{\hat{\boldsymbol{x}}}(\hat{\boldsymbol{u}}+\hat{\boldsymbol{p}})\|_{r_1,\hat{K}}\right) \\
&\le C\left(|\hat{\boldsymbol{u}}|_{r_1,\hat{K}} + |\mathrm{rot}_{\hat{\boldsymbol{x}}}\,\hat{\boldsymbol{u}}|_{[r_1],\hat{K}} + |\mathrm{rot}_{\hat{\boldsymbol{x}}}\,\hat{\boldsymbol{u}}|_{r_1,\hat{K}}\right),
\end{aligned}$$

and when $r = k+2$ (in this case $r_1 = r_2 + 1$),

$$\begin{aligned}
\|\hat{\boldsymbol{u}} - \Pi_{\hat{K}}\hat{\boldsymbol{u}}\|_{\hat{K}} &= \inf_{\hat{\boldsymbol{p}}\in \boldsymbol{P}_{\widetilde{r}_1}(\hat{K})} \|(I-\Pi_{\hat{K}})\,(\hat{\boldsymbol{u}}+\hat{\boldsymbol{p}})\|_{\hat{K}} \\
&\le \inf_{\hat{\boldsymbol{p}}\in \boldsymbol{P}_{\widetilde{r}_1}(\hat{K})} C\,\|\hat{\boldsymbol{u}}+\hat{\boldsymbol{p}}\|_{r_1,\hat{K}} \le C\,|\hat{\boldsymbol{u}}|_{r_1,\hat{K}}\,.
\end{aligned}$$

Collecting the above two equations with (5.3.7), using Lemma 5.3.5, and summing over $K \in \mathcal{T}_h$ leads to

$$\|\boldsymbol{u} - \Pi_h\boldsymbol{u}\| = \sum_{K\in\mathcal{T}_h} \|\boldsymbol{u} - \Pi_K\boldsymbol{u}\|_K \le Ch^{r_1}(\|\boldsymbol{u}\|_{\max\{s+(r-k-1),1/2+\delta\},K} + \|\mathrm{rot}\,\boldsymbol{u}\|_{s,K}).$$

(ii). From (5.3.3), we have for $i = 0, 1$,

$$\|\mathrm{rot}(\boldsymbol{u} - \Pi_h\boldsymbol{u})\|_i = \|(I - \widetilde{\pi}_h)\,\mathrm{rot}\,\boldsymbol{u}\|_i$$

which, together with the error estimate of Lagrange interpolation [49, Theorem 5.48], leads to

$$\|\mathrm{rot}(\boldsymbol{u} - \Pi_h\boldsymbol{u})\|_i \le Ch^{r_2-i}\,\|\mathrm{rot}\,\boldsymbol{u}\|_{s,K}\,.$$

□

5.4 Applications to $-\mathrm{curl}\,\Delta\,\mathrm{rot}$ Problems

In this section, we use the three families of the grad rot-conforming finite elements to solve a problem slightly different from the problem (3.2.14).

For $\boldsymbol{f} \in H(\operatorname{div}^0;\Omega)$, find $\boldsymbol{u}$, such that

$$\begin{aligned} -\operatorname{curl}\Delta\operatorname{rot}\boldsymbol{u}+\boldsymbol{u}&=\boldsymbol{f} \quad \text{in } \Omega,\\ \operatorname{div}\boldsymbol{u}&=0 \quad \text{in } \Omega,\\ \boldsymbol{u}\times\boldsymbol{n}&=0 \quad \text{on } \partial\Omega,\\ \operatorname{rot}\boldsymbol{u}&=0 \quad \text{on } \partial\Omega. \end{aligned} \tag{5.4.1}$$

Here $H(\operatorname{div}^0;\Omega)$ is the space of $L^2(\Omega)\otimes\mathbb{V}$ functions with vanishing divergence, i.e.,

$$H(\operatorname{div}^0;\Omega) := \{\boldsymbol{u}\in L^2(\Omega)\otimes\mathbb{V} : \ \operatorname{div}\boldsymbol{u}=0\}.$$

Taking divergence on both sides of the first equation of (5.4.1), we see that the divergence-free condition $\operatorname{div}\boldsymbol{u}=0$ holds automatically.

We define $H_0(\operatorname{grad}\operatorname{rot};\Omega)$ with vanishing boundary conditions:

$$H_0(\operatorname{grad}\operatorname{rot};\Omega) := \{\boldsymbol{u}\in H(\operatorname{grad}\operatorname{rot};\Omega) : \ \boldsymbol{n}\times\boldsymbol{u}=0 \text{ and } \operatorname{rot}\boldsymbol{u}=0 \ \text{ on } \partial\Omega\}.$$

The variational formulation reads: find $\boldsymbol{u}\in H_0(\operatorname{grad}\operatorname{rot};\Omega)$ such that

$$a(\boldsymbol{u},\boldsymbol{v}) = (\boldsymbol{f},\boldsymbol{v}), \quad \forall \boldsymbol{v}\in H_0(\operatorname{grad}\operatorname{rot};\Omega) \tag{5.4.2}$$

with $a(\boldsymbol{u},\boldsymbol{v}) := (\operatorname{grad}\operatorname{rot}\boldsymbol{u},\operatorname{grad}\operatorname{rot}\boldsymbol{v}) + (\boldsymbol{u},\boldsymbol{v})$. Taking $\boldsymbol{v}=\operatorname{grad} p$ with $p\in H_0^1(\Omega)$ in (5.4.2), we see that $(\boldsymbol{u},\nabla p) = (\boldsymbol{f},\nabla p) = (\operatorname{div}\boldsymbol{f},p)=0$, which implies $\operatorname{div}\boldsymbol{u}=0$.

The strong formulation (5.4.1) and the weak formulation (5.4.2) are equivalent. By suitable modification to the proof of [6, Theorem 4.8]) and [6, Theorem 4.9]), we can show the problem (5.4.1) is well-posed, and it holds

$$\|\boldsymbol{u}\| + \|\operatorname{grad}\operatorname{rot}\boldsymbol{u}\| + \|\operatorname{curl}\Delta\operatorname{rot}\boldsymbol{u}\| \le C\|\boldsymbol{f}\|. \tag{5.4.3}$$

We assume further Ω is a polygon. If we have (4.2.2), proceeding as the proof of Theorem 4.2.1, we can show that

$$\|\boldsymbol{u}\|_{\alpha} + \|\operatorname{rot}\boldsymbol{u}\|_{1+\alpha} \le C\|\boldsymbol{f}\|, \tag{5.4.4}$$

with the constant α defined in Theorem 4.2.1. When Ω is convex, $\alpha = 1$.

Now we prove (4.2.2) for the problem (5.4.1).

Lemma 5.4.1. *It holds the following estimate*

$$\|\Delta \operatorname{rot} \boldsymbol{u}\| \leq C\|\boldsymbol{f}\|.$$

Proof. Let $q = \Delta \operatorname{rot} \boldsymbol{u} - \frac{(\Delta \operatorname{rot} \boldsymbol{u}, 1)}{|\Omega|}$, then $(q, 1) = 0$, and hence

$$\|q\| \leq C\|\operatorname{curl} q\|.$$

Using the triangle inequality, we have

$$\|\Delta \operatorname{rot} \boldsymbol{u}\| \leq \|q\| + \frac{|(\Delta \operatorname{rot} \boldsymbol{u}, 1)|}{|\Omega|^{1/2}} \leq C\|\operatorname{curl} q\| + \frac{|(\Delta \operatorname{rot} \boldsymbol{u}, 1)|}{|\Omega|^{1/2}} \tag{5.4.5}$$

Since $C_0^\infty(\Omega)$ is dense in $L^2(\Omega)$, there exists a function $\rho \in C_0^\infty(\Omega) \subset H_0^1(\Omega)$ satisfying

$$\|1 - \rho\| < 1/2|\Omega|^{1/2},$$

and hence,

$$\begin{aligned} |(\Delta \operatorname{rot} \boldsymbol{u}, 1)| &\leq |(\Delta \operatorname{rot} \boldsymbol{u}, \rho)| + |(\Delta \operatorname{rot} \boldsymbol{u}, 1 - \rho)| \\ &\leq \|\Delta \operatorname{rot} \boldsymbol{u}\|_{-1}\|\rho\|_1 + \|\Delta \operatorname{rot} \boldsymbol{u}\|\|1 - \rho\|. \end{aligned}$$

Taking (5.4.5) into consideration, we get

$$\|\Delta \operatorname{rot} \boldsymbol{u}\| \leq C\left(\|\operatorname{curl} q\| + \|\Delta \operatorname{rot} \boldsymbol{u}\|_{-1}\right) + \frac{1}{2}\|\Delta \operatorname{rot} \boldsymbol{u}\|,$$

which leads to

$$\|\Delta \operatorname{rot} \boldsymbol{u}\| \leq C\left(\|\operatorname{curl} q\| + \|\Delta \operatorname{rot} \boldsymbol{u}\|_{-1}\right). \tag{5.4.6}$$

According to the definition of the negative norm, we have

$$\|\Delta \operatorname{rot} \boldsymbol{u}\|_{-1} = \sup_{0 \neq p \in H_0^1(\Omega)} \frac{(\Delta \operatorname{rot} \boldsymbol{u}, p)}{\|p\|_1} = \sup_{0 \neq p \in H_0^1(\Omega)} \frac{(\operatorname{grad} \operatorname{rot} \boldsymbol{u}, \operatorname{grad} p)}{\|p\|_1} \leq \|\operatorname{grad} \operatorname{rot} \boldsymbol{u}\|.$$

Plugging the above estimate to (5.4.6) and applying (5.4.3), we obtain

$$\|\Delta \operatorname{rot} \boldsymbol{u}\| \leq C\left(\|\operatorname{curl} q\| + \|\operatorname{grad} \operatorname{rot} \boldsymbol{u}\|\right) = C\left(\|\operatorname{curl} \Delta \operatorname{rot} \boldsymbol{u}\| + \|\operatorname{grad} \operatorname{rot} \boldsymbol{u}\|\right) \leq C\|\boldsymbol{f}\|.$$

□

We define the finite element space with vanishing boundary conditions

$$\mathring{V}_h^{r-1,k+1} = \{\boldsymbol{v}_h \in V_h^{r-1,k+1},\ \boldsymbol{n} \times \boldsymbol{v}_h = 0 \text{ and } \operatorname{rot} \boldsymbol{v}_h = 0 \text{ on } \partial\Omega\}.$$

Remark 5.4.1. To enforce the vanishing boundary conditions, we only need to set all the DOFs on $\partial\Omega$ to be 0.

The grad rot-conforming finite element method reads: seek $\boldsymbol{u}_h \in \mathring{V}_h^{r-1,k+1}$ such that

$$a(\boldsymbol{u}_h, \boldsymbol{v}_h) = (\boldsymbol{f}, \boldsymbol{v}_h), \quad \forall \boldsymbol{v}_h \in \mathring{V}_h^{r-1,k+1}. \tag{5.4.7}$$

Taking $\boldsymbol{v}_h = \operatorname{grad} p_h$ with $p_h \in \mathring{\Sigma}_h^r = \{q \in \Sigma_h^r : q = 0 \text{ on } \partial\Omega\}$ in (5.4.7), we have $(\boldsymbol{u}_h, \nabla p_h) = 0$. The div-free condition holds in a weak sense. If there is no term $\boldsymbol{u}$ in the problem (5.4.1), we usually introduce a Lagrange multiplier to enforce the div-free condition.

To get the error estimate in the sense of $H(\text{rot})$-norm, we introduce the following auxiliary problem. Find $\boldsymbol{w}$ such that

$$\begin{aligned} -\operatorname{curl} \Delta \operatorname{rot} \boldsymbol{w} + \boldsymbol{w} &= \operatorname{curl} \operatorname{rot}(\boldsymbol{u} - \boldsymbol{u}_h) \text{ in } \Omega, \\ \operatorname{div} \boldsymbol{w} &= 0 \text{ in } \Omega, \\ \boldsymbol{w} \times \boldsymbol{n} &= 0 \text{ on } \partial\Omega, \\ \operatorname{rot} \boldsymbol{w} &= 0 \text{ on } \partial\Omega. \end{aligned} \tag{5.4.8}$$

Due to the special form of the right-hand side in the auxiliary problem, we can have a better result than (5.4.4). This result will play an important role in the dual argument in the approximation analysis below.

Theorem 5.4.2. *In addition to the assumptions on Ω, we further assume that Ω is a polygon. The solution $\boldsymbol{w}$ of* (5.4.8) *satisfies*

$$\|\boldsymbol{w}\|_\alpha + \|\operatorname{rot} \boldsymbol{w}\|_{1+\alpha} \le C\|\operatorname{rot}(\boldsymbol{u} - \boldsymbol{u}_h)\|.$$

Proof. Multiplying both sides of the first equation in (7.4.5) by $\boldsymbol{w}$, integrating over Ω, and dividing by $\|\boldsymbol{w}\|_{H(\mathrm{grad\,rot};\Omega)}$ lead to

$$\|\boldsymbol{w}\|_{H(\mathrm{grad\,rot};\Omega)} \leq \|\operatorname{rot}(\boldsymbol{u}-\boldsymbol{u}_h)\|. \tag{5.4.9}$$

Since $H_0(\mathrm{grad\,rot};\Omega)\cap H(\mathrm{div}^0;\Omega) \subset H_0(\mathrm{rot};\Omega)\cap H(\mathrm{div};\Omega) \hookrightarrow H^\alpha(\Omega)\otimes\mathbb{V}$ with $\alpha > 1/2$ [4], it holds

$$\|\boldsymbol{w}\|_\alpha \leq C\left(\|\boldsymbol{w}\| + \|\operatorname{rot}\boldsymbol{w}\|\right) \leq C\|\boldsymbol{w}\|_{H(\mathrm{grad\,rot};\Omega)} \leq C\|\operatorname{rot}(\boldsymbol{u}-\boldsymbol{u}_h)\|.$$

Rewriting the first equation of (7.4.5) gives

$$\boldsymbol{w} = \operatorname{curl}\left(\operatorname{rot}(\boldsymbol{u}-\boldsymbol{u}_h) + \Delta\operatorname{rot}\boldsymbol{w}\right) \in L^2(\Omega)\otimes\mathbb{V}.$$

Let $q = \operatorname{rot}(\boldsymbol{u}-\boldsymbol{u}_h) + \Delta\operatorname{rot}\boldsymbol{w} - \frac{(\Delta\operatorname{rot}\boldsymbol{w},1)}{|\Omega|}$, then we have $(q,1)=0$ and hence

$$\|q\| \leq C\|\operatorname{curl} q\| = C\|\boldsymbol{w}\|. \tag{5.4.10}$$

The definition of q gives

$$-\Delta\operatorname{rot}\boldsymbol{w} = \operatorname{rot}(\boldsymbol{u}-\boldsymbol{u}_h) - q - \frac{(\Delta\operatorname{rot}\boldsymbol{w},1)}{|\Omega|} \in L^2(\Omega).$$

Moreover, $\operatorname{rot}\boldsymbol{w}$ satisfies the boundary condition

$$\operatorname{rot}\boldsymbol{w} = 0.$$

By the regularity of the Laplace problem [49], there exists a constant $\alpha > 1/2$ such that

$$\|\operatorname{rot}\boldsymbol{w}\|_{1+\alpha} \leq C\|\Delta\operatorname{rot}\boldsymbol{w}\|. \tag{5.4.11}$$

It remains to show

$$\|\Delta\operatorname{rot}\boldsymbol{w}\| \leq C\|\operatorname{rot}(\boldsymbol{u}-\boldsymbol{u}_h)\|.$$

By the triangle inequality,

$$\|\Delta\operatorname{rot}\boldsymbol{w}\| \leq \|\operatorname{rot}(\boldsymbol{u}-\boldsymbol{u}_h)\| + \|q\| + \frac{|(\Delta\operatorname{rot}\boldsymbol{w},1)|}{|\Omega|^{1/2}}.$$

Proceeding as the proof of Lemma 5.4.1, we obtain

$$\begin{aligned}\|\Delta \operatorname{rot} \boldsymbol{w}\| &\le C\left(\|\operatorname{rot}(\boldsymbol{u}-\boldsymbol{u}_h)\| + \|\operatorname{curl} q\| + \operatorname{grad}\operatorname{rot}\boldsymbol{w}\|\right)\\ &\le C\left(\|\operatorname{rot}(\boldsymbol{u}-\boldsymbol{u}_h)\| + \|\boldsymbol{w}\|_{H(\operatorname{grad}\operatorname{rot};\Omega)}\right) \le C\|\operatorname{rot}(\boldsymbol{u}-\boldsymbol{u}_h)\|.\end{aligned}$$

□

Theorem 5.4.3. *Suppose* $\boldsymbol{u} \in H^{s+(r-k-1)}(\Omega)\otimes\mathbb{V}$ *and* $\operatorname{rot}\boldsymbol{u} \in H^s(\Omega)$ *with* $s \ge 1+\alpha$, *we have the following error estimates for the numerical solution* $\boldsymbol{u}_h$*:*

$$\|\boldsymbol{u}-\boldsymbol{u}_h\|_{H(\operatorname{grad}\operatorname{rot};\Omega)} \le Ch^{r_2-1}\left(\|\boldsymbol{u}\|_{s+(r-k-1)} + \|\operatorname{rot}\boldsymbol{u}\|_s\right), \tag{5.4.12}$$

$$\|\operatorname{rot}(\boldsymbol{u}-\boldsymbol{u}_h)\| \le Ch^{\min\{r_2,2\alpha\}}\left(\|\boldsymbol{u}\|_{s+(r-k-1)} + \|\operatorname{rot}\boldsymbol{u}\|_s\right), \tag{5.4.13}$$

$$\|\boldsymbol{u}-\boldsymbol{u}_h\| \le Ch^{\min\{r_2,2\alpha\}}\left(\|\boldsymbol{u}\|_s + \|\operatorname{rot}\boldsymbol{u}\|_s\right) \ \textit{when}\ r = k+1, k+2, \tag{5.4.14}$$

where $r_2 = \min\{s, k+1\}$.

Remark 5.4.2. The estimate for $\|\boldsymbol{u}-\boldsymbol{u}_h\|$ is not optimal for the family $r = k+2$. In the numerical experiment, we can observe one-order higher accuracy when $k \ge 2$ if $\boldsymbol{u}$ is sufficiently smooth.

Proof. The estimates (5.4.12) and (5.4.13) follow immediately from the Céa's lemma, dual argument, and Theorem 5.3.6. Proceeding as in the proof of [61, Theorem 6], we can show that (5.4.14) holds. □

5.5 Numerical Experiments

We now turn to a concrete example. We consider the problem (5.4.1) on a unit square $\Omega = (0,1)\times(0,1)$ with an exact solution

$$\boldsymbol{u} = \begin{pmatrix} 3\pi\sin^3(\pi x_1)\sin^2(\pi x_2)\cos(\pi x_2) \\ \\ -3\pi\sin^3(\pi x_2)\sin^2(\pi x_1)\cos(\pi x_1)\end{pmatrix}. \tag{5.5.1}$$

Then the source term $\boldsymbol{f}$ can be obtained by a simple calculation.

To measure the error between the exact solution and the finite element solution, we denote

$$\boldsymbol{e}_h = \boldsymbol{u} - \boldsymbol{u}_h.$$

5.5.1 The New Family of Elements with $r = k$

We first use the lowest-order element in the new family with $r = k$ to solve the problem (5.4.1). In this test, we use uniform triangular meshes and uniform rectangular meshes with the mesh size h varying from 1/20 to 1/320 by the bisection strategy. For $\boldsymbol{u} = (u_1, u_2)^{\mathrm{T}}$, we define two discrete norms:

$$\|\!|\boldsymbol{u}|\!\|_V^2 = \sum_{K\in\mathcal{T}_h} 2h_1^K \int_{x_2^K-h_2^K}^{x_2^K+h_2^K} u_1^2(x_1^K, x_2)\mathrm{d}x_2 + \sum_{K\in\mathcal{T}_h} 2h_2^K \int_{x_1^K-h_1^K}^{x_1^K+h_1^K} u_2^2(x_1, x_2^K)\mathrm{d}x_1,$$

$$\|\!|\boldsymbol{u}|\!\|_W^2 = \sum_{K\in\mathcal{T}_h} 4h_1^K h_2^K \left(u_1^2(x_1^K, x_2^K) + u_2^2(x_1^K, x_2^K)\right),$$

where $K = (x_1^K - h_1^K, x_1^K + h_1^K) \times (x_2^K - h_2^K, x_2^K + h_2^K)$ with the center (x_1^K, x_2^K) and the side length $2h_1^K, 2h_2^K$.

Table 5.5.1 illustrates various errors and convergence rates for triangular elements. Table 5.5.2 shows errors measured in various norms for rectangular elements. We also depict error curves for rectangular elements with a log-log scale in Fig. 5.5.1. We observe that the numerical solution converges to the exact solution with convergence order 1 in the L^2-norm, 2 in the $H(\mathrm{rot})$-norm, and 1 in the $H(\mathrm{grad\,rot})$-norm, respectively. From Fig. 5.5.1, we also observe some superconvergence phenomena of $\boldsymbol{e}_h$ and $\mathrm{grad\,rot}\,\boldsymbol{e}_h$ measured in the sense of $\|\!|\cdot|\!\|_V$ and $\|\!|\cdot|\!\|_W$, respectively. Using these superconvergent results, together with some recovery techniques, we can construct a solution with higher accuracy if needed.

5.5.2 The Family of Elements with $r = k + 1$

We then use the lowest-order element $V_h^{k,k+1}$ in the family with $r = k + 1$.

Again, we use the uniform mesh. Table 5.5.3 and Table 5.5.4 demonstrate the numer-

Table 5.5.1: Numerical results of the triangular element with $r = k$ and $k = 1$

h	$\lVert \boldsymbol{e}_h \rVert$	rates	$\lVert \mathrm{rot}\, \boldsymbol{e}_h \rVert$	rates	$\lVert \mathrm{grad}\,\mathrm{rot}\, \boldsymbol{e}_h \rVert$	rates
1/20	2.099367e-01		7.598390e-01		2.510488e+01	
1/40	9.736039e-02	1.1085	1.960868e-01	1.9542	1.258823e+01	0.9959
1/80	4.759381e-02	1.0326	4.941757e-02	1.9884	6.297909e+00	0.9991
1/160	2.365626e-02	1.0086	1.237934e-02	1.9971	3.149406e+00	0.9998
1/320	1.183872e-02	0.9987	3.096531e-03	1.9992	1.574759e+00	0.9999

Table 5.5.2: Numerical results of the rectangular element with $r = k$ and $k = 1$

h	$\lVert \boldsymbol{e}_h \rVert$	$\lVert \boldsymbol{e}_h \rVert_V$	$\lVert \mathrm{rot}\, \boldsymbol{e}_h \rVert$	$\lVert \mathrm{grad}\,\mathrm{rot}\, \boldsymbol{e}_h \rVert$	$\lVert \mathrm{grad}\,\mathrm{rot}\, \boldsymbol{e}_h \rVert_W$
1/20	1.56953e-01	3.83651e-02	2.63065e-01	1.48431e+01	3.23332e+00
1/40	5.76799e-02	9.62913e-03	6.58847e-02	7.41177e+00	8.08779e-01
1/80	2.84156e-02	2.40963e-03	1.64788e-02	3.70484e+00	2.02224e-01
1/160	1.41756e-02	6.02611e-04	4.12019e-03	1.85230e+00	5.05578e-02
1/320	7.08507e-03	2.08784e-04	1.03009e-03	9.26132e-01	1.26397e-02

ical results with h varying from 1/10 to 1/160. We observe a second-order convergence in the sense of $H(\mathrm{rot})$-norm and a first-order convergence in the sense of $H(\mathrm{grad}\,\mathrm{rot})$-norm.

Table 5.5.3: Numerical results of the triangular element with $r = k + 1$ and $k = 1$

h	$\lVert \boldsymbol{e}_h \rVert$	rates	$\lVert \mathrm{rot}\, \boldsymbol{e}_h \rVert$	rates	$\lVert \mathrm{grad}\,\mathrm{rot}\, \boldsymbol{e}_h \rVert$	rates
1/10	1.924001e-01		1.836748e+00		4.822043e+01	
1/20	5.037761e-02	1.9333	4.924701e-01	1.8990	2.491412e+01	0.9527
1/40	1.275089e-02	1.9822	1.253756e-01	1.9738	1.256258e+01	0.9878
1/80	3.197749e-03	1.9955	3.148802e-02	1.9934	6.294644e+00	0.9969
1/160	8.016954e-04	1.9959	7.881059e-03	1.9983	3.148996e+00	0.9992

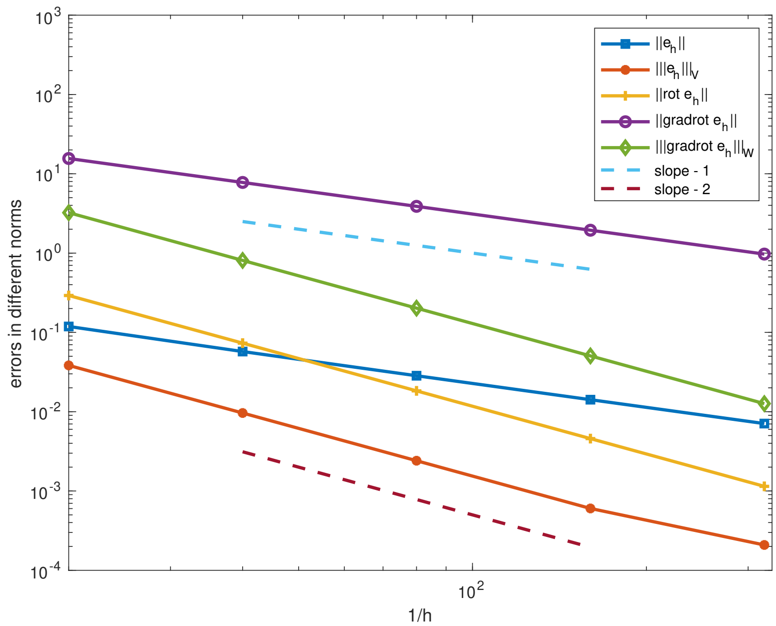

Figure 5.5.1: Error curves in different norms

Table 5.5.4: Numerical results of the rectangular element with $r = k + 1$ and $k = 1$

h	$\|\boldsymbol{e}_h\|$	rates	$\|\text{rot}\,\boldsymbol{e}_h\|$	rates	$\|\text{grad}\,\text{rot}\,\boldsymbol{e}_h\|$	rates
$1/10$	8.545193e-02		7.742300e-01		3.116513e+01	
$1/20$	2.117547e-02	2.0127	1.924503e-01	2.0083	1.556844e+01	1.0013
$1/40$	5.283250e-03	2.0029	4.804726e-02	2.0020	7.782876e+00	1.0002
$1/80$	1.320165e-03	2.0007	1.200780e-02	2.0005	3.891283e+00	1.0001
$1/160$	3.301818e-04	1.9994	3.001698e-03	2.0001	1.945622e+00	1.0000

5.5.3 The Family of Elements with $r = k + 2$

We now test elements in the family with $r = k + 2$. We apply the same mesh as before. Tables 5.5.5, 5.5.6, and 5.5.7 show the numerical results for various mesh sizes and elements. We observe one-order higher convergence rate than the estimate in Theorem 8.4.2 when $k \geq 2$.

We conclude this section by pointing out that the three families of elements bear

Table 5.5.5: Numerical results of the triangular element with $r = k + 2$ and $k = 1$

h	$\|\boldsymbol{e}_h\|$	rates	$\|\mathrm{rot}\, \boldsymbol{e}_h\|$	rates	$\|\mathrm{grad}\,\mathrm{rot}\, \boldsymbol{e}_h\|$	rates
1/10	1.916204e-01		1.831377e+00		4.821773e+01	
1/20	4.953536e-02	1.9517	4.921121e-01	1.8959	2.491403e+01	0.9526
1/40	1.254233e-02	1.9817	1.253529e-01	1.9730	1.256258e+01	0.9878
1/80	3.145763e-03	1.9953	3.148659e-02	1.9932	6.294644e+00	0.9969
1/160	7.897003e-04	1.9940	7.880958e-03	1.9983	3.148996e+00	0.9992

Table 5.5.6: Numerical results of the rectangular element with $r = k + 2$ and $k = 1$

h	$\|\boldsymbol{e}_h\|$	rates	$\|\mathrm{rot}\, \boldsymbol{e}_h\|$	rates	$\|\mathrm{grad}\,\mathrm{rot}\, \boldsymbol{e}_h\|$	rates
1/10	8.399241e-02		7.736407e-01		3.117602e+01	
1/20	2.055671e-02	2.0306	1.924122e-01	2.0075	1.556987e+01	1.0017
1/40	5.125523e-03	2.0038	4.804486e-02	2.0017	7.783057e+00	1.0003
1/80	1.280556e-03	2.0009	1.200764e-02	2.0004	3.891305e+00	1.0001
1/160	3.203172e-04	1.9992	3.001689e-03	2.0001	1.945625e+00	1.0000

Table 5.5.7: Numerical results of the rectangular element with $r = k + 2$ and $k = 2$

h	$\|\boldsymbol{e}_h\|$	rates	$\|\mathrm{rot}\, \boldsymbol{e}_h\|$	rates	$\|\mathrm{grad}\,\mathrm{rot}\, \boldsymbol{e}_h\|$	rates
1/4	6.482470e-02		9.955505e-01		2.796216e+01	
1/8	4.580398e-03	3.8230	1.388809e-01	2.8416	7.337119e+00	1.9302
1/16	2.927226e-04	3.9679	1.780427e-02	2.9636	1.854476e+00	1.9842
1/32	1.838464e-05	3.9930	2.239038e-03	2.9913	4.648552e-01	1.9962
1/64	1.166284e-06	3.9785	2.802981e-04	2.9978	1.162907e-01	1.9990

their own advantages. The family with $r = k$ can be the best choice if we pursue a low computational cost, while the family with $r = k + 2$ stands out for its higher accuracy in the sense of L^2-norm.

CHAPTER 6 3D GRADCURL-CONFORMING ELEMENTS I

In this chapter, to construct the grad curl-conforming elements, we consider the Stokes complex (1.4.3). We present it here again:

$$0 \longrightarrow \mathbb{R} \xrightarrow{\subset} H^1(\Omega) \xrightarrow{\text{grad}} H(\text{grad curl};\Omega) \xrightarrow{\text{curl}} H^1(\Omega)\otimes\mathbb{V} \xrightarrow{\text{div}} L^2(\Omega) \longrightarrow 0. \quad (6.0.1)$$

From the complex, we can see the construction of the grad curl-conforming elements is related to the incompressible flows since the last two spaces $H^1(\Omega)\otimes\mathbb{V} - L^2(\Omega)$ in the complex is actually a Stokes pair.

We will construct the following finite element subcomplexes of (6.0.1) on tetrahedral meshes:

$$0 \longrightarrow \mathbb{R} \xrightarrow{\subset} \Sigma_h^r \xrightarrow{\text{grad}} V_h^{r-1,k+1} \xrightarrow{\text{curl}} Z_h^k \xrightarrow{\text{div}} W_h^{k-1} \longrightarrow 0. \quad (6.0.2)$$

Same as Chapter 5, we take $r = k$, $k+1$, or $k+2$. In [53], Neilan constructed a finite element subcomplex for another Stokes complex:

$$0 \longrightarrow \mathbb{R} \xrightarrow{\subset} H^2(\Omega) \xrightarrow{\text{grad}} H^1(\text{curl};\Omega) \xrightarrow{\text{curl}} H^1(\Omega)\otimes\mathbb{V} \xrightarrow{\text{div}} L^2(\Omega) \longrightarrow 0,$$

where $H^1(\text{curl};\Omega) = \{\boldsymbol{u} \in H^1(\Omega)\otimes\mathbb{V} : \text{curl}\,\boldsymbol{u} \in H^1(\Omega)\otimes\mathbb{V}\}$. This discrete complex contains a finite element Stokes pair, but the first two spaces in the complex have higher smoothness. We will apply the Stokes pair in [53] to construct the whole complex (6.0.2).

6.1 Local Shape Function Spaces and Polynomial Complexes

On each $K \in \mathcal{T}_h$, we construct the local complex of the shape function spaces of (6.0.2):

$$0 \longrightarrow \mathbb{R} \xrightarrow{\subset} \Sigma_h^r(K) \xrightarrow{\text{grad}} V_h^{r-1,k+1}(K) \xrightarrow{\text{curl}} Z_h^k(K) \xrightarrow{\text{div}} W_h^{k-1}(K) \longrightarrow 0. \quad (6.1.1)$$

To this end, we first consider the following local complex on the reference element

$\hat{K}$:

$$0 \longrightarrow \mathbb{R} \xrightarrow{\subset} \hat{\Sigma}_h^r(\hat{K}) \xrightarrow{\operatorname{grad}_{\hat{\boldsymbol{x}}}} \hat{V}_h^{r-1,k+1}(\hat{K}) \xrightarrow{\operatorname{curl}_{\hat{\boldsymbol{x}}}} \hat{Z}_h^k(\hat{K}) \xrightarrow{\operatorname{div}_{\hat{\boldsymbol{x}}}} \hat{W}_h^{k-1}(\hat{K}) \longrightarrow 0. \tag{6.1.2}$$

We choose $\hat{\Sigma}_h^r(\hat{K}) := P_r(\hat{K})$, $\hat{W}_h^{k-1}(\hat{K}) := P_{k-1}(\hat{K})$, and $\hat{Z}_h^k(\hat{K}) := \boldsymbol{P}_k(\hat{K})$. Define

$$\hat{V}_h^{r-1,k+1}(\hat{K}) = \operatorname{grad}_{\hat{\boldsymbol{x}}} \hat{\Sigma}_h^r(\hat{K}) \oplus \mathfrak{p}_{\hat{\boldsymbol{x}}}^2 \hat{Z}_h^k(K), \tag{6.1.3}$$

where $\mathfrak{p}_{\hat{\boldsymbol{x}}}^2$ is defined in (2.1.21) with $W = 0$.

As a special case of the Poincaré operators, $\mathfrak{p}_{\hat{\boldsymbol{x}}}^2$ satisfies the following null-homotopy identities:

$$\mathfrak{p}_{\hat{\boldsymbol{x}}}^2 \operatorname{curl}_{\hat{\boldsymbol{x}}} \hat{\boldsymbol{u}} + \operatorname{grad}_{\hat{\boldsymbol{x}}} \mathfrak{p}_{\hat{\boldsymbol{x}}}^1 \hat{\boldsymbol{u}} = \hat{\boldsymbol{u}}, \ \forall \hat{\boldsymbol{u}} \in C^\infty \Lambda^1(\hat{K}); \tag{6.1.4}$$

$$\operatorname{curl}_{\hat{\boldsymbol{x}}} \mathfrak{p}_{\hat{\boldsymbol{x}}}^2 \hat{\boldsymbol{u}} + \mathfrak{p}_{\hat{\boldsymbol{x}}}^3 \operatorname{div}_{\hat{\boldsymbol{x}}} \hat{\boldsymbol{u}} = \hat{\boldsymbol{u}}, \ \forall \hat{\boldsymbol{u}} \in C^\infty \Lambda^2(\hat{K}). \tag{6.1.5}$$

Remark 6.1.1. We can replace $\mathfrak{p}_{\hat{\boldsymbol{x}}}^2$ in (6.1.3) with $\kappa_{\hat{\boldsymbol{x}}}^2$.

The right-hand side of (6.1.3) is a direct sum. In fact, if $\hat{\boldsymbol{u}} \in \operatorname{grad}_{\hat{\boldsymbol{x}}} \hat{\Sigma}_h^r(\hat{K}) \cap \mathfrak{p}_{\hat{\boldsymbol{x}}}^2 \hat{Z}_h^k(\hat{K})$, then $\operatorname{curl}_{\hat{\boldsymbol{x}}} \hat{\boldsymbol{u}} = 0$ and $\mathfrak{p}_{\hat{\boldsymbol{x}}}^1 \hat{\boldsymbol{u}} = 0$. By the null-homotopy identity (6.1.4), $\hat{\boldsymbol{u}} = \mathfrak{p}_{\hat{\boldsymbol{x}}}^2 \operatorname{curl}_{\hat{\boldsymbol{x}}} \hat{\boldsymbol{u}} + \operatorname{grad}_{\hat{\boldsymbol{x}}} \mathfrak{p}_{\hat{\boldsymbol{x}}}^1 \hat{\boldsymbol{u}} = 0$.

By the definitions of the shape function spaces, it is easy to show that the sequence (6.1.2) is a complex. By the properties of the Poincaré operators, we can verify that the sequence

$$0 \longleftarrow \hat{\Sigma}_h^r(\hat{K}) \xleftarrow{\mathfrak{p}_{\hat{\boldsymbol{x}}}^1} \hat{V}_h^{r-1,k+1}(\hat{K}) \xleftarrow{\mathfrak{p}_{\hat{\boldsymbol{x}}}^2} \hat{Z}_h^k(\hat{K}) \xleftarrow{\mathfrak{p}_{\hat{\boldsymbol{x}}}^3} \hat{W}_h^{k-1}(\hat{K}) \longleftarrow 0 \tag{6.1.6}$$

is also a complex with the Poincaré operators in (2.1.20) – (2.1.22). From Lemma 2.1.3, we obtain the exactness.

Lemma 6.1.1. *The complex* (6.1.2) *is exact.*

We demonstrate that $\hat{V}_h^{r-1,k+1}(\hat{K})$ contains polynomials of certain degree.

Lemma 6.1.2. *The inclusion* $\boldsymbol{P}_{r-1}(\hat{K}) \subseteq \hat{V}_h^{r-1,k+1}(\hat{K})$ *holds.*

Proof. From the null-homotopy property (6.1.4),

$$\boldsymbol{P}_{r-1}(\hat{K}) = \operatorname{grad}_{\hat{\boldsymbol{x}}} \mathfrak{p}^1_{\hat{\boldsymbol{x}}} \boldsymbol{P}_{r-1}(\hat{K}) + \mathfrak{p}^2_{\hat{\boldsymbol{x}}} \operatorname{curl}_{\hat{\boldsymbol{x}}} \boldsymbol{P}_{r-1}(\hat{K}).$$

By definition, $\hat{V}_h^{r-1,k+1}(\hat{K}) = \operatorname{grad}_{\hat{\boldsymbol{x}}} \hat{\Sigma}_h^r(\hat{K}) \oplus \mathfrak{p}^2_{\hat{\boldsymbol{x}}} \hat{Z}_h^k(\hat{K})$. We have $\mathfrak{p}^1_{\hat{\boldsymbol{x}}} \boldsymbol{P}_{r-1}(\hat{K}) \subseteq P_r(\hat{K}) = \hat{\Sigma}_h^r(\hat{K})$ and $\operatorname{curl}_{\hat{\boldsymbol{x}}} \boldsymbol{P}_{r-1}(\hat{K}) \subseteq \boldsymbol{P}_k(\hat{K}) = \hat{Z}_h^k(\hat{K})$. Therefore the desired inclusion holds. □

We adopt the transformation (5.1.7) to relate the function $\hat{\boldsymbol{u}} \in \hat{V}_h^{r-1,k+1}(\hat{K})$ to a function $\boldsymbol{u} \in V_h^{r-1,k+1}(K)$. By a simple computation, we have

$$\operatorname{curl} \boldsymbol{u} \circ F_K = \frac{B_K}{\det(B_K)} \operatorname{curl}_{\hat{\boldsymbol{x}}} \hat{\boldsymbol{u}}. \tag{6.1.7}$$

We are now in a position to define the spaces in (6.1.1):

$$\begin{aligned} \Sigma_h^r(K) &= \left\{ u : u \circ F_K \in \hat{\Sigma}_h^r(\hat{K}) \right\}, \\ V_h^{r-1,k+1}(K) &= \left\{ \boldsymbol{u} : B_K^{\mathrm{T}} \boldsymbol{u} \circ F_K \in \hat{V}_h^{r-1,k+1}(\hat{K}) \right\}, \\ Z_h^k(K) &= \left\{ \boldsymbol{u} : B_K^{-1} \boldsymbol{u} \circ F_K \in \hat{Z}_h^k(\hat{K}) \right\}. \end{aligned} \tag{6.1.8}$$

By the definition of the spaces and Lemma 6.1.1, we can show (6.1.1) is also an exact complex.

6.2 Degrees of Freedom

In this section, we define DOFs for each space in (6.1.1). Taking $r = k$, $k+1$, and $k+2$ in (6.1.1) yields three versions of grad curl-conforming element spaces $V_h^{k-1,k+1}(K)$, $V_h^{k,k+1}(K)$, and $V_h^{k+1,k+1}(K)$.

The DOFs for the Lagrange element $\Sigma_h^r(K)$ $(r \geq 1)$ can be given as follows.

- Vertex DOFs $M_v(u)$ at all the vertices $v_i \in \mathcal{V}_h(K)$:

$$M_v(u) = \{u(v_i)\}. \tag{6.2.1}$$

- Edge DOFs $M_e(u)$ on all the edges $e_i \in \mathcal{E}_h(K)$:

$$M_e(u) = \left\{ \int_{e_i} uv \mathrm{d}s \text{ for all } v \in P_{r-2}(e_i) \right\}. \tag{6.2.2}$$

- Face DOFs $M_f(u)$ on all the faces $f_i \in \mathcal{F}_h(K)$:

$$M_f(u) = \left\{ \int_{f_i} uv \mathrm{d}A \text{ for all } v \in P_{r-3}(f_i) \right\}. \tag{6.2.3}$$

- Interior DOFs $M_K(u)$ in the element $K \in \mathcal{T}_h$:

$$M_K(u) = \left\{ \int_{K} uv \mathrm{d}V \text{ for all } v \in P_{r-4}(K) \right\}. \tag{6.2.4}$$

We equip the space $V_h^{r-1,k+1}(K)$ ($r \geq 1, k \geq 6$) with the following DOFs:

- Vertex DOFs $M_v(\boldsymbol{u})$ at all the vertices $v_i \in \mathcal{V}_h(K)$:

$$\begin{aligned} M_v(\boldsymbol{u}) = \{ & D^\alpha(\operatorname{curl} \boldsymbol{u})(v_i) \text{ for all } |\alpha| \leq 2 \text{ except for } \partial_{x_3}(\operatorname{curl} \boldsymbol{u})_3(v_i), \\ & \partial^2_{x_1x_1}(\operatorname{curl} \boldsymbol{u})_1(v_i), \partial^2_{x_2x_2}(\operatorname{curl} \boldsymbol{u})_2(v_i), \partial^2_{x_3x_3}(\operatorname{curl} \boldsymbol{u})_3(v_i) \}. \end{aligned} \tag{6.2.5}$$

- Edge DOFs $\boldsymbol{M}_e(\boldsymbol{u})$ at all edges $e_i \in \mathcal{E}_h(K)$ (with two mutually orthogonal unit normal vector $\boldsymbol{n}_i$ and $\boldsymbol{m}_i$ to the edge e_i and the unit tangential vector $\boldsymbol{\tau}_i$):

$$\begin{aligned} \boldsymbol{M}_e(\boldsymbol{u}) = & \left\{ \int_{\boldsymbol{e}_i} \boldsymbol{u} \cdot \boldsymbol{\tau}_i q \mathrm{d}s \text{ for all } q \in P_{r-1}(e_i) \right\} \\ & \cup \left\{ \int_{e_i} \operatorname{curl} \boldsymbol{u} \cdot \boldsymbol{q} \mathrm{d}s \text{ for all } \boldsymbol{q} \in \boldsymbol{P}_{k-6}(e_i) \right\} \\ & \cup \left\{ \int_{e_i} \operatorname{grad}(\operatorname{curl} \boldsymbol{u} \cdot \boldsymbol{l}_i) \cdot \boldsymbol{n}_i q \mathrm{d}s \text{ with } \boldsymbol{l}_i = \boldsymbol{\tau}_i, \boldsymbol{n}_i, \boldsymbol{m}_i, \text{ for all } q \in P_{k-5}(e_i) \right\} \\ & \cup \left\{ \int_{e_i} \operatorname{grad}(\operatorname{curl} \boldsymbol{u} \cdot \boldsymbol{l}_i) \cdot \boldsymbol{m}_i q \mathrm{d}s \text{ with } \boldsymbol{l}_i = \boldsymbol{\tau}_i, \boldsymbol{n}_i, \text{ for all } q \in P_{k-5}(e_i) \right\}. \end{aligned} \tag{6.2.6}$$

- Face DOFs $\boldsymbol{M}_f(\boldsymbol{u})$ at all faces $f_i \in \mathcal{F}_h(K)$ (with two mutually orthogonal unit vector $\boldsymbol{\tau}_i^1$ and $\boldsymbol{\tau}_i^2$ in the face f_i and the unit normal vector $\boldsymbol{n}_i$):

$$\begin{aligned} \boldsymbol{M}_f(\boldsymbol{u}) = & \left\{ \int_{f_i} \operatorname{curl} \boldsymbol{u} \cdot \boldsymbol{n}_i q \mathrm{d}A \text{ for all } q \in P_{k-6}(f_i)/\mathbb{R} \right\} \\ & \cup \left\{ \int_{f_i} \operatorname{curl} \boldsymbol{u} \cdot \boldsymbol{\tau}_i^1 q \mathrm{d}A \text{ for all } q \in P_{k-6}(f_i) \right\} \\ & \cup \left\{ \int_{f_i} \operatorname{curl} \boldsymbol{u} \cdot \boldsymbol{\tau}_i^2 q \mathrm{d}A \text{ for all } q \in P_{k-6}(f_i) \right\} \\ & \cup \left\{ \int_{f_i} \boldsymbol{u} \cdot \boldsymbol{q} \mathrm{d}A \text{ for all } \boldsymbol{q} = B_K \hat{\boldsymbol{q}}, \hat{\boldsymbol{q}} \in P_{r-3}(\hat{f}_i) \hat{\boldsymbol{x}}_{\hat{f}_i} \right\}, \end{aligned} \tag{6.2.7}$$

where $\hat{\boldsymbol{x}}_{\hat{f}_i} = [\hat{\boldsymbol{x}} - (\hat{\boldsymbol{x}} \cdot \hat{\boldsymbol{n}}_i)\, \hat{\boldsymbol{n}}_i]\,|_{\hat{f}_i}$.

- Interior DOFs $\boldsymbol{M}_K(\boldsymbol{u})$ in the element $K \in \mathcal{T}_h$:

$$\begin{aligned}\boldsymbol{M}_K(\boldsymbol{u}) = &\left\{ \int_K \operatorname{curl} \boldsymbol{u} \cdot \boldsymbol{q} \mathrm{d}V \text{ for all } \boldsymbol{q} \circ F_K = B_K^{-\mathrm{T}} \hat{\boldsymbol{q}}, \hat{\boldsymbol{q}} \in \boldsymbol{P}_{k-6}(\hat{K}) \times \hat{\boldsymbol{x}} \right\} \\ &\cup \left\{ \int_K \boldsymbol{u} \cdot \boldsymbol{q} \mathrm{d}V \text{ for all } \boldsymbol{q} \circ F_K = B_K \hat{\boldsymbol{q}}, \hat{\boldsymbol{q}} \in P_{r-4}(\hat{K}) \hat{\boldsymbol{x}} \right\}, \end{aligned} \tag{6.2.8}$$

We choose the finite element Stokes pair proposed in [53] for $Z_h^k(K) - W_h^{k-1}(K)$ ($k \geq 5$). The DOFs for $Z_h^k(K)$ are given as follows.

- Vertex DOFs $\boldsymbol{M}_v(\boldsymbol{u})$ at all the vertices $v_i \in \mathcal{V}_h(K)$:

$$\boldsymbol{M}_v(\boldsymbol{u}) = \{ D^\alpha \boldsymbol{u}(v_i) \text{ for all } |\alpha| \leq 2 \}. \tag{6.2.9}$$

- Edge DOFs $\boldsymbol{M}_e(\boldsymbol{u})$ at all edges $e_i \in \mathcal{E}_h(K)$ (with two mutually orthogonal unit normal vector $\boldsymbol{n}_i$ and $\boldsymbol{m}_i$ to the edge e_i):

$$\begin{aligned}\boldsymbol{M}_e(\boldsymbol{u}) = &\left\{ \int_{e_i} \boldsymbol{u} \cdot \boldsymbol{q} \mathrm{d}s \text{ for all } \boldsymbol{q} \in \boldsymbol{P}_{k-6}(e_i) \right\} \\ \cup &\left\{ \int_{e_i} (\operatorname{grad} \boldsymbol{u}) \boldsymbol{n}_i \cdot \boldsymbol{q} \mathrm{d}s \text{ for all } \boldsymbol{q} \in \boldsymbol{P}_{k-5}(e_i) \right\} \\ \cup &\left\{ \int_{e_i} (\operatorname{grad} \boldsymbol{u}) \boldsymbol{m}_i \cdot \boldsymbol{q} \mathrm{d}s \text{ for all } \boldsymbol{q} \in \boldsymbol{P}_{k-5}(e_i) \right\}, \end{aligned} \tag{6.2.10}$$

  where grad is applied rowwise.

- Face DOFs $\boldsymbol{M}_f(\boldsymbol{u})$ at all faces $f_i \in \mathcal{F}_h(K)$:

$$\boldsymbol{M}_f(\boldsymbol{u}) = \left\{ \int_{f_i} \boldsymbol{u} \cdot \boldsymbol{q} \mathrm{d}A \text{ for all } \boldsymbol{q} \in \boldsymbol{P}_{k-6}(f_i) \right\}. \tag{6.2.11}$$

- Interior DOFs $\boldsymbol{M}_K(\boldsymbol{u})$ in the element $K \in \mathcal{T}_h$:

$$\boldsymbol{M}_K(\boldsymbol{u}) = \left\{ \int_K \boldsymbol{u} \cdot \boldsymbol{q} \mathrm{d}V \text{ for all } \boldsymbol{q} \in \boldsymbol{P}_{k-4}(K) \right\}. \tag{6.2.12}$$

The DOFs for $W_h^{k-1}(K)$ are given as follows.

- Vertex DOFs $M_v(u)$ at all faces $v_i \in \mathcal{V}_h(K)$:

$$M_v(u) = \{D^\alpha u(v_i) \text{ for all } |\alpha| \le 1\}.$$

- Edge DOFs $M_e(u)$ at all edges $e_i \in \mathcal{E}_h(K)$:

$$M_e(u) = \left\{ \int_{e_i} uq\mathrm{d}s \text{ for all } q \in P_{k-5}(e_i) \right\}.$$

- Interior DOFs $M_K(u)$ in the element $K \in \mathcal{T}_h$:

$$M_K(u) = \left\{ \int_K uv\mathrm{d}V \text{ for all } v \in P_{k-1}(K) \text{ such that } v|_{\partial K} = 0 \right\}.$$

Lemma 6.2.1. *The DOFs* (6.2.9) – (6.2.12) *are well-defined for any* $\boldsymbol{u} \in H^{1/2+\delta}(\Omega) \otimes \mathbb{V}$ *and* $\operatorname{curl} \boldsymbol{u} \in H^{7/2+\delta}(\Omega) \otimes \mathbb{V}$ *with* $\delta > 0$.

Proof. By the embedding theorem, we have $\operatorname{curl} \boldsymbol{u} \in H^{7/2+\delta}(\Omega) \otimes \mathbb{V} \hookrightarrow C^{2,\delta}(\Omega) \otimes \mathbb{V}$, then the DOFs involving $\operatorname{curl} \boldsymbol{u}$ are well-defined. Proceeding as in the proof of [49, Lemma 5.38], we see that the remaining DOFs are well-defined since $\boldsymbol{u} \in H^{1/2+\delta}(\Omega) \otimes \mathbb{V}$ and $\operatorname{curl} \boldsymbol{u} \in H^{7/2+\delta}(\Omega) \otimes \mathbb{V} \hookrightarrow C^{2,\delta}(\Omega) \otimes \mathbb{V} \subset L^p(\Omega) \otimes \mathbb{V}$ with $p > 2$. □

Lemma 6.2.2. *The DOFs for* $V_h^{r-1,k+1}(K)$ *are unisolvent.*

Proof. Since the complex (6.1.1) is exact, we have

$$\dim V_h^{r-1,k+1}(K) = \dim Z_h^k(K) + \dim \Sigma_h^r(K) - \dim W_h^{k-1}(K) - 1. \tag{6.2.13}$$

We can check that the DOF set has the same dimension. Then it suffices to show that if all the DOFs vanish on $\boldsymbol{u} \in V_h^{r-1,k+1}(K)$, then $\boldsymbol{u} = 0$. To see this, we first show that $\operatorname{curl} \boldsymbol{u} = 0$. Since the sequence (6.1.1) is a complex, we have $\operatorname{curl} V_h^{r-1,k+1}(K) \subset Z_h^k(K)$. By integration by parts, the following face DOFs for $Z_h^k(K)$ vanish on $\operatorname{curl} \boldsymbol{u}$:

$$\int_{f_i} \operatorname{curl} \boldsymbol{u} \cdot \boldsymbol{n}_i \mathrm{d}A = \int_{\partial f_i} \boldsymbol{u} \cdot \boldsymbol{\tau}_{\partial f_i} \mathrm{d}s = 0.$$

The conformity of $Z_h^k(K)$ leads to $\operatorname{curl} \boldsymbol{u} = 0$ on ∂K. We relate $\boldsymbol{u}$ to $\hat{\boldsymbol{u}}$ via (5.1.7), and then $\operatorname{curl}_{\hat{\boldsymbol{x}}} \hat{\boldsymbol{u}} = 0$ on $\partial\hat{K}$. We can rewrite $\operatorname{curl}_{\hat{\boldsymbol{x}}} \hat{\boldsymbol{u}}$ as:

$$\operatorname{curl}_{\hat{\boldsymbol{x}}} \hat{\boldsymbol{u}} = \hat{x}_1\hat{x}_2\hat{x}_3(1-\hat{x}_1-\hat{x}_2-\hat{x}_3)\hat{\boldsymbol{\Phi}} \text{ with } \hat{\boldsymbol{\Phi}} = (\hat{\Phi}_1, \hat{\Phi}_2, \hat{\Phi}_3)^{\mathrm{T}} \in \boldsymbol{P}_{k-4}(\hat{K}),$$

and hence

$$\partial_{\hat{x}_1}(\operatorname{curl}_{\hat{\boldsymbol{x}}} \hat{\boldsymbol{u}})_1 = \hat{x}_2\hat{x}_3[(1-2x_1-\hat{x}_2-\hat{x}_3)\hat{\Phi}_1 + (1-\hat{x}_1-\hat{x}_2-\hat{x}_3)\hat{x}_1\partial_{\hat{x}_1}\hat{\Phi}_1],$$

$$\partial_{\hat{x}_2}(\operatorname{curl}_{\hat{\boldsymbol{x}}} \hat{\boldsymbol{u}})_2 = \hat{x}_1\hat{x}_3[(1-2\hat{x}_2-\hat{x}_1-\hat{x}_3)\hat{\Phi}_2 + (1-\hat{x}_1-\hat{x}_2-\hat{x}_3)\hat{x}_2\partial_{\hat{x}_2}\hat{\Phi}_2],$$

$$\partial_{\hat{x}_3}(\operatorname{curl}_{\hat{\boldsymbol{x}}} \hat{\boldsymbol{u}})_3 = \hat{x}_1\hat{x}_2[(1-2\hat{x}_3-\hat{x}_1-\hat{x}_2)\hat{\Phi}_3 + (1-\hat{x}_1-\hat{x}_2-\hat{x}_3)\hat{x}_3\partial_{\hat{x}_3}\hat{\Phi}_3].$$

When $\hat{x}_1 = 0$, $\partial_{\hat{x}_2}(\operatorname{curl}_{\hat{\boldsymbol{x}}} \hat{\boldsymbol{u}})_2 + \partial_{\hat{x}_3}(\operatorname{curl}_{\hat{\boldsymbol{x}}} \hat{\boldsymbol{u}})_3 = 0$ which leads to $\partial_{\hat{x}_1}(\operatorname{curl}_{\hat{\boldsymbol{x}}} \hat{\boldsymbol{u}})_1 = 0$ because $\operatorname{div}\operatorname{curl}_{\hat{\boldsymbol{x}}} \hat{\boldsymbol{u}} = \partial_{\hat{x}_1}(\operatorname{curl}_{\hat{\boldsymbol{x}}} \hat{\boldsymbol{u}})_1 + \partial_{\hat{x}_2}(\operatorname{curl}_{\hat{\boldsymbol{x}}} \hat{\boldsymbol{u}})_2 + \partial_{\hat{x}_3}(\operatorname{curl}_{\hat{\boldsymbol{x}}} \hat{\boldsymbol{u}})_3 = 0$. It implies $\hat{\Phi}_1$ has a factor $\hat{x}_1$. Similarly, $\hat{\Phi}_2$ has a factor $\hat{x}_2$ and $\hat{\Phi}_3$ has a factor $\hat{x}_3$. Then

$$\operatorname{curl}_{\hat{\boldsymbol{x}}} \hat{\boldsymbol{u}} = \hat{x}_1\hat{x}_2\hat{x}_3(1-\hat{x}_1-\hat{x}_2-\hat{x}_3)[\hat{x}_1\widetilde{\Phi}_1, \hat{x}_2\widetilde{\Phi}_2, \hat{x}_3\widetilde{\Phi}_3]^{\mathrm{T}}$$

with $\widetilde{\boldsymbol{\Phi}} = [\widetilde{\Phi}_1, \widetilde{\Phi}_2, \widetilde{\Phi}_3] \in \boldsymbol{P}_{k-5}(\hat{K})$. By integration by parts,

$$\int_K \operatorname{curl}\boldsymbol{u} \cdot \operatorname{grad} v \mathrm{d}V = \int_{\partial K} \operatorname{curl}\boldsymbol{u} \cdot \boldsymbol{n}_{\partial K} v \mathrm{d}A = 0 \text{ for any } v \in P_{k-4}(K),$$

which together with the vanishing interior DOFs involving $\operatorname{curl}\boldsymbol{u}$ leads to

$$0 = \int_K \operatorname{curl}\boldsymbol{u} \cdot B_K^{-\mathrm{T}}\widetilde{\boldsymbol{\Phi}} \circ F_K^{-1}\mathrm{d}V = \int_{\hat{K}} \operatorname{curl}_{\hat{\boldsymbol{x}}} \hat{\boldsymbol{u}} \cdot \widetilde{\boldsymbol{\Phi}}\mathrm{d}\hat{V}.$$

Then $\operatorname{curl}\boldsymbol{u} = \frac{B_K}{\det(B_K)} \operatorname{curl}_{\hat{\boldsymbol{x}}} \hat{\boldsymbol{u}} = 0$ since $\widetilde{\boldsymbol{\Phi}} = 0$.

Since $\operatorname{curl}\boldsymbol{u} \cdot \boldsymbol{n}_i = 0$ on each f_i, there exists a $\phi_i \in P_r(f_i)$ such that $\boldsymbol{n}_i \times \boldsymbol{u}|_{f_i} \times \boldsymbol{n}_i = \operatorname{grad}_{f_i} \phi_i$. Here $\operatorname{grad}_{f_i}$ is the face gradient on f_i. By the edge DOFs of $V_h^{r-1,k+1}(K)$, we get $\boldsymbol{u} \cdot \boldsymbol{\tau}_i = 0$ on each edge e_i. Therefore ϕ_i is a constant on the boundary of f_i. Without loss of generality, we can choose this constant to be zero. Then ϕ_i has the form $\phi_i = B_i|_{f_i}\psi_i$ with $\psi_i \in P_{r-3}(f_i)$. By the property of Koszul operators in 2D (see Chapter 2), for any function $\psi_i \in P_{r-3}(f_i)$, there exists $\boldsymbol{q}_i \in P_{r-3}(f_i)B_K\hat{\boldsymbol{x}}_{\hat{f}_i}$ satisfying $\boldsymbol{q}_i \perp \boldsymbol{n}_i$ and $\operatorname{div}_{f_i} \boldsymbol{q}_i = \psi_i$. By the DOFs in (6.2.9), we have

$$0 = (\boldsymbol{u}, \boldsymbol{q}_i)_{f_i} = -(\phi_i, \operatorname{div}_{f_i} \boldsymbol{q}_i)_{f_i} = -\left(B_i|_{f_i}\psi_i, \psi_i\right)_{f_i}.$$

This implies that $\psi_i = 0$, i.e., $\boldsymbol{u} \times \boldsymbol{n}_i = 0$ on f_i.

Therefore there exists $\phi = B_0\psi$ with $\psi \in P_{r-4}(K)$ such that $\boldsymbol{u} = \operatorname{grad}\phi$. We choose $\boldsymbol{q} \in P_{r-4}(K)B_K\hat{\boldsymbol{x}}$ such that $\operatorname{div}\boldsymbol{q} = \psi$. Then

$$0 = (\boldsymbol{u}, \boldsymbol{q}) = (\operatorname{grad}\phi, \boldsymbol{q}) = -(\phi, \operatorname{div}\boldsymbol{q}) = -(B_0\psi, \psi).$$

This implies that $\psi = 0$ and hence $\phi = 0$ and $\boldsymbol{u} = 0$.

□

6.3 Global Finite Element Complexes

Equipping the local spaces with the above DOFs, we obtain the global finite element spaces Σ_h^r, $V_h^{r-1,k+1}$, Z_h^k, and W_h^{k-1} with $k \geq 6$ in the complex (6.0.2). The number of DOFs of the space $V_h^{r-1,k+1}(K)$ is at least 279.

Lemma 6.3.1. *The following conformity holds:*

$$V_h^{r-1,k+1} \subset H(\operatorname{grad}\operatorname{curl};\Omega).$$

Proof. To prove the conformity, we must show $\boldsymbol{u} \times \boldsymbol{n}_i = 0$ and $\operatorname{curl}\boldsymbol{u} = 0$ for all $f_i \in \mathcal{F}_h(K)$ if the DOFs (6.2.9) – (6.2.11) vanish on $\boldsymbol{u} \in V_h^{r-1,k+1}(K)$. Proceeding as in the proof of Lemma 6.2.2, we can show that $\operatorname{curl}\boldsymbol{u} = 0$ and $\boldsymbol{u} \times \boldsymbol{n}_i = 0$ on each f_i. □

Theorem 6.3.2. *The complex* (6.0.2) *is exact on contractible domains.*

Proof. The exactness at Σ_h^r is trivial. The exactness at $V_h^{r-1,k+1}$ follows from the exactness of the standard finite element differential forms (see Theorem 5.3.2). The exactness at W_h^{k-1}, i.e., the surjectivity of $\operatorname{div} : Z_h^k \to W_h^{k-1}$ has been verified in [53, Lemma 4.5].

Finally, the exactness at Z_h^k follows from a dimension count. Let $\mathcal{V}$, $\mathcal{E}$, $\mathcal{F}$, and $\mathcal{K}$ denote the number of vertices, edges, faces, and 3D cells, respectively. Then we have

$$\dim \Sigma_h^r = \mathcal{V} + (r-1)\mathcal{E} + \frac{1}{2}(r-2)(r-1)\mathcal{F} + \frac{1}{6}(r-3)(r-2)(r-1)\mathcal{K},$$

$$\dim W_h^{k-1} = \frac{k(k+1)(k+2)}{6}\mathcal{K} - 16\mathcal{K} - 6(k-4)\mathcal{K} + 4\mathcal{V} + (k-4)\mathcal{E}.$$

From the DOFs (6.2.9) – (6.2.9),

$$\dim V_h^{r-1,k+1} - \dim Z_h^k = -4\mathcal{V} + r\mathcal{E} - (k-4)\mathcal{E} + \frac{1}{2}(r-2)(r-1)\mathcal{F} - \mathcal{F} + \frac{1}{6}\big[(r-3)(r-2)(r-1) + (k-5)(k-4)(4k-15) - 3(k-3)(k-2)(k-1)\big]\mathcal{K}.$$

From the above dimension count, we have

$$-1 + \dim \Sigma_h^r - \dim V_h^{r-1,k+1} + \dim Z_h^k - \dim W_h^{k-1} = 0,$$

where we have used Euler's formula $\mathcal{V} - \mathcal{E} + \mathcal{F} - \mathcal{K} = 1$. This completes the proof. □

We now consider the following complex with vanishing boundary conditions:

$$0 \longrightarrow H_0^1(\Omega) \xrightarrow{\text{grad}} H_0(\text{grad}\,\text{curl};\Omega) \xrightarrow{\text{curl}} H_0^1(\Omega)\otimes\mathbb{V} \xrightarrow{\text{div}} L_0^2(\Omega) \longrightarrow 0, \tag{6.3.1}$$

where $H_0(\text{grad}\,\text{curl};\Omega) = \{\boldsymbol{u} \in H(\text{grad}\,\text{curl};\Omega) : \ \boldsymbol{u}\times\boldsymbol{n} = 0 \text{ and } \text{curl}\,\boldsymbol{u} = 0 \text{ on } \partial\Omega\}$. By a standard argument, the sequence (6.3.1) is a complex and is exact on contractible domains, see, e.g., [25].

However, if we simply take $\mathring{\Sigma}_h^r = \Sigma_h^r \cap H_0^1(\Omega)$, $\mathring{V}_h^{r-1,k+1} = V_h^{r-1,k+1} \cap H_0(\text{grad}\,\text{curl};\Omega)$, $\mathring{Z}_h^k = Z_h^k \cap H_0^1(\Omega)\otimes\mathbb{V}$, and $\mathring{W}_h^{k-1} = W_h^{k-1} \cap L_0^2(\Omega)$, the complex

$$0 \xrightarrow{\subset} \mathring{\Sigma}_h^r \xrightarrow{\text{grad}} \mathring{V}_h^{r-1,k+1} \xrightarrow{\text{curl}} \mathring{Z}_h^k \xrightarrow{\text{div}} \mathring{W}_h^{k-1} \longrightarrow 0 \tag{6.3.2}$$

is not exact. This is because the construction in this chapter involves supersmoothness on lower-dimensional simplices of the mesh. Actually it is a non-trivial issue to construct such finite element spaces with homogeneous boundary conditions that can fit into an exact complex. We will not discuss this issue here, but only mention that the construction in the next chapter will not suffer from this issue.

6.4 Approximation Property of V_h

Denote $V(D) = \{\boldsymbol{u} \in H^{1/2+\delta}(D)\otimes\mathbb{V} : \text{curl}\,\boldsymbol{u} \in H^{7/2+\delta}(D)\otimes\mathbb{V}\}$ (see Lemma 6.2.1). We define an $H(\text{grad}\,\text{curl})$ interpolation operator $\Pi_K : V(K) \to V_h^{r-1,k+1}(K)$ by the DOFs for $V_h^{r-1,k+1}(K)$. Similarly, we can define an interpolation operator $\widetilde{\boldsymbol{\pi}}_K$:

$H^{7/2+\delta}(K)\otimes\mathbb{V}\to Z_h^k(K)$ by the DOFs for $Z_h^k(K)$. The global interpolation operators Π_h and $\widetilde{\boldsymbol{\pi}}_h$ are defined piecewisely by

$$\Pi_h|_K=\Pi_K \text{ and } \widetilde{\boldsymbol{\pi}}_h|_K=\widetilde{\boldsymbol{\pi}}_K.$$

The DOFs for $V_h^{r-1,k+1}(K)$ involve normal derivatives to edges, we can not relate the interpolation Π_K on a general element K to $\Pi_{\hat{K}}$ on the reference element $\hat{K}$ by the mapping (5.1.7). To estimate the interpolation error, we follow the method in [23]. We define a new element by replacing the DOFs $\boldsymbol{M}_e(\boldsymbol{u})$ for $V_h^{r-1,k+1}(K)$ with the following DOFs:

$$\widetilde{\boldsymbol{M}_e}(\boldsymbol{u})=\left\{\int_{\boldsymbol{e}_i}\boldsymbol{u}\cdot\boldsymbol{\tau}_i q\mathrm{d}s \text{ for all } q\in P_{r-1}(e_i)\right\}\cup\left\{\int_{e_i}\operatorname{curl}\boldsymbol{u}\cdot\boldsymbol{q}\mathrm{d}s \text{ for all } \boldsymbol{q}\in\boldsymbol{P}_{k-6}(e_i)\right\}$$
$$\cup\left\{\frac{1}{|e_i|}\int_{e_i}\operatorname{grad}(\operatorname{curl}\boldsymbol{u}\cdot\boldsymbol{l}_i^j)\cdot\boldsymbol{t}_i^j q\mathrm{d}s \text{ with } \boldsymbol{l}_i^j\in\boldsymbol{L}_i^j, j=1,2, \text{ for all } q\in P_{k-5}(e_i)\right\},$$

where $|e_i|=\operatorname{length}(e_i)$, $\boldsymbol{t}_i^1$ and $\boldsymbol{t}_i^2$ are the vectors connecting the midpoint of edge e_i and the other two vertices other than the endpoints of e_i, and

$$\boldsymbol{L}_i^j=\begin{cases}\left\{\boldsymbol{t}_i^1\times\boldsymbol{t}_i^3,\boldsymbol{t}_i^2\times\boldsymbol{t}_i^3\right\} & j=1,\\ \left\{\boldsymbol{t}_i^1\times\boldsymbol{t}_i^3,\boldsymbol{t}_i^2\times\boldsymbol{t}_i^3,\boldsymbol{t}_i^1\times\boldsymbol{t}_i^2\right\} & j=2,\end{cases}$$

with $\boldsymbol{t}_i^3=|e_i|\boldsymbol{\tau}_i$.

With these DOFs, the element is no longer grad curl-conforming.

We denote the interpolation defined by the above DOFs as Λ_K. Now we show that Λ_K and $\Lambda_{\hat{K}}$ can be related via the mapping (5.1.7).

Lemma 6.4.1. *Assume that Λ_K is well-defined. Then under the transformation* (5.1.7), *we have $\Lambda_K\boldsymbol{u}\circ F_K=B_K^{-\mathrm{T}}\Lambda_{\hat{K}}\hat{\boldsymbol{u}}$.*

Proof. Under the transformation (5.1.7), the new DOFs satisfy

$$\frac{1}{|e_i|}\int_{e_i}\operatorname{grad}(\operatorname{curl}\boldsymbol{u}\cdot\boldsymbol{l}_i^j)\cdot\boldsymbol{t}_i^j q\mathrm{d}s=\frac{1}{|\hat{e}_i|}\int_{\hat{e}_i}\operatorname{grad}_{\hat{\boldsymbol{x}}}(\operatorname{curl}_{\hat{\boldsymbol{x}}}\hat{\boldsymbol{u}}\cdot\hat{\boldsymbol{l}}_i^j)\cdot\hat{\boldsymbol{t}}_i^j\hat{q}\mathrm{d}\hat{s},$$

since $\boldsymbol{l}_i^j=\frac{B_K^{-\mathrm{T}}}{\det(B_K^{-\mathrm{T}})}\hat{\boldsymbol{l}}_i^j$. Therefore, the DOFs to define Λ_K are either identical with or linear combinations of those to define $\Lambda_{\hat{K}}$. According to Proposition 3.4.7 in [16], we complete the proof. □

Correspondingly, we define a new interpolation I_K by replacing the DOFs $\boldsymbol{M}_e(\boldsymbol{u})$ to define $\widetilde{\boldsymbol{\pi}}_K$ with the following:

$$\begin{aligned}\widetilde{\boldsymbol{M}}_e(\boldsymbol{u}) = &\left\{\int_{e_i} \boldsymbol{u}\cdot\boldsymbol{q}\mathrm{d}s \text{ for all } \boldsymbol{q}\in\boldsymbol{P}_{k-6}(e_i)\right\}\\ \cup &\left\{\frac{1}{|e_i|}\int_{e_i} \operatorname{grad}(\boldsymbol{u}\cdot\boldsymbol{l}_i)\cdot\boldsymbol{t}_i^1 q\mathrm{d}s \text{ with } \boldsymbol{l}_i\in\boldsymbol{L}_i^2 \text{ for all } q\in P_{k-5}(e_i)\right\}\\ \cup &\left\{\frac{1}{|e_i|}\int_{e_i} \operatorname{grad}(\boldsymbol{u}\cdot\boldsymbol{l}_i)\cdot\boldsymbol{t}_i^2 q\mathrm{d}s \text{ with } \boldsymbol{l}_i\in\boldsymbol{L}_i^2 \text{ for all } q\in P_{k-5}(e_i)\right\}.\end{aligned}$$

Lemma 6.4.2. *If $\boldsymbol{w}\in H^s(K)\otimes\mathbb{V}$ with $s>7/2$ and there exists a pair $\{m,q\}$ such that $H^s(K)\hookrightarrow W^{m,q}(K)$, then we have the following error estimates for the interpolation I_K,*

$$\|\boldsymbol{w}-I_K\boldsymbol{w}\|_{m,q,K}\le C|K|^{1/q-1/2}h_K^{\min\{s,k+1\}-m}\|\boldsymbol{w}\|_{s,K},$$

where $|K|$ is the volume of K.

Proof. The proof is standard, see, e.g., Theorem 3.1.4 in [23]. □

Lemma 6.4.3. *If $\operatorname{curl}\boldsymbol{u}\in H^s(K)\otimes\mathbb{V}$ with $s>7/2$ and there exists a pair $\{m,q\}$ such that $H^s(K)\hookrightarrow W^{m,q}(K)$, then*

$$\|I_K\operatorname{curl}\boldsymbol{u}-\operatorname{curl}\Lambda_K\boldsymbol{u}\|_{m,q,K}\le C|K|^{1/q-1/2}h_K^{\min\{s,k+1\}-m}\|\operatorname{curl}\boldsymbol{u}\|_{s,K}.$$

Proof. For simplicity of notation, we let $\boldsymbol{w}=I_K\operatorname{curl}\boldsymbol{u}-\operatorname{curl}\Lambda_K\boldsymbol{u}$. Since $\boldsymbol{w}\in Z_h^k(K)$, we have $\boldsymbol{w}=I_K\boldsymbol{w}=\sum_i d_i(\boldsymbol{w})\boldsymbol{N}_i$, where $d_i(\boldsymbol{w})$ are the DOFs to define $I_K\boldsymbol{w}$ and $\boldsymbol{N}_i$ are the corresponding dual basis functions. It is easy to see all the DOFs $d_i(\boldsymbol{w})$ vanish, except for $\frac{1}{|e_i|}\int_{e_i}\operatorname{grad}(\boldsymbol{w}\cdot\boldsymbol{l}_i)\cdot\boldsymbol{t}_i^1 q\mathrm{d}s, \boldsymbol{l}_i\in L_i^2$. We estimate only the non-vanishing term. By the definition of I_K, we have

$$\begin{aligned}\frac{1}{|e_i|}\int_{e_i}\operatorname{grad}(\boldsymbol{w}\cdot\boldsymbol{l}_i)\cdot\boldsymbol{t}_i^1 q\mathrm{d}s &= \frac{1}{|e_i|}\int_{e_i}\operatorname{grad}\left(\operatorname{curl}(\boldsymbol{u}-\Lambda_K\boldsymbol{u})\cdot\boldsymbol{l}_i\right)\cdot\boldsymbol{t}_i^1 q\mathrm{d}s\\ &= \frac{1}{|e_i|}\int_{e_i}\operatorname{grad}\left(\operatorname{curl}(\boldsymbol{u}-\Lambda_K\boldsymbol{u})\cdot(\boldsymbol{t}_i^1\times\boldsymbol{t}_i^2)\right)\cdot\boldsymbol{t}_i^1 q\mathrm{d}s.\end{aligned}$$

Let $\boldsymbol{L}_i^3 = \boldsymbol{L}_i^2$. Since the divergence of $\operatorname{curl}(\boldsymbol{u} - \Lambda_K \boldsymbol{u})$ is 0, we can find 8 constants $C_{\boldsymbol{l}_i^j}$ with $\boldsymbol{l}_i^j \in \boldsymbol{L}_i^j$ for $j = 1, 2, 3$ independent of h_K such that

$$
\begin{aligned}
&\frac{1}{|e_i|}\int_{e_i} \operatorname{grad}\left(\operatorname{curl}(\boldsymbol{u} - \Lambda_K \boldsymbol{u}) \cdot (\boldsymbol{t}_i^1 \times \boldsymbol{t}_i^2)\right) \cdot \boldsymbol{t}_i^1 q \mathrm{d}s \\
=& \sum_{j=1}^{3} \sum_{\boldsymbol{l}_i^3 \in \boldsymbol{L}_i^j} C_{\boldsymbol{l}_i^j} \frac{1}{|e_i|}\int_{e_i} \operatorname{grad}\left(\operatorname{curl}(\boldsymbol{u} - \Lambda_K \boldsymbol{u}) \cdot \boldsymbol{l}_i^j\right) \cdot \boldsymbol{t}_i^j q \mathrm{d}s,
\end{aligned}
$$

which can be finished by mapping to the reference element, finding the constants and then mapping back. Furthermore, by the definition of $\Lambda_K \boldsymbol{u}$, we have

$$
\begin{aligned}
&\sum_{j=1}^{3} \sum_{\boldsymbol{l}_i^j \in \boldsymbol{L}_i^j} C_{\boldsymbol{l}_i^j} \frac{1}{|e_i|}\int_{e_i} \operatorname{grad}\left(\operatorname{curl}(\boldsymbol{u} - \Lambda_K \boldsymbol{u}) \cdot \boldsymbol{l}_i^j\right) \cdot \boldsymbol{t}_i^j q \mathrm{d}s \\
=& \sum_{\boldsymbol{l}_i^3 \in \boldsymbol{L}_i^3} C_{\boldsymbol{l}_i^j} \frac{1}{|e_i|}\int_{e_i} \operatorname{grad}\left(\operatorname{curl}(\boldsymbol{u} - \Lambda_K \boldsymbol{u}) \cdot \boldsymbol{l}_i^3\right) \cdot \boldsymbol{t}_i^3 q \mathrm{d}s.
\end{aligned}
$$

Since $\operatorname{curl} \Lambda_K \boldsymbol{u}$ restricted on the edge e_i is a polynomial of order k, it can be determined by the vertex DOFs $D^\alpha\big(\operatorname{curl} \Lambda_K \boldsymbol{u}\big)(v_i) = D^\alpha\big(I_K \operatorname{curl} \boldsymbol{u}\big)(v_i)$ for $|\alpha| \leq 2$ and the edge DOFs $\int_{e_i} \operatorname{curl} \Lambda_K \boldsymbol{u} \cdot \boldsymbol{q} \mathrm{d}s = \int_{e_i} I_K \operatorname{curl} \boldsymbol{u} \cdot \boldsymbol{q} \mathrm{d}s$ for $\boldsymbol{q} \in \boldsymbol{P}_{k-6}(e_i)$. By Lemma 6.4.2, we have

$$
\begin{aligned}
&\sum_{\boldsymbol{l}_i^3 \in \boldsymbol{L}_i^3} C_{\boldsymbol{l}_i^3} \frac{1}{|e_i|}\int_{e_i} \operatorname{grad}\left(\operatorname{curl}(\boldsymbol{u} - \Lambda_K \boldsymbol{u}) \cdot \boldsymbol{l}_i^3\right) \cdot \boldsymbol{t}_i^3 q \mathrm{d}s \\
=& \sum_{\boldsymbol{l}_i^3 \in \boldsymbol{L}_i^3} C_{\boldsymbol{l}_i^3} \frac{1}{|e_i|}\int_{e_i} \operatorname{grad}\left(\operatorname{curl} \boldsymbol{u} - I_K \operatorname{curl} \boldsymbol{u}) \cdot \boldsymbol{l}_i^3\right) \cdot \boldsymbol{t}_i^3 q \mathrm{d}s \\
\leq& C h_K^3 \left|\operatorname{curl} \boldsymbol{u} - I_K(\operatorname{curl} \boldsymbol{u})\right|_{1,\infty,K} \\
\leq& C|K|^{-1/2} h_K^3 h_K^{\min\{s-1,k\}} \left|\operatorname{curl} \boldsymbol{u}\right|_{s,K}. \qquad (6.4.1)
\end{aligned}
$$

Suppose $\boldsymbol{N}_i$ are the basis functions associated with the non-vanishing DOFs. Then

$$
\|\boldsymbol{N}_i\|_{m,q,K} \leq C h^{-2-m} |K|^{1/q} \|\hat{\boldsymbol{N}}_i\|_{m,q,\hat{K}}, \qquad (6.4.2)
$$

where $\hat{\boldsymbol{N}}_i = \det(B_K) B_K^{-1} \boldsymbol{N}_i$ are the basis functions on the reference element.

Combining (6.4.1) and (6.4.2), we complete the proof. □

Theorem 6.4.4. *If* $\boldsymbol{u} \in H^{s+(r-k-1)}(K) \otimes \mathbb{V}$ *and* $\operatorname{curl} \boldsymbol{u} \in H^s(K) \otimes \mathbb{V}$ *with* $s > \frac{7}{2}$, *then* *we have the following error estimates for the interpolation* Λ_K*,*

$$\|\boldsymbol{u}-\Lambda_K\boldsymbol{u}\|_K \le Ch_K^{r_1}(\|\boldsymbol{u}\|_{s+(r-k-1),K}+\|\operatorname{curl}\boldsymbol{u}\|_{s,K}), \tag{6.4.3}$$

$$\|\operatorname{curl}(\boldsymbol{u}-\Lambda_K\boldsymbol{u})\|_{m,q,K} \le C|K|^{1/q-1/2}h_K^{r_2-m}\|\operatorname{curl}\boldsymbol{u}\|_{s,K}. \tag{6.4.4}$$

where $r_1=\min\{s+(r-k-1),r\}$ *and* $r_2=\min\{s,k+1\}$*.*

Proof. Due to the relationship $\Lambda_K\boldsymbol{u}\circ F_K = B_K^{-\mathrm{T}}\Lambda_{\hat{K}}\hat{\boldsymbol{u}}$ obtained in Lemma 7.3.8, the proof of (6.4.3) is standard, see the proof of Theorem 5.3.6. Combining Lemma 6.4.2 and Lemma 6.4.3, we obtain

$$\begin{aligned}\|\operatorname{curl}(\boldsymbol{u}-\Lambda_K\boldsymbol{u})\|_{m,q,K} &\le \|\operatorname{curl}\boldsymbol{u}-I_K\operatorname{curl}\boldsymbol{u})\|_{m,q,K}+\|I_K\operatorname{curl}\boldsymbol{u}-\operatorname{curl}\Lambda_K\boldsymbol{u})\|_{m,q,K}\\ &\le C|K|^{1/q-1/2}h_K^{s-m}\|\operatorname{curl}\boldsymbol{u}\|_{s,K}.\end{aligned}$$

□

Theorem 6.4.5. *If* $\boldsymbol{u}\in H^{s+(r-k-1)}(\Omega)\otimes\mathbb{V}$ *and* $\operatorname{curl}\boldsymbol{u}\in H^s(\Omega)\otimes\mathbb{V}$ *with* $s>\frac{7}{2}$*, then we have the following error estimates for the interpolation* Π_h*,*

$$\|\boldsymbol{u}-\Pi_h\boldsymbol{u}\| \le Ch_K^{r_1}(\|\boldsymbol{u}\|_{s+(r-k-1)}+\|\operatorname{curl}\boldsymbol{u}\|_s), \tag{6.4.5}$$

$$\|\operatorname{curl}(\boldsymbol{u}-\Pi_h\boldsymbol{u})\| \le Ch_K^{r_2}\|\operatorname{curl}\boldsymbol{u}\|_s, \tag{6.4.6}$$

$$\|\operatorname{grad}\operatorname{curl}(\boldsymbol{u}-\Pi_h\boldsymbol{u})\| \le Ch_K^{r_2-1}\|\operatorname{curl}\boldsymbol{u}\|_s. \tag{6.4.7}$$

Proof. We estimate $\|\boldsymbol{u}-\Pi_h\boldsymbol{u}\|_K$ and $\|\operatorname{curl}(\boldsymbol{u}-\Pi_h\boldsymbol{u})\|_{i,K}$ for $i=0,1$. Since $\boldsymbol{u}-\Pi_K\boldsymbol{u} = \boldsymbol{u}-\Lambda_K\boldsymbol{u}+\Lambda_K\boldsymbol{u}-\Pi_K\boldsymbol{u}$, it remains to estimate $\Lambda_K\boldsymbol{u}-\Pi_K\boldsymbol{u}$ in three different norms or semi-norms. We denote $\boldsymbol{\Delta}=\Lambda_K\boldsymbol{u}-\Pi_K\boldsymbol{u}$ which is a polynomial with a degree of no more than $k+1$. The DOFs to define $\Lambda_K\boldsymbol{\Delta}$ vanish except for $\frac{1}{|e_i|}\int_{e_i}\operatorname{grad}(\operatorname{curl}\boldsymbol{\Delta}\cdot\boldsymbol{l}_i^j)\cdot\boldsymbol{t}_i^j q\mathrm{d}s$ with $\boldsymbol{l}_i^j\in\boldsymbol{L}_i^j, j=1,2,$ and $q\in P_{k-5}(e_i)$. Then

$$\boldsymbol{\Delta}=\sum_{i=1}^{6}\sum_{l=1}^{k-4}\sum_{j=1}^{2}\sum_{\boldsymbol{l}_i^j\in\boldsymbol{L}_i^j}\frac{1}{|e_i|}\int_{e_i}\operatorname{grad}(\operatorname{curl}\boldsymbol{\Delta}\cdot\boldsymbol{l}_i^j)\cdot\boldsymbol{t}_i^j q_l\mathrm{d}s\boldsymbol{N}_{ijl}^{\boldsymbol{l}_i^j},$$

where $N_{ijl}^{\boldsymbol{l}_i^j}$ are the corresponding dual basis functions. Since $\operatorname{curl}\boldsymbol{\Delta}$ is a div-free polynomial, we can represent $\operatorname{grad}(\operatorname{curl}\boldsymbol{\Delta}\cdot\boldsymbol{m}_i)\cdot\boldsymbol{m}_i$ as a linear combination of $\operatorname{grad}(\operatorname{curl}\boldsymbol{\Delta}\cdot\boldsymbol{\tau}_i)\cdot\boldsymbol{m}_i$, $\operatorname{grad}(\operatorname{curl}\boldsymbol{\Delta}\cdot\boldsymbol{\tau}_i)\cdot\boldsymbol{n}_i$, $\operatorname{grad}(\operatorname{curl}\boldsymbol{\Delta}\cdot\boldsymbol{n}_i)\cdot\boldsymbol{m}_i$, $\operatorname{grad}(\operatorname{curl}\boldsymbol{\Delta}\cdot\boldsymbol{n}_i)\cdot\boldsymbol{n}_i$, and $\operatorname{grad}(\operatorname{curl}\boldsymbol{\Delta}\cdot\boldsymbol{m}_i)\cdot\boldsymbol{n}_i$ with weights independent of h. Therefore,

$$
\begin{aligned}
&\operatorname{grad}(\operatorname{curl}\boldsymbol{\Delta}\cdot\boldsymbol{l}_i^j)\cdot\boldsymbol{t}_i^j\\
=&\operatorname{grad}\Big(\operatorname{curl}\boldsymbol{\Delta}\cdot\big[(\boldsymbol{l}_i^j\cdot\boldsymbol{\tau}_i)\boldsymbol{\tau}_i+(\boldsymbol{l}_i^j\cdot\boldsymbol{n}_i)\boldsymbol{n}_i+(\boldsymbol{l}_i^j\cdot\boldsymbol{m}_i)\boldsymbol{m}_i\big]\Big)\\
&\cdot\big[(\boldsymbol{t}_i^j\cdot\boldsymbol{\tau}_i)\boldsymbol{\tau}_i+(\boldsymbol{t}_i^j\cdot\boldsymbol{n}_i)\boldsymbol{n}_i+(\boldsymbol{t}_i^j\cdot\boldsymbol{m}_i)\boldsymbol{m}_i\big]\\
\le& Ch_K^3\Big(\big|\operatorname{grad}\big(\operatorname{curl}(\boldsymbol{u}-\Lambda_K\boldsymbol{u})\cdot\boldsymbol{\tau}_i\big)\cdot\boldsymbol{n}_i\big|+\big|\operatorname{grad}\big(\operatorname{curl}(\boldsymbol{u}-\Lambda_K\boldsymbol{u})\cdot\boldsymbol{\tau}_i\big)\cdot\boldsymbol{m}_i\big|\\
&+\big|\operatorname{grad}\big(\operatorname{curl}(\boldsymbol{u}-\Lambda_K\boldsymbol{u})\cdot\boldsymbol{n}_i\big)\cdot\boldsymbol{n}_i\big|+\big|\operatorname{grad}\big(\operatorname{curl}(\boldsymbol{u}-\Lambda_K\boldsymbol{u})\cdot\boldsymbol{n}_i\big)\cdot\boldsymbol{m}_i\big|\\
&+\big|\operatorname{grad}\big(\operatorname{curl}(\boldsymbol{u}-\Lambda_K\boldsymbol{u})\cdot\boldsymbol{m}_i\big)\cdot\boldsymbol{n}_i\big|\Big)
\end{aligned}
$$

Each term has the following estimate. We show only the first term

$$
\begin{aligned}
&\operatorname{grad}\big(\operatorname{curl}(\boldsymbol{u}-\Lambda_K\boldsymbol{u})\cdot\boldsymbol{\tau}_i\big)\cdot\boldsymbol{n}_i\\
\le& C\left|\operatorname{curl}(\boldsymbol{u}-\Lambda_K\boldsymbol{u})\right|_{1,\infty,K}\\
\le& C|K|^{-1/2}h_K^{r_2-1}\left|\operatorname{curl}\boldsymbol{u}\right|_{s,K}.
\end{aligned}
$$

According to the mapping (5.1.7), the basis functions $\boldsymbol{N}_{ijl}^{\boldsymbol{l}_i^j}$ satisfy

$$
\begin{aligned}
&\big\|\boldsymbol{N}_{ijl}^{\boldsymbol{l}_i^j}\big\|\le Ch_K^{1/2}\big\|\hat{\boldsymbol{N}}_{ijl}^{\boldsymbol{l}_i^j}\big\|,\\
&\big\|\operatorname{curl}\boldsymbol{N}_{ijl}^{\boldsymbol{l}_i^j}\big\|\le Ch_K^{-1/2}\big\|\operatorname{curl}_{\hat{\boldsymbol{x}}}\hat{\boldsymbol{N}}_{ijl}^{\boldsymbol{l}_i^j}\big\|,\\
&\big\|\operatorname{grad}\operatorname{curl}\boldsymbol{N}_{ijl}^{\boldsymbol{l}_i^j}\big\|\le Ch_K^{-3/2}\big\|\operatorname{grad}_{\hat{\boldsymbol{x}}}\operatorname{curl}_{\hat{\boldsymbol{x}}}\hat{\boldsymbol{N}}_{ijl}^{\boldsymbol{l}_i^j}\big\|,
\end{aligned}
$$

where $\hat{\boldsymbol{N}}_{ijl}^{\boldsymbol{l}_i^j}$ are the corresponding basis functions on $\hat{K}$ and satisfy $\boldsymbol{N}_{ijl}^{\boldsymbol{l}_i^j}=B_K^{-\mathrm{T}}\hat{\boldsymbol{N}}_{ijl}^{\boldsymbol{l}_i^j}$. By combining the above estimates, we complete the proof. □

CHAPTER 7 3D GRADCURL-CONFORMING ELEMENTS II

The construction in the last chapter involves supersmoothness on lower-dimensional simplices. As a consequence, the grad curl-conforming elements have a large number of DOFs, and it is hard to construct exact discrete complexes with vanishing boundary conditions.

In this chapter, we will construct finite element subcomplexes of (6.0.1) with fewer DOFs:

$$0 \longrightarrow \mathbb{R} \xrightarrow{\subset} \Sigma_h^r \xrightarrow{\text{grad}} V_h^{r-1,k+1} \xrightarrow{\text{curl}} \boldsymbol{\Sigma}_h^{k,+} \xrightarrow{\text{div}} W_h^{k-1} \longrightarrow 0, \qquad (7.0.1)$$

where $r = k$, $k+1$, or $k+2$. To construct the discrete complex, we first need an inf-sup stable finite element Stokes pair $\boldsymbol{\Sigma}_h^{k,+} - W_h^{k-1}$. To satisfy the complex property, the Stokes pair should satisfy

$$\operatorname{div} \boldsymbol{\Sigma}_h^{k,+} \subseteq W_h^{k-1},$$

which guarantees the divergence-free condition at the discrete level. Recently, Guzmán and Neilan [34] constructed such a finite element Stokes pair by enriching the first-order vector-valued Lagrange finite element space with modified Bernardi-Raugel bubbles. The pair has only 16 and 1 DOFs on each element. Therefore, it is a good candidate for $\boldsymbol{\Sigma}_h^{+} - W_h$. However, the extension to high-order cases is still not available yet. In this chapter, we will first extend Guzmán and Neilan's construction in [34] to high-order cases and apply it to construct the whole complex (7.0.1).

7.1 Local Shape Function Spaces and Polynomial Complexes

7.1.1 Modified Bubble Functions

For each $K \in \mathcal{T}_h$, let x_K be the barycenter of K. We denote K^r as the partition of K by adjoining the vertices of K with the new vertex x_K, known as the Alfeld split of

K [1]. We also denote

$$\boldsymbol{P}_k^c(K^r) = \{\boldsymbol{v} \in H^1(K)\otimes\mathbb{V} : \boldsymbol{v}|_T \in \boldsymbol{P}_k(T) \text{ for all } T \in K^r\},$$

$$\mathring{\boldsymbol{P}}_k^c(K^r) = \{\boldsymbol{v} \in H_0^1(K)\otimes\mathbb{V} : \boldsymbol{v}|_T \in \boldsymbol{P}_k(T) \text{ for all } T \in K^r\},$$

$$\mathring{P}_k(K^r) = \{q \in L_0^2(K) : q|_T \in P_k(T) \text{ for all } T \in K^r\}.$$

Let $x_1, \cdots, x_4$ be the four vertexes of the element K, and $x_0 = x_K$. Let λ_0 be the continuous piecewise linear function satisfying $\lambda_0(x_j) = \delta_{0j}$ for $0 \le j \le 4$. Denote

$$\boldsymbol{M}_k(K^r) = \Big\{\boldsymbol{v} \in \mathring{\boldsymbol{P}}_k^c(K^r) : \boldsymbol{v} = \sum_{j=1}^{k} \lambda_0^j \boldsymbol{w}_{k-j} \text{ with } \boldsymbol{w}_{k-j} \in \boldsymbol{P}_{k-j}^{\perp}(K)\Big\}, \tag{7.1.1}$$

where $\boldsymbol{P}_l^{\perp}(K) = \big\{\boldsymbol{v} \in \boldsymbol{P}_l(K) : \int_K \boldsymbol{v}\cdot\boldsymbol{\kappa}\,\mathrm{d}V = 0 \text{ for all } \boldsymbol{\kappa} \in \mathcal{R}_{l-1}\big\}$ with $\mathcal{R}_l$ defined in (1.5.4) for $l \ge 1$ and $\mathcal{R}_l = 0$ for $l = 0, -1$.

We will construct modified bubbles using the following properties of polynomial spaces on K^r [34, Theorem 3.3].

Lemma 7.1.1. *Let $k \ge 1$. For any $K \in \mathcal{T}_h$ and for any $p \in \mathring{P}_{k-1}(K^r)$, there exists a unique $\boldsymbol{v} \in \mathring{\boldsymbol{M}}_k(K^r)$ satisfying*

$$\operatorname{div}\boldsymbol{v} = p \text{ on } K.$$

Let $\lambda_i (i = 1, 2, 3, 4)$ be the barycentric coordinates of K, i.e., $\lambda_i(x_j) = \delta_{ij}$. We define the scalar face bubbles

$$B_i = \prod_{j=1, j\ne i}^{4} \lambda_j \text{ for } 1 \le i \le 4$$

and the scalar interior bubble

$$B_0 = \prod_{j=1}^{4} \lambda_j.$$

The Bernardi-Raugel face bubbles are given as

$$\boldsymbol{b}_i^f = B_i \boldsymbol{n}_i \text{ for } 1 \le i \le 4,$$

where $\boldsymbol{n}_i$ is the outward unit normal to $f_i \in \mathcal{F}_h(K)$.

According to [34, Propsition 4.2], we can modify the Bernardi-Raugel face bubbles such that they have constant divergence.

Lemma 7.1.2 ([34])**.** *There exists* $\boldsymbol{\beta}_i^f \in \boldsymbol{P}_3^c(K^r)$ *such that*

$$\boldsymbol{\beta}_i^f|_{\partial K} = \boldsymbol{b}_i^f|_{\partial K}, \quad \operatorname{div} \boldsymbol{\beta}_i^f \in P_0(K). \tag{7.1.2}$$

We refer to the functions $\boldsymbol{\beta}_i^f \in \boldsymbol{P}_3^c(K^r)$, $i = 1, 2, 3, 4$ which satisfy (7.1.2) as the *modified Bernardi-Raugel bubbles* on a tetrahedron K (see [34]). Denote

$$B^1 := \operatorname{span}\{\boldsymbol{\beta}_i^f,\ i = 1, 2, 3, 4\},$$

To construct higher-order elements, we will use certain interior bubbles. Denote

$$\mathcal{S}_k(K) = \begin{cases} \widetilde{P}_k(K), & k = 1, \\ \widetilde{P}_k(K) \oplus \widetilde{P}_{k-1}(K), & k \geq 2, \end{cases}$$

and

$$\mathring{\mathcal{S}}_k(K) := \left\{ u - \frac{1}{|K|} \int_K u \mathrm{d}V : u \in \mathcal{S}_k(K) \right\}.$$

According to Lemma 7.1.1, for $k \geq 2$, there exists a unique subspace $B^k \subset \boldsymbol{M}_k(K^r)$ such that $\operatorname{div} B^k = \mathring{\mathcal{S}}_{k-1}(K)$ and $\dim B^k = \dim \mathring{\mathcal{S}}_{k-1}(K)$. We refer to the functions in B^k as *modified interior bubbles* on a tetrahedron K.

Remark 7.1.1. With the constructive proof of Lemma 7.1.1 (see [34, Theorem 3.3]), we can obtain explicit forms of the interior bubbles in the implementation.

Lemma 7.1.3. *For* $k \geq 2$*, a function* $\boldsymbol{v} \in B^k$ *is uniquely determined by*

$$\int_K \boldsymbol{v} \cdot \operatorname{grad} q dS \text{ for all } q \in \mathring{\mathcal{S}}_{k-1}(K). \tag{7.1.3}$$

Proof. From the construction, $\dim B^k = \dim \mathring{\mathcal{S}}_{k-1}(K)$. Suppose that the functionals in (7.1.3) vanish on $\boldsymbol{v}$. It suffices to show $\boldsymbol{v} = 0$. Indeed, we have from integration by parts

$$0 = \int_K \boldsymbol{v} \cdot \operatorname{grad} q \mathrm{d}V = \int_K \operatorname{div} \boldsymbol{v} q \mathrm{d}V.$$

Taking $q = \operatorname{div} \boldsymbol{v}$, we obtain $\operatorname{div} \boldsymbol{v} = 0$ and therefore $\boldsymbol{v} = 0$ since $\operatorname{div} : B^k \to \mathring{\mathcal{S}}_{k-1}(K)$ is bijective by the construction of B^k. □

7.1.2 Local Shape Function Spaces

On each $K \in \mathcal{T}_h$, we construct the local complex of the shape function spaces of (7.0.1) as follows:

$$0 \longrightarrow \mathbb{R} \xrightarrow{\subset} \Sigma_h^r(K) \xrightarrow{\text{grad}} V_h^{r-1,k+1}(K) \xrightarrow{\text{curl}} \boldsymbol{\Sigma}_h^{k,+}(K) \xrightarrow{\text{div}} W_h^{k-1}(K) \longrightarrow 0. \quad (7.1.4)$$

As before, we first consider the following local complex on the reference element $\hat{K}$:

$$0 \longrightarrow \mathbb{R} \xrightarrow{\subset} \hat{\Sigma}_h^r(\hat{K}) \xrightarrow{\text{grad}_{\hat{\boldsymbol{x}}}} \hat{V}_h^{r-1,k+1}(\hat{K}) \xrightarrow{\text{curl}_{\hat{\boldsymbol{x}}}} \hat{\boldsymbol{\Sigma}}_h^{k,+}(\hat{K}) \xrightarrow{\text{div}_{\hat{\boldsymbol{x}}}} \hat{W}_h^{k-1}(\hat{K}) \longrightarrow 0 \quad (7.1.5)$$

We choose $\hat{\Sigma}_h^r(\hat{K}) := P_r(\hat{K})$ and $W_h^{k-1}(\hat{K}) := P_{k-1}(\hat{K})$. Denote by $\hat{B}^k$ the set of modified bubbles on $\hat{K}$. Set $\hat{\boldsymbol{\Sigma}}_h^{k,+}(\hat{K}) = \boldsymbol{P}_k(\hat{K}) \oplus \hat{B}$, where

$$\hat{B} = \begin{cases} \hat{B}^1, & k = 1, \\ \hat{B}^1 \oplus \hat{B}^2, & k = 2, \\ \hat{B}^k, & k \geq 3. \end{cases}$$

Note that for $k = 1$, we only supply $\boldsymbol{P}_1(\hat{K})$ with modified Bernardi-Raugel face bubbles; for $k = 2$, we supply $\boldsymbol{P}_2(\hat{K})$ with both face and interior bubbles, while for $k \geq 3$ we only need supply $\boldsymbol{P}_k(\hat{K})$ with interior bubbles. It is easy to see that the face bubbles $\{\boldsymbol{\beta}_i^f\}_{i=1}^4$ and $\boldsymbol{P}_2(\hat{K})$ are linearly independent, and hence, $\boldsymbol{P}_2(\hat{K}) \oplus \hat{B}^1$ and $\boldsymbol{P}_1(\hat{K}) \oplus \hat{B}^1$ are direct sums. From the explicit form (7.1.1) of the functions in $\boldsymbol{M}_k(\hat{K}^r)$, we see that $\boldsymbol{M}_k(\hat{K}^r) \oplus \boldsymbol{P}_k(\hat{K})$ is a direct sum, and hence, $\hat{B}^k \oplus \boldsymbol{P}_k(\hat{K})$ is also a direct sum.

Remark 7.1.2. The idea of enriching with modified bubbles is inspired by [34], where the case of $k = 1$ is defined and used to construct a stable Stokes finite element pair. Here we extend it to high-order cases.

Define

$$\hat{V}_h^{r-1,k+1}(\hat{K}) = \operatorname{grad}_{\hat{\boldsymbol{x}}} \hat{\Sigma}_h^r(\hat{K}) \oplus \mathfrak{p}_{\hat{\boldsymbol{x}}}^2 \hat{\boldsymbol{\Sigma}}_h^{k,+}(\hat{K}). \tag{7.1.6}$$

The right-hand side of (7.1.6) is a direct sum.

Remark 7.1.3. For the modified bubble functions in $\hat{\boldsymbol{\Sigma}}_h^{k,+}(\hat{K})$, we choose the barycenter $x_{\hat{K}}$ as the base point W in the definition of $\mathfrak{p}_{\hat{\boldsymbol{x}}}^2$ (see [21]). For other functions, we choose $W = 0$.

Remark 7.1.4. For polynomial bases in $\hat{\boldsymbol{\Sigma}}_h^{k,+}(\hat{K})$ other than the bubbles, we can replace the Poincaré operator $\mathfrak{p}_{\hat{\boldsymbol{x}}}^2$ by the Koszul operator $\kappa_{\hat{\boldsymbol{x}}}^2$. However, to get the complex property it seems necessary to use the Poincaré operator for the bubbles.

By the definitions of the shape function spaces, it is easy to show that the sequence (7.1.5) is a complex. By the properties of the Poincaré operators, we can verify that the sequence

$$0 \longleftarrow \hat{\Sigma}_h^r(\hat{K}) \xleftarrow{\mathfrak{p}_{\hat{\boldsymbol{x}}}^1} \hat{V}_h^{r-1,k+1}(\hat{K}) \xleftarrow{\mathfrak{p}_{\hat{\boldsymbol{x}}}^2} \hat{\boldsymbol{\Sigma}}_h^{k,+}(\hat{K}) \xleftarrow{\mathfrak{p}_{\hat{\boldsymbol{x}}}^3} \hat{W}_h^{k-1}(\hat{K}) \longleftarrow 0 \tag{7.1.7}$$

is also a complex with the Poincaré operators in (2.1.20) – (2.1.22). From Lemma 2.1.3, we obtain the exactness.

Lemma 7.1.4. *The complex* (7.1.4) *is exact.*

From the definition, we see that $\hat{V}_h^{r-1,k+1}(\hat{K})$ has two parts: one from the gradient on $\hat{\Sigma}_h^r(\hat{K})$ and the other from the Poincaré operator on $\hat{\boldsymbol{\Sigma}}_h^{k,+}(\hat{K})$. The first part is easy to implement: we may remove the constant (kernel of gradient) from the bases of $\hat{\Sigma}_h^r(\hat{K})$ and apply gradient to the rest. The $\mathfrak{p}_{\hat{\boldsymbol{x}}}^2 \hat{\boldsymbol{\Sigma}}_h^{k,+}(\hat{K})$ part calls for more explanation as we cannot obtain a basis by applying the Poincaré operator to a basis of $\hat{\boldsymbol{\Sigma}}_h^{k,+}(\hat{K})$ (as the results are not linearly independent). Now we show how to obtain a basis for the $\mathfrak{p}_{\hat{\boldsymbol{x}}}^2 \hat{\boldsymbol{\Sigma}}_h^{k,+}(\hat{K})$ part to implement $\hat{V}_h^{r-1,k+1}(\hat{K})$.

We first claim $\boldsymbol{P}_k(\hat{K}) = \operatorname{curl}_{\hat{\boldsymbol{x}}} \boldsymbol{P}_{k+1}(\hat{K}) \oplus \mathfrak{p}^3_{\hat{\boldsymbol{x}}} P_{k-1}(\hat{K})$. In fact, for all $\hat{\boldsymbol{u}} \in \boldsymbol{P}_k(\hat{K})$, the null-homotopy identity (6.1.5) leads to $\hat{\boldsymbol{u}} = \operatorname{curl}_{\hat{\boldsymbol{x}}} \mathfrak{p}^2_{\hat{\boldsymbol{x}}} \hat{\boldsymbol{u}} + \mathfrak{p}^3_{\hat{\boldsymbol{x}}} \operatorname{div}_{\hat{\boldsymbol{x}}} \hat{\boldsymbol{u}} \in \operatorname{curl}_{\hat{\boldsymbol{x}}} \boldsymbol{P}_{k+1}(\hat{K}) + \mathfrak{p}^3_{\hat{\boldsymbol{x}}} P_{k-1}(\hat{K})$. Moreover, if $\hat{\boldsymbol{u}} \in \operatorname{curl}_{\hat{\boldsymbol{x}}} \boldsymbol{P}_{k+1}(\hat{K}) \cap \mathfrak{p}^3_{\hat{\boldsymbol{x}}} P_{k-1}(\hat{K})$, then $\operatorname{div}_{\hat{\boldsymbol{x}}} \hat{\boldsymbol{u}} = 0$ and $\mathfrak{p}^2_{\hat{\boldsymbol{x}}} \hat{\boldsymbol{u}} = 0$, which follows from (6.1.5) again that $\hat{\boldsymbol{u}} = 0$.

We then have the decomposition $\hat{\boldsymbol{\Sigma}}^{k,+}_h(\hat{K}) = \operatorname{curl}_{\hat{\boldsymbol{x}}} \boldsymbol{P}_{k+1}(\hat{K}) \oplus \mathfrak{p}^3_{\hat{\boldsymbol{x}}} P_{k-1}(\hat{K}) \oplus \hat{B}$, which leads to

$$\begin{aligned} \mathfrak{p}^2_{\hat{\boldsymbol{x}}} \hat{\boldsymbol{\Sigma}}^{k,+}_h(\hat{K}) =& \mathfrak{p}^2_{\hat{\boldsymbol{x}}} \operatorname{curl}_{\hat{\boldsymbol{x}}} \boldsymbol{P}_{k+1}(\hat{K}) + \mathfrak{p}^2_{\hat{\boldsymbol{x}}} \hat{B} + \mathfrak{p}^2_{\hat{\boldsymbol{x}}} \mathfrak{p}^3_{\hat{\boldsymbol{x}}} P_{k-1}(\hat{K}) \\ =& \mathfrak{p}^2_{\hat{\boldsymbol{x}}} \operatorname{curl}_{\hat{\boldsymbol{x}}} \boldsymbol{P}_{k+1}(\hat{K}) + \mathfrak{p}^2_{\hat{\boldsymbol{x}}} \hat{B}, \end{aligned} \tag{7.1.8}$$

where we used $\mathfrak{p}^2_{\hat{\boldsymbol{x}}} \mathfrak{p}^3_{\hat{\boldsymbol{x}}} = 0$.

From the exactness and the decomposition of $\hat{\boldsymbol{\Sigma}}^{k,+}_h(\hat{K})$, we obtain

$$\begin{aligned} \dim \mathfrak{p}^2_{\hat{\boldsymbol{x}}} \hat{\boldsymbol{\Sigma}}^{k,+}_h &= \dim \hat{V}^{r-1,k+1}_h(\hat{K}) - \dim \operatorname{grad}_{\hat{\boldsymbol{x}}} \hat{\Sigma}^r_h(\hat{K}) \\ &= \dim \hat{\boldsymbol{\Sigma}}^{k,+}_h(\hat{K}) - \dim \hat{W}^{k-1}_h(\hat{K}) \\ &= \dim \operatorname{curl}_{\hat{\boldsymbol{x}}} \boldsymbol{P}_{k+1}(\hat{K}) + \dim \mathfrak{p}^3_{\hat{\boldsymbol{x}}} P_{k-1}(\hat{K}) + \dim \hat{B} - \dim \hat{W}^{k-1}_h(\hat{K}) \\ &= \dim \operatorname{curl}_{\hat{\boldsymbol{x}}} \boldsymbol{P}_{k+1}(\hat{K}) + \dim \hat{B} \\ &\geq \dim \mathfrak{p}^2_{\hat{\boldsymbol{x}}} \operatorname{curl}_{\hat{\boldsymbol{x}}} \boldsymbol{P}_{k+1}(\hat{K}) + \dim \mathfrak{p}^2_{\hat{\boldsymbol{x}}} \hat{B}, \end{aligned}$$

which together with (7.1.8) leads to

$$\mathfrak{p}^2_{\hat{\boldsymbol{x}}} \hat{\boldsymbol{\Sigma}}^{k,+}_h(\hat{K}) = \mathfrak{p}^2_{\hat{\boldsymbol{x}}} \operatorname{curl}_{\hat{\boldsymbol{x}}} \boldsymbol{P}_{k+1}(\hat{K}) \oplus \mathfrak{p}^2_{\hat{\boldsymbol{x}}} \hat{B}.$$

Therefore, to implement $\mathfrak{p}^2_{\hat{\boldsymbol{x}}} \hat{V}^{r-1,k+1}_h(\hat{K})$, we take the bases of $\hat{B}$ and the bases of $\operatorname{curl}_{\hat{\boldsymbol{x}}} \boldsymbol{P}_{k+1}(\hat{K})$, and apply the Poincaré operator on them.

We demonstrate that $\hat{V}^{r-1,k+1}_h(\hat{K})$ contains polynomials of certain degree.

Lemma 7.1.5. *The inclusion* $\boldsymbol{P}_{r-1}(\hat{K}) \subseteq V^{r-1,k+1}_h(\hat{K})$ *holds.*

Proof. Proceeding as the proof of Lemma 6.1.2, we can prove this lemma. □

Define $\Sigma^r_h(K)$, $V^{r-1,k+1}_h(K)$, and $\boldsymbol{\Sigma}^{k,+}_h$ as in (6.1.8). Then the complex (7.1.4) is an exact complex.

7.2 Degrees of Freedom

In this section, we define DOFs for each space in (7.1.4). Taking $r = k$, $k+1$, and $k+2$ in (7.1.4) yields three versions of grad curl-conforming element spaces $V_h^{k-1,k+1}(K)$, $V_h^{k,k+1}(K)$, and $V_h^{k+1,k+1}(K)$.

The DOFs for the Lagrange element $\Sigma_h^r(K)$ can be given as follows.

- Vertex DOFs $M_v(u)$ at all the vertices $v_i \in \mathcal{V}_h(K)$:

$$M_v(u) = \{u(v_i)\}. \tag{7.2.1}$$

- Edge DOFs $M_e(u)$ on all the edges $e_i \in \mathcal{E}_h(K)$:

$$M_e(u) = \left\{\int_{e_i} uv\mathrm{d}s \text{ for all } v \in P_{r-2}(e_i)\right\}. \tag{7.2.2}$$

- Face DOFs $M_f(u)$ on all the faces $f_i \in \mathcal{F}_h(K)$:

$$M_f(u) = \left\{\int_{f_i} uv\mathrm{d}A \text{ for all } v \in P_{r-3}(f_i)\right\}. \tag{7.2.3}$$

- Interior DOFs $M_K(u)$ in the element $K \in \mathcal{T}_h$:

$$M_K(u) = \left\{\int_{K} uv\mathrm{d}V \text{ for all } v \in P_{r-4}(K)\right\}. \tag{7.2.4}$$

We equip the space $V_h^{r-1,k+1}(K)$ with the following DOFs:

- Vertex DOFs $\boldsymbol{M}_v(\boldsymbol{u})$ at all vertices $v_i \in \mathcal{V}_h(K)$:

$$\boldsymbol{M}_v(\boldsymbol{u}) = \{\mathrm{curl}\,\boldsymbol{u}(v_i)\}. \tag{7.2.5}$$

- Edge DOFs $\boldsymbol{M}_e(\boldsymbol{u})$ on all edges $e_i \in \mathcal{E}_h(K)$:

$$\begin{aligned}\boldsymbol{M}_e(\boldsymbol{u}) = &\left\{\int_{e_i} \boldsymbol{u}\cdot\boldsymbol{\tau}_i q\mathrm{d}s \text{ for all } q \in P_{r-1}(e_i)\right\}\\ &\cup\left\{\int_{e_i} \mathrm{curl}\,\boldsymbol{u}\cdot\boldsymbol{q}\mathrm{d}s \text{ for all } \boldsymbol{q} \in \boldsymbol{P}_{k-2}(e_i)\right\}.\end{aligned} \tag{7.2.6}$$

- Face DOFs $\boldsymbol{M}_f(\boldsymbol{u})$ at all faces $f_i \in \mathcal{F}_h(K)$ (with two mutually orthogonal unit vector $\boldsymbol{\tau}_i^1$ and $\boldsymbol{\tau}_i^2$ in the face f_i and the unit normal vector $\boldsymbol{n}_i$):

$$\begin{aligned}\boldsymbol{M}_f(\boldsymbol{u}) = &\left\{\int_{f_i} \operatorname{curl}\boldsymbol{u}\cdot\boldsymbol{n}_i q \mathrm{d}A \text{ for all } q\in P_{k-3}(f_i)/\mathbb{R}\right\}\\ &\cup\left\{\int_{f_i} \operatorname{curl}\boldsymbol{u}\cdot\boldsymbol{\tau}_i^1 q\mathrm{d}A \text{ for all } q\in P_{k-3}(f_i)\right\}\\ &\cup\left\{\int_{f_i} \operatorname{curl}\boldsymbol{u}\cdot\boldsymbol{\tau}_i^2 q\mathrm{d}A \text{ for all } q\in P_{k-3}(f_i)\right\}\\ &\cup\left\{\int_{f_i} \boldsymbol{u}\cdot\boldsymbol{q}\mathrm{d}A \text{ for all } \boldsymbol{q}=B_K\hat{\boldsymbol{q}}, \hat{\boldsymbol{q}}\in P_{r-3}(\hat{f}_i)\hat{\boldsymbol{x}}_{\hat{f}_i}\right\},\end{aligned} \tag{7.2.7}$$

where $\hat{\boldsymbol{x}}_{\hat{f}_i} = [\hat{\boldsymbol{x}} - (\hat{\boldsymbol{x}}\cdot\hat{\boldsymbol{n}}_i)\,\hat{\boldsymbol{n}}_i]\,|_{\hat{f}_i}$.

- Interior DOFs $\boldsymbol{M}_K(\boldsymbol{u})$ in the element $K\in\mathcal{T}_h$:

$$\begin{aligned}\boldsymbol{M}_K(\boldsymbol{u}) = &\left\{\int_K \operatorname{curl}\boldsymbol{u}\cdot\boldsymbol{q}\mathrm{d}V \text{ for all } \boldsymbol{q}\circ F_K = B_K^{-\mathrm{T}}\hat{\boldsymbol{q}}, \hat{\boldsymbol{q}}\in \operatorname{curl}_{\hat{\boldsymbol{x}}} \mathring{\hat{V}}_h^{r-1,k+1}(\hat{K})\right\}\\ &\cup\left\{\int_K \boldsymbol{u}\cdot\boldsymbol{q}\mathrm{d}V \text{ for all } \boldsymbol{q}\circ F_K = B_K\hat{\boldsymbol{q}}, \hat{\boldsymbol{q}}\in P_{r-4}(\hat{K})\hat{\boldsymbol{x}}\right\},\end{aligned} \tag{7.2.8}$$

where $\mathring{\hat{V}}_h^{r-1,k+1}(\hat{K}) = \{\boldsymbol{u}\in \hat{V}_h^{r-1,k+1}(\hat{K}) : \text{DOFs (7.2.5) } - \text{ (7.2.7) vanish on } \hat{\boldsymbol{u}}\}$.

The DOFs for $\boldsymbol{\Sigma}_h^{k,+}(K)$ can be given similarly to $\Sigma_h^r(K)$ with some additional face or interior integration DOFs to take care of the bubble functions (see Lemma 7.1.2 and Lemma 7.1.3).

- Vertex DOFs $\boldsymbol{M}_v(\boldsymbol{u})$ at all the vertices $v_i\in\mathcal{V}_h(K)$:

$$\boldsymbol{M}_v(\boldsymbol{u}) = \{\boldsymbol{u}(v_i)\}. \tag{7.2.9}$$

- Edge DOFs $\boldsymbol{M}_e(\boldsymbol{u})$ on all the edges $e_i\in\mathcal{E}_h(K)$:

$$\boldsymbol{M}_e(\boldsymbol{u}) = \left\{\int_{e_i} \boldsymbol{u}\cdot\boldsymbol{v}\mathrm{d}s \text{ for all } \boldsymbol{v}\in\boldsymbol{P}_{k-2}(e_i)\right\}. \tag{7.2.10}$$

- Face DOFs $\boldsymbol{M}_f(\boldsymbol{u})$ on all the faces $f_i\in\mathcal{F}_h(K)$:

$$\begin{aligned}\boldsymbol{M}_f(\boldsymbol{u}) = &\left\{\int_{f_i} \boldsymbol{u}\cdot\boldsymbol{v}\mathrm{d}A \text{ for all } \boldsymbol{v}\in\boldsymbol{P}_{k-3}(f_i)\right\}\\ &\cup\left\{\int_{f_i} \boldsymbol{u}\cdot\boldsymbol{n}_i\mathrm{d}A \text{ when } k=1,2\right\}.\end{aligned} \tag{7.2.11}$$

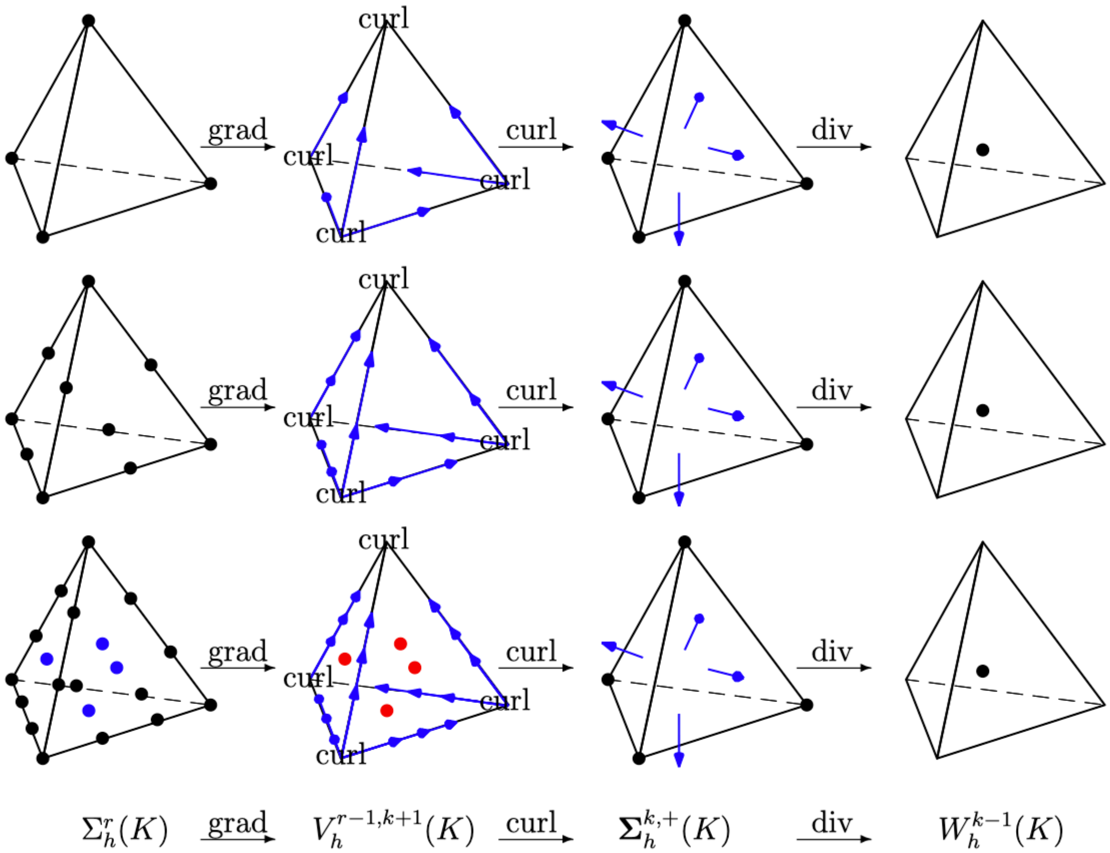

Figure 7.2.1: The lowest-order ($k = 1$) finite element complex (7.1.4) on tetrahedra with $r = k$ in the first row, $r = k + 1$ in the second row, and $r = k + 2$ in the third row.

- Interior DOFs $\boldsymbol{M}_K(\boldsymbol{u})$ in the element $K \in \mathcal{T}_h$:

$$\boldsymbol{M}_K(\boldsymbol{u}) = \left\{ \int_K \boldsymbol{u} \cdot \boldsymbol{v} \mathrm{d}V \text{ for all } \boldsymbol{v} = B_K^{-\mathrm{T}} \hat{\boldsymbol{v}}, \hat{\boldsymbol{v}} \in \operatorname{curl}_{\hat{\boldsymbol{x}}} \mathring{\hat{V}}_h^{r-1,k+1}(\hat{K}) \right\} \cup \left\{ \int_K \boldsymbol{u} \cdot \operatorname{grad} v \mathrm{d}V \text{ for all } v \in P_{k-1}(K)/\mathbb{R} \ (k \geq 2) \right\}. \tag{7.2.12}$$

The DOFs for $W_h^{k-1}(K)$ can be given as follows.

- Interior DOFs $M_K(u)$ in the element $K \in \mathcal{T}_h$:

$$M_K(u) = \left\{ \int_K u \cdot v \mathrm{d}V \text{ for all } v \in P_{k-1}(K) \right\}.$$

Lemma 7.2.1. *The DOFs for $\boldsymbol{\Sigma}_h^{k,+}(K)$ are unisolvent.*

Proof. The case of $k = 1$ is proved in [34, Lemma 4.3], and the case of $k = 2$ can be proved similarly. We only prove the lemma for $k \geq 3$. Denote $N_{k-1} = \dim B^k$. For $\boldsymbol{u} \in \boldsymbol{\Sigma}_h^{k,+}(K)$, rewrite $\boldsymbol{u} = \boldsymbol{w} + \sum_i^{N_{k-1}} b_i \mathring{\boldsymbol{\beta}}_i$ with $b_i \in \mathbb{R}$, $\boldsymbol{w} \in \boldsymbol{P}_k(K)$, and $\mathring{\boldsymbol{\beta}}_i \in B^k$. Suppose that the DOFs (7.2.9) – (7.2.12) vanish on $\boldsymbol{u}$. We must show that $\boldsymbol{u} = 0$. Since $\mathring{\boldsymbol{\beta}}_i$ vanish on ∂K, $\boldsymbol{w}$ vanishes on ∂K by the DOFs in (7.2.9) – (7.2.11). The DOFs in the second set of (7.2.12) leads to $\operatorname{div} \boldsymbol{u} = 0$ since $\operatorname{div} \boldsymbol{u} \in P_{k-1}(K)/\mathbb{R}$. Therefore $\boldsymbol{u} = \operatorname{curl} \boldsymbol{v}$ with $\boldsymbol{v} \in \mathring{V}_h^{r-1,k+1}(K)$. Using the DOFs in the first set of (7.2.12), we obtain $\boldsymbol{u} = 0$. □

Lemma 7.2.2. *The DOFs* (7.2.5) – (7.2.8) *are well-defined for any* $\boldsymbol{u} \in H^{1/2+\delta}(\Omega) \otimes \mathbb{V}$ *and* $\operatorname{curl} \boldsymbol{u} \in H^{3/2+\delta}(\Omega) \otimes \mathbb{V}$ *with* $\delta > 0$.

Proof. By the embedding theorem, we have $\operatorname{curl} \boldsymbol{u} \in H^{3/2+\delta}(\Omega) \otimes \mathbb{V} \hookrightarrow C^{0,\delta}(\Omega) \otimes \mathbb{V}$, then the DOFs involving $\operatorname{curl} \boldsymbol{u}$ are well-defined. Proceeding as in the proof of [49, Lemma 5.38], we see that the remaining DOFs are well-defined since $\boldsymbol{u} \in H^{1/2+\delta}(\Omega) \otimes \mathbb{V}$ and $\operatorname{curl} \boldsymbol{u} \in H^{3/2+\delta}(\Omega) \otimes \mathbb{V} \hookrightarrow C^{0,\delta}(\Omega) \otimes \mathbb{V} \subset L^p(\Omega) \otimes \mathbb{V}$ with $p > 2$. □

Lemma 7.2.3. *The DOFs for* $V_h^{r-1,k+1}(K)$ *are unisolvent.*

Proof. Since the complex (7.1.4) is exact, we have

$$\dim V_h^{r-1,k+1}(K) = \dim \boldsymbol{\Sigma}_h^{k,+}(K) + \dim \Sigma_h^r(K) - \dim W_h^{k-1}(K) - 1. \tag{7.2.13}$$

We can check that the DOF set has the same dimension. Then it suffices to show that if all the DOFs vanish on $u \in V_h^{r-1,k+1}(K)$, then $\boldsymbol{u} = 0$. To see this, we first show that $\operatorname{curl} \boldsymbol{u} = 0$. Using the properties of the Poincaré operators, we have $\operatorname{curl} V_h^{r-1,k+1}(K) \subset \boldsymbol{\Sigma}_h^{k,+}(K)$. By integration by parts, the following DOFs for $\boldsymbol{\Sigma}_h^{k,+}(K)$ vanish on $\operatorname{curl} \boldsymbol{u}$:

$$\int_{f_i} \operatorname{curl} \boldsymbol{u} \cdot \boldsymbol{n}_i \mathrm{d}A = \int_{\partial f_i} \boldsymbol{u} \cdot \boldsymbol{\tau}_{\partial f_i} \mathrm{d}s = 0,$$

and

$$\int_K \operatorname{curl} \boldsymbol{u} \cdot \operatorname{grad} v \mathrm{d}V = \int_{\partial K} \operatorname{curl} \boldsymbol{u} \cdot \boldsymbol{n}_{\partial K} v \mathrm{d}A = 0 \text{ for any } v \in P_{k-1}(K).$$

By the unisolvence of the DOFs for $\boldsymbol{\Sigma}_h^{k,+}(K)$, we get $\operatorname{curl} \boldsymbol{u} = 0$ in K.

Therefore on each f_i, there exists a $\phi_i \in P_r(f_i)$ such that $\boldsymbol{n}_i \times \boldsymbol{u}|_{f_i} \times \boldsymbol{n}_i = \operatorname{grad}_{f_i} \phi_i$. Here $\operatorname{grad}_{f_i}$ is the face gradient on f_i. By the edge DOFs of $V_h^{r-1,k+1}(K)$, we get $\boldsymbol{u} \cdot \boldsymbol{\tau}_i = 0$ on the edge $\boldsymbol{e}_i$. Therefore ϕ_i is a constant on all the edges of f_i. Without loss of generality, we can choose this constant to be zero. Then ϕ_i has the form $\phi_i = B_i|_{f_i}\psi_i$ with $\psi_i \in P_{r-3}(f_i)$. By the property of Koszul operators in 2D (see Chapter 2), for any function $\psi_i \in P_{r-3}(f_i)$, there exists $\boldsymbol{q}_i \in P_{r-3}(f_i) B_K \hat{\boldsymbol{x}}_{\hat{f}_i}$ satisfying $\boldsymbol{q}_i \perp \boldsymbol{n}_i$ and $\operatorname{div}_{f_i} \boldsymbol{q}_i = \psi_i$. By the DOFs in (7.2.7), we have

$$0 = (\boldsymbol{u}, \boldsymbol{q}_i)_{f_i} = -(\phi_i, \operatorname{div}_{f_i} \boldsymbol{q}_i)_{f_i} = -\left(B_i|_{f_i}\psi_i, \psi_i\right)_{f_i}.$$

This implies that $\psi_i = 0$, i.e., $\boldsymbol{u} \times \boldsymbol{n}_i = 0$ on f_i.

Therefore, there exists $\psi \in P_{r-4}(K)$ such that $\phi = B_0\psi$. We choose $\boldsymbol{q} \in P_{r-4}(K) B_K \hat{\boldsymbol{x}}$ such that $\operatorname{div} \boldsymbol{q} = \psi$. Then

$$0 = (\boldsymbol{u}, \boldsymbol{q}) = (\operatorname{grad} \phi, \boldsymbol{q}) = -\left(\phi, \operatorname{div} \boldsymbol{q}\right) = -\left(B_0\psi, \psi\right).$$

This implies that $\psi = 0$ and hence $\phi = 0$ and $\boldsymbol{u} = 0$.

□

For $\delta > 0$ and $D \subset \Omega$, denote $\Sigma(D) = H^{3/2+\delta}(D)$ and $V(D) = \{\boldsymbol{u} \in H^{1/2+\delta}(D) \otimes \mathbb{V} : \operatorname{curl} \boldsymbol{u} \in H^{3/2+\delta}(D) \otimes \mathbb{V}\}$.

For $u \in \Sigma(K)$, we can define an H^1 interpolation operator $\pi_K : H^{3/2+\delta}(K) \to \Sigma_h^r(K)$ by the DOFs for $\Sigma_h^r(K)$. We use $\widetilde{\boldsymbol{\pi}}_K$ to denote the interpolation operator to $\boldsymbol{\Sigma}_K^{k,+}$. Provided $\boldsymbol{u} \in V(K)$ (see Lemma 7.2.2), we can define an $H(\operatorname{grad}\operatorname{curl})$ interpolation operator $\Pi_K : V(K) \to V_h^{r-1,k+1}(K)$ by the DOFs for $V_h^{r-1,k+1}(K)$. We denote the interpolation defined by the DOFs for $W_h^{k-1}(K)$ as r_K.

7.3 Global Finite Element Complexes

7.3.1 Complexes without Boundary Conditions

Equipping the local spaces with the above DOFs, we obtain the global finite element spaces Σ_h^r, $V_h^{r-1,k+1}$, $\boldsymbol{\Sigma}_h^{k,+}$, and W_h^{k-1} in the complex (7.0.1).

Lemma 7.3.1. *The following conformity holds:*

$$V_h^{r-1,k+1} \subset H(\operatorname{grad}\operatorname{curl};\Omega).$$

Proof. To prove the conformity, we must show $\boldsymbol{u}\times\boldsymbol{n}_i = 0$ and $\operatorname{curl}\boldsymbol{u} = 0$ for all $f_i \in \mathcal{F}_h(K)$ if the DOFs (7.2.5) – (7.2.7) vanish on $\boldsymbol{u}\in V_h^{r-1,k+1}(K)$. By integration by parts,

$$\int_{f_i}\operatorname{curl}\boldsymbol{u}\cdot\boldsymbol{n}_i\mathrm{d}A = \int_{\partial f_i}\boldsymbol{u}\cdot\boldsymbol{\tau}_{\partial f_i}\mathrm{d}s = 0,$$

which together with vanishing DOFs involving $\operatorname{curl}\boldsymbol{u}$ leads to $\operatorname{curl}\boldsymbol{u} = 0$ on ∂K. Proceeding as in the proof of Lemma 7.2.3, we can show that $\boldsymbol{u}\times\boldsymbol{n}_i = 0$ on each f_i. □

We now present properties of the complex (7.0.1) with the global finite element spaces. The first property we will show is the surjectivity of $\operatorname{div}:\boldsymbol{\Sigma}_h^{k,+}\to W_h^{k-1}$. To this end, we need the following property for the local complex.

Lemma 7.3.2. *For any $q\in W_h^{k-1}(K)\cap L_0^2(K)$, there exists $\boldsymbol{v}\in\boldsymbol{\Sigma}_h^{k,+}(K)\cap H_0^1(K)\otimes\mathbb{V}$ such that $\operatorname{div}\boldsymbol{v} = q$ and $\|\boldsymbol{v}\|_{1,K}\le C\|q\|_K$.*

Proof. For a fixed $q\in W_h^{k-1}(K)\cap L_0^2(K)$, there exists $\boldsymbol{w}\in H_0^1(K)\otimes\mathbb{V}$ such that (see e.g., [30, Corollary 2.4])

$$\operatorname{div}\boldsymbol{w} = q \text{ in } \Omega.$$

Let $\boldsymbol{v}\in\boldsymbol{\Sigma}_h^{k,+}(K)$ be the unique function that satisfies

$$\int_K \boldsymbol{v}\cdot\operatorname{grad}p\mathrm{d}V = \int_K \boldsymbol{w}\cdot\operatorname{grad}p\mathrm{d}V,\ \forall p\in P_{k-1}(K),$$

with the remaining DOFs in (7.2.9) – (7.2.12) vanishing on $\boldsymbol{v}$. Then $\boldsymbol{v} \in \boldsymbol{\Sigma}_h^{k,+}(K) \cap H_0^1(K) \otimes \mathbb{V}$. Moreover, integrating by parts, we have

$$(\operatorname{div} \boldsymbol{v}, p) = (\boldsymbol{v}, \operatorname{grad} p) = (\boldsymbol{w}, \operatorname{grad} p) = (\operatorname{div} \boldsymbol{w}, p) = (q, p), \ \forall p \in P_{k-1}(K)/\mathbb{R},$$
$$(\operatorname{div} \boldsymbol{v}, 1) = \langle \boldsymbol{v} \cdot \boldsymbol{n}, 1 \rangle = 0 = (q, 1).$$

This implies $\operatorname{div} \boldsymbol{v} - q = 0$ since $\operatorname{div} \boldsymbol{v} - q \in P_{k-1}(K)$.

We now prove $\|\boldsymbol{v}\|_{1,K} \leq C\|q\|_K$ by a scaling argument. Denote

$$n_{k-1} = \dim P_{k-1}(K),$$

we can express $\boldsymbol{v}$ as

$$\boldsymbol{v} = \sum_{i=2}^{n_{k-1}} (\boldsymbol{w}, \operatorname{grad} p_i) \boldsymbol{N}_i,$$

where $\{p_i\}_{i=2}^{n_{k-1}}$ is a set of basis functions of $P_{k-1}(K)/\mathbb{R}$ and $\boldsymbol{N}_i$ is the dual basis of p_i with respect to the DOFs $(\boldsymbol{w}, \operatorname{grad} p_i)$, i.e., $(\boldsymbol{N}_i, \operatorname{grad} q_j) = \delta_{ij}$. Setting $\hat{\boldsymbol{v}} = \det(B_K) B_K^{-1} \boldsymbol{v} \circ F_K$ and $\hat{p} = p \circ F_K$ with B_K and F_K defined in (1.5.1), we obtain

$$\|\boldsymbol{v}\|_{1,K}^2 \leq C h_K^{-3} \|\hat{\boldsymbol{v}}\|_{1,\hat{K}}^2 \leq C h_K^{-3} \sup_{2 \leq i \leq n_{k-1}} |(\hat{\boldsymbol{w}}, \operatorname{grad}_{\hat{\boldsymbol{x}}} \hat{p}_i)|^2$$
$$= C h_K^{-3} \sup_{2 \leq i \leq n_{k-1}} |(\operatorname{div}_{\hat{\boldsymbol{x}}} \hat{\boldsymbol{w}}, \hat{p}_i)|^2 \leq C h_K^{-3} \| \operatorname{div}_{\hat{\boldsymbol{x}}} \hat{\boldsymbol{w}} \|_{\hat{K}}^2 \leq C \|\operatorname{div} \boldsymbol{w}\|_K^2 = C\|q\|_K^2.$$

□

Lemma 7.3.3. *For any* $q \in W_h^{k-1}$, *there exists* $\boldsymbol{v} \in \boldsymbol{\Sigma}_h^{k,+}$ *such that* $\operatorname{div} \boldsymbol{v} = q$ *and* $\|\boldsymbol{v}\|_1 \leq C\|q\|$.

Proof. Given $q \in W_h^{k-1} \subset L^2(\Omega)$, according to [12, Theorem 2], there exists $\boldsymbol{w} \in H^1(\Omega) \otimes \mathbb{V}$ satisfying $\operatorname{div} \boldsymbol{w} = q$ and $\|\boldsymbol{w}\|_1 \leq C\|q\|$. Let $\boldsymbol{I}_h \boldsymbol{w} \in \Sigma_h^k \otimes \mathbb{V} \subset \boldsymbol{\Sigma}_h^{k,+}$ denote the Scott-Zhang interpolation of $\boldsymbol{w}$ (see [59, (2.13)] for its definition). We also let $\boldsymbol{v}_1 \in \boldsymbol{\Sigma}_h^{k,+}$ be the unique function that satisfies

$$\int_{f_i} \boldsymbol{v}_1 \cdot \boldsymbol{n}_i \mathrm{d}A = \int_{f_i} (\boldsymbol{w} - \boldsymbol{I}_h \boldsymbol{w}) \cdot \boldsymbol{n}_i \mathrm{d}A, \ \forall f_i \in \mathcal{F}_h,$$

with other DOFs in (7.2.9) – (7.2.12) vanishing on $\boldsymbol{v}_1$. Then we have, for any $K \in \mathcal{T}_h$,

$$(\operatorname{div} \boldsymbol{v}_1 + \operatorname{div} \boldsymbol{I}_h \boldsymbol{w}, 1)_K = \langle \boldsymbol{v}_1 \cdot \boldsymbol{n} + \boldsymbol{I}_h \boldsymbol{w} \cdot \boldsymbol{n}, 1\rangle_{\partial K} = \langle \boldsymbol{w} \cdot \boldsymbol{n}, 1\rangle_{\partial K} = (\operatorname{div} \boldsymbol{w}, 1)_K = (q, 1)_K,$$

which means $(q - \operatorname{div} \boldsymbol{v}_1 - \operatorname{div} \boldsymbol{I}_h \boldsymbol{w})|_K \in W_h^{k-1}(K) \cap L_0^2(K)$. By Lemma 7.3.2, there exists $\boldsymbol{v}_{2,K} \in \boldsymbol{\Sigma}_h^{k,+}(K) \cap H_0^1(K) \otimes \mathbb{V}$ such that

$$\operatorname{div} \boldsymbol{v}_{2,K} = (q - \operatorname{div} \boldsymbol{v}_1 - \operatorname{div} \boldsymbol{I}_h \boldsymbol{w})|_K, \ \forall K \in \mathcal{T}_h$$

and

$$\|\boldsymbol{v}_{2,K}\|_{1,K} \leq C(\|\boldsymbol{v}_1\|_{1,K} + \|\boldsymbol{I}_h \boldsymbol{w}\|_{1,K} + \|q\|_K).$$

Define $\boldsymbol{v}_2 \in H_0^1(\Omega) \otimes \mathbb{V} \cap \boldsymbol{\Sigma}_h^{k,+}$ by $\boldsymbol{v}_2|_K = \boldsymbol{v}_{2,K}$. Setting $\boldsymbol{v} = \boldsymbol{v}_1 + \boldsymbol{v}_2 + \boldsymbol{I}_h \boldsymbol{w}$, we have

$$\operatorname{div} \boldsymbol{v} = \operatorname{div}(\boldsymbol{v}_1 + \boldsymbol{v}_2 + \boldsymbol{I}_h \boldsymbol{w}) = q \text{ and } \|\boldsymbol{v}\|_1 \leq C(\|\boldsymbol{v}_1\|_1 + \|\boldsymbol{I}_h \boldsymbol{w}\|_1 + \|q\|).$$

We apply the same scaling argument as used in Lemma 7.3.2 and the approximation property of the Scott-Zhang interpolation $\boldsymbol{I}_h \boldsymbol{w}$ [59, (4.1)] to obtain

$$\begin{aligned}\|\boldsymbol{v}_1\|_{1,K}^2 \leq & C h_K^{-3} \|\hat{\boldsymbol{v}}_1\|_{1,\hat{K}}^2 \leq C h_K^{-3} \left|\langle (\boldsymbol{w} - \boldsymbol{I}_h \boldsymbol{w}) \cdot \boldsymbol{n}_i, 1\rangle_{\partial K}\right|^2 \leq C h_K^{-1} \|\boldsymbol{w} - \boldsymbol{I}_h \boldsymbol{w}\|_{\partial K}^2 \\ & \leq C \left(h_K^{-2} \|\boldsymbol{w} - \boldsymbol{I}_h \boldsymbol{w}\|_K^2 + \|\boldsymbol{w} - \boldsymbol{I}_h \boldsymbol{w}\|_{1,K}^2\right) \leq C \|\boldsymbol{w}\|_{1,\omega(K)}^2\end{aligned}$$

with $\omega(K) = \operatorname{Int}\left\{\overline{K}_i | \overline{K}_i \cap \overline{K} \neq \emptyset, K_i \in \mathcal{T}_h\right\}$. Summing over $K \in \mathcal{T}_h$, we obtain

$$\|\boldsymbol{v}_1\|_1 \leq C \|\boldsymbol{w}\|_1,$$

which together with $\|\boldsymbol{I}_h \boldsymbol{w}\|_1 \leq C \|\boldsymbol{w}\|_1$ [59, (4.5)] and $\|\boldsymbol{w}\|_1 \leq C \|q\|$ leads to

$$\|\boldsymbol{v}\|_1 \leq C \|q\|.$$

□

Corollary 7.3.4. *The inf-sup condition for the Stokes problem holds, i.e., there exists a positive constant $\alpha > 0$ not depending on h, such that*

$$\sup_{0 \neq \boldsymbol{v} \in \boldsymbol{\Sigma}_h^{k,+}} \frac{(\operatorname{div} \boldsymbol{v}, q)}{\|\boldsymbol{v}\|_1} \geq \alpha \|q\|, \ \forall q \in W_h^{k-1}.$$

Corollary 7.3.4 implies that $\boldsymbol{\Sigma}_h^{k,+} - W_h^{k-1}$ leads to convergent algorithms for solving the Stokes problem with a precise divergence-free condition.

Theorem 7.3.5. *The complex* (7.0.1) *is exact on contractible domains.*

Proof. The exactness at Σ_h^r and $V_h^{r-1,k+1}$ follows from the exactness of the standard finite element differential forms (e.g., [49]). The exactness at W_h^{k-1}, i.e., the surjectivity of div : $\boldsymbol{\Sigma}_h^{k,+} \to W_h^{k-1}$ is verified in Lemma 7.3.3.

Finally, the the exactness at $\boldsymbol{\Sigma}_h^{k,+}$ follows from a dimension count. Let $\mathcal{V}$, $\mathcal{E}$, $\mathcal{F}$, and $\mathcal{K}$ denote the number of vertices, edges, faces, and 3D cells, respectively. Then we have

$$\dim \Sigma_h^r = \mathcal{V} + (r-1)\mathcal{E} + \frac{1}{2}(r-2)(r-1)\mathcal{F} + \frac{1}{6}(r-3)(r-2)(r-1)\mathcal{K},$$

$$\dim W_h^{k-1} = \frac{k(k+1)(k+2)}{6}\mathcal{K}.$$

From the DOFs (7.2.5) – (7.2.8),

$$\begin{aligned}\dim V_h^{r-1,k+1} - \dim \boldsymbol{\Sigma}_h^{+,k} &= r\mathcal{E} + \frac{1}{2}(r-2)(r-1)\mathcal{F} \\ &- \mathcal{F} + \frac{1}{6}\big[(r-3)(r-2)(r-1) - k(k+1)(k+2) + 6\big]\mathcal{K}.\end{aligned}$$

From the above dimension count, we have

$$-1 + \dim \Sigma_h^r - \dim V_h^{r-1,k+1} + \dim \boldsymbol{\Sigma}_h^{k,+} - \dim W_h^{k-1} = 0,$$

where we have used Euler's formula $\mathcal{V} - \mathcal{E} + \mathcal{F} - \mathcal{K} = 1$. This completes the proof. □

To ease the notation, we drop Ω in $\Sigma(\Omega)$ and $V(\Omega)$, and denote $\boldsymbol{\Sigma} = \Sigma \otimes \mathbb{V}$. We define four global interpolations $\pi_h : \Sigma \to \Sigma_h^r$, $\widetilde{\boldsymbol{\pi}}_h : \boldsymbol{\Sigma} \to \boldsymbol{\Sigma}_h^{k,+}$, $\Pi_h : V \to V_h^{r-1,k+1}$, and $r_h : L^2(\Omega) \to W_h^{k-1}$ in the following way:

$$(\pi_h u)|_K = \pi_K u,\ (\widetilde{\boldsymbol{\pi}}_h \boldsymbol{u})|_K = \widetilde{\boldsymbol{\pi}}_K \boldsymbol{u}, (\Pi_h \boldsymbol{u})|_K = \Pi_K \boldsymbol{u},\ \text{and}\ (r_h u)|_K = r_K u.$$

The interpolations π_K, $\widetilde{\boldsymbol{\pi}}_K$, Π_K, r_K are defined in Section 7.2.

We summarize the interpolations in the following diagram:

$$
\begin{array}{ccccccccccc}
\mathbb{R} & \xrightarrow{\subset} & H^1(\Omega) & \xrightarrow{\text{grad}} & H(\operatorname{grad}\operatorname{curl};\Omega) & \xrightarrow{\text{curl}} & H^1(\Omega)\otimes\mathbb{V} & \xrightarrow{\text{div}} & L^2(\Omega) & \longrightarrow & 0 \\
 & & \big\downarrow & & \big\downarrow & & \big\downarrow & & \big\downarrow & & \\
\mathbb{R} & \xrightarrow{\subset} & \Sigma & \xrightarrow{\text{grad}} & V & \xrightarrow{\text{curl}} & \boldsymbol{\Sigma} & \xrightarrow{\text{div}} & L^2(\Omega) & \longrightarrow & 0 \\
 & & \big\downarrow \pi_h & & \big\downarrow \Pi_h & & \big\downarrow \widetilde{\boldsymbol{\pi}}_h & & \big\downarrow r_h & & \\
\mathbb{R} & \xrightarrow{\subset} & \Sigma_h^r & \xrightarrow{\text{grad}} & V_h^{r-1,k+1} & \xrightarrow{\text{curl}} & \boldsymbol{\Sigma}_h^{+,k} & \xrightarrow{\text{div}} & W_h^{k-1} & \longrightarrow & 0.
\end{array}
\tag{7.3.1}
$$

By a similar argument as Lemma 5.3.3, the interpolations in (7.3.1) commute with the differential operators.

Lemma 7.3.6. *The last two rows of the complex* (7.3.1) *are a commuting diagram, i.e.,*

$$\operatorname{grad}\pi_h u = \Pi_h \operatorname{grad} u \text{ for all } u \in \Sigma, \tag{7.3.2}$$

$$\operatorname{curl}\Pi_h \boldsymbol{u} = \widetilde{\boldsymbol{\pi}}_h \operatorname{curl}\boldsymbol{u} \text{ for all } \boldsymbol{u} \in V, \tag{7.3.3}$$

$$\operatorname{div}\widetilde{\boldsymbol{\pi}}_h \boldsymbol{u} = r_h \operatorname{div}\boldsymbol{u} \text{ for all } \boldsymbol{u} \in \boldsymbol{\Sigma}. \tag{7.3.4}$$

We adopt the Piola mapping (5.1.7) to transform the finite element function $\boldsymbol{u}$ on a general element K to a function $\hat{\boldsymbol{u}}$ on the reference element $\hat{K}$.

Lemma 7.3.7 ([49, 2])**.** *Suppose that $\boldsymbol{v}$ and $\hat{\boldsymbol{v}}$ are related by the transformation* (5.1.7)*. Then for any $s \geq 0$, we have*

$$
\begin{aligned}
|\hat{\boldsymbol{v}}|_{s,\hat{K}} &\leq Ch_K^{s-1/2}\|\boldsymbol{v}\|_{s,K}, \\
\left|\operatorname{curl}_{\hat{\boldsymbol{x}}}\hat{\boldsymbol{v}}\right|_{s,\hat{K}} &\leq Ch_K^{s+1/2}\|\operatorname{curl}\boldsymbol{v}\|_{s,K}.
\end{aligned}
$$

The following lemma relates the interpolation on K to that on $\hat{K}$.

Lemma 7.3.8. *For $\boldsymbol{u} \in V$, we have $\widehat{\Pi_K \boldsymbol{u}} = \Pi_{\hat{K}}\hat{\boldsymbol{u}}$ with the transformation* (5.1.7)*.*

Proof. As in the proof of Lemma 5.3.4, we show the DOFs in (7.2.5) – (7.2.8) are linear combinations of those for defining $\Pi_{\hat{K}}\hat{\boldsymbol{u}}$.

By the transformations (5.1.7), (6.1.7), (1.5.2), and (1.5.3), we have that all the DOFs in (7.2.5) – (7.2.8) are linear combinations of those for $\hat{\boldsymbol{u}}$ on $\hat{K}$. For instance,

$$\begin{aligned}
&\int_{f_i} \operatorname{curl} \boldsymbol{u} \cdot \boldsymbol{\tau}_i^1 \mathrm{d}A = \frac{|f_i|}{\det(B_K)|\hat{f}_i|} \int_{\hat{f}_i} \operatorname{curl}_{\hat{\boldsymbol{x}}} \hat{\boldsymbol{u}} \cdot \boldsymbol{B}_K^{\mathrm{T}} \boldsymbol{\tau}_i^1 \mathrm{d}\hat{A} \\
=&\frac{|f_i|}{\det(B_K)|\hat{f}_i|} \int_{\hat{f}_i} \operatorname{curl}_{\hat{\boldsymbol{x}}} \hat{\boldsymbol{u}} \cdot \left((\boldsymbol{B}_K^{\mathrm{T}} \boldsymbol{\tau}_i^1 \cdot \hat{\boldsymbol{\tau}}_i^1) \hat{\boldsymbol{\tau}}_i^1 + (\boldsymbol{B}_K^{\mathrm{T}} \boldsymbol{\tau}_i^1 \cdot \hat{\boldsymbol{\tau}}_i^2) \hat{\boldsymbol{\tau}}_i^2 + (\boldsymbol{B}_K^{\mathrm{T}} \boldsymbol{\tau}_i^1 \cdot \hat{\boldsymbol{n}}_i) \hat{\boldsymbol{n}}_i \right) \mathrm{d}\hat{A} \\
=&\frac{|f_i|}{\det(B_K)|\hat{f}_i|} \int_{\hat{f}_i} \operatorname{curl}_{\hat{\boldsymbol{x}}} \hat{\boldsymbol{u}} \cdot \left((\boldsymbol{B}_K^{\mathrm{T}} \boldsymbol{\tau}_i^1 \cdot \hat{\boldsymbol{\tau}}_i^1) \hat{\boldsymbol{\tau}}_i^1 + (\boldsymbol{B}_K^{\mathrm{T}} \boldsymbol{\tau}_i^1 \cdot \hat{\boldsymbol{\tau}}_i^2) \hat{\boldsymbol{\tau}}_i^2 \right) \mathrm{d}\hat{A} \\
&+ \frac{|f_i| (\boldsymbol{B}_K^{\mathrm{T}} \boldsymbol{\tau}_i^1 \cdot \hat{\boldsymbol{n}}_i)}{|\hat{f}_i| \det(B_K)} \int_{\partial \hat{f}_i} \hat{\boldsymbol{u}} \cdot \hat{\boldsymbol{\tau}}_{\partial f_i} \mathrm{d}\hat{s},
\end{aligned}$$

where $|f_i| = \operatorname{area}(f_i)$. □

Next, we establish the approximation property of the interpolation operators.

Theorem 7.3.9. *Assume that* $\boldsymbol{u} \in H^{s+(r-k-1)}(\Omega) \otimes \mathbb{V}$ *and* $\operatorname{curl} \boldsymbol{u} \in H^s(\Omega) \otimes \mathbb{V}$, $s \geq 3/2 + \delta$ *with* $\delta > 0$. *Then we have the following error estimates for the interpolation* Π_h,

$$\|\boldsymbol{u} - \Pi_h \boldsymbol{u}\| \leq C h^{\min\{s+(r-k-1), r\}} (\|\boldsymbol{u}\|_{s+(r-k-1)} + \|\operatorname{curl} \boldsymbol{u}\|_s), \tag{7.3.5}$$

$$\|\operatorname{curl}(\boldsymbol{u} - \Pi_h \boldsymbol{u})\| \leq C h^{\min\{s, k+1\}} \|\operatorname{curl} \boldsymbol{u}\|_s, \tag{7.3.6}$$

$$|\operatorname{curl}(\boldsymbol{u} - \Pi_h \boldsymbol{u})|_1 \leq C h^{\min\{s-1, k\}} \|\operatorname{curl} \boldsymbol{u}\|_s. \tag{7.3.7}$$

Proof. With the identity $\widehat{\Pi_K \boldsymbol{u}} = \Pi_{\hat{K}} \hat{\boldsymbol{u}}$ and the inclusion $\boldsymbol{P}_{r-1}(\hat{K}) \subseteq \hat{V}_h^{r-1,k+1}(\hat{K})$ (Lemma 7.3.8 and Lemma 7.1.5), the estimate (7.3.5) can be obtained by following the proof of Theorem 5.3.6. To prove (7.3.6) and (7.3.7), we apply Lemma 7.3.6 and the approximation property of the Lagrange interpolation. □

7.3.2 Complexes with Homogeneous Boundary Conditions

We define the following finite element spaces with vanishing boundary conditions

$$\mathring{\Sigma}_h^r = \{v_h \in \Sigma_h^r : \ v_h = 0 \text{ on } \partial\Omega\},$$

$$\mathring{\boldsymbol{\Sigma}}_h^{k,+} = \{\boldsymbol{v}_h \in \boldsymbol{\Sigma}_h^{k,+} : \ \boldsymbol{v}_h = 0 \text{ on } \partial\Omega\},$$

$$\mathring{W}_h^{k-1} = \{v_h \in W_h^{k-1} : \ \int_\Omega v_h \mathrm{d}V = 0\},$$

$$\mathring{V}_h^{r-1,k+1} = \{\boldsymbol{v}_h \in V_h^{r-1,k+1} : \ \boldsymbol{n} \times \boldsymbol{v}_h = 0 \text{ and } \operatorname{curl} \boldsymbol{v}_h = 0 \text{ on } \partial\Omega\}.$$

We can impose the above vanishing boundary conditions by setting all the boundary DOFs for the spaces $\mathring{\Sigma}_h^r$, $\mathring{\boldsymbol{\Sigma}}_h^{k,+}$, and $\mathring{V}_h^{r-1,k+1}$ to be 0. These finite element spaces form a complex:

$$0 \xrightarrow{\subset} \mathring{\Sigma}_h^r \xrightarrow{\text{grad}} \mathring{V}_h^{r-1,k+1} \xrightarrow{\text{curl}} \mathring{\boldsymbol{\Sigma}}_h^{k,+} \xrightarrow{\text{div}} \mathring{W}_h^{k-1} \longrightarrow 0, \tag{7.3.8}$$

We can show the exactness of (7.3.8).

Lemma 7.3.10. *The discrete complex* (7.3.8) *is exact.*

Proof. The exactness at $\mathring{\Sigma}_h^r$ and $\mathring{W}_h^{k-1}$ is similar to Theorem 7.3.5. We only verify the dimension condition to show the exactness of (7.3.8).

Let $\mathcal{V}_\partial$, $\mathcal{E}_\partial$, $\mathcal{F}_\partial$ be the number of vertices, edges, and faces on the boundary, respectively. We have the following dimension count:

$$\begin{aligned}
\dim \mathring{\Sigma}_h^r &= \dim \Sigma_h^r - \mathcal{V}_\partial - (r-1)\mathcal{E}_\partial - \frac{(r-2)(r-1)}{2}\mathcal{F}_\partial,\\
\dim \mathring{\boldsymbol{\Sigma}}_h^{k,+} &= \dim \boldsymbol{\Sigma}_h^{k,+} - 3\mathcal{V}_\partial - 3(k-1)\mathcal{E}_\partial - \frac{3(k-2)(k-1)}{2}\mathcal{F}_\partial,\\
\dim \mathring{V}_h^{r-1,k+1} &= \dim V_h^{r-1,k+1} - 3\mathcal{V}_\partial - (r+3k-3)\mathcal{E}_\partial\\
&\quad - \frac{(r-2)(r-1)+3(k-2)(k-1)-2}{2}\mathcal{F}_\partial,\\
\dim \mathring{W}_h^{k-1} &= \dim W_h^{k-1} - 1.
\end{aligned}$$

Therefore, we have

$$\begin{aligned}
&\dim \mathring{\Sigma}_h^r - \dim \mathring{V}_h^{r-1,k+1} + \dim \mathring{\boldsymbol{\Sigma}}_h^{k,+} - \dim \mathring{W}_h^{k-1}\\
=& \dim \Sigma_h^r - \dim V_h^{r-1,k+1} + \dim \boldsymbol{\Sigma}_h^{k,+} - \dim W_h^{k-1} - \mathcal{V}_\partial + \mathcal{E}_\partial - \mathcal{F}_\partial + 1 = 0,
\end{aligned}$$

where we have used the relation $-\mathcal{V}_\partial + \mathcal{E}_\partial - \mathcal{F}_\partial = -2$. This shows the dimension condition of exactness. ∎

7.4 Applications to $-\operatorname{curl}\Delta\operatorname{curl}$ Problems

In this section, we use the three grad curl-conforming finite element families to solve a problem with the curl Δ curl operator: for $\boldsymbol{f} \in H(\operatorname{div}^0;\Omega)$, find $\boldsymbol{u}$, such that

$$
\begin{aligned}
-\operatorname{curl}\Delta\operatorname{curl}\boldsymbol{u} + \boldsymbol{u} = \boldsymbol{f} \quad & \text{in } \Omega,\\
\operatorname{div}\boldsymbol{u} = 0 \quad & \text{in } \Omega,\\
\boldsymbol{u}\times\boldsymbol{n} = 0 \quad & \text{on } \partial\Omega,\\
\operatorname{curl}\boldsymbol{u} = 0 \quad & \text{on } \partial\Omega.
\end{aligned}
\tag{7.4.1}
$$

Here $H(\operatorname{div}^0;\Omega)$ is defined in Section 5.4. Taking divergence on both sides of the first equation of (7.4.1), we see that $\operatorname{div}\boldsymbol{u} = 0$ automatically holds with $\boldsymbol{f} \in H(\operatorname{div}^0;\Omega)$.

The variational formulation reads: find $\boldsymbol{u} \in H_0(\operatorname{grad}\operatorname{curl};\Omega)$, such that

$$
a(\boldsymbol{u},\boldsymbol{v}) = (\boldsymbol{f},\boldsymbol{v}) \quad \forall \boldsymbol{v} \in H_0(\operatorname{grad}\operatorname{curl};\Omega), \tag{7.4.2}
$$

with $a(\boldsymbol{u},\boldsymbol{v}) := (\operatorname{grad}\operatorname{curl}\boldsymbol{u}, \operatorname{grad}\operatorname{curl}\boldsymbol{v}) + (\boldsymbol{u},\boldsymbol{v})$. The weak form (7.4.2) can be regarded as a higher-order model problem in either MHD, e.g., [19, (1)] or continuum mechanics with size effects, e.g., [48, (3.27)], [54, (35)].

Remark 7.4.1. The problem (7.4.2) is closely related to the Hodge Laplacian (3.1.11).

Remark 7.4.2. With the given boundary conditions and the identity for vector Laplacian $-\Delta\boldsymbol{u} = -\operatorname{grad}\operatorname{div}\boldsymbol{u} + \operatorname{curl}\operatorname{curl}\boldsymbol{u}$, the above weak form is equivalent to the quad-curl problem, i.e., $(\operatorname{grad}\operatorname{curl}\boldsymbol{u}, \operatorname{grad}\operatorname{curl}\boldsymbol{v}) = (\operatorname{curl}\operatorname{curl}\boldsymbol{u}, \operatorname{curl}\operatorname{curl}\boldsymbol{v})$.

Theorem 7.4.1. *We assume that Ω is a simply-connected Lipschitz polyhedral domain with a connected boundary. There exists a constant $\alpha > 1/2$ such that the solution $\boldsymbol{u}$ of* (7.4.1) *satisfies*

$$
\boldsymbol{u} \in H^{\alpha}(\Omega)\otimes\mathbb{V}, \ \operatorname{curl}\boldsymbol{u} \in H^{1+\alpha}(\Omega)\otimes\mathbb{V},
$$

and it holds

$$\|\boldsymbol{u}\|_\alpha + \|\operatorname{curl}\boldsymbol{u}\|_{1+\alpha} \le C\|\boldsymbol{f}\|.$$

Proof. The result will follow from the proof of Theorem 4.2.1 if $\Delta\operatorname{curl}\boldsymbol{u}$ belongs to $L^2(\Omega)\otimes\mathbb{V}$ and $\|\Delta\operatorname{curl}\boldsymbol{u}\| \le C\|\boldsymbol{f}\|$. It suffices to show that $\operatorname{curl}^3\boldsymbol{u} \in L^2(\Omega)\otimes\mathbb{V}$ and $\|\operatorname{curl}^3\boldsymbol{u}\| \le C\|\boldsymbol{f}\|$ since $-\Delta\operatorname{curl}\boldsymbol{u} = -\operatorname{grad}\operatorname{div}\operatorname{curl}\boldsymbol{u} + \operatorname{curl}^3\boldsymbol{u} = \operatorname{curl}^3\boldsymbol{u}$. If we can prove

$$g(\boldsymbol{v}) := (\operatorname{curl}\operatorname{curl}\boldsymbol{u}, \operatorname{curl}\boldsymbol{v}) \le C_0\|\boldsymbol{v}\|, \text{ for all } \boldsymbol{v} \in H_0(\operatorname{curl};\Omega), \tag{7.4.3}$$

then, by Hahn Banach theorem, there is a unique extension of the map $g(\boldsymbol{v})$ for $\boldsymbol{v} \in H_0(\operatorname{curl};\Omega)$ to a bounded linear functional from all of $L^2(\Omega)\otimes\mathbb{V}$ to $\mathbb{R}$ with the bound C_0. Moreover, by Riesz representation theorem, there exists a unique function $\boldsymbol{\phi} \in L^2(\Omega)\otimes\mathbb{V}$ such that

$$g(\boldsymbol{v}) = (\operatorname{curl}\operatorname{curl}\boldsymbol{u}, \operatorname{curl}\boldsymbol{v}) = (\boldsymbol{\phi}, \boldsymbol{v}), \text{ for } \boldsymbol{v} \in H_0(\operatorname{curl};\Omega).$$

From the definition of the adjoint of curl operator, we have $\operatorname{curl}^3\boldsymbol{u} = \boldsymbol{\phi} \in L^2(\Omega)\otimes\mathbb{V}$ and $\|\boldsymbol{\phi}\| = \|g\|_{\mathcal{L}(L^2(\Omega)\otimes\mathbb{V},\mathbb{R})} \le C_0$.

To prove (7.4.3), we first seek $q \in H_0^1(\Omega)$ such that

$$-\Delta q = \operatorname{div}\boldsymbol{v} \in H^{-1}(\Omega).$$

Then it holds $\|\operatorname{grad} q\| \le \|\boldsymbol{v}\|$. Applying [30, Theorem 3.6] to $\boldsymbol{v} - \operatorname{grad} q$, there exists a divergence-free vector potential $\boldsymbol{w} \in H_0(\operatorname{curl};\Omega)$ satisfying

$$\boldsymbol{v} - \operatorname{grad} q = \operatorname{curl}\boldsymbol{w} \quad \text{and} \quad \langle \boldsymbol{w}\cdot\boldsymbol{n}, 1\rangle_{\partial\Omega} = 0. \tag{7.4.4}$$

Since $\boldsymbol{v} - \operatorname{grad} q \in H_0(\operatorname{curl};\Omega)$, then $\boldsymbol{w} \in H_0(\operatorname{curl}\operatorname{curl};\Omega)$. From (7.4.4) and the Poincaré inequality [6, Theorem 4.6], we have

$$\begin{aligned}(\operatorname{curl}\operatorname{curl}\boldsymbol{u}, \operatorname{curl}\boldsymbol{v}) &= (\operatorname{curl}\operatorname{curl}\boldsymbol{u}, \operatorname{curl}\operatorname{curl}\boldsymbol{w})\\ &= (\boldsymbol{f} - \boldsymbol{u}, \boldsymbol{w}) \le \|\boldsymbol{f} - \boldsymbol{u}\|\|\boldsymbol{w}\| \le C\|\boldsymbol{f} - \boldsymbol{u}\|\|\operatorname{curl}\boldsymbol{w}\|\end{aligned}$$

$$\le C\|\boldsymbol{f}-\boldsymbol{u}\|\left(\|\boldsymbol{v}\|+\|\operatorname{grad} q\|\right) \le C\|\boldsymbol{f}-\boldsymbol{u}\|\|\boldsymbol{v}\| \le C\|\boldsymbol{f}\|\|\boldsymbol{v}\|,$$

which leads to (7.4.3) with $C_0 = C\|\boldsymbol{f}\|$. □

To estimate the error in the sense of $H(\text{curl})$-norm, we introduce the following auxiliary problem. Find $\boldsymbol{w}$ such that

$$\begin{aligned} -\operatorname{curl}\Delta\operatorname{curl}\boldsymbol{w}+\boldsymbol{w} &= \operatorname{curl}\operatorname{curl}(\boldsymbol{u}-\boldsymbol{u}_h) \text{ in } \Omega,\\ \operatorname{div}\boldsymbol{w} &= 0 \text{ in } \Omega,\\ \boldsymbol{w}\times\boldsymbol{n} &= 0 \text{ on } \partial\Omega,\\ \operatorname{curl}\boldsymbol{w} &= 0 \text{ on } \partial\Omega. \end{aligned} \tag{7.4.5}$$

Due to the special form of the right-hand side in the auxiliary problem, we can have a better regularity estimate by a suitable modification to the proof of Theorem 7.4.1. This result will play an important role in the dual argument in the approximation analysis below.

Theorem 7.4.2. *We assume that Ω is a simply-connected Lipschitz polyhedral domain with a connected boundary. The solution $\boldsymbol{w}$ of* (7.4.5) *satisfies*

$$\|\boldsymbol{w}\|_\alpha + \|\operatorname{curl}\boldsymbol{w}\|_{1+\alpha} \le C\|\operatorname{curl}(\boldsymbol{u}-\boldsymbol{u}_h)\|.$$

Remark 7.4.3. Furthermore, if Ω is convex, then the constant α in Theorem 7.4.1 and Theorem 7.4.2 can be 1.

The $H(\operatorname{grad}\operatorname{curl})$-conforming finite element method for (7.4.2) reads: seek $\boldsymbol{u}_h \in \mathring{V}_h^{r-1,k+1}$, such that

$$a(\boldsymbol{u}_h, \boldsymbol{v}_h) = (\boldsymbol{f}, \boldsymbol{v}_h) \quad \forall \boldsymbol{v}_h \in \mathring{V}_h^{r-1,k+1}. \tag{7.4.6}$$

It follows immediately from Céa's lemma and the duality argument that the following approximation property of $\boldsymbol{u}_h$ holds.

Theorem 7.4.3. *For $r = k$, $r = k+1$, or $r = k+2$, if $\boldsymbol{u} \in H^{s+(r-k-1)}(\Omega) \otimes \mathbb{V}$ and $\operatorname{curl} \boldsymbol{u} \in H^s(\Omega) \otimes \mathbb{V}$, $s \geq 3/2 + \delta$ with $\delta > 0$, we have the following error estimates for the numerical solution $\boldsymbol{u}_h$:*

$$\|\boldsymbol{u} - \boldsymbol{u}_h\|_{H(\operatorname{grad}\operatorname{curl};\Omega)} \leq Ch^{r_2 - 1}\left(\|\boldsymbol{u}\|_{s+(r-k-1)} + \|\operatorname{curl}\boldsymbol{u}\|_s\right), \tag{7.4.7}$$

$$\|\operatorname{curl}(\boldsymbol{u} - \boldsymbol{u}_h)\| \leq Ch^{\min\{r_2, 2\alpha\}}\left(\|\boldsymbol{u}\|_{s+(r-k-1)} + \|\operatorname{curl}\boldsymbol{u}\|_s\right), \tag{7.4.8}$$

$$\|\boldsymbol{u} - \boldsymbol{u}_h\| \leq Ch^{\min\{r_2, 2\alpha\}}\left(\|\boldsymbol{u}\|_s + \|\operatorname{curl}\boldsymbol{u}\|_s\right) \text{ when } r = k+1, k+2, \tag{7.4.9}$$

where $r_2 = \min\{k+1, s\}$.

7.5 Numerical Experiments

We now carry out several numerical tests to validate our new elements. We consider the problem (7.4.1) on a unit cube $\Omega = (0,1) \times (0,1) \times (0,1)$ with an exact solution

$$\boldsymbol{u} = \begin{pmatrix} \sin(\pi x_1)^3 \sin(\pi x_2)^2 \sin(\pi x_3)^2 \cos(\pi x_2)\cos(\pi x_3) \\ \\ \sin(\pi x_2)^3 \sin(\pi x_3)^2 \sin(\pi x_1)^2 \cos(\pi x_3)\cos(\pi x_1) \\ \\ -2\sin(\pi x_3)^3 \sin(\pi x_1)^2 \sin(\pi x_2)^2 \cos(\pi x_1)\cos(\pi x_2) \end{pmatrix}.$$

Then, by a simple calculation, we can obtain the source term $\boldsymbol{f}$.

For the mesh, we partition the unit cube into N^3 small cubes and then partition each small cube into 6 congruent tetrahedra.

We first use the lowest-order ($k = 1$) elements in the families $r = k$ and $r = k+1$ to solve the problem (7.4.1) on the uniform tetrahedral mesh. Tables 8.5.1 and 8.5.2 illustrate errors and convergence rates for the two families. We observe that the numerical solution converges to the exact one at rate h for the case $r = k = 1$, and at rate h^2 for $r = k+1 = 2$ in the sense of the L^2-norm. In addition, the two families have the same convergence rate h^2 in the $H(\text{curl})$-norm and h in the $H(\text{grad}\,\text{curl})$-norm, respectively. All results agree with Theorem 8.4.2.

We now test the third-order element ($k = 3$) in the family $r = k$. Tables 7.5.3 demonstrates numerical data, again they are consistent with Theorem 8.4.2.

Table 7.5.1: Numerical results of the tetrahedral element with $r = k$ and $k = 1$

N	$\|\boldsymbol{e}_h\|$	rates	$\|\text{curl}\, \boldsymbol{e}_h\|$	rates	$\|\text{grad}\,\text{curl}\, \boldsymbol{e}_h\|$	rates
45	8.642113e-03		7.620755e-02		2.862735e+00	
50	7.401715e-03	1.4705	6.317760e-02	1.7797	2.601358e+00	0.9087
55	6.443660e-03	1.4544	5.314638e-02	1.8141	2.382186e+00	0.9235
60	5.687783e-03	1.4340	4.527838e-02	1.8414	2.196043e+00	0.9351

Table 7.5.2: Numerical results of the tetrahedral element with $r = k + 1$ and $k = 1$

N	$\|\boldsymbol{e}_h\|$	rates	$\|\text{curl}\, \boldsymbol{e}_h\|$	rates	$\|\text{grad}\,\text{curl}\, \boldsymbol{e}_h\|$	rates
30	1.334051e-02		1.453615e-01		4.055510e+00	
35	1.033747e-02	1.6544	1.135563e-01	1.6018	3.567777e+00	0.8312
40	8.212073e-03	1.7237	9.077071e-02	1.6772	3.178759e+00	0.8646
45	6.662599e-03	1.7753	7.399883e-02	1.7344	2.862553e+00	0.8896

Table 7.5.3: Numerical results of the tetrahedral element with $r = k$ and $k = 3$

N	$\|\boldsymbol{e}_h\|$	rates	$\|\text{curl}\, \boldsymbol{e}_h\|$	rates	$\|\text{grad}\,\text{curl}\, \boldsymbol{e}_h\|$	rates
10	3.047288e-04		2.974941e-03		2.909078e-01	
12	1.719285e-04	3.1392	1.403569e-03	4.1202	1.779005e-01	2.6973
14	1.070064e-04	3.0761	7.353798e-04	4.1932	1.162168e-01	2.7620
16	7.125639e-05	3.0450	4.174453e-04	4.2405	7.986321e-02	2.8094

CHAPTER 8 3D GRADDIV-CONFORMING ELEMENTS

By a rotation, the 2D grad rot-conforming elements in Chapter 5 are grad div-conforming. To construct 3D grad div-conforming elements, in this chapter, we consider the following de Rham complex:

$$0 \longrightarrow \mathbb{R} \xrightarrow{\subset} H^1(\Omega) \xrightarrow{\text{grad}} H(\text{curl};\Omega) \xrightarrow{\text{curl}} H(\text{grad}\,\text{div};\Omega) \xrightarrow{\text{div}} H^1(\Omega) \longrightarrow 0. \quad (8.0.1)$$

We will construct finite element subcomplexes of (8.0.1):

$$0 \longrightarrow \mathbb{R} \xrightarrow{\subset} \Sigma_h^r \xrightarrow{\text{grad}} V_h^r \xrightarrow{\text{curl}} W_h^{r-1,k+1} \xrightarrow{\text{div}} \Sigma_h^{k,+} \longrightarrow 0. \quad (8.0.2)$$

As before, we take $r = k$, $k+1$, or $k+2$.

Through out the chapter, we denote $\mathcal{Q}_k^-\Lambda^1(K) = Q_{k,k-1,k-1}(K) \times Q_{k-1,k,k-1}(K) \times Q_{k-1,k-1,k}(K)$ and $\mathcal{Q}_k^-\Lambda^2(K) = Q_{k-1,k,k}(\hat{K}) \times Q_{k,k-1,k}(\hat{K}) \times Q_{k,k-1,k-1}(\hat{K})$.

8.1 Local Shape Function Spaces and Polynomial Complexes

In this section, we define the following local complex of the shape functions for each space in (8.0.2):

$$0 \longrightarrow \mathbb{R} \xrightarrow{\subset} \Sigma_h^r(K) \xrightarrow{\text{grad}} V_h^r(K) \xrightarrow{\text{curl}} W^{r-1,k+1}(K) \xrightarrow{\text{div}} \Sigma_h^{k,+}(K) \longrightarrow 0. \quad (8.1.1)$$

We first consider the local complex on $\hat{K}$:

$$0 \longrightarrow \mathbb{R} \xrightarrow{\subset} \hat{\Sigma}_h^r(\hat{K}) \xrightarrow{\text{grad}_{\hat{x}}} \hat{V}_h^r(\hat{K}) \xrightarrow{\text{curl}_{\hat{x}}} \hat{W}^{r-1,k+1}(\hat{K}) \xrightarrow{\text{div}_{\hat{x}}} \hat{\Sigma}_h^{k,+}(\hat{K}) \longrightarrow 0. \quad (8.1.2)$$

We let $\hat{\Sigma}_h^r(\hat{K})$ be $P_r(\hat{K})$ for a tetrahedral element or $Q_r(\hat{K})$ for a cubical element, and let $\hat{V}_h^r(K)$ be $\mathcal{R}_r(\hat{K})$ for a tetrahedral element or $\mathcal{Q}_r^-\Lambda^1(\hat{K})$ for a cubical element. Note that $\mathcal{R}_k$ is defined in For a tetrahedral element $\hat{K}$, we set

$$\hat{\Sigma}_h^{k,+}(\hat{K}) = \begin{cases} \hat{\Sigma}_h^k(\hat{K}), & k \geq 4, \\ \hat{\Sigma}_h^k(\hat{K}) \oplus \text{span}\{\hat{B}_t\}, & k = 1,2,3, \end{cases}$$

where $\hat{B}_t = \hat{x}_1\hat{x}_2\hat{x}_3(1-\hat{x}_1-\hat{x}_2-\hat{x}_3)$. For a cubical element $\hat{K}$, we set

$$\hat{\Sigma}_h^{k,+}(\hat{K}) = \begin{cases} \hat{\Sigma}_h^k(\hat{K}), & k \geq 2, \\ \hat{\Sigma}_h^k(\hat{K}) \oplus \mathrm{span}\{\hat{B}_c\}, & k = 1, \end{cases}$$

where $\hat{B}_c = (1-\hat{x}_1)(1+\hat{x}_1)(1-\hat{x}_2)(1+\hat{x}_2)(1-\hat{x}_3)(1+\hat{x}_3)$. We define

$$\hat{W}_h^{r-1,k+1}(\hat{K}) = \mathrm{curl}_{\hat{\boldsymbol{x}}}\, \hat{V}_h^r(\hat{K}) \oplus \mathfrak{p}_{\hat{\boldsymbol{x}}}^3 \hat{\Sigma}_h^{k,+}(\hat{K}) \tag{8.1.3}$$

with $\mathfrak{p}_{\hat{\boldsymbol{x}}}^3$ defined by (2.1.22). As a special case of the Poincaré operators, $\mathfrak{p}_{\hat{\boldsymbol{x}}}^3$ satisfies the following the null-homotopy identity:

$$\mathrm{div}_{\hat{\boldsymbol{x}}}\, \mathfrak{p}_{\hat{\boldsymbol{x}}}^3 \hat{u} = \hat{u},\ \forall \hat{u} \in C^\infty\Lambda^3(\hat{K}). \tag{8.1.4}$$

By the null-homotopy identity (8.1.4), the right hand side of (8.1.3) is a direct sum.

By the definitions of the shape function spaces on $\hat{K}$, it is easy to show that the sequence (8.1.2) is a complex. By the definitions and properties of the Poincaré operators, we can verify that the sequence

$$0 \longleftarrow \hat{\Sigma}_h^r(\hat{K}) \xleftarrow{\mathfrak{p}_{\hat{\boldsymbol{x}}}^1} \hat{V}_h^r(\hat{K}) \xleftarrow{\mathfrak{p}_{\hat{\boldsymbol{x}}}^2} \hat{W}_h^{r-1,k+1}(\hat{K}) \xleftarrow{\mathfrak{p}_{\hat{\boldsymbol{x}}}^3} \hat{\Sigma}_h^{k,+}(\hat{K}) \longleftarrow 0 \tag{8.1.5}$$

is also a complex with the Poincaré operators in (2.1.20) – (2.1.22). By Lemma 2.1.3, we obtain the exactness.

Lemma 8.1.1. *The complex* (8.1.2) *is exact.*

In the following lemma, we show that $\hat{W}_h^{r-1,k+1}(\hat{K})$ contains some polynomial spaces. It plays an essential role in analyzing the approximation properties of the finite element space $W_h^{r-1,k+1}$.

Lemma 8.1.2. *The inclusion* $\boldsymbol{P}_{r-1}(\hat{K}) \subseteq \hat{W}_h^{r-1,k+1}(\hat{K})$ *holds.*

Proof. From the null-homotopy property (6.1.5),

$$\boldsymbol{P}_{r-1}(\hat{K}) = \mathrm{curl}_{\hat{\boldsymbol{x}}}\, \mathfrak{p}_{\hat{\boldsymbol{x}}}^2 \boldsymbol{P}_{r-1}(\hat{K}) + \mathfrak{p}_{\hat{\boldsymbol{x}}}^3\, \mathrm{div}_{\hat{\boldsymbol{x}}}\, \boldsymbol{P}_{r-1}(\hat{K}).$$

By definition, $\hat{W}_h^{r-1,k+1}(\hat{K}) = \operatorname{curl}_{\hat{\boldsymbol{x}}} \hat{V}_h^r(\hat{K}) + \mathfrak{p}_{\hat{\boldsymbol{x}}}^3 \hat{\Sigma}_h^{k,+}(\hat{K})$. It is easy to check $\operatorname{div}_{\hat{\boldsymbol{x}}} \boldsymbol{P}_{r-1}(\hat{K}) \subseteq P_{r-2}(\hat{K}) \subseteq \hat{\Sigma}_h^{k,+}(\hat{K})$. If we can prove $\mathfrak{p}_{\hat{\boldsymbol{x}}}^2 \boldsymbol{P}_{r-1}(\hat{K}) \subseteq \hat{V}_h^r(\hat{K})$, then the desired inclusion holds.

To prove $\mathfrak{p}_{\hat{\boldsymbol{x}}}^2 \boldsymbol{P}_{r-1}(\hat{K}) \subseteq \hat{V}_h^r(\hat{K})$, we claim that

$$\hat{V}_h^r(\hat{K}) = \operatorname{grad}_{\hat{\boldsymbol{x}}} \hat{\Sigma}_h^r(\hat{K}) \oplus \mathfrak{p}_{\hat{\boldsymbol{x}}}^2 \mathcal{W}_h^{r-1}(\hat{K}), \tag{8.1.6}$$

where $\mathcal{W}_h^{r-1}(\hat{K}) = \mathcal{Q}_r^- \Lambda^2(\hat{K})$ when $\hat{K}$ is a cube, and $\mathcal{W}_h^{r-1}(\hat{K}) = \boldsymbol{P}_{r-1}(\hat{K})$ when $\hat{K}$ is a tetrahedron. It is easy to check $\operatorname{grad}_{\hat{\boldsymbol{x}}} \hat{\Sigma}_h^r(\hat{K}) \oplus \mathfrak{p}_{\hat{\boldsymbol{x}}}^2 \mathcal{W}_h^{r-1}(\hat{K}) \subseteq \hat{V}_h^r(\hat{K})$. For $\hat{\boldsymbol{u}} \in \hat{V}_h^r(\hat{K})$, from the null-homotopy identity (6.1.4), we have $\hat{\boldsymbol{u}} \in \operatorname{grad}_{\hat{\boldsymbol{x}}} \hat{\Sigma}_h^r(\hat{K}) + \mathfrak{p}_{\hat{\boldsymbol{x}}}^2 \mathcal{W}_h^{r-1}(\hat{K})$. Therefore, $\hat{V}_h^r(\hat{K}) \subseteq \operatorname{grad}_{\hat{\boldsymbol{x}}} \hat{\Sigma}_h^r(\hat{K}) \oplus \mathfrak{p}_{\hat{\boldsymbol{x}}}^2 \mathcal{W}_h^{r-1}(\hat{K})$. Moreover, the right hand side of (8.1.6) is a direct sum since if $\hat{\boldsymbol{u}} \in \operatorname{grad}_{\hat{\boldsymbol{x}}} \hat{\Sigma}_h^r(\hat{K}) \cap \mathfrak{p}_{\hat{\boldsymbol{x}}}^2 \mathcal{W}_h^{r-1}(\hat{K})$, then $\hat{\boldsymbol{u}} = 0$ from the null-homotopy identity (6.1.4). From the claim (8.1.6), we have $\mathfrak{p}_{\hat{\boldsymbol{x}}}^2 \boldsymbol{P}_{r-1}(\hat{K}) \subseteq \mathfrak{p}_{\hat{\boldsymbol{x}}}^2 \mathcal{W}_h^{r-1}(\hat{K}) \subseteq \hat{V}_h^r(\hat{K})$.

□

We adopt the following transformation to relate the function $\hat{\boldsymbol{u}} \in \hat{W}_h^{r-1,k+1}(\hat{K})$ to a function $\boldsymbol{u} \in W_h^{r-1,k+1}(K)$:

$$\boldsymbol{u} \circ F_K = \frac{B_K}{\det(B_K)} \hat{\boldsymbol{u}}, \tag{8.1.7}$$

where the affine mapping F_K is defined in (1.5.1). By a simple computation, we have

$$\operatorname{div} \boldsymbol{u} \circ F_K = \frac{1}{\det(B_K)} \operatorname{div}_{\hat{\boldsymbol{x}}} \hat{\boldsymbol{u}}, \tag{8.1.8}$$

Therefore, we define

$$\begin{aligned}
\Sigma_h^r(K) &= \left\{ u : u \circ F_K \in \hat{\Sigma}_h^r(\hat{K}) \right\}, \\
V_h^r(K) &= \left\{ \boldsymbol{u} : B_K^{\mathrm{T}} \boldsymbol{u} \circ F_K \in \hat{V}_h^r(\hat{K}) \right\}, \\
W_h^{r-1,k+1}(K) &= \left\{ \boldsymbol{u} : B_K^{-1} \boldsymbol{u} \circ F_K \in \hat{W}_h^{r-1,k+1}(\hat{K}) \right\}, \\
\Sigma_h^{k,+}(K) &= \left\{ u : u \circ F_K \in \hat{\Sigma}_h^{k,+}(\hat{K}) \right\}.
\end{aligned}$$

By the definition of the spaces and Lemma 8.1.1, we can show (8.1.1) is also an exact complex.

8.2 Degrees of Freedom

In this section, we define DOFs for each space in (8.1.1). Assigning $r = k,\ k+1$, and $k+2$ in (8.1.1) leads to three versions of grad div-conforming element spaces $W_h^{k-1,k+1}(K)$, $W_h^{k,k+1}(K)$, and $W_h^{k+1,k+1}(K)$. Figure 8.2.1 demonstrates the complex (8.1.1) for the case $k = 1$ when K is a tetrahedral element. Figure 8.2.2 demonstrates the three versions of grad div-conforming elements on a cubical element.

The DOFs for the Lagrange element $\Sigma_h^r(K)$ is shown as follows:

- Vertex DOFs $M_v(u)$ at all the vertices $v_i \in \mathcal{V}_h(K)$:

$$M_v(u) = \left\{u\left(v_i\right)\right\}.$$

- Edge DOFs $M_e(u)$ on all the edges $e_i \in \mathcal{E}_h(K)$:

$$M_e(u) = \left\{\int_{e_i} uv\mathrm{d}s \text{ for all } v \in P_{r-2}(e_i)\right\}.$$

- Face DOFs $M_f(u)$ on all the faces $f_i \in \mathcal{F}_h(K)$:

$$M_f(u) = \left\{\int_{f_i} uv\mathrm{d}A \text{ for all } v \in P_{r-3}(f_i)\right\}, \text{ when } K \text{ is a tetrahedral element;}$$
$$M_f(u) = \left\{\int_{f_i} uv\mathrm{d}A \text{ for all } v \in Q_{r-2}(f_i)\right\}, \text{ when } K \text{ is a cubical element.}$$

- Interior DOFs $M_K(u)$ in the element $K \in \mathcal{T}_h$:

$$M_K(u) = \left\{\int_{K} uv\mathrm{d}V \text{ for all } v \in P_{r-4}(K)\right\}, \text{ when } K \text{ is a tetrahedral element;}$$

$$M_K(u) = \left\{\int_{K} uv\mathrm{d}V \text{ for all } v \in Q_{r-2}(K)\right\}, \text{ when } K \text{ is a cubical element.}$$

For $u \in H^{3/2+\delta}(K)$ with $\delta > 0$, we can define an H^1 interpolation operator π_K :

$H^{3/2+\delta}(K) \to \Sigma_h^r(K)$ by the above DOFs s.t.

$$M_v(u - \pi_K u) = \{0\},\ M_e(u - \pi_K u) = \{0\},$$
$$M_f(u - \pi_K u) = \{0\},\ \text{and}\ M_K(u - \pi_K u) = \{0\}.$$

The DOFs for $\Sigma_h^{k,+}(K)$ can be given similarly, with only one additional interior integration DOF on K to deal with the interior bubble function. We denote $\widetilde{\pi}_K$ as the H^1 interpolation operator to $\Sigma_h^{k,+}(K)$ by these DOFs.

We choose the space $V_h^r(K)$ as the first family of Nédélec elements, which has the following DOFs:

- Edge DOFs $\boldsymbol{M}_e(\boldsymbol{u})$ on all the edges $e_i \in \mathcal{E}_h(K)$(with a unit tangential vector $\boldsymbol{\tau}_i$):
$$\boldsymbol{M}_e(\boldsymbol{u}) = \left\{ \int_{e_i} \boldsymbol{u} \cdot \boldsymbol{\tau}_i v \mathrm{d}s \text{ for all } v \in P_{r-1}(e_i) \right\}.$$
- Face DOFs $\boldsymbol{M}_f(\boldsymbol{u})$ on all the faces $f_i \in \mathcal{F}_h(K)$ (with a unit normal vector $\boldsymbol{n}_i$):
$$\boldsymbol{M}_f(\boldsymbol{u}) = \left\{ \int_{f_i} \boldsymbol{u} \cdot \boldsymbol{v} \mathrm{d}A \text{ for all } \boldsymbol{v} \in \boldsymbol{P}_{r-2}(f_i) \text{ such that } \boldsymbol{v} \cdot \boldsymbol{n}_i = 0 \right\},$$
when K is a tetrahedral element;
$$\boldsymbol{M}_f(\boldsymbol{u}) = \left\{ \int_{f_i} \boldsymbol{u} \times \boldsymbol{n}_i \cdot \boldsymbol{v} \mathrm{d}A \text{ for all } \boldsymbol{v} \in Q_{r-2,r-1}(f_i) \times Q_{r-1,r-2}(f_i) \right\},$$
when K is a cubical element.
- Interior DOFs $\boldsymbol{M}_K(\boldsymbol{u})$ in the element $K \in \mathcal{T}_h$:
$$\boldsymbol{M}_K(\boldsymbol{u}) = \left\{ \int_K \boldsymbol{u} \cdot \boldsymbol{v} \mathrm{d}V \text{ for all } \boldsymbol{v} \in \boldsymbol{P}_{r-3}(K) \right\} \text{ when } K \text{ is a tetrahedral element,}$$
$$\boldsymbol{M}_K(\boldsymbol{u}) = \left\{ \int_K \boldsymbol{u} \cdot \boldsymbol{v} \mathrm{d}V \text{ for all } \boldsymbol{v} \in \mathcal{Q}_{r-1}^{-}\Lambda^2(K) \right\} \text{ when } K \text{ is a cubical element.}$$

Assuming that $\boldsymbol{u} \in H^{1/2+\delta}(\Omega) \otimes \mathbb{V}$ and $\operatorname{curl} \boldsymbol{u} \in L^{2+\delta}(\Omega) \otimes \mathbb{V}$ with $\delta > 0$ [49, Lemma 5.38]. By the above DOFs, we define an $H(\text{curl})$ interpolation operator Π_K which maps $\boldsymbol{u}$ to $V_h^r(K)$ and satisfies

$$\boldsymbol{M}_e(\boldsymbol{u} - \Pi_K \boldsymbol{u}) = \{0\}, \boldsymbol{M}_f(\boldsymbol{u} - \Pi_K \boldsymbol{u}) = \{0\},\ \text{and}\ \boldsymbol{M}_K(\boldsymbol{u} - \Pi_K \boldsymbol{u}) = \{0\}.$$

We now equip the space $W_h^{r-1,k+1}(K)$ with the following DOFs:

- Vertex DOFs $\boldsymbol{M}_v(\boldsymbol{u})$ at all vertices $v_i \in \mathcal{V}_h(K)$:

$$\boldsymbol{M}_v(\boldsymbol{u}) = \{\operatorname{div} \boldsymbol{u}(v_i)\}. \tag{8.2.1}$$

- Edge DOFs $\boldsymbol{M}_e(\boldsymbol{u})$ on all edges $e_i \in \mathcal{E}_h(K)$:

$$\boldsymbol{M}_e(\boldsymbol{u}) = \left\{ \int_{e_i} \operatorname{div} \boldsymbol{u} q \mathrm{d}s \text{ for all } q \in P_{k-2}(e_i) \right\}. \tag{8.2.2}$$

- Face DOFs $\boldsymbol{M}_f(\boldsymbol{u})$ on all faces $f_i \in \mathcal{F}_h(K)$ (with the unit normal vector $\boldsymbol{n}_i$):

$$\begin{aligned} \boldsymbol{M}_f(\boldsymbol{u}) = & \left\{ \int_{f_i} \operatorname{div} \boldsymbol{u} q \mathrm{d}A, \ \forall q \in P_{k-3}(f_i) \right\} \\ & \cup \left\{ \int_{f_i} \boldsymbol{u} \cdot \boldsymbol{n}_i q \mathrm{d}A \text{ for all } q \in P_{r-1}(f_i) \right\}, \end{aligned} \tag{8.2.3}$$

  when K is a tetrahedral element;

$$\begin{aligned} \boldsymbol{M}_f(\boldsymbol{u}) = & \left\{ \int_{f_i} \operatorname{div} \boldsymbol{u} q \mathrm{d}A \text{ for all } q \in Q_{k-2,k-2}(f_i) \right\} \\ & \cup \left\{ \int_{f_i} \boldsymbol{u} \cdot \boldsymbol{n}_i q \mathrm{d}A \text{ for all } q \in Q_{r-1,r-1}(f_i) \right\}, \end{aligned} \tag{8.2.4}$$

  when K is a cubical element.

- Interior DOFs $\boldsymbol{M}_K(\boldsymbol{u})$ for the element $K \in \mathcal{T}_h$:

$$\begin{aligned} \boldsymbol{M}_K(\boldsymbol{u}) = & \left\{ \int_K \boldsymbol{u} \cdot \boldsymbol{q} \mathrm{d}V \text{ for all } \boldsymbol{q} = B_K^{-\mathrm{T}} \hat{\boldsymbol{q}}, \ \hat{\boldsymbol{q}} \in \boldsymbol{P}_{r-3}(\hat{K}) \times \hat{\boldsymbol{x}} \right\} \\ & \cup \left\{ \int_K \operatorname{div} \boldsymbol{u} q \mathrm{d}V \text{ for all } q \in P_{k-4}(K)/\mathbb{R} \right\}, \end{aligned} \tag{8.2.5}$$

  when K is a tetrahedral element;

$$\begin{aligned} \boldsymbol{M}_K(\boldsymbol{u}) = & \left\{ \int_K \boldsymbol{u} \cdot \boldsymbol{q} \mathrm{d}V \text{ for all } \boldsymbol{q} = B_K^{-\mathrm{T}} \hat{\boldsymbol{q}}, \ \hat{\boldsymbol{q}} \in \mathcal{Q}_{r-1}^{-} \Lambda^2(\hat{K}) \times \hat{\boldsymbol{x}} \right\} \\ & \cup \left\{ \int_K \operatorname{div} \boldsymbol{u} q \mathrm{d}V \text{ for all } q \in Q_{k-2}(K)/\mathbb{R} \right\}, \end{aligned} \tag{8.2.6}$$

  when K is a tetrahedral element.

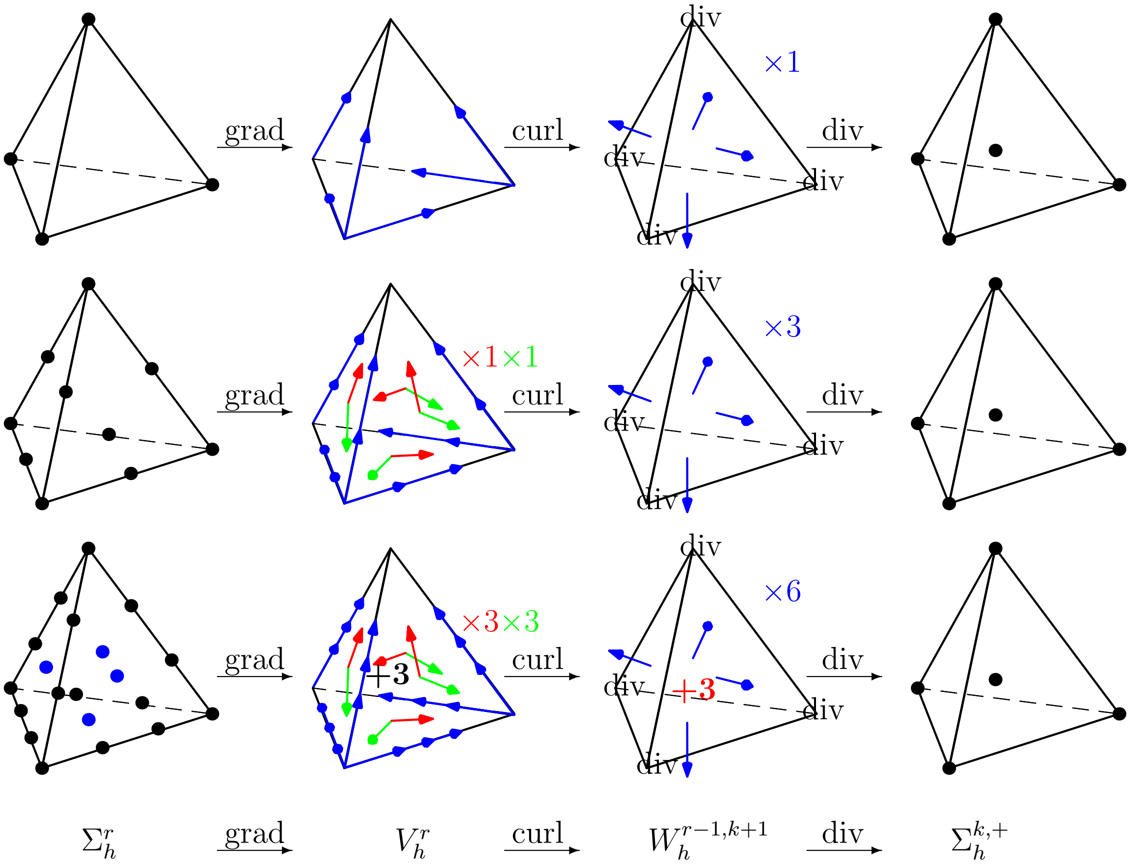

Figure 8.2.1: The lowest-order ($k = 1$) finite element complex (8.1.1) on tetrahedra with $r = k - 1$ in the first row, $r = k$ in the second row, and $r = k + 1$ in the third row.

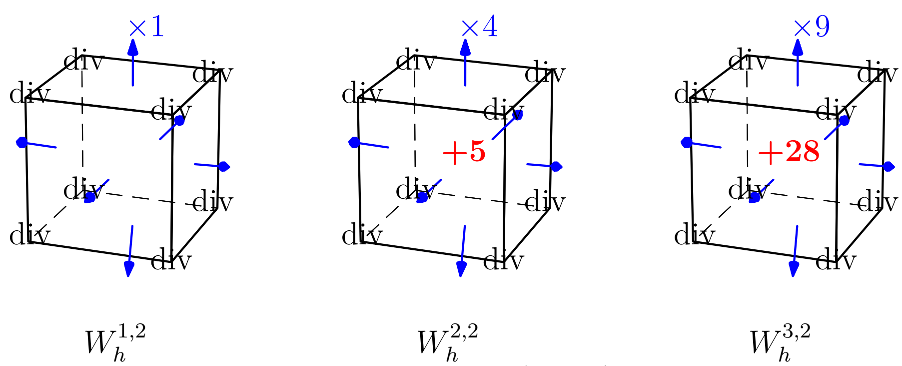

Figure 8.2.2: The three versions of lowest-order ($k = 1$) grad-div finite elements on cubes

Lemma 8.2.1. *The DOFs for $W_h^{r-1,k+1}(K)$ are unisolvent.*

Proof. Since the complex (8.1.1) is exact, $\dim W_h^{r-1,k+1}(K) = \dim V_h^r - \dim \Sigma_h^r + 1 + \dim \Sigma_h^{k,+}(K)$. By counting the number of DOFs, we find the DOF set has the same dimension. Then it suffices to show that if all the DOFs vanish on a function $\boldsymbol{u} \in W_h^{r-1,k+1}(K)$, then $\boldsymbol{u} = 0$. To see this, we first show that $\operatorname{div} \boldsymbol{u} = 0$. By integration by parts,

$$(\operatorname{div} \boldsymbol{u}, 1) = \langle \boldsymbol{u} \cdot \boldsymbol{n}_{\partial K}, 1 \rangle = 0.$$

Since $\operatorname{div} W_h^{r-1,k+1}(K) \subseteq \Sigma_h^{k,+}(K)$, the unisolvence of the DOFs of $\Sigma_h^{k,+}(K)$ leads to $\operatorname{div} \boldsymbol{u} = 0$.

There exists a $\boldsymbol{\phi} \in V_h^r(K)$ such that $\boldsymbol{u} = \operatorname{curl} \boldsymbol{\phi}$, and hence $\boldsymbol{u}|_{f_i} \cdot \boldsymbol{n}_i \in P_{r-1}(f_i)$ or $Q_{r-1,r-1}(f_i)$. By the face DOFs (8.2.3) or (8.2.4), $\boldsymbol{u} \cdot \boldsymbol{n}_i = 0$ on the face f_i. Recalling that $\boldsymbol{u}$ and $\hat{\boldsymbol{u}}$ are related by (8.1.7) , $\hat{\boldsymbol{u}} = (\hat{x}_1\hat{\varphi}_1, \hat{x}_2\hat{\varphi}_2, \hat{x}_3\hat{\varphi}_3)^{\mathrm{T}}$ when K is a tetrahedron, and $\hat{\boldsymbol{u}} = \big((1-\hat{x}_1)(1+\hat{x}_1)\hat{\varphi}_1, (1-\hat{x}_2)(1+\hat{x}_2)\hat{\varphi}_2, (1-\hat{x}_3)(1+\hat{x}_3)\hat{\varphi}_3\big)^{\mathrm{T}}$ when K is a cube. Here $\hat{\boldsymbol{\varphi}} = (\hat{\varphi}_1, \hat{\varphi}_2, \hat{\varphi}_3)^{\mathrm{T}} \in \boldsymbol{P}_{r-2}(\hat{K})$ or $\mathcal{Q}_{r-1}^{-}\Lambda^1(\hat{K})$. By integration by parts, we have, for any $q \in P_{r-1}(K)$ or $Q_{r-1}(K)$

$$(\boldsymbol{u}, \operatorname{grad} q)_K = (\operatorname{curl} \boldsymbol{\phi}, \operatorname{grad} q)_K = \langle \operatorname{curl} \boldsymbol{\phi} \cdot \boldsymbol{n}_{\partial K}, q \rangle_{\partial K} = \langle \boldsymbol{u} \cdot \boldsymbol{n}_{\partial K}, q \rangle_{\partial K} = 0,$$

which, together with the interior DOFs, leads to

$$(\boldsymbol{u}, \boldsymbol{q})_K = 0 \text{ for any } \boldsymbol{q} \circ F_K = B_K^{-\mathrm{T}} \hat{\boldsymbol{q}},\ \hat{\boldsymbol{q}} \in \mathcal{Q}_{r-1}^{-}\Lambda^1(\hat{K}) \text{ or } \boldsymbol{P}_{r-2}(\hat{K}). \tag{8.2.7}$$

Choosing $\boldsymbol{\varphi} = B_K^{-\mathrm{T}} \hat{\boldsymbol{\varphi}}$, we have

$$0 = (\boldsymbol{u}, \boldsymbol{\varphi})_K = (\hat{\boldsymbol{u}}, \hat{\boldsymbol{\varphi}})_{\hat{K}}.$$

This implies that $\hat{\boldsymbol{\varphi}} = 0$ and hence $\boldsymbol{u} = 0$. □

Provided $\boldsymbol{u} \in H^{1/2+\delta}(K) \otimes \mathbb{V}$ and $\operatorname{div} \boldsymbol{u} \in H^{3/2+\delta}(K)$ with $\delta > 0$, we can define an

$H(\operatorname{grad}\operatorname{div})$ interpolation $\boldsymbol{r}_K\boldsymbol{u} \in W_h^{r-1,k+1}(K)$ by

$$\boldsymbol{M}_v(\boldsymbol{u}-\boldsymbol{r}_K\boldsymbol{u}) = \{0\},\ \boldsymbol{M}_e(\boldsymbol{u}-\boldsymbol{r}_K\boldsymbol{u}) = \{0\},$$

$$\boldsymbol{M}_f(\boldsymbol{u}-\boldsymbol{r}_K\boldsymbol{u}) = \{0\},\ \text{and}\ \boldsymbol{M}_K(\boldsymbol{u}-\boldsymbol{r}_K\boldsymbol{u}) = \{0\},$$

where $\boldsymbol{M}_v,\ \boldsymbol{M}_e,\ \boldsymbol{M}_f$, and $\boldsymbol{M}_K$ are the sets of DOFs in (8.2.1) – (8.2.6).

8.3 Global Finite Element Complexes

Gluing the local spaces by the above DOFs, we obtain the global finite element spaces Σ_h^r, V_h^r, $W_h^{r-1,k+1}$, and $\Sigma_h^{k,+}$ in the complex (8.0.2). We now develop some properties of the complex (8.0.2) containing these spaces.

Lemma 8.3.1. *The following conformity holds:*

$$W_h^{r-1,k+1} \subset H(\operatorname{grad}\operatorname{div};\Omega).$$

Proof. To verify $W_h^{r-1,k+1} \subset H(\operatorname{grad}\operatorname{div};\Omega)$, we must show $\boldsymbol{u}\cdot\boldsymbol{n}_i = 0$ and $\operatorname{div}\boldsymbol{u} = 0$ on each $f_i \in \mathcal{F}_h(K)$ if the DOFs (8.2.1) – (8.2.4) vanish on $\boldsymbol{u} \in W_h^{r-1,k+1}(K)$. It is easy to see that $(\operatorname{div}\boldsymbol{u})|_{f_i} \in Q_{k,k}(K)$ or $P_k(f_i)$. Restricted on f_i, $\boldsymbol{u}\cdot\boldsymbol{n}_i = \frac{(\hat{\boldsymbol{u}}\cdot\hat{\boldsymbol{n}}_i)\circ F_K^{-1}}{\det(B_K)|B_K^{-\mathrm{T}}\hat{\boldsymbol{n}}_i|} = \frac{(\operatorname{curl}_{\hat{\boldsymbol{x}}}\mathfrak{p}_{\hat{\boldsymbol{x}}}^2\hat{\boldsymbol{u}}\cdot\hat{\boldsymbol{n}}_i + \mathfrak{p}_{\hat{\boldsymbol{x}}}^3\operatorname{div}_{\hat{\boldsymbol{x}}}\hat{\boldsymbol{u}}\cdot\hat{\boldsymbol{n}}_i)\circ F_K^{-1}}{\det(B_K)|B_K^{-\mathrm{T}}\hat{\boldsymbol{n}}_i|} = \frac{(\operatorname{curl}_{\hat{\boldsymbol{x}}}\mathfrak{p}_{\hat{\boldsymbol{x}}}^2\hat{\boldsymbol{u}}\cdot\hat{\boldsymbol{n}}_i)\circ F_K^{-1}}{\det(B_K)|B_K^{-\mathrm{T}}\hat{\boldsymbol{n}}_i|} \in Q_{r-1,r-1}(f_i)$ or $P_{r-1}(f_i)$ since $\hat{\boldsymbol{x}}\cdot\hat{\boldsymbol{n}}_i = 0$ on $\hat{f}_i$. From the vanishing DOFs in (8.2.1) – (8.2.4), we have $\boldsymbol{u}\cdot\boldsymbol{n}_i = 0$ and $\operatorname{div}\boldsymbol{u} = 0$ on f_i. □

Theorem 8.3.2. *The complex* (8.0.2) *is exact on contractible domains.*

Proof. We first show the exactness at V_h^r and $W_h^{r-1,k+1}$. To this end, we show that for any $\boldsymbol{v}_h \in V_h^r \subset H(\operatorname{curl};\Omega)$ and $\boldsymbol{u}_h \in W_h^{r-1,k+1} \subset H(\operatorname{grad}\operatorname{div};\Omega) \subset H(\operatorname{div};\Omega)$ satisfying $\operatorname{curl}\boldsymbol{v}_h = 0$ and $\operatorname{div}\boldsymbol{u}_h = 0$, there exists $p_h \in \Sigma_h^r$ and $\boldsymbol{\phi}_h \in V_h^r$ such that $\boldsymbol{v}_h = \operatorname{grad} p_h$ and $\boldsymbol{u}_h = \operatorname{curl}\boldsymbol{\phi}_h$. Actually, this follows from the exactness of the standard finite element differential forms (e.g., [49]). To prove the exactness at $\Sigma_h^{k,+}$, that is to prove the operator div from $W_h^{r-1,k+1}$ to $\Sigma_h^{k,+}$ is surjective, we count the dimensions. We take the complex (8.0.2) on tetrahedral meshes as an example. The dimension count of the Lagrange elements reads:

$$\dim \Sigma_h^r = \mathcal{V} + (r-1)\mathcal{E} + \frac{1}{2}(r-2)(r-1)\mathcal{F} + \frac{1}{6}(r-3)(r-2)(r-1)\mathcal{K},$$

where $\mathcal{V}$, $\mathcal{E}$, $\mathcal{F}$, and $\mathcal{K}$ denote the number of vertices, edges, faces, and 3D cells, respectively. The dimension count of the space V_h^r reads:

$$\dim V_h^r = r\mathcal{E} + r(r-1)\mathcal{F} + \frac{1}{2}r(r-1)(r-2)\mathcal{K}.$$

From the DOFs (8.2.1) – (8.2.6),

$$\dim W_h^{r-1,k+1} - \dim \Sigma_h^{k,+} = \frac{1}{2}r(r+1)\mathcal{F} + \frac{1}{6}r(r+1)(2r-5)\mathcal{K}.$$

From the above dimension count, we have

$$-1 + \dim \Sigma_h^r - \dim V_h^r + \dim W_h^{r-1,k+1} - \dim \Sigma_h^{k,+} = 0,$$

where we have used Euler's formula $\mathcal{V} - \mathcal{E} + \mathcal{F} - \mathcal{K} = 1$. This completes the proof. □

For $\delta > 0$, denote $\Sigma = H^{3/2+\delta}(\Omega)$, $V = \{\boldsymbol{u} \in H^{1/2+\delta}(\Omega) \otimes \mathbb{V} : \operatorname{curl} \boldsymbol{u} \in L^{2+\delta}(\Omega) \otimes \mathbb{V}\}$, and $W = \{\boldsymbol{u} \in H^{1/2+\delta}(\Omega) \otimes \mathbb{V} : \operatorname{div} \boldsymbol{u} \in H^{3/2+\delta}(\Omega)\}$. We define four global interpolations $\pi_h : \Sigma \to \Sigma_h^r$, $\widetilde{\pi}_h : \Sigma \to \Sigma_h^{k,+}$, $\Pi_h : V \to V_h^r$, and $\boldsymbol{r}_h : W \to W_h^{r-1,k+1}$ in the following way:

$$(\pi_h u)|_K = \pi_K u, \ (\widetilde{\pi}_h \boldsymbol{u})|_K = \widetilde{\pi}_K \boldsymbol{u}, (\Pi_h \boldsymbol{u})|_K = \Pi_K \boldsymbol{u}, \text{ and } (\boldsymbol{r}_h u)|_K = \boldsymbol{r}_K u.$$

The interpolations π_K, $\widetilde{\pi}_K$, Π_K, $\boldsymbol{r}_K$ are defined in Section 8.2.

We summarize these interpolations in the following diagram:

$$\begin{array}{ccccccccccc}
\mathbb{R} & \xrightarrow{\subset} & H^1(\Omega) & \xrightarrow{\text{grad}} & H(\text{curl};\Omega) & \xrightarrow{\text{curl}} & H(\text{grad div};\Omega) & \xrightarrow{\text{div}} & H^1(\Omega) & \longrightarrow & 0 \\
 & & \downarrow & & \downarrow & & \downarrow & & \downarrow & & \\
\mathbb{R} & \xrightarrow{\subset} & \Sigma & \xrightarrow{\text{grad}} & V & \xrightarrow{\text{curl}} & W & \xrightarrow{\text{div}} & \Sigma & \longrightarrow & 0 \\
 & & \downarrow{\scriptstyle \pi_h} & & \downarrow{\scriptstyle \Pi_h} & & \downarrow{\scriptstyle \boldsymbol{r}_h} & & \downarrow{\scriptstyle \widetilde{\pi}_h} & & \\
\mathbb{R} & \xrightarrow{\subset} & \Sigma_h^r & \xrightarrow{\text{grad}} & V_h^r & \xrightarrow{\text{curl}} & W_h^{r-1,k+1} & \xrightarrow{\text{div}} & \Sigma_h^{k,+} & \longrightarrow & 0.
\end{array} \tag{8.3.1}$$

Now we show that the interpolations in (8.3.1) commute with the differential operators. In addition to Lemma 8.1.2, this result also plays a key role in the error analysis below for the interpolations.

Lemma 8.3.3. *The last two rows of the complex* (8.3.1) *are a commuting diagram, i.e.,*

$$\operatorname{grad} \pi_h u = \Pi_h \operatorname{grad} u \text{ for all } u \in \Sigma, \tag{8.3.2}$$

$$\operatorname{curl} \Pi_h \boldsymbol{u} = \boldsymbol{r}_h \operatorname{curl} \boldsymbol{u} \text{ for all } \boldsymbol{u} \in V, \tag{8.3.3}$$

$$\operatorname{div} \boldsymbol{r}_h \boldsymbol{u} = \widetilde{\pi}_h \operatorname{div} \boldsymbol{u} \text{ for all } \boldsymbol{u} \in W. \tag{8.3.4}$$

Proof. A similar trick as Lemma 5.3.3 can be used to prove this lemma. For simplicity of presentation, we omit it. □

The following lemma relates the interpolation on K to that on $\hat{K}$.

Lemma 8.3.4. *For $\boldsymbol{u} \in W$, under the transformation* (8.1.7)*, we have $\widehat{\boldsymbol{r}_K \boldsymbol{u}} = \boldsymbol{r}_{\hat{K}} \hat{\boldsymbol{u}}$.*

Next, we establish the approximation property of the interpolation operator.

Theorem 8.3.5. *Assume that $\boldsymbol{u} \in H^{s+(r-k-1)}(\Omega) \otimes \mathbb{V}$ and $\operatorname{div} \boldsymbol{u} \in H^s(\Omega)$, $s \geq 3/2 + \delta$ with $\delta > 0$. Then we have the following error estimates for the interpolation $\boldsymbol{r}_h$,*

$$\|\boldsymbol{u} - \boldsymbol{r}_h \boldsymbol{u}\| \leq C h^{\min\{s+(r-k-1),r\}} (\|\boldsymbol{u}\|_{s+(r-k-1)} + \|\operatorname{div} \boldsymbol{u}\|_s), \tag{8.3.5}$$

$$\|\operatorname{div}(\boldsymbol{u} - \boldsymbol{r}_h \boldsymbol{u})\| \leq C h^{\min\{s,k+1\}} \|\operatorname{div} \boldsymbol{u}\|_s \,, \tag{8.3.6}$$

$$|\operatorname{div}(\boldsymbol{u} - \boldsymbol{r}_h \boldsymbol{u})|_1 \leq C h^{\min\{s-1,k\}} \|\operatorname{div} \boldsymbol{u}\|_s \,. \tag{8.3.7}$$

Proof. With the identity $\widehat{\boldsymbol{r}_K \boldsymbol{u}} = \boldsymbol{r}_{\hat{K}} \hat{\boldsymbol{u}}$ and the inclusion $\boldsymbol{P}_{r-1}(\hat{K}) \subseteq \hat{W}_h^{r-1,k+1}(\hat{K})$ (Lemma 8.3.4 and Lemma 8.1.2), the estimate (8.3.5) can be obtained by following the proof of Theorem 5.3.6. To prove (8.3.6) and (8.3.7), we apply Lemma 8.3.3 and the approximation property of the Lagrange interpolation. □

8.4 Applications to $\operatorname{grad} \Delta \operatorname{div}$ Problems

In this section, we use the grad div-conforming finite elements to solve the following $\operatorname{grad} \Delta \operatorname{div}$ problem which is closely related to the Hodge Laplacian problem (3.3.6).

For $\boldsymbol{f} \in H(\text{curl};\Omega)$ and $\boldsymbol{g} \in L^2(\Omega)\otimes\mathbb{V}$, find $\boldsymbol{u}$ such that

$$\begin{aligned} \operatorname{grad}\Delta\operatorname{div}\boldsymbol{u} + \boldsymbol{u} &= \boldsymbol{f} \quad \text{in } \Omega,\\ \operatorname{curl}\boldsymbol{u} &= \boldsymbol{g} \quad \text{in } \Omega,\\ \boldsymbol{u}\cdot\boldsymbol{n} &= 0 \quad \text{on } \partial\Omega,\\ \operatorname{div}\boldsymbol{u} &= 0 \quad \text{on } \partial\Omega. \end{aligned} \tag{8.4.1}$$

Here, to make the problem consistent, $\boldsymbol{g} = \operatorname{curl}\boldsymbol{f}$. By taking curl on both sides of the first equation of (8.4.1), we see that the condition $\operatorname{curl}\boldsymbol{u} = \boldsymbol{g}$ holds automatically.

We define $H_0(\operatorname{grad}\operatorname{div};\Omega)$ with vanishing boundary conditions:

$$H_0(\operatorname{grad}\operatorname{div};\Omega) := \{\boldsymbol{u} \in H(\operatorname{grad}\operatorname{div};\Omega) : \ \boldsymbol{u}\cdot\boldsymbol{n} = 0 \text{ and } \operatorname{div}\boldsymbol{u} = 0 \ \text{ on } \partial\Omega\}.$$

The variational formulation is to seek $\boldsymbol{u} \in H_0(\operatorname{grad}\operatorname{div};\Omega)$ such that

$$a(\boldsymbol{u},\boldsymbol{v}) = (\boldsymbol{f},\boldsymbol{v}) \quad \forall \boldsymbol{v} \in H_0(\operatorname{grad}\operatorname{div};\Omega), \tag{8.4.2}$$

with $a(\boldsymbol{u},\boldsymbol{v}) := \big(\operatorname{grad}\operatorname{div}\boldsymbol{u}, \operatorname{grad}\operatorname{div}\boldsymbol{v}\big) + (\boldsymbol{u},\boldsymbol{v})$.

It follows from Lax-Milgram Lemma that (8.4.2) is well-posedness. Taking $\boldsymbol{v} = \operatorname{curl}\boldsymbol{\psi}$ with $\boldsymbol{\psi} \in H_0(\text{curl};\Omega)$ in (8.4.2) leads to

$$(\boldsymbol{u}, \operatorname{curl}\boldsymbol{\psi}) = (\boldsymbol{f}, \operatorname{curl}\boldsymbol{\psi}) = (\boldsymbol{g}, \boldsymbol{\psi}),$$

which implies $\operatorname{curl}\boldsymbol{u} = \boldsymbol{g}$ holds in the sense of $L^2(\Omega)\otimes\mathbb{V}$. Since the regularity of the solution plays a crucial role in the error analysis, we will first derive a regularity result for the $\operatorname{grad}\Delta\operatorname{div}$ problem before proceeding further.

Theorem 8.4.1. *Assume Ω is Lipschitz polyhedron. There exist a constant $\alpha > 1/2$ such that the solution $\boldsymbol{u}$ of* (8.4.1) *satisfies $\boldsymbol{u} \in H^{\alpha}(\Omega)\otimes\mathbb{V}$ and $\operatorname{div}\boldsymbol{u} \in H^{1+\alpha}(\Omega)$. Moreover,*

$$\|\boldsymbol{u}\|_{\alpha} + \|\operatorname{div}\boldsymbol{u}\|_{1+\alpha} \le C(\|\boldsymbol{f}\| + \|\boldsymbol{g}\|).$$

Proof. Since $\boldsymbol{u} \in H_0(\text{div};\Omega)\cap H(\text{curl};\Omega) \hookrightarrow H^{\alpha}(\Omega)\otimes\mathbb{V}$ [4, Proposition 3.7], we have

$\boldsymbol{u} \in H^{\alpha}(\Omega) \otimes \mathbb{V}$, and

$$\|\boldsymbol{u}\|_{\alpha} \leq C(\|\boldsymbol{u}\| + \|\operatorname{div} \boldsymbol{u}\| + \|\operatorname{curl} \boldsymbol{u}\|)$$
$$\leq C(\|\boldsymbol{u}\| + \|\operatorname{grad}\operatorname{div} \boldsymbol{u}\| + \|\operatorname{curl} \boldsymbol{u}\|) \leq C(\|\boldsymbol{f}\| + \|\boldsymbol{g}\|).$$

Proceeding similarly to the proof of 5.4.1, we can get

$$\|\Delta \operatorname{div} \boldsymbol{u}\| \leq C\|\boldsymbol{f}\|.$$

From the regularity estimate of the Laplace problem [49], we have $\operatorname{div} \boldsymbol{u} \in H^{1+\alpha}(\Omega)$ and $\|\operatorname{div} \boldsymbol{u}\|_{1+\alpha} \leq C\|\Delta \operatorname{div} \boldsymbol{u}\| \leq C\|\boldsymbol{f}\|$.

□

We now present the finite element scheme. We define the finite element space with vanishing boundary conditions

$$\mathring{W}_h^{r-1,k+1} = \{\boldsymbol{v}_h \in W_h^{r-1,k+1},\ \boldsymbol{n} \cdot \boldsymbol{v}_h = 0 \text{ and } \operatorname{div} \boldsymbol{v}_h = 0 \text{ on } \partial\Omega\}.$$

The grad div-conforming finite element method reads: seek $\boldsymbol{u}_h \in \mathring{W}_h^{r-1,k+1}$ such that

$$a(\boldsymbol{u}_h, \boldsymbol{v}_h) = (\boldsymbol{f}, \boldsymbol{v}_h) \quad \forall \boldsymbol{v}_h \in \mathring{W}_h^{r-1,k+1}. \tag{8.4.3}$$

By suitable modification to the proof of Theorem 5.4.3, we have the following approximation property.

Theorem 8.4.2. *Suppose $\boldsymbol{u} \in H^{s+(r-k-1)}(\Omega) \otimes \mathbb{V}$ and $\operatorname{div} \boldsymbol{u} \in H^s(\Omega)$ with $s \geq 1 + \alpha$, we have the following error estimates for the numerical solution $\boldsymbol{u}_h$:*

$$\|\boldsymbol{u} - \boldsymbol{u}_h\|_{H(\operatorname{grad}\operatorname{div};\Omega)} \leq Ch^{r_2-1}\left(\|\boldsymbol{u}\|_{s+(r-k-1)} + \|\operatorname{div} \boldsymbol{u}\|_s\right), \tag{8.4.4}$$

$$\|\operatorname{div}(\boldsymbol{u} - \boldsymbol{u}_h)\| \leq Ch^{\min\{r_2, 2\alpha\}}\left(\|\boldsymbol{u}\|_{s+(r-k-1)} + \|\operatorname{div} \boldsymbol{u}\|_s\right), \tag{8.4.5}$$

$$\|\boldsymbol{u} - \boldsymbol{u}_h\| \leq Ch^{\min\{r_2, 2\alpha\}}\left(\|\boldsymbol{u}\|_s + \|\operatorname{div} \boldsymbol{u}\|_s\right) \text{ when } r = k+1, k+2, \tag{8.4.6}$$

where $r_2 = \min\{s, k+1\}$.

8.5 Numerical Experiments

We now turn to a concrete example to test our new elements. We consider the problem (8.4.1) on a unit cube $\Omega = (0,1) \times (0,1) \times (0,1)$ with an exact solution

$$\boldsymbol{u} = \operatorname{grad}\left(x_1^3 x_2^3 x_3^3 (x_1-1)^3 (x_2-1)^3 (x_3-1)^3\right). \tag{8.5.1}$$

The source term $\boldsymbol{f}$ can be derived by a simple calculation. Note that in this case $\boldsymbol{g} = 0$.

Example 8.5.1. In this example, we test the tetrahedral elements. To this end, we partition the unit cube into N^3 small cubes and then partition each small cubes into 6 congruent tetrahedra. We use the lowest-order elements in three families to solve the problem (8.4.1) on the uniform tetrahedral mesh.

Tables 8.5.1, 8.5.2, and 8.5.3 illustrate various errors and convergence rates for three families. We observe from the tables that the numerical solution converges to the exact solution with a convergence order 1 for the family $r = k$, 2 for the family $r = k+1$, and 2 for the family $r = k+2$ in the sense of L^2-norm. In addition, the three families have the same convergence order 2 in the $H(\text{div})$-norm and 1 in the $H(\operatorname{grad}\operatorname{div})$-norm, respectively. All the results coincide with Theorem 8.4.2, which confirms the correctness of the elements and their properties.

Table 8.5.1: Numerical results of the tetrahedral grad div-conforming element with $r = k$ and $k = 1$

N	$\\|\boldsymbol{e}_h\\|$	rates	$\\|\operatorname{div}\boldsymbol{e}_h\\|$	rates	$\\|\operatorname{grad}\operatorname{div}\boldsymbol{e}_h\\|$	rates
16	7.338806e-07		3.773907e-06		1.261805e-04	
20	5.585337e-07	1.2236	2.462834e-06	1.9127	1.016297e-04	0.9697
24	4.511530e-07	1.1711	1.728736e-06	1.9412	8.500500e-05	0.9797
28	3.788654e-07	1.1328	1.278389e-06	1.9578	7.302452e-05	0.9855
32	3.268841e-07	1.1052	9.829309e-07	1.9682	6.398944e-05	0.9891

Example 8.5.2. In this example, we test the cubical grad div-conforming elements. We

Table 8.5.2: Numerical results of the tetrahedral grad div-conforming element with $r = k+1$ and $k = 1$

N	$\|\boldsymbol{e}_h\|$	rates	$\|\mathrm{div}\,\boldsymbol{e}_h\|$	rates	$\|\mathrm{grad}\,\mathrm{div}\,\boldsymbol{e}_h\|$	rates
8	1.232033e-06		1.150197e-05		3.902786e-04	
12	5.905553e-07	1.8136	5.614381e-06	1.7688	1.654137e-04	0.8952
16	3.416300e-07	1.9026	3.269987e-06	1.8790	1.259942e-04	0.9462
20	2.215699e-07	1.9404	2.127621e-06	1.9260	1.015312e-04	0.9674
24	1.549977e-07	1.9599	1.490982e-06	1.9502	8.494707e-05	0.9782

Table 8.5.3: Numerical results of the tetrahedral grad div-conforming element with $r = k+2$ and $k = 1$

N	$\|\boldsymbol{e}_h\|$	rates	$\|\mathrm{div}\,\boldsymbol{e}_h\|$	rates	$\|\mathrm{grad}\,\mathrm{div}\,\boldsymbol{e}_h\|$	rates
8	1.224295e-06		1.149723e-05		2.377994e-04	
10	8.220074e-07	1.7853	7.812974e-06	1.7313	1.954954e-04	0.8779
12	5.864916e-07	1.8516	5.613355e-06	1.8135	1.654135e-04	0.9165
14	4.381462e-07	1.8917	4.211742e-06	1.8636	1.431136e-04	0.9394
16	3.391664e-07	1.9176	3.269652e-06	1.8961	1.259941e-04	0.9541

use uniform cubical meshes with the mesh size h varying from 1/12 to 1/20. Unlike tetrahedral elements, in this test, we explore superconvergence of the cubical elements. To this end, we denote $\{w_n\}_{n=1}^p$ and $\{g_n\}_{n=1}^p$ as the weights and nodes of Legendre-Gauss quadrature rule of order p. We also denote $\{w_n^l\}_{n=1}^p$ and $\{l_n\}_{n=1}^p$ as the weights and nodes of Legendre-Gauss-Lobbato quadrature rule of order p. For $\boldsymbol{u} = (u_1, u_2, u_3)^{\mathrm{T}}$, we define three discrete norms.

$$|||\boldsymbol{u}|||_U^2 = \sum_{K\in\mathcal{T}_h} \sum_{r,s,t=1}^{k+1} \omega_r^l \omega_s^l \omega_t^l \Big(h_1^K h_2^K h_3^K \big|\boldsymbol{u}(x_1^K + h_1^K l_r, x_2^K + h_2^K l_s, x_3^K + h_3^K l_t)\big|^2 \Big),$$

$$|||\boldsymbol{u}|||_V^2 = \sum_{K\in\mathcal{T}_h} \sum_{m,n=1}^{k+r-1} \omega_m \omega_n \Big(h_2^K h_3^K \left\| u_1(\cdot, x_2^K + h_2^K g_m, x_3^K + h_3^K g_n) \right\|^2 + h_1^K h_3^K$$

$$\left\| u_2(x_1^K + h_1^K g_m, \cdot, x_3^K + h_3^K g_n) \right\|^2 + h_1^K h_2^K \left\| u_3(x_1^K + h_1^K g_m, x_2^K + h_2^K g_n, \cdot) \right\|^2 \Big),$$

and

$$|||\boldsymbol{u}|||_W^2 = \sum_{K\in\mathcal{T}_h}\sum_{n=1}^{k}\omega_l\Big(h_1^K\left\|u_1(x_1^K+h_1^K g_n,\cdot,\cdot)\right\|^2 + h_2^K\left\|u_2(\cdot,x_2^K+h_2^K g_n,\cdot)\right\|^2 + h_3^K\left\|u_3(\cdot,\cdot,x_3^K+h_3^K g_n)\right\|^2\Big),$$

where $K = (x_1^K - h_1^K, x_1^K + h_1^K) \times (x_2^K - h_2^K, x_2^K + h_2^K) \times (x_3^K - h_3^K, x_3^K + h_3^K)$ with the center (x_1^K, x_2^K, x_3^K) and the side length $2h_1^K, 2h_2^K, 2h_3^K$.

Tables 8.5.4, 8.5.5, and 8.5.6 show errors measured in various norms for the lowest-order cubical elements in the three familes. We also depict error curves with a log-log scale in Figure 8.5.1. From Figure 8.5.1 (A), we can observe superconvergence phenomena that $|||\operatorname{grad}\operatorname{div}\boldsymbol{e}_h|||_W$ and $|||\boldsymbol{e}_h|||_V$ converge to 0 with one order higher than $\|\operatorname{grad}\operatorname{div}\boldsymbol{e}_h\|$ and $\|\boldsymbol{e}_h\|$. In addition, from Figure 8.5.1 (B)(C), we can observe superconvergence of $|||\operatorname{grad}\operatorname{div}\boldsymbol{e}_h|||_W$.

When $k = 1$, we can not observe any superconvergence of $|||\boldsymbol{e}_h|||_V$ for $r = 2, 3$ and $|||\operatorname{div}\boldsymbol{e}_h|||_U$ for all the 3 families. To further investigate the superconvergence of $\operatorname{div}\boldsymbol{e}_h$, we test the element with $k = 2$ and $r = k$. The results are shown in Table 8.5.7 and Figure 8.5.1(D). In this case, we can observe superconvergence of $\operatorname{div}\boldsymbol{e}_h$.

Using these superconvergent results, together with some recovery techniques, we can construct a solution with higher accuracy if needed, which is one of the reasons that we explore the superconvergence of cubical elements.

Table 8.5.4: Numerical results of the cubical grad div-conforming element with $r = k$ and $k = 1$

h	$\|\boldsymbol{e}_h\|$	$\|\boldsymbol{e}_h\|_V$	$\|\mathrm{div}\,\boldsymbol{e}_h\|$	$\|\mathrm{div}\,\boldsymbol{e}_h\|_U$	$\|\mathrm{grad}\,\mathrm{div}\,\boldsymbol{e}_h\|$	$\|\mathrm{grad}\,\mathrm{div}\,\boldsymbol{e}_h\boldsymbol{e}_h\|_W$
1/8	1.2939e-06	8.2349e-07	6.6566e-06	2.7601e-06	1.5795e-04	6.2427e-05
1/16	5.6099e-07	2.1371e-07	1.7020e-06	6.6734e-07	7.6700e-05	1.5975e-05
1/24	3.6063e-07	9.5663e-08	7.5957e-07	2.9471e-07	5.0814e-05	7.1306e-06
1/32	2.6677e-07	5.3946e-08	4.2787e-07	1.6541e-07	3.8025e-05	4.0170e-06
1/40	2.1201e-07	3.4566e-08	2.7402e-07	1.0575e-07	3.0388e-05	2.5726e-06

Table 8.5.5: Numerical results of the cubical grad div-conforming element with $r = k+1$ and $k = 1$

h	$\|\boldsymbol{e}_h\|$	$\|\boldsymbol{e}_h\|_V$	$\|\mathrm{div}\,\boldsymbol{e}_h\|$	$\|\mathrm{div}\,\boldsymbol{e}_h\|_U$	$\|\mathrm{grad}\,\mathrm{div}\,\boldsymbol{e}_h\|$	$\|\mathrm{grad}\,\mathrm{div}\,\boldsymbol{e}_h\boldsymbol{e}_h\|_W$
1/4	2.2275e-06	2.1791e-06	2.0877e-05	1.4226e-05	3.2323e-04	2.0116e-04
1/10	3.2909e-07	3.2124e-07	3.2354e-06	2.4023e-06	1.2317e-04	3.1825e-05
1/16	1.2730e-07	1.2419e-07	1.2547e-06	9.2031e-07	7.6282e-05	1.2340e-05
1/22	6.7137e-08	6.5485e-08	6.6217e-07	4.8348e-07	5.5322e-05	6.5115e-06
1/28	4.1395e-08	4.0373e-08	4.0839e-07	2.9756e-07	4.3414e-05	4.0157e-06

Table 8.5.6: Numerical results of the cubical grad div-conforming element with $r = k+2$ and $k = 1$

h	$\|\boldsymbol{e}_h\|$	$\|\boldsymbol{e}_h\|_V$	$\|\mathrm{div}\,\boldsymbol{e}_h\|$	$\|\mathrm{div}\,\boldsymbol{e}_h\|_U$	$\|\mathrm{grad}\,\mathrm{div}\,\boldsymbol{e}_h\|$	$\|\mathrm{grad}\,\mathrm{div}\,\boldsymbol{e}_h\boldsymbol{e}_h\|_W$
1/4	2.5839e-06	2.5818e-06	2.0796e-05	1.4263e-05	3.2318e-04	2.0132e-04
1/10	3.2119e-07	3.2115e-07	3.2315e-06	2.4030e-06	1.2317e-04	3.1829e-05
1/16	1.2417e-07	1.2416e-07	1.2541e-06	9.2042e-07	7.6282e-05	1.2340e-05
1/22	6.5478e-08	6.5476e-08	6.6200e-07	4.8351e-07	5.5322e-05	6.5117e-06

Table 8.5.7: Numerical results of the cubical grad div-conforming element with $r = k$ and $k = 2$

h	$\|\boldsymbol{e}_h\|$	$\|\boldsymbol{e}_h\|_V$	$\|\mathrm{div}\,\boldsymbol{e}_h\|$	$\|\mathrm{div}\,\boldsymbol{e}_h\|_U$	$\|\mathrm{grad}\,\mathrm{div}\,\boldsymbol{e}_h\|$	$\|\mathrm{grad}\,\mathrm{div}\,\boldsymbol{e}_h\boldsymbol{e}_h\|_W$
1/4	6.3209e-07	2.2806e-07	2.9623e-06	8.8580e-07	7.8540e-05	2.5723e-05
1/10	7.6991e-08	1.1031e-08	1.8971e-07	2.8011e-08	1.2378e-05	1.9063e-06
1/16	2.8833e-08	2.5640e-09	4.6416e-08	4.3703e-09	4.8272e-06	4.7467e-07
1/22	1.5050e-08	9.7038e-10	1.7869e-08	1.2319e-09	2.5519e-06	1.8377e-07

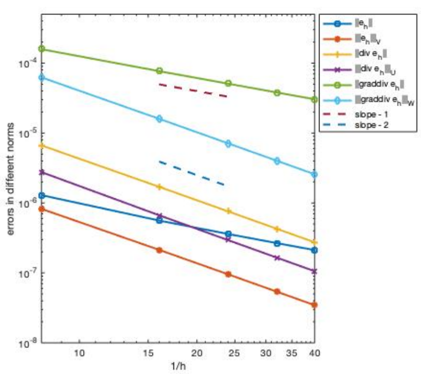

(a) $r = k, k = 1$

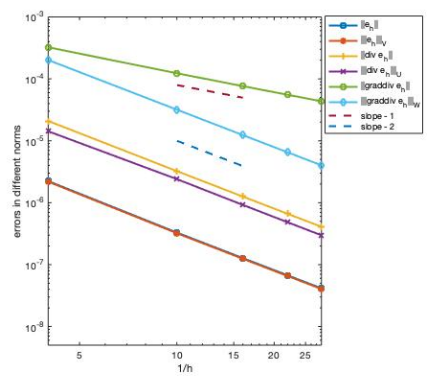

(b) $r = k + 1, k = 1$

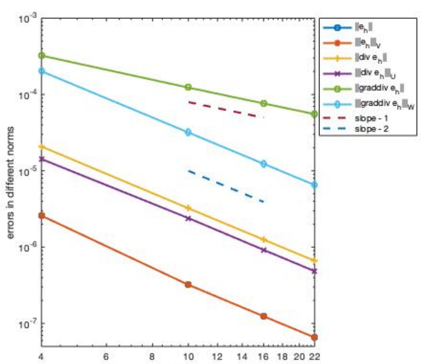

(c) $r = k + 2, k = 1$

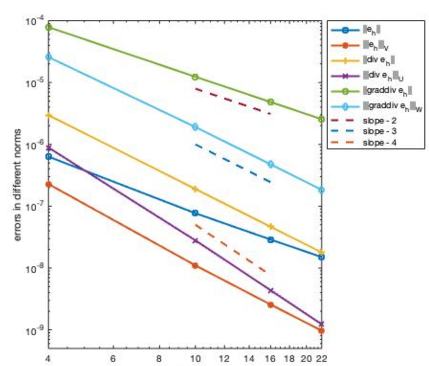

(d) $r = k, k = 2$

Figure 8.5.1: Error curves in different norms

CHAPTER 9 CONCLUSION

In this dissertation, we considered the construction of grad curl-conforming and grad div-conforming finite elements in both 2D and 3D based on discrete de Rham complexes. We briefly summarize our work below:

- By theoretical framework in [12], we derived the cohomology of the grad curl complex, the grad rot complex, and the grad div complex. We proved the density of $C^\infty(\overline{\Omega}) \otimes \mathbb{V}$ in $H(\operatorname{grad}\operatorname{curl};\Omega)$, $H(\operatorname{grad}\operatorname{rot};\Omega)$, and $H(\operatorname{grad}\operatorname{div};\Omega)$. We defined the trace operators $\gamma_{\tau,\mathrm{curl}} : H(\operatorname{grad}\operatorname{curl};\Omega) \to H^{-1/2}(\partial\Omega) \otimes \mathbb{V} \times H^{1/2}(\partial\Omega) \otimes \mathbb{V}$, $\gamma_{\tau,\mathrm{rot}} : H(\operatorname{grad}\operatorname{rot};\Omega) \to H^{-1/2}(\partial\Omega) \times H^{1/2}(\partial\Omega)$ and $\gamma_{n,\mathrm{div}} : H(\operatorname{grad}\operatorname{div};\Omega) \to H^{-1/2}(\partial\Omega) \times H^{1/2}(\partial\Omega)$, and proved their boundedness. We also proved the surjectivity of $\gamma_{\tau,\mathrm{rot}}$ and $\gamma_{n,\mathrm{div}}$. With these theoretical basis, we provided characterizations for $H_0(\operatorname{grad}\operatorname{curl};\Omega)$ and spaces in the dual complexes of the grad rot complex and the grad div complex. As a result, we obtain the explicit boundary conditions of the Hodge Laplacian problems.

- We investigated the spurious solutions of the $\operatorname{curl}\Delta\operatorname{rot}$ problems. We applied four finite element schemes to solve Hodge Laplacian source and eigenvalue problems of the grad rot complex. We found the primal formulations with the Argyris element and the $H^1(\mathrm{rot})$-conforming element lead to spurious solutions in certain cases, whereas the mixed formulations with the grad rot-conforming element and the $H^1(\mathrm{rot})$-conforming elements lead to the correct solutions. We provided a theoretical explanation for the numerical phenomena and a convergence analysis on simply-connected domains for the mixed formulation with the grad rot-conforming finite element.

- We constructed a smooth finite element de Rham complex in 2D. This leads to three families of grad rot-conforming elements, among which one family is consistent with our previous construction in high-order cases. We extended the existing family of elements by removing the restriction on the polynomial degree and fit it into the discrete complex. Among the three families, the simplest elements have only 6 DOFs for a triangle and 8 DOFs for a rectangle.

- We constructed a finite element Stokes complex on tetrahedral meshes, which contains three families of grad curl-conforming elements. Since the construction involves supersmoothness on lower-dimensional simplices of the tetrahedral mesh, the number of DOFs is at least 279. We proved that the discrete complex is exact on contractable domains. However, it is hard to construct an exact complex with vanishing boundary conditions. In addition, the canonical interpolations defined by the DOFs can not fit into a commuting diagram.

- We constructed another finite element Stokes complex, which contains three families of grad curl-conforming elements with fewer DOFs. The simplest element has only 18 DOFs, which, compared with the 279 DOFs in our previous construction, is a huge step forward. Besides, the discrete complex is exact on contractable domains, and hence it also contains a family of inf-sup stable finite element Stokes pairs which is the extension of the lower-order Stokes pair in [34]. Unlike our previous construction, we can show the finite element spaces with vanishing traces can form an exact complex and the canonical interpolations can fit into a commuting diagram.

- We constructed a finite element de Rham complex with enhanced smoothness, which leads to the first grad div-conforming elements in 3D. The simplest element has only 8 DOFs for a tetrahedron and 14 DOFs for a cube. We can also prove the exactness and the commuting diagram property of the proposed complex.

This dissertation inspires some new research directions:

- For the Hodge Laplacian problems of the grad curl complex, we obtained the explicit boundary conditions for only (3.1.8). We will characterize the boundary conditions for other Hodge Laplacian problems.

- The construction of discrete grad rot and grad div complexes is trivial, which can be realized by combining two finite elements de Rham complexes. However, it is not the case for the grad curl complex. We will construct a finite element subcomplex for the grad curl complex (3.1.6).

- In Chapter 4, we proved only the convergence on simply-connected domains. To obtain the convergence on general domains, we can apply the theoretical framework in FEEC [9], which requires the bounded cochain projections. Therefore, in the future, we will construct bounded cochain projections for the discrete grad rot, grad div, and even grad curl complexes.

- Only tetrahedral grad curl-conforming elements were considered in this dissertation. We will extend the construction in Chapter 7 to cubical meshes in the future.

- Despite the significant progress in the construction of the H^2-conforming finite elements mentioned in Introduction, the large number of DOFs makes it hard to implement these elements in practice. We will apply the idea of enriching with modified bubbles to construct new H^2-conforming elements with fewer DOFs.

- A discrete subcomplex provides an explicit characterization for the kernel of differential operators, which is crucial for the construction of robust preconditioners in the framework of the subspace correction methods [45, 57]. With an explicit characterization of the kernel spaces in the discrete complex in Chapter 7, one may construct parameter robust preconditioners for solving the Navier-Stokes equations.

REFERENCES

[1] P. Alfeld. A trivariate Clough-Tocher scheme for tetrahedral data. *Computer Aided Geometric Design*, 1(2):169–181, 1984.

[2] A. Alonso and A. Valli. An optimal domain decomposition preconditioner for low-frequency time-harmonic Maxwell equations. *Mathematics of Computation*, 68(226):607–631, 1999.

[3] S. Altan and E. Aifantis. On the structure of the mode III crack-tip in gradient elasticity. *Scripta Metallurgica et Materialia*, 26(2):319–324, 1992.

[4] C. Amrouche, C. Bernardi, M. Dauge, and V. Girault. Vector potentials in three-dimensional non-smooth domains. *Mathematical Methods in the Applied Sciences*, 21(9):823–864, 1998.

[5] J. Argyris, I. Fried, and D. Scharpf. The TUBA family of plate elements for the matrix displacement method. *The Aeronautical Journal*, 72(692):701–709, 1968.

[6] D. N. Arnold. *Finite Element Exterior Calculus*, volume 93. SIAM, 2018.

[7] D. N. Arnold and G. Awanou. The serendipity family of finite elements. *Foundations of Computational Mathematics*, 11(3):337–344, 2011.

[8] D. N. Arnold and G. Awanou. Finite element differential forms on cubical meshes. *Mathematics of Computation*, 83(288):1551–1570, 2014.

[9] D. N. Arnold, G. Awanou, and R. Winther. Finite elements for symmetric tensors in three dimensions. *Mathematics of Computation*, 77(263):1229–1251, 2008.

[10] D. N. Arnold, R. Falk, and R. Winther. Finite element exterior calculus, homological techniques, and applications. *Acta Numerica*, 15:1–155, 2006.

[11] D. N. Arnold, R. Falk, and R. Winther. Finite element exterior calculus: from hodge theory to numerical stability. *Bulletin of the American Mathematical Society*, 47(2):281–354, 2010.

[12] D. N. Arnold and K. Hu. Complexes from complexes. *arXiv preprint: arXiv:2005.12437*, 2020.

[13] D. N. Arnold and A. Logg. Periodic table of the finite elements. *SIAM News*, 47(9):212, 2014.

[14] I. Babuška and J. Osborn. Eigenvalue problems. *Elsevier*, 2:641–787, 1991.

[15] K. Bell. A refined triangular plate bending finite element. *International journal for numerical methods in engineering*, 1(1):101–122, 1969.

[16] S. C. Brenner and L. R. Scott. *The Mathematical Theory of Finite Element Methods*, volume 15. Springer Science & Business Media, 2008.

[17] F. Brezzi, J. Douglas, and L. D. Marini. Two families of mixed finite elements for second order elliptic problems. *Numerische Mathematik*, 47(2):217–235, 1985.

[18] F. Cakoni and H. Haddar. A variational approach for the solution of the electromagnetic interior transmission problem for anisotropic media. *Inverse Problems and Imaging*, 1(3):443–456, 2017.

[19] L. Chacón, A. N. Simakov, and A. Zocco. Steady-state properties of driven magnetic reconnection in 2D electron magnetohydrodynamics. *Physical review letters*, 99(23):235001, 2007.

[20] S. Christiansen, J. Hu, and K. Hu. Nodal finite element de Rham complexes. *Numerische Mathematik*, 139(2):411–446, 2018.

[21] S. Christiansen and K. Hu. Generalized finite element systems for smooth differential forms and stokes problem. *Numerische Mathematik*, 140(2):327–371, 2018.

[22] P. G. Ciarlet. Interpolation error estimates for the reduced Hsieh-Clough-Tocher triangle. *Mathematics of Computation*, 32(142):335–344, 1978.

[23] P. G. Ciarlet. *The finite element method for elliptic problems.* SIAM, 2002.

[24] R. Clough and J. Tocher. Finite element stiffness matrices for analysis of plates in bending. *In Proceedings of the Conference on Matrix Methods in Structural*

Mechanics, Wright-Patterson Air Force Base, OH, pages 515 – 547.

[25] M. Costabel and A. McIntosh. On Bogovskiĭ and regularized Poincaré integral operators for de Rham complexes on Lipschitz domains. *Mathematische Zeitschrift*, 265(2):297–320, 2010.

[26] R. Courant. Variational methods for the solution of problems of equilibrium and vibrations. *Bulletin of the American Mathematical Society*, 49:1–23, 1943.

[27] F. Demengel, G. Demengel, and R. Erné. *Functional spaces for the theory of elliptic partial differential equations*. Springer, 2012.

[28] R. Falk and M. Neilan. Stokes complexes and the construction of stable finite elements with pointwise mass conservation. *SIAM Journal on Numerical Analysis*, 51(2):1308–1326, 2013.

[29] G. Farin. Bézier polynomials over triangles and the construction of piecewise c^r polynomials. *Brunel University Mathematics Technical Papers collection*, 1980.

[30] V. Girault and P. Raviart. *Finite element methods for Navier-Stokes equations: theory and algorithms*, volume 5. Springer Science & Business Media, 2012.

[31] J. Guzmán, A. Lischke, and M. Neilan. Exact sequences on Powell-Sabin splits. *Calcolo*, 57(2):1–25, 2020.

[32] J. Guzmán, A. Lischke, and M. Neilan. Exact sequences on Worsey-Farin splits. *arXiv preprint, arXiv:2008.05431*, 2020.

[33] J. Guzmán and M. Neilan. Conforming and divergence-free stokes elements in three dimensions. *IMA Journal of Numerical Analysis*, 34(4):1489–1508, 2014.

[34] J. Guzmán and M. Neilan. Inf-sup stable finite elements on barycentric refinements producing divergence-free approximations in arbitrary dimensions. *SIAM Journal on Numerical Analysis*, 56(5):2826–2844, 2018.

[35] J. He, K. Hu, and J. Xu. Generalized Gaffney inequality and discrete compactness for discrete differential forms. *Numerische Mathematik*, 143(4):781–795, 2019.

[36] R. Hiptmair. Canonical construction of finite elements. *Mathematics of Computation*, 68(228):1325–1346, 1999.

[37] R. Hiptmair. Higher order whitney forms. *Progress in Electromagnetics Research*, 32:271–299, 2001.

[38] R. Hiptmair. Finite elements in computational electromagnetism. *Acta Numerica*, 11:237, 2002.

[39] K. Hu, Q. Zhang, and Z. Zhang. A family of finite element Stokes complexes in three dimensions. *arXiv preprint arXiv:2008.03793*, 2020.

[40] K. Hu, Q. Zhang, and Z. Zhang. Simple curl-curl-conforming finite elements in two dimensions. *SIAM Journal on Scientific Computing*, 42(6):A3859–A3877, 2020.

[41] V. John, A. Linke, C. Merdon, M. Neilan, and L. Rebholz. On the divergence constraint in mixed finite element methods for incompressible flows. *SIAM review*, 59(3):492–544, 2017.

[42] M. Krizek, P. Neittaanmaki, and R. Stenberg. *Finite element methods: fifty years of the Courant element*. CRC Press, 2016.

[43] M. J. Lai and L. L. Schumaker. *Spline functions on triangulations*, volume 110. Cambridge University Press, 2007.

[44] S. Lang. *Fundamentals of differential geometry*, volume 191. Springer Science & Business Media, 2012.

[45] Y. Lee, J. Wu, J. Xu, and L. Zikatanov. Robust subspace correction methods for nearly singular systems. *Mathematical Models and Methods in Applied Sciences*, 17(11):1937–1963, 2007.

[46] R. Mindlin. Micro-structure in linear elasticity. *Arch. Ration. Mech. Anal.*, 16:51–78, 1964.

[47] R. Mindlin. Second gradient of strain and surface-tension in linear elasticity. *International Journal of Solids and Structures*, 1(4):417–438, 1965.

[48] R. D. Mindlin and H. F. Tiersten. Effects of couple-stresses in linear elasticity. *Archive for Rational Mechanics and Analysis*, 11(1):415–448, 1962.

[49] P. Monk. *Finite Element Methods for Maxwell's Equations.* Oxford University Press, 2003.

[50] P. Monk and J. Sun. Finite element methods for Maxwell's transmission eigenvalues. *SIAM Journal on Scientific Computing*, 34(3):B247–B264, 2012.

[51] J. C. Nédélec. Mixed finite elements in $\diagdown^3$. *Numerische Mathematik*, 35(3):315–341, 1980.

[52] J. C. Nédélec. A new family of mixed finite elements in $\diagdown^3$. *Numerische Mathematik*, 50(1):57–81, 1986.

[53] M. Neilan. Discrete and conforming smooth de Rham complexes in three dimensions. *Mathematics of Computation*, 84(295):2059–2081, 2015.

[54] S. K. Park and X. Gao. Variational formulation of a modified couple stress theory and its application to a simple shear problem. *Zeitschrift für angewandte Mathematik und Physik*, 59(5):904–917, 2008.

[55] M. J. D. Powell and M.A. Sabin. Piecewise quadratic approximations on triangles. *ACM Transactions on Mathematical Software (TOMS)*, 3(4):316–325, 1977.

[56] P. A. Raviart and J. M. Thomas. Primal hybrid finite element methods for 2nd order elliptic equations. *Mathematics of computation*, 31(138):391–413, 1977.

[57] J. Schöberl. *Robust multigrid methods for parameter dependent problems.* PhD thesis, Johannes Kepler Universität Linz, 1999.

[58] L. R. Scott and Michael Vogelius. Norm estimates for a maximal right inverse of the divergence operator in spaces of piecewise polynomials. *ESAIM: Mathematical Modelling and Numerical Analysis*, 19(1):111–143, 1985.

[59] L. R. Scott and S. Zhang. Finite element interpolation of nonsmooth functions satisfying boundary conditions. *Mathematics of Computation*, 54(190):483–493,

1990.

[60] T. Sorokina. Intrinsic supersmoothness of multivariate splines. *Numerische Mathematik*, 116(3):421–434, 2010.

[61] J. Sun. A mixed FEM for the quad-curl eigenvalue problem. *Numerische Mathematik*, 132(1):185–200, 2016.

[62] X. C. Tai and R. Winther. A discrete de Rham complex with enhanced smoothness. *Calcolo*, 43(4):287–306, 2006.

[63] H. Whitney. *Geometric integration theory*. Princeton university press, 2015.

[64] A. J. Worsey and B. Piper. A trivariate Powell-Sabin interpolant. *Computer Aided Geometric Design*, 5(3):177–186, 1988.

[65] A. Ženíšek. Polynomial approximation on tetrahedrons in the finite element method. *Journal of Approximation Theory*, 7(4):334–351, 1973.

[66] Q. Zhang, L. Wang, and Z. Zhang. H(curl^2)-conforming finite elements in 2 dimensions and applications to the quad-curl problem. *SIAM Journal on Scientific Computing*, 41(3):A1527–A1547, 2019.

[67] Q. Zhang and Z. Zhang. A family of curl-curl conforming finite elements on tetrahedral meshes. *CSIAM Transactions on Applied Mathematics*, 1(4):639–663, 2020.

[68] Q. Zhang and Z. Zhang. Three families of grad-div-conforming finite elements. *arXiv preprint arXiv:2007.10856*, 2020.

[69] Shangyou Zhang. A new family of stable mixed finite elements for the 3D Stokes equations. *Mathematics of computation*, 74(250):543–554, 2005.

[70] Shangyou Zhang. A family of 3D continuously differentiable finite elements on tetrahedral grids. *Applied Numerical Mathematics*, 59(1):219–233, 2009.

ABSTRACT

NEW CONFORMING FINITE ELEMENTS BASED ON THE DE RHAM COMPLEXES FOR SOME FOURTH-ORDER PROBLEMS

by

QIAN ZHANG

August 2021

Advisor: Dr. Zhimin Zhang

Major: Mathematics

Degree: Doctor of Philosophy

In this dissertation, we discuss the conforming finite element discretization of high-order equations involving operators such as $(\operatorname{curl}\operatorname{curl})^2$, $\operatorname{grad}\Delta\operatorname{div}$, and $-\operatorname{curl}\Delta\operatorname{curl}$. These operators appear in various models, such as continuum mechanics, inverse electromagnetic scattering theory, magnetohydrodynamics, and linear elasticity. Naively discretizing these operators and their corresponding eigenvalue problems using the existing H^2-conforming element would lead to spurious solutions in certain cases. Therefore, it is desirable to design conforming finite elements for equations containing these high-order differential operators.

The $\operatorname{curl}\operatorname{curl}$-conformity or $\operatorname{grad}\operatorname{curl}$-conformity requires that the tangential component of $\operatorname{curl}\boldsymbol{u}_h$ is continuous. Recall that the Nédélec element requires only the continuity of the tangential component of $\boldsymbol{u}_h$. Due to the continuity requirement and the naturally divergence-free property of the curl operator, it is challenging to construct $\operatorname{grad}\operatorname{curl}$-conforming elements. We start from the two dimensional case, where $\operatorname{curl}\boldsymbol{u}_h$ is a scalar. Our previous construction [66] is based on the existing polynomial spaces $Q_{k-1,k}\times Q_{k,k-1}$ and $\mathcal{R}_k$. The restriction of $k\geq 4$ for a triangular element or $k\geq 3$ for

a rectangular element has to be imposed since an interior bubble should be included in the shape function space of $\operatorname{curl} \boldsymbol{u}_h$, and hence the simplest triangular or rectangular element has 24 degrees of freedom. To reduce the degrees of freedom, we resort to the discrete de Rham complex to construct elements. The Poincaré operator enables us to tailor the shape function space to our needs (not necessarily the existing polynomial spaces). As a result, we construct a finite element complex, which contains three families of $\operatorname{grad}\operatorname{curl}$-conforming elements without the restriction on polynomial degrees. One of three families is consistent with the previous construction in high-order cases. The lowest-order triangular and rectangular finite elements have only 6 and 8 degrees of freedom, respectively.

Unlike the two-dimensional case, $\operatorname{curl} \boldsymbol{u}_h$ in three dimensions should be a divergence-free vector in the space $H^1 \otimes \mathbb{V}$, which relates the $\operatorname{curl}\Delta\operatorname{curl}$ problems to the Stokes problem. However, it is challenging to construct an inf-sup stable finite element Stokes pair that preserves the divergence-free condition at the discrete level. Neilan [53] constructed a finite element complex that includes a stable Stokes pair and an $H^1(\operatorname{curl})$-conforming element on tetrahedral meshes. Based on the same Stokes pair, we construct a finite element complex which contains three families of $\operatorname{grad}\operatorname{curl}$-conforming elements. Compared to the $H^1(\operatorname{curl})$-conforming elements [53] which have at least 360 DOFs, our $\operatorname{grad}\operatorname{curl}$-conforming elements have weaker continuity ($\boldsymbol{u}_h$ is in $H(\operatorname{curl})$ instead of $H^1 \otimes \mathbb{V}$) and thus fewer degrees of freedom. However, our elements still have at least 279 degrees of freedom. Recently, Guzmán and Neilan stabilized the lowest-order three dimensional Scott-Vogelius pair by enriching the velocity space with modified Bernardi-Raugel bubbles [34], which inspires us to use it to construct $\operatorname{grad}\operatorname{curl}$-conforming elements with fewer degrees of freedom. To obtain a family of elements, we first generalize their construction to an arbitrary order by enriching the velocity space with modified face or/and interior bubbles. Then we construct the whole finite element complex which contains three families of grad curl-conforming elements on tetrahedral meshes. The lowest-order element has only 18 degrees of freedom.

The grad div-conformity requires that the normal component and divergent of the finite element function $\boldsymbol{u}_h$ are continuous. Since div $\boldsymbol{u}_h$ is a scalar, the construction of the finite element complex and the grad div-conforming elements is similar to the grad curl elements in two dimensions. The simplest tetrahedral and cubical elements have only 8 and 14 degrees of freedom, respectively.

AUTOBIOGRAPHICAL STATEMENT

Qian Zhang

Education

- Ph.D. in Mathematics, 2021
  Wayne State University, Detroit, Michigan, USA
- M.S. in Computational Mathematics, 2018
  Beijing Computational Science Research Center, Beijing, China
- B.S. in Computational Mathematics, 2015
  Jilin University, Changchun, Jilin, China

Selected List of Awards and Scholarships

1. Outstanding Graduate Award, Wayne State University, 2021.
2. Thomas C. Rumble University Graduate Fellowship, Wayne State University, 2020-2021.
3. M.F. Janowitz Endowed Mathematics Scholarship, Wayne State University, 2020.

Selected List of Publications and Preprints

1. K. Hu, Q. Zhang, and Z. Zhang, *A family of finite element Stokes complexes in three dimensions*, submitted to SIAM J. Numer. Anal., arXiv:2008.03793.
2. Q. Zhang and Z. Zhang, *Three families of grad-div-conforming finite elements*, submitted to Numer. Math., arXiv:2007.10856.
3. K. Hu, Q. Zhang, and Z. Zhang, *Simple curl-curl-conforming finite elements in two dimensions*, SIAM J. Sci. Comput., Vol. 42, No. 6, 2020, A3859–A3877.
4. Q. Zhang and Z. Zhang, *A family of curl-curl conforming elements on tetrahedral meshes,* CSIAM Trans. Appl. Math., Vol. 1, No. 4, 2020, 639–663.
5. Q. Zhang, L. Wang, and Z. Zhang, $H(\text{curl}^2)$-*conforming finite elements in 2 dimensions and applications to the quad-curl problem*, SIAM J. Sci. Comput., Vol. 41, No. 3, 2019, A1527–A1547.
6. K. Hu, Q. Zhang, J. Han, L. Wang, and Z. Zhang, *Spurious solutions for high order curl problems*, 2021.